

**The Effect of Variations in Component Positioning and Swing Phase Load
on the Occurrence and Severity of Edge Loading and Wear in Hip Joint
Replacements**

Oscar Gilbert O'Dwyer Lancaster-Jones

Submitted in accordance with the requirements for a degree of
Doctor of Philosophy

The University of Leeds
School of Mechanical Engineering

Sep 2017

The candidate confirms that the work submitted is his own, except where work which has formed part of jointly authored publications has been included. The contribution of the candidate and the other authors to this work has been explicitly indicated below. The candidate confirms that appropriate credit has been given within the thesis where reference has been made to work of others.

The work in Chapter 3.6, specifically, the wear study under a 4 mm translational mismatch with a 45° and 65° cup inclination angle, was predominantly carried out by Mazen Al-Hajjar and used as training of the hip joint simulator for Oscar O'Dwyer Lancaster-Jones.

The work in Chapter 3.5 of this thesis has appeared in publication as follows:

Dynamic virtual simulation of the occurrence and severity of edge loading in hip replacements associated with variation in the rotational and translational surgical position, April 2017, Joanna Leng, Mazen Al-Hajjar, Ruth Wilcox, Alison Jones, David Barton and John Fisher

I was responsible for the *in vitro* testing used to compare against the *in silico* work of this publication. The contribution of the other authors included the study design, development of the *in silico* model and writing of the publication.

This copy has been supplied on the understanding that it is copyright material and that no quotation from thesis may be published without proper acknowledgement

© 2017 The University of Leeds and Oscar O'Dwyer Lancaster-Jones

The right of Oscar O'Dwyer Lancaster-Jones to be identified as Author of this work has been asserted by him in accordance with the Copyright, Design and Patents Act 1988.

Acknowledgments

I would firstly like to thank both my supervisors Mazen Al-Hajjar and John Fisher for their valuable time, providing me with the opportunities for development, their help and continuous support throughout the years.

I would like to thank the incredible staff in the School of Mechanical Engineering, many people have given me their time and helped me and without their input and support this work would have not been accomplished.

Also, with many hours of work there were also many hours that were spent with the people from iMBE. I took that place as my second home. Socialising and laughing with such a great bunch of people made the years go by very easily and I have many good memories. Thank you for your friendship.

I would also like to thank Amy Kinbrum, you always made the meetings very valuable and thanks to you I have learned a lot.

Finally, to my mother, truly without you I wouldn't be where I am.

Abstract

Edge loading is multifactorial and has been identified as a risk leading to the revision of hip joint replacements. Pre-clinical testing requirements currently do not incorporate edge loading. Previous testing of edge loading has been carried out as controlled dynamic microseparation of 0.5 mm via a spring, where the femoral head contacts the rim section of the acetabular cup. The input conditions of these tests did not allow the individual evaluation of other variables due to the constraints of the methodology.

The aim of these studies was to evaluate the effect on the occurrence and severity of edge loading, and wear, under edge loading due to different parameters in a hip joint simulator.

A translational mismatch of 1, 2, 3 and 4 mm were applied between the centres of rotation of the head and the cup in order to evaluate the effect on the dynamic separation and severity of edge loading. This allowed differentiating the effect of the 45°, 55° and 65° cup inclination angle studied in the test matrix. Three studies were developed to determine the effect of the cup inclination angle (45°, 55° and 65°), the effect of the swing phase load (50-500 N) and the effect of the spring constant (50, 100 and 200 N/mm), where short biomechanical studies determined the effect and aided to provide an informed decision on the specific test conditions selected for wear testing.

The results indicated how the decrease in cup inclination angle and increase in swing phase load decreased the dynamic separation and severity of edge loading and wear.

These studies have elaborated on the potential conditions leading to edge loading and their outcome. Overall the severity of edge loading had a positive linear correlation ($R^2=0.90$) with the wear rate for all the conditions tested. This project has emphasised the criteria required to individually evaluate different parameters when considering edge loading and presented a format to develop an ISO standard to consider the risks associated with edge loading.

Table of contents

1.	Introduction	1
1.1.	The natural adult hip joint	1
1.1.1.	Anatomy	1
1.1.2.	Biomechanics	4
1.1.3.	Synovial fluid	5
1.1.4.	Joint degeneration	5
1.2.	Hip joint prostheses	6
1.2.1.	Articulating materials.....	6
1.2.2.	Design.....	9
1.2.3.	Design considerations	9
1.2.4.	Head size	9
1.2.5.	Clearance.....	10
1.2.6.	Jumping distance.....	10
1.2.7.	Cup coverage.....	10
1.3.	Tribology	10
1.3.1.	Contact mechanics	10
1.3.2.	Friction	10
1.3.3.	Lubrication	11
1.3.4.	Wear mechanisms.....	12
1.4.	Biological response to wear debris	13
1.5.	Implant position	15
1.5.1.	Surgical approach.....	15
1.5.2.	Clinical studies of hip prostheses	18
a)	Imaging for total hip replacement alignment.....	18
b)	Centre of rotation (premorbid centre) and tissue tension	20
c)	Femoral offset.....	20
d)	Leg lengthening.....	21
e)	Stem migration.....	21
f)	Cup migration.....	22
1.5.3.	Edge loading and stripe wear.....	22
a)	Rotational and translational malposition	23
b)	Retrievals related to edge loading	25
c)	In vivo translation	27
d)	Effect of the translational mismatch on the biomechanics	28
1.6.	Wear of hip joint replacement bearings	29
1.6.1.	Hip joint replacement biomechanics	29

a)	In vivo forces	29
b)	In vivo motions.....	30
1.6.2.	In vitro hip simulator studies	32
a)	Factors.....	32
b)	Influence of kinematics	33
c)	Wear of hip joint replacements	34
1.6.3.	In vitro malposition and adverse conditions.....	41
a)	Rotational malposition.....	41
b)	Microseparation simulation (translational malposition)	42
c)	Wear particle size.....	44
d)	Effect of rotational malposition in combination with microseparation	45
1.7.	Rationale	46
1.8.	Aims and objectives	47
1.9.	Outline of studies.....	48
1.10.	Hypothesis and research questions	49
2.	Methodology.....	50
2.1.	Materials	50
2.2.	Hip joint simulator	51
2.2.1.	Leeds Mark II Physiological Anatomical Hip Joint Wear Simulator.....	51
2.2.2.	Fixtures.....	51
2.2.3.	Kinematics.....	53
2.2.4.	Medial-lateral component translational mismatch	53
Definitions:.....		53
Springs.....		56
2.2.5.	Monitoring and Data Acquisition System (MDAS).....	56
2.2.6.	Lubrication	58
2.3.	Measurements	59
2.3.1.	Gravimetric wear analysis.....	59
2.3.2.	Clearance measurements	60
2.3.3.	Volumetric wear analysis	60
2.3.4.	Surface topography analysis	61
2.3.5.	Dynamic separation	62
Effect of the input mismatch on the cup displacement due to the tilt of the cup holder		62
Dynamic separation calculation		64
Budget of uncertainty		64
2.3.6.	Duration of edge loading	65

2.3.7.	Maximum vertical force under of edge loading.....	66
2.3.8.	Severity of edge loading.....	66
3.	The Combined Effect of the Mismatch between the Head and Cup Centres and the Cup Inclination Angle on the Occurrence and Severity of Edge Loading and Wear in Ceramic-on-ceramic Hip Joint Replacements.....	68
3.1.	Introduction	68
3.2.	Aim	70
3.3.	Methodology of the study	71
3.4.	Biomechanical study Phase 1: Evaluation of the biomechanics under a medial-lateral component translational mismatch between the head and the cup for different cup inclination angles	72
3.4.1.	Aim	72
3.4.2.	Methodology.....	72
3.4.3.	Results.....	74
3.5.	Biomechanical study Phase 2: Evaluation of severity of edge loading for specific testing conditions under a medial-lateral component translational mismatch between the head and the cup centre.....	81
3.5.1.	Aim	81
3.5.2.	Methodology.....	81
3.5.3.	Results.....	83
3.6.	The wear of 36 mm CoC (BIOLOX® delta) under edge loading due to a medial-lateral component translational mismatch of 2, 3 and 4 mm for a 45° and 65° cup inclination angle 84	
3.6.1.	Aim	84
3.6.2.	Methodology.....	84
3.6.3.	Results.....	86
3.7.	Discussion.....	98
3.7.1.	Dynamic separation	98
3.7.2.	Wear correlations	100
3.7.3.	Maximum vertical force under edge loading.....	104
3.7.4.	Medial-lateral load.....	105
3.7.5.	Type of edge loading.....	106
3.7.6.	Severity of edge loading.....	107
3.7.7.	Wear under a translational mismatch	107
3.7.8.	Limitations.....	109
3.8.	Conclusion.....	112
4.	The Influence of the Swing Phase Load on the Occurrence and Severity of Edge Loading and Wear for Ceramic-on-ceramic Total Hip Replacement under Variations of Component Positioning	113

4.1.	Introduction	113
4.2.	Aim	114
4.3.	Methodology of the study	114
4.4.	Biomechanical study Phase 1. Evaluation of the biomechanics for different swing phase loads under variations in translational mismatch and cup inclination angle.....	116
4.4.1.	Aim	116
4.4.2.	Methodology.....	116
4.4.3.	Results	118
4.5.	Biomechanical study Phase 2. Evaluation of severity of edge loading of specific swing phase load conditions under a translational mismatch.....	127
4.5.1.	Aim & methodology	127
4.5.2.	Results	128
4.6.	The wear of 36 mm CoC (BIOLOX® delta) under edge loading due to a medial-lateral component translational mismatch of 4 mm for 150 N and 300 N swing phase load with a cup inclination of 65°	130
4.6.1.	Aim	130
4.6.2.	Methodology.....	130
4.6.3.	Results	132
4.7.	Discussion.....	137
4.7.1.	Dynamic separation	137
4.7.2.	Wear correlations	141
4.7.3.	In vivo biomechanics.....	144
4.7.4.	Type of edge loading.....	145
4.7.5.	Severity of edge loading.....	148
4.7.6.	Limitations.....	149
4.8.	Conclusion.....	152
5.	The Influence of the Spring Stiffness on the Occurrence and Severity of Edge Loading and Wear for Ceramic-on-ceramic Total Hip Replacement under Variations of Component Positioning in vitro	153
5.1.	Introduction	153
5.2.	Aim	154
5.3.	Methodology.....	154
5.4.	Biomechanical study Phase 1. Evaluation of the biomechanics for different spring constants under variations in translational mismatch and cup inclination angle	156
5.4.1.	Aim	156
5.4.2.	Methodology.....	156
5.4.3.	Results	158
5.5.	Biomechanical study Phase 2. Evaluation of the severity of edge loading for specific spring constant test conditions under a translational mismatch	174

5.5.1.	Aim & methodology	174
5.5.2.	Results	175
5.6.	The wear of 36 mm CoC (BIOLOX® delta) under edge loading due to a medial-lateral component translational mismatch of 4 mm for 50 and 200 N/mm spring constants with a cup inclination of 65°	177
5.6.1.	Aim	177
5.6.2.	Methodology	177
5.6.3.	Results	179
5.7.	Discussion	185
5.7.1.	Dynamic separation	185
5.7.2.	Wear correlations	188
5.7.3.	Separation ratio and threshold	191
5.7.4.	Type of edge loading	192
5.7.5.	Limitations	193
5.8.	Conclusion	194
6.	Discussion and conclusion	195
6.1.	Summary	195
6.2.	Conclusion	199
6.3.	Future work	200
7.	Publications and abstracts	201
8.	References	203
9.	Appendices	216
	Appendix A. Type of edge loading for different conditions based on the analysis of data and interpretation of the observer	216
	Appendix B. Variability of the springs close end finish and the effect on its performance under axial compression	219
	Appendix C. Effect of the input translational mismatch on the displacement and tilt of the cup holder	222

List of figures

Figure 1-1. Anterior view of the top section of the right femur (a), anterior view of pelvis (b) indicating A) anterior posterior iliac spine, B) acetabulum, C) coccyx, D) iliac spine, E) obturator foramen, F) ischial tuberosity, and G) ischial tuberosity (adapted from p. 5 and p. 7, Paul 1967).	1
Figure 1-2. Outer ligaments surrounding the hip joint (A) anterior view and (B) posterior view (adapted from p. 54, Wasielewski 2007).	2
Figure 1-3. Variation with time of the components of the upper bounds of the hip joint force (adapted from p. 202, Paul 1967). Heel strike left foot (HSLF), toe off left foot (TOLF). LB stands for pounds.	4
Figure 1-4. Generic total hip replacement device, showing components and elements (adapted from p.103, Black <i>et al.</i> 2007).....	7
Figure 1-5. Effect of protein concentration upon friction factor, tested with 100 N swing phase load (Brockett <i>et al.</i> , 2007).	11
Figure 1-6. Stribeck diagram showing friction factor against Sommerfeld number and the lubrication regimens (Jin <i>et al.</i> , 2006).....	12
Figure 1-7. Schematic of different parameters to consider during hip joint replacement surgery.	19
Figure 1-8. Schematic representing medial-lateral malposition.	23
Figure 1-9. Schematic representing rotational malposition.	24
Figure 1-10. Kinematics on the Leeds Mark II Anatomical Hip Simulator	33
Figure 1-11. Summary graph to elaborate on how a favourable film-thickness-to-surface-roughness ratio (λ ratio) is desirable in order to maintain low friction between the articulating surfaces for MoM studies under optimal testing conditions. Figure 1 from Silva <i>et al.</i> , 2005.	38
Figure 1-12. Schematic of the test methodology to apply edge loading with a dynamic microseparation.....	43
Figure 1-13. Schematic of the analysis of data and the test structure.	48
Figure 2-1. AMC Ceramic bearings (BIOLOX® delta).	50
Figure 2-2. C-STEM™ AMT (A) and, ceramic head mounted in the stem fixture with bone cement (B).....	51
Figure 2-3. PINNACLE® shell (A) and, ceramic liner inserter in the cup fixture (B).....	52
Figure 2-4. Two designs of cup the fixtures, top is 65° and bottom is 45° inclination angle.....	52
Figure 2-5. Schematic of the inputs in the Leeds Hip Joint Simulator.	53
Figure 2-6. Schematic of the cup holder and mounting fixture at different points a) axially aligned, b) and c) with a displacement in the medial-lateral axis away from the reference plane.	54

Figure 2-7. Schematic of the medial-lateral component translational mismatch input between the head and cup centre and without a vertical load applied on the cup, and axially aligned when a load is applied.	55
Figure 2-8. LVDT set-up for routine check (A), and visualisation of the cup holder displacement in an oscilloscope (B).....	55
Figure 2-9. Photograph of a spring used in these studies to illustrating geometrical-end finish.	56
Figure 2-10. Diagram of the Monitoring and Data Acquisition System (MDAS) for the Leeds II (A) Hip Joint Simulator.	58
Figure 2-11. Leeds Hip Simulator with lubricant serum applied on the stations	59
Figure 2-12. CMM and ceramic head set-up.....	61
Figure 2-13. Schematic of the three traces performed on the heads before testing.....	61
Figure 2-14. Schematic of the two traces performed on the heads after testing.	62
Figure 2-15. Schematic illustrating the tilt on the cup holder due to the position of the spring applying a force at a different position than that of the head and cup centre.	63
Figure 2-16. Schematic illustrating the effect of the translational mismatch on the cup holder displacement medial-laterally during cyclic loading.....	63
Figure 2-17. Schematic illustrating the mismatch, the tilt calibration and dynamic separation during cyclic and axially aligned conditions. In order to calculate the dynamic separation, first the axial alignment point was defined (Phase A), then a mismatch was applied (Phase B), the tilt calibration was measured (Phase C), this defined the assembly point (Phase D) and the dynamic separation was calculated (Phase E).	64
Figure 2-18. Schematic of the duration of edge loading from a load and dynamic separation curves.....	65
Figure 2-19. Example of raw output force (blue) and displacement (red) data under a translational mismatch. The zero point of the displacement indicates when the head and the cup were axially aligned.....	65
Figure 2-20. Schematic of the measured maximum vertical force under edge loading from a load and dynamic separation profile.	66
Figure 2-21. Schematic of the evaluation of the severity of edge loading from the load and separation curves.....	67
Figure 2-22. Example of output axial (F_y , in blue) and medial-lateral (F_x , in black) force data under a translational mismatch.....	67
Figure 3-1. Schematic of the acetabular cup and femoral head conforming to each other at the hip joint centre set by the cup position.	69
Figure 3-2. Schematic of a total hip joint replacement where a translational mismatch is present between the centre of the head and the centre of the cup.....	69

Figure 3-3. Schematic representing the hip simulator testing conditions with reconstructed head and cup medial-lateral centre mismatch.....	73
Figure 3-4. Mean (n=3, $\pm 95\%$ CI) dynamic separation of 36 mm ceramic-on-ceramic (BIOLOX® delta) bearings under 1, 2, 3 and 4 mm translational mismatch conditions for three cup inclination angle conditions, 45°, 55° and 65°.....	74
Figure 3-5. Mean (n=3, $\pm 95\%$ CI) maximum load recorded at 0.1 mm separation during edge loading at different component positions including acetabular cup and femoral head translational mismatch.....	75
Figure 3-6. Mean minimum and maximum medial-lateral load (n=3, $\pm 95\%$ CI) of 36 mm ceramic-on-ceramic (BIOLOX® delta) bearings under 1, 2, 3 and 4 mm translational mismatch conditions (color coded and shaded against increased in translational mismatch) for three cup inclination angle conditions, 45° (green), 55° (blue) and 65° (red).	77
Figure 3-7. Schematic representing the relocation of the cup into the head in a single action.	78
Figure 3-8. Schematic representing an interrupted edge loading condition.....	78
Figure 3-9. Mean (n=3, $\pm 95\%$ CI) severity of edge loading of 36 mm ceramic-on-ceramic (BIOLOX® delta) bearings under 1, 2, 3 and 4 mm translational mismatch conditions for three cup inclination angle conditions, 45°, 55° and 65°.....	79
Figure 3-10. Schematic of the input translational mismatch between the centre of the head and the centre of the cup in the Hip Joint Simulator.....	82
Figure 3-11. Mean (n=6, $\pm 95\%$ CI) severity of edge loading of 36 mm ceramic-on-ceramic (BIOLOX® delta) bearings under 2, 3 and 4 mm translational mismatch conditions for two cup inclination angle conditions, 45° and 65°.....	83
Figure 3-12. Schematic of the inputs on the Hip Joint Simulator.	84
Figure 3-13. Average displacement of the cup holder ($\pm 95\%$ CI) for standard and steep inclination angles under a 2 mm translational mismatch.....	86
Figure 3-14. Average displacement of the cup holder ($\pm 95\%$ CI) for standard and steep inclination angles under a 3 mm translational mismatch.....	87
Figure 3-15. Average displacement of the cup holder ($\pm 95\%$ CI) for standard and steep inclination angles under a 4 mm translational mismatch.....	87
Figure 3-16. Individual volumetric wear for standard (45°) and steep (65°) cup inclination angles under 2 mm medial-lateral component translational mismatch. Stn = Station.....	88
Figure 3-17. Mean (n=6, $\pm 95\%$ CI) wear rates for standard (45°) and steep (65°) inclination angles under 2 mm medial-lateral component translational mismatch.	89
Figure 3-18. Individual volumetric wear for standard (green) and steep (red) cup inclination angles under 3 mm medial-lateral component translational mismatch. Stn = Station.....	90
Figure 3-19. Mean (n=6, $\pm 95\%$ CI) wear rates for standard and steep inclination angles under 3 mm medial-lateral component translational mismatch.....	90

Figure 3-20. Individual volumetric wear for standard (green) and steep (red) inclination angles under 4 mm medial-lateral component translational mismatch. Stn = Station.	91
Figure 3-21. Mean (n=6, $\pm 95\%$ CI) wear rates for standard and steep inclination angles under 4 mm medial-lateral component translational mismatch.	92
Figure 3-22. Mean (n=6, $\pm 95\%$ CI) wear rate of 36 mm ceramic-on-ceramic (BIOLOX [®] delta) bearings under 2, 3 and 4 mm translational mismatch conditions with a cup inclination angle conditions of 45° and 65°.....	92
Figure 3-23. Visualisation of the heads tested under a 2 mm medial-lateral component translational mismatch via RedLux software after 3 million cycles. The maximum depth of the scar is labelled beside each head accordingly.	93
Figure 3-24. Visualisation of the heads under a 3 mm medial-lateral component translational mismatch via RedLux software after 3 million cycles. The maximum depth of the scar is aligned to each head accordingly.	93
Figure 3-25. Visualisation of the heads under a 4 mm medial-lateral component translational mismatch via RedLux software after 3 million cycles. The maximum depth of the scar is aligned to each head accordingly.	94
Figure 3-26. Mean (n=6, $\pm 95\%$ CI) maximum scar penetration after 3 million cycles under a 2, 3 and 4 mm medial-lateral component translational mismatch conditions for standard (45°) and steep (65°) cup inclination angles.	95
Figure 3-27. Mean surface roughness (Ra) for unworn head samples (P1-P3), and post-test at the pole (P1), and the wear scar (P2) under 2 mm medial-lateral component translational mismatch for standard (45°, n=6) and steep (65°, n=6) cup inclination angles.....	95
Figure 3-28. Mean surface roughness (Ra) for unworn head samples (P1-P3), and post-test at the pole (P1), and the wear scar (P2) under 3 mm medial-lateral component translational mismatch for standard (45°, n=6) and steep (65°, n=6) cup inclination angles.....	96
Figure 3-29. Mean (n=6, $\pm 95\%$ CI) surface roughness (Ra) for head samples post-test at the pole 'P1 (tested)', and the wear scar 'P2 (tested)' under 4 mm medial-lateral component translational mismatch for standard (45°) and steep (65°) cup inclination angles.	96
Figure 3-30. Schematic showing the acetabular cup at two inclination angle conditions highlighting the additional bearing surface with the cup at lower inclination angle which aids in the resistance of the separation due to medial-lateral force from the component translational mismatch.....	100
Figure 3-31. Mean wear rate ($\pm 95\%$ CI, n=6) of 36 mm ceramic-on-ceramic (BIOLOX [®] delta) bearings against the mean dynamic separation ($\pm 95\%$ CI, n=3) under 2, 3 and 4 mm translational mismatch conditions with a cup inclination angle conditions of 45° and 65°.....	101
Figure 3-32. Mean wear rate ($\pm 95\%$ CI, n=6) of 36 mm ceramic-on-ceramic (BIOLOX [®] delta) bearings against the maximum force under edge loading ($\pm 95\%$ CI, n=3) under 2, 3 and 4 mm translational mismatch conditions with a cup inclination angle conditions of 45° and 65°.....	101

Figure 3-33. Mean wear rate ($\pm 95\%$ CI, n=6) of 36 mm ceramic-on-ceramic (BIOLOX [®] delta) bearings against the severity of edge loading ($\pm 95\%$ CI, n=3) under 2, 3 and 4 mm translational mismatch conditions with a cup inclination angle conditions of 45° and 65°.	102
Figure 3-34. Mean wear rate ($\pm 95\%$ CI, n=6) of 36 mm ceramic-on-ceramic (BIOLOX [®] delta) bearings against the severity of edge loading ($\pm 95\%$ CI, n=6) under 2, 3 and 4 mm translational mismatch conditions with a cup inclination angle conditions of 45° and 65°.	103
Figure 3-35. Input (in black) and output (Stn #1, #2, #4 and #5') readings from the Leeds II Hip Joint Simulator during the wear study under a 3 mm translational mismatch and 65° inclination angle condition.	111
Figure 4-1. Schematic of the input translational mismatch between the centre of the head and the centre of the cup in the Hip Joint Simulator.	117
Figure 4-2. Mean (n=3, $\pm 95\%$ CI) dynamic separation for 36 mm ceramic-on-ceramic (BIOLOX [®] delta) bearings under 1, 2, 3 and 4 mm translational mismatch conditions (A, B, C and D respectively) with a cup inclination angle of 45°, 55° and 65°.	119
Figure 4-3. Schematic of Separation Ratio (SR) versus the dynamic separation.	121
Figure 4-4. Schematic of Separation Threshold (ST) versus the dynamic separation.	122
Figure 4-5. Dynamic separation against separation ratio for 1, 2, 3 and 4 mm translational mismatches grouped per inclination angle of 45° (green), 55° (blue) and 65° (red) for different swing phase loads conditions.	123
Figure 4-6. Dynamic separation against separation threshold for 1, 2, 3 and 4 mm translational mismatches grouped per inclination angle of 45° (green), 55° (blue) and 65° (red) for different swing phase loads conditions.	123
Figure 4-7. Schematic for the type of edge loading and the variables affecting it.	124
Figure 4-8. Mean (n=3, $\pm 95\%$ CI) severity of edge loading for 36 mm ceramic-on-ceramic (BIOLOX [®] delta) bearings under 1, 2, 3 and 4 mm translational mismatch conditions (A, B, C and D respectively) with a cup inclination angle of 45°, 55° and 65° for different swing phase load conditions.	126
Figure 4-9. Mean (n=6, $\pm 95\%$ CI) maximum force under edge loading for 36 mm ceramic-on-ceramic (BIOLOX [®] delta) bearings under 4 mm translational mismatch conditions with a cup inclination angle of 65° for three swing phase loads (70, 150 and 300 N).	128
Figure 4-10. Mean (n=6, $\pm 95\%$ CI) severity of edge loading for 36 mm ceramic-on-ceramic (BIOLOX [®] delta) bearings under 4 mm translational mismatch conditions with a cup inclination angle of 65° for three swing phase loads (70, 150 and 300 N).	129
Figure 4-11. Schematic of the 4 mm translational mismatch input on the Hip Simulator.	130
Figure 4-12. Average displacement of the cup holder ($\pm 95\%$ CI) for 65° inclination angles under a 4 mm translational mismatch and 150 N swing phase load.	132
Figure 4-13. Individual volumetric wear under 4 mm translational mismatch for 65° cup inclination angle and 150 N swing phase load. Stn = Station.	133

Figure 4-14. Individual volumetric wear under 4 mm translational mismatch for 65° cup inclination angle and 300 N swing phase load. Stn = Station. 133

Figure 4-15 Mean (n=6, ±95% CI) wear rates for 150 and 300 N swing phase load under a 4 mm translational mismatch and 65° inclination angle. 134

Figure 4-16. Visualisation of surface of the heads under a 4 mm translational mismatch and 150 N swing phase load via RedLux software at the end of the wear test. The maximum depth of the scar is aligned to each head accordingly. 134

Figure 4-17. Visualisation of the heads under a 4 mm translational mismatch and 300 N swing phase load via RedLux software after 3 million cycles. The maximum depth of the scar is aligned to each head accordingly. 135

Figure 4-18. Mean (n=6, ±95% CI) maximum scar penetration after 3 million cycles under 50 and 300 N swing phase loads and a 4 mm translational mismatch condition with a 65° cup inclination angle. 135

Figure 4-19. Mean (n=6, ±95% CI) surface roughness (Ra) for head samples post-test at the pole 'P1 (tested)', and the wear scar 'P2 (tested)' under 4 mm translational mismatch and 65° cup inclination angle for 150 and 300 N swing phase load compared against the pre-test 'P1-P3 (unworn)'. 136

Figure 4-20. Mean (n=3, ±95% CI) dynamic separation for 36 mm ceramic-on-ceramic (BIOLOX® delta) bearings under variations in translational mismatch and cup inclination angle for a 150 N swing phase load conditions. 138

Figure 4-21. Mean (n=3, ±95% CI) dynamic separation for 36 mm ceramic-on-ceramic (BIOLOX® delta) bearings under variations in translational mismatch and cup inclination angle for a 300 N swing phase load conditions. 138

Figure 4-22. Mean (n=3, ±95% CI) dynamic separation for 36 mm ceramic-on-ceramic (BIOLOX® delta) bearings under 1, 2, 3 and 4 mm translational mismatch with a cup inclination angle of 65° for three swing phase load conditions (70, 150 and 300 N). 139

Figure 4-23. Mean (n=6, ±95% CI) wear rate for 36 mm ceramic-on-ceramic (BIOLOX® delta) bearings under 4 mm translational mismatch with a cup inclination angle of 65° and three swing phase loads (70, 150 and 300 N) conditions. 141

Figure 4-24. Mean (n=3, ±95% CI) dynamic separation against mean (n=6, ±95% CI) wear rate for 36 mm ceramic-on-ceramic (BIOLOX® delta) bearings under 2, 3 and 4 mm translational mismatches with a cup inclination angle of 45° and 65° under 70 N swing phase load (black circles), and 150 N (red square) and 300 N (red diamond) swing phase loads under a 4 mm translational mismatch and 65° cup inclination angle. 142

Figure 4-25. Mean (n=6, ±95% CI) severity of edge loading against mean (n=6, ±95% CI) wear rate for 36 mm ceramic-on-ceramic (BIOLOX® delta) bearings under 4 mm translational mismatch with a cup inclination angle of 65° for 70 (circle), 150 (square) and 300 (diamond) swing phase loads. 143

Figure 4-26. Mean (n=6, ±95% CI) severity of edge loading against mean (n=6, ±95% CI) wear rate for 36 mm ceramic-on-ceramic (BIOLOX® delta) bearings under 2, 3 and 4 mm translational mismatches with a cup inclination angle of 45° and 65° under 70 N swing phase

load (black circles), and 150 N (red square) and 300 N (red diamond) swing phase loads under a 4 mm translational mismatch and 65° cup inclination angle.....	143
Figure 4-27. Mean (n=6, ±95% CI) severity of edge loading against mean (n=6, ±95% CI) wear rate for 36 mm ceramic-on-ceramic (BIOLOX® delta) bearings adapted from Figure 4-26 were the 150 N swing phase load under a 4 mm translational mismatch with a cup inclination angle of 65° is split with interrupted relocation (red '+') and with-out interrupted relocation (red 'x'). All other conditions from Figure 4-26 remain the same (black circles).....	147
Figure 4-28. Input (black) for a 300 N swing phase load, and outputs for a 50 N swing phase load (orange) and 300 N swing phase load (blue) readings from the Leeds II Hip Joint Simulator during wear study under a 4 mm translational mismatch and a 65° inclination angle condition.	151
Figure 5-1. Schematic of the input translational mismatch applied with a spring between the centre of the head and the centre of the cup in the Hip Joint Simulator while no load is applied.	157
Figure 5-2. Mean (n=3, ±95% CI) dynamic separation for 36 mm ceramic-on-ceramic (BIOLOX® delta) bearings under 1, 2, 3 and 4 mm translational mismatch conditions (A, B, C and D respectively) with a cup inclination angle of 45°, 55° and 65° and a spring stiffness of 50 N/mm.	159
Figure 5-3. Mean (n=3, ±95% CI) severity of edge loading for 36 mm ceramic-on-ceramic (BIOLOX® delta) bearings under 1, 2, 3 and 4 mm translational mismatch conditions (A, B, C and D respectively) with a cup inclination angle of 45°, 55° and 65°, different swing phase loads and a spring stiffness of 50 N/mm.....	161
Figure 5-4. Mean (n=3, ±95% CI) dynamic separation for 36 mm ceramic-on-ceramic (BIOLOX® delta) bearings under 1, 2, 3 and 4 mm translational mismatch conditions (A, B, C and D respectively) with a cup inclination angle of 45°, 55° and 65°, different swing phase loads and a spring stiffness of 100 N/mm.....	163
Figure 5-5. Mean (n=3, ±95% CI) severity of edge loading for 36 mm ceramic-on-ceramic (BIOLOX® delta) bearings under 1, 2, 3 and 4 mm translational mismatch conditions (A, B, C and D respectively) with a cup inclination angle of 45°, 55° and 65°, different swing phase loads and a spring stiffness of 100 N/mm.....	164
Figure 5-6. Mean (n=3, ±95% CI) dynamic separation for 36 mm ceramic-on-ceramic (BIOLOX® delta) bearings under 1, 2, 3 and 4 mm translational mismatch conditions (A, B, C and D respectively) with a cup inclination angle of 45°, 55° and 65°, different swing phase loads and a spring stiffness of 200 N/mm.....	166
Figure 5-7. Mean (n=3, ±95% CI) severity of edge loading for 36 mm ceramic-on-ceramic (BIOLOX® delta) bearings under 1, 2, 3 and 4 mm translational mismatch conditions (A, B, C and D respectively) with a cup inclination angle of 45°, 55° and 65°, different swing phase loads and a spring stiffness of 200 N/mm.....	169
Figure 5-8. Dynamic separation against separation ratio for 1, 2, 3 and 4 mm translational mismatches grouped per inclination angle of 45° (green), 55° (blue) and 65° (red) for different swing phase loads conditions with a spring constant of 50 N/mm.	171

Figure 5-9. Dynamic separation against separation ratio for 1, 2, 3 and 4 mm translational mismatches grouped per inclination angle of 45° (green), 55° (blue) and 65° (red) for different swing phase loads conditions with a spring constant of 100 N/mm.	171
Figure 5-10. Dynamic separation against separation ratio for 1, 2, 3 and 4 mm translational mismatches grouped per inclination angle of 45° (green), 55° (blue) and 65° (red) for different swing phase loads conditions with a spring constant of 200 N/mm.	171
Figure 5-11. Separation threshold against dynamic separation for 1, 2, 3 and 4 mm translational mismatches grouped per inclination angle of 45° (green), 55° (blue) and 65° (red) for different swing phase loads conditions with a spring constant of 50 N/mm.	172
Figure 5-12. Separation threshold against dynamic separation for 1, 2, 3 and 4 mm translational mismatches grouped per inclination angle of 45° (green), 55° (blue) and 65° (red) for different swing phase loads conditions with a spring constant of 100 N/mm.	172
Figure 5-13. Separation threshold against dynamic separation for 1, 2, 3 and 4 mm translational mismatches grouped per inclination angle of 45° (green), 55° (blue) and 65° (red) for different swing phase loads conditions with a spring constant of 200 N/mm.	172
Figure 5-14. Schematic for the type of edge loading observed from the variables considered for testing.	173
Figure 5-15. Mean (n=6, ±95% CI) maximum force under edge loading for 36 mm ceramic-on-ceramic (BIOLOX® delta) bearings under 4 mm translational mismatch conditions with a cup inclination angle of 65° for two spring constants (50, 100 and 200 N/mm).	175
Figure 5-16. Mean (n=6, ±95% CI) severity of edge loading for 36 mm ceramic-on-ceramic (BIOLOX® delta) bearings under 4 mm translational mismatch conditions with a cup inclination angle of 65° for three spring constants (50, 100 and 200 N/mm).	176
Figure 5-17. Schematic of the 4 mm translational mismatch input in the Hip Simulator.	177
Figure 5-18. Average displacement of the cup holder (±CV) for 65° inclination angle under a 4 mm translational mismatch with a 70 N swing phase load and 50 N/mm spring constant.	179
Figure 5-19. Average displacement of the cup holder (±CV) for 65° inclination angle under a 4 mm translational mismatch with a 70 N swing phase load and 200 N/mm spring constant. ...	180
Figure 5-20. Individual volumetric wear under a 4 mm translational mismatch for 65° cup inclination angle with a 70 N swing phase load and 50 N/mm spring constant. Stn = Station.	180
Figure 5-21. Individual volumetric wear under a 4 mm translational mismatch for 65° cup inclination angle with a 70 N swing phase load and a 200 N/mm spring constant. Stn = Station.	181
Figure 5-22 Mean (n=6, ±95% CI) wear rates for 50 and 200 N/mm spring constant under a 4 mm translational mismatch and 65° inclination angles with a 70 N swing phase load.	181
Figure 5-23. Visualisation of the heads under a 4 mm translational mismatch and 50 N/mm spring constant via RedLux software at the end of the wear test. The maximum depth of the scar is aligned to each head accordingly.	182

- Figure 5-24. Visualisation of the heads under a 4 mm translational mismatch and 200 N/mm spring constant via RedLux software at the end of the wear test. The maximum depth of the scar is aligned to each head accordingly..... 182
- Figure 5-25. Mean (n=6, $\pm 95\%$ CI) maximum scar penetration after 3 million cycles under 50 and 200 N/mm spring constant and a 4 mm translational mismatch condition with a 65° cup inclination angle and a 70 N swing phase load..... 183
- Figure 5-26. Mean (n=6, $\pm 95\%$ CI) surface roughness (Ra) for head samples post-test at the pole 'P1 (tested)', and the wear scar 'P2 (tested)' under 4 mm translational mismatch with a 65° cup inclination angle and a 70 N swing phase load for 50 and 200 N/mm spring constant. 184
- Figure 5-27. Mean (n=3, $\pm 95\%$ CI) dynamic separation of 36 mm ceramic-on-ceramic (BIOLOX® delta) bearings under 1, 2, 3 and 4 mm translational mismatch conditions for three cup inclination angle conditions, 45°, 55° and 65° for a 70 N swing phase load and a 50 N/mm spring constant. 186
- Figure 5-28. Mean (n=3, $\pm 95\%$ CI) dynamic separation of 36 mm ceramic-on-ceramic (BIOLOX® delta) bearings under 1, 2, 3 and 4 mm translational mismatch conditions for three cup inclination angle conditions, 45°, 55° and 65° for a 70 N swing phase load and a 100 N/mm spring constant. 186
- Figure 5-29. Mean (n=3, $\pm 95\%$ CI) dynamic separation of 36 mm ceramic-on-ceramic (BIOLOX® delta) bearings under 1, 2, 3 and 4 mm translational mismatch conditions for three cup inclination angle conditions, 45°, 55° and 65° for a 70 N swing phase load and a 200 N/mm spring constant. 186
- Figure 5-30. Mean (n=3, $\pm 95\%$ CI) dynamic separation for 36 mm ceramic-on-ceramic (BIOLOX® delta) bearings under a 4 mm translational mismatch with a cup inclination angle of 65° and a swing phase load of 70 N for three spring constants (50, 100 and 200 N/mm) conditions..... 187
- Figure 5-31. Mean (n=6, $\pm 95\%$ CI) wear rates 36 mm ceramic-on-ceramic (BIOLOX® delta) bearings under a 4 mm translational mismatch with a cup inclination angle of 65° for three spring constants (50, 100 and 200 N/mm) conditions. 188
- Figure 5-32. Mean (n=3, $\pm 95\%$ CI) dynamic separation against mean (n=6, $\pm 95\%$ CI) wear rate for 36 mm ceramic-on-ceramic (BIOLOX® delta) bearings under 100 N/mm spring constant with a 2, 3 and 4 mm translational mismatches with a cup inclination angle of 45° and 65° under 70 N swing phase load, and 4 mm translational mismatch with a cup inclination angle of 65° under 150 and 300 N (black circles), and 50 N/mm (red triangle) and 200 N/mm (red square) spring constants under a 4 mm translational mismatch and 65° cup inclination angle. 189
- Figure 5-33. Mean (n=6, $\pm 95\%$ CI) severity of edge loading against mean (n=6, $\pm 95\%$ CI) wear rate for 36 mm ceramic-on-ceramic (BIOLOX® delta) bearings under 100 N/mm spring constant with a 2, 3 and 4 mm translational mismatch with a cup inclination angle of 45° and 65° under 70 N swing phase load, and 4 mm translational mismatch with a cup inclination angle of 65° under 150 and 300 N (black circles), and 50 N/mm (red circle) and 200 N/mm (red triangle) spring constants under a 4 mm translational mismatch and 65° cup inclination angle..... 190

Figure 5-34. Schematic to describe the overall effect between the dynamic separation and separation ratio relationship for different spring constants and different input conditions...	191
Figure 5-35. Schematic to describe the overall effect between the dynamic separation and separation threshold relationship for different spring constants and different input conditions.	192
Figure 5-36. Mean (n=6, $\pm 95\%$ CI) severity of edge loading against mean (n=6, $\pm 95\%$ CI) wear rate for 36 mm ceramic-on-ceramic (BIOLOX® delta) bearings adapted from Figure 5-33 were the 50 N/mm spring constant under a 4 mm translational mismatch, a cup inclination angle of 65° with a swing phase load of 70 N is split with interrupted relocation (red '+') and with-out interrupted relocation (red 'x'). All other conditions from Figure 5-33 remain the same (black circles).	193
Figure 6-1. Schematic demonstrating a higher dynamic separation under the same translational mismatch for a low (A) and high (B) cup inclination angle.....	196
Figure 6-2. Schematic demonstrating dynamic separation occurring during the swing phase load of the walking cycle, leading to edge loading conditions in the hip joint simulator.	197
Figure 6-3. Mean (n=6, $\pm 95\%$ CI) severity of edge loading against mean (n=6, $\pm 95\%$ CI) wear rate for 36 mm ceramic-on-ceramic (BIOLOX® delta) bearings under different translational mismatches (2, 3 and 4 mm) for different cup inclination angles (45° and 65°) under 100 N/mm spring constant along with two different swing phase load (150 and 300 N) conditions (tested under 4 mm, 65° and 100 N/mm), and two different spring constants (50 and 200 N/mm) conditions (tested under 4 mm, 65° and 70 N).	198
Figure 9-1. Load vs displacement curve for a 100 N/mm spring tested under a 1 mm/min compressive load.	219
Figure 9-2. Distance required to grip the 50 N/mm spring constant before the active coils respond to the appropriate spring stiffness for the 6 stations of the Leeds II Hip Joint Simulator.	220
Figure 9-3. Distance required to grip the 100 N/mm spring constant before the active coils respond to the appropriate spring stiffness for the 6 stations of the Leeds II Hip Joint Simulator.	220
Figure 9-4. Distance required to grip the 200 N/mm spring constant before the active coils respond to the appropriate spring stiffness for the 6 stations of the Leeds II Hip Joint Simulator.	221
Figure 9-5. Schematic of the cup holder and the positions where the LVDTs were placed in the Leeds Mark II Hip Joint Simulator to measure the displacement of the cup centre relative to the head centre.	222
Figure 9-6. Mean (n=3, $\pm SD$) defined centre assembly point for different translational mismatches (1, 2, 3 and 4 mm) and different cup inclination angles (45°, 55° and 65°) for the 100 N/mm spring constant.	223
Figure 9-7. Mean (n=3, $\pm SD$) defined centre assembly point for different translational mismatches (1, 2, 3 and 4 mm) for the 65° cup inclination angle for the 50, 100 and 200 N/mm spring constant.	224

List of tables

Table 1-1. Muscles of the hip joint and their function group	3
Table 1-2. Range of motion of the hip joint	4
Table 1-3. Nominal range of motion from total hip replacement gait studies	31
Table 1-4. <i>In vitro</i> wear of MoM joint replacement with increased head size	37
Table 1-5. Wear of MoM joint replacement with increased clearance <i>in vitro</i>	39
Table 1-6. Comparison of material properties for metal and ceramic THR bearings	42
Table 1-7. Matrix of hip simulator test conditions	48
Table 2-1. Properties of BIOLOX® delta adapted from the scientific information and performance data, CeramTec (2014)	50
Table 3-1. Details of the biomechanical study for the evaluation of the medial-lateral component translational mismatch in a hip joint simulator.	73
Table 3-2. Two-way ANOVA with Tukey analysis for the dynamic separation under a 1, 2, 3 and 4 mm translational mismatch and 45°, 55° and 65° cup inclination angle for n = 3.	75
Table 3-3. Two-way ANOVA with Tukey analysis for the maximum force during edge loading under a 1, 2, 3 and 4 mm translational mismatch and 45°, 55° and 65° cup inclination angle for n = 3.	76
Table 3-4. Two-way ANOVA with Tukey analysis for the severity of edge loading under a 1, 2, 3 and 4 mm translational mismatch and 45°, 55° and 65° cup inclination angle for n = 3.	80
Table 3-5. Details of the biomechanical study for the evaluation of the severity of edge loading under selective medial-lateral component translational mismatch conditions.	82
Table 3-6. Details of the medial-lateral component translational mismatch wear study under 2, 3 and 4 mm.	85
Table 4-1. Details of the biomechanical study for the evaluation of different swing phase loads under a translational mismatch in a hip joint simulator	117
Table 4-2. Details of the biomechanical study for the evaluation of the severity of edge loading for selective swing phase load conditions under a translational mismatch	127
Table 4-3. Details of the swing phase load wear study under a translational mismatch.	131
Table 5-1. Details of the biomechanical study for the evaluation of different spring constants under a translational mismatch in a hip joint simulator	157
Table 5-2. Details of the biomechanical study for the evaluation of the severity of edge loading for selective spring constants under a translational mismatch	174
Table 5-3. Details of the spring constant wear study under a translational mismatch	178
Table 9-1. Details of the study to define the centre assembly point of the head and the cup under a translational mismatch condition to replicate edge loading	223

1. Introduction

1.1. The natural adult hip joint

1.1.1. Anatomy

The hip joint is essentially a combination of bone and soft tissue that allows movement. It can be classified as a simple model consisting of the femoral head and the acetabulum. This configuration is categorised as an enarthrosis (ball and socket) type of joint. Unlike other ball and socket joints, the hip joint has intrinsic stability (Frankel and Nordin, 1980).

The femoral head is relatively convex in shape (Figure 1-1, a), and it articulates against a relative hemispherical shaped acetabulum (Figure 1-1, b). The acetabulum is deepened by the labrum, but on its own only allows for about 170° coverage of the femoral head (Wasielowski, 2007). Muscles surround the outskirts of the acetabulum on all sides. The angle between the femoral neck and the longitudinal axis of the femur is about 125° in the adult hip. After infancy the neck of the hip decreases from a high angle of approximately 145° (Wasielowski, 2007). However, an adult hip neck angle can vary from 90-135° (Frankel and Nordin, 1980). A deviation from these angles is considered a medical condition; a low angle is termed coxa vara, while a high angle is termed coxa valga. The femoral anteversion is approximately 14° (Wasielowski, 2007). Similarly, this angle gradually decreases from birth to adult development (Wasielowski, 2007).

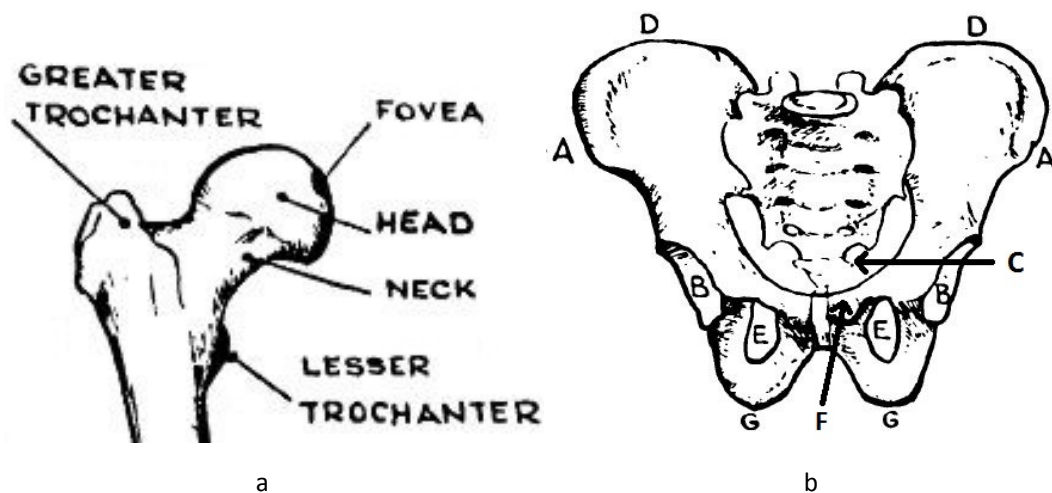


Figure 1-1. Anterior view of the top section of the right femur (a), anterior view of pelvis (b) indicating A) anterior posterior iliac spine, B) acetabulum, C) coccyx, D) iliac spine, E) obturator foramen, F) ischial tuberosity, and G) ischial tuberosity (adapted from p. 5 and p. 7, Paul 1967).

Ligaments:

The ligaments are a cluster of fibres that are attached to two different bone points and provide restraint depending on the rotation, as they are taut (van Arkel *et al.*, 2015). Three segmented ligaments reinforce the hip joint capsule; the iliofemoral, the pubofemoral and the ischiofemoral (Figure 1-2). These also serve as a mechanism for muscular feedback and pain (Wasielowski, 2007).

The ligamentum teres and the iliofemoral ligaments maintain stability at extreme rotations of the hip joint (Buechel and Pappas, 2012). The teres is joined between the acetabular capsule and the femoral head (near the polar region in an area called the fovea, Figure 1-1). The iliofemoral surrounds the femoral head anteriorly and laterally (Figure 1-2, A). This ligament is connected between the outskirts of the acetabulum (Anterior Inferior Iliac Spine (AIIS) and the iliopectineal eminence) and the end section of the neck of the femur between the greater trochanter and the lesser trochanter, called the intertrochanter line (Wasielowski, 2007). The iliofemoral ligaments are especially strong as they support much of the body's stability when standing. They limit hyperextension and lateral rotation and during extension they force the head into the acetabulum (Wasielowski, 2007). The pubofemoral ligaments are located in the inferior part of the acetabular capsule, joining the pubic region of the acetabular rim and the inferior-most of the iliofemoral ligament (Figure 1-2, A). Both, the iliofemoral and pubofemoral reinforce the anterior portion of the hip joint capsule (Wasielowski, 2007). Posteriorly, the capsule is reinforced by the ischiofemoral ligament (Figure 1-2, B). It joins the ischial section of the acetabular rim and partial fibres attach to the inner surface of the greater trochanter (Wasielowski, 2007).

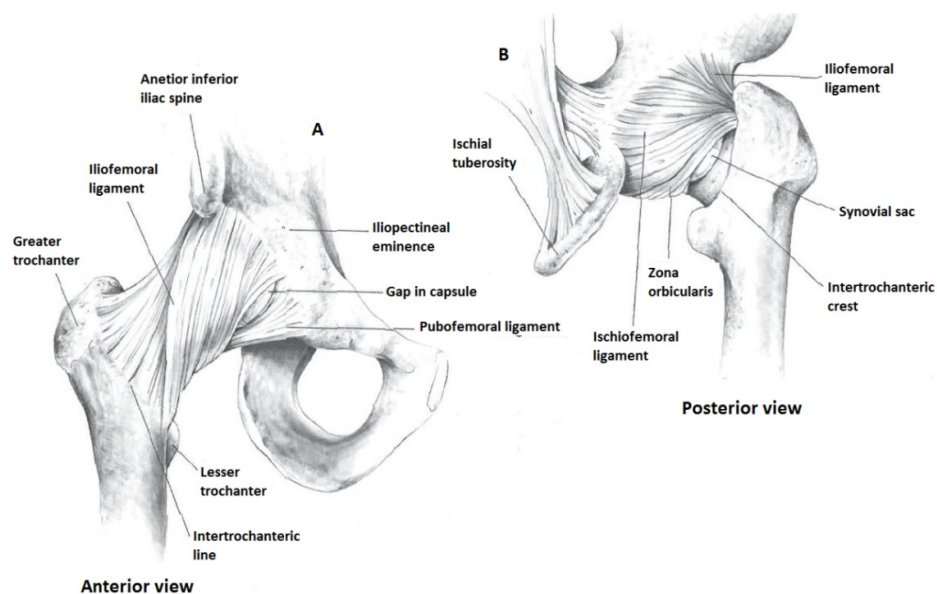


Figure 1-2. Outer ligaments surrounding the hip joint (A) anterior view and (B) posterior view (adapted from p. 54, Wasielowski 2007).

Muscles:

The muscles are bundles of tissue that provide movement. The hip joint is surrounded by many muscles (Table 1-1) which allow a large range of motion. Mainly, these muscles are connected from the pelvis to the femur, however the psoas are connected to the vertebral column (TH12, L1 and L2) instead of the pelvis. The extension is generated by the gluteus maximus, and the flexion is mainly provided by the iliacus and psoas major (Buechel and Pappas, 2012), formally known as the combination muscles “iliopsoas”. The adduction is generated by the adductor brevis, longus and magnus, while the abduction is mainly generated by the gluteus medius and minimus (Buechel and Pappas, 2012).

Table 1-1. Muscles of the hip joint and their function group

Muscle	Muscle group
Iliopsoas (Psaos major and Iliacus)	Flexor , External rotator
Rectus femoris	Flexor
Pectineus	Flexor , Adductor, Internal rotator
Gluteus maximus	Extensor , Flexor
Semimembranosus	Extensor , Internal rotator
Semitendinosus	Extensor , Internal rotator
Biceps femoris	Extensor
Adductor magnus	Extensor , Adductor , Internal rotator
Adductor brevis	Adductor
Adductor longus	Adductor
Tensor fascia lata	Abductor , Flexor, Internal rotator
Gracilis	Adductor
Obturator externus	Adductor
Hamstrings	Adductor
Gluteus minimus	Abductor , Internal rotator
Gluteus medius	Abductor , Internal rotator
Sartorius	Abductor
Quadratus femoris	External rotator
Piriformis	External rotator
Superior gemellus	External rotator
Inferior gemellus	External rotator
Obturator internus	External rotator

Bold signifies major contribution to muscle action

Articulating structures:

The surface structure of the natural hip joint which is articulating (femoral head and acetabulum), is a damped tissue called the articular cartilage. The head is completely covered with cartilage except for a small region in the fovea. Cartilage has a water phase of 65-80% (Amadò *et al.*, 1976) which provides low friction and resistance to wear. Due to the matrix mixture of tissue and fluid, and its time dependent properties, it is considered poro-elastic like many other tissues in the body. At a mature age, the thickening of the bone cuts off the blood

supply. Without the blood supply, cartilage can bear loading without developing any inflammation.

1.1.2. Biomechanics

The range of motion of the hip joint (Frankel and Nordin, 1980) is shown in Table 1-2. Flexion has the largest degree of motion. Not all motions can be carried out at one time, e.g. less rotation can be achieved when the hip is extended due to the constrictions of the soft tissue around the joint (Frankel and Nordin, 1980).

Table 1-2. Range of motion of the hip joint

Action	Flexion	Extension	Abduction	Adduction	Internal Rotation	External Rotation
Range of motion	0° to 140°	0° to 15°	0° to 30°	0° to 25°	0° to 90°	0° to 70°

Walking gait cycle:

The hip joint is designed to withstand the forces exerted by the body. During the walking cycle these tend to be three to five times the body weight in the vertical axis. The maximum force is typically observed by a double peak at two intervals, heel strike and toe off (Figure 1-3). The vertical forces are approximately 1400 N (or twice body weight), while the medial-lateral force are approximately 700 N (Crowninshield *et al.*, 1978). Individuals may have a distinct range of motion while walking, however it generally conforms within the following range; 30° flexion up to 15° extension, 5° abduction up to 5° adduction and 5° of internal rotation up to 5° external rotation. During the walking cycle, the flexion can reach a maximum motion of about 35°-40° at the end of the swing phase just before heel strike (Frankel and Nordin, 1980).

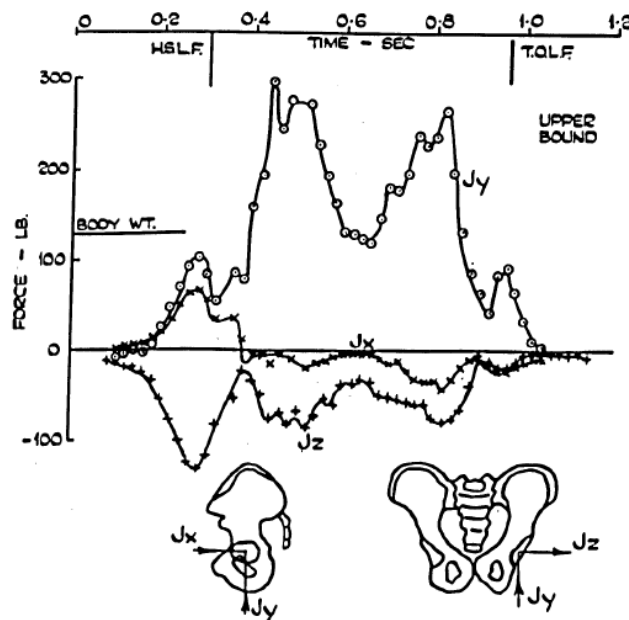


Figure 1-3. Variation with time of the components of the upper bounds of the hip joint force (adapted from p. 202, Paul 1967). Heel strike left foot (HSLF), toe off left foot (TOLF). LB stands for pounds.

1.1.3. Synovial fluid

The lubricant within the hip joint capsule is called the synovial fluid. It consists of water, plasma proteins, hyaluronic acid (polysaccharide) and other substances. This fluid keeps the cartilage damp, and provides the nutrients to the chondrocytes which are cells that are dispersed within the cartilage. After the formation of the subchondral plate, this fluid is the only supply of nutrients which maintains the cartilage in a healthy condition. The change in pressure due to loading and unloading causes the fluid to enter in (negative pressure) and out (positive pressure) of the joint cavity. The synovium (like egg white) is the surrounding tissue that produces and maintains the synovial fluid. The labrum peripheral tissue, consisting of fibro-cartilage, helps to seal and maintain the synovial fluid around the joint capsule (Buechel and Pappas, 2012).

The synovial fluid is considered viscous-elastic (Unsworth *et al.*, 1975, O'Kelly *et al.*, 1978, (Dowson *et al.*, 1967). It is very viscous due to the hyaluronan (acid content), and the content level plays a role on its viscosity. Since the viscosity can also decrease with increasing shear rate (shear thinning), it is appropriately defined as pseudo-plastic. However, for shear thinning to occur on the synovial fluid, a high pressure of up to 100 MPa are required to change its viscosity (Jin *et al.*, 1997).

1.1.4. Joint degeneration

Joint degeneration can occur via many pathways, but the terminology is sometimes interpreted as osteoarthritis. There are many types of articular disorders but in terms of the pathology, the hip can be categorised into six; where the first three tend to be treated without a joint replacement (Buechel and Pappas, 2012).

1. Congenital; incomplete or poor embryonic development.
2. Neuromuscular; problems associated with gait and stability due to diseases on the nerves and muscles.
3. Infectious; bacteria affecting the hip joint.
4. Autoimmune; self-host destruction leading to articular disorders.

Evidence suggests there is a genetic characteristic relating osteoarthritis to an autoimmune phenomenon (Buechel and Pappas, 2012). Joint narrowing is a very common characteristic of presence of osteoarthritis. In this particular type, the gap between the femoral head and acetabulum narrows such that bone to bone contact occurs. This leads to pain and reduction of motion. The gap or cartilage tissue breaks down by an enzymatic, chemical or by a mechanical pathway (Armfield and Towers,

2007). There are two types of osteoarthritis, primary (or idiopathic) and secondary. Secondary types are followed after a primary type.

In rheumatoid arthritis, articular cartilage damage also occurs but due to the increase in synovial fluid and thickening of the joint capsule. The body attempts to neutralize the situation, but instead it destroys the cartilage structure.

5. Metabolic; deficiencies in the bones or ligaments;

Another articular disorder is avascular necrosis (or ischemic bone necrosis) which develops from a lack of blood supply to the bone. Early in the disease, it affects cellular but not crystalline elements, this later turns into detectable difference in bone density (Armfield and Towers, 2007).

6. Post-traumatic

Other causes for joint replacement could originate from trauma, such as fracture, dislocation or femoroacetabular impingement.

1.2. Hip joint prostheses

1.2.1. Articulating materials

When an arthroplasty (Arth(o)- related to the joint, and -plasty from Greek meaning “to form”) is necessary, this requires a surgical intervention, and in the case of total joint reconstruction, non-biological components are implanted to replace the articulating surfaces. Typical joint replacements are based on a metallic stem to hold a femoral component, which articulates against an acetabular cup (Figure 1-4). In order to restore the function of an articulating joint, one must understand the concept on which it works and the mechanisms which holds the system together. One of the important features of prostheses is that the materials used are biocompatible. In 1960's, John Charnley used low friction polymer components coupled with good fixation mechanisms using Polymethylmethacrylate (PMMA) which is known as bone cement (Charnley, 1961). This metal-on-polyethylene hip joint replacement has become very successful in the elderly (Callaghan, 2007). In the UK, 2010/11 figures suggested that approximately 90,000 hip procedures were performed, of which 10,000 were revisions (NICE, 2013). One of the drawbacks and limitations of prostheses is that they are not a living tissue and it does not remodel to the needs of the body like healthy bone does.

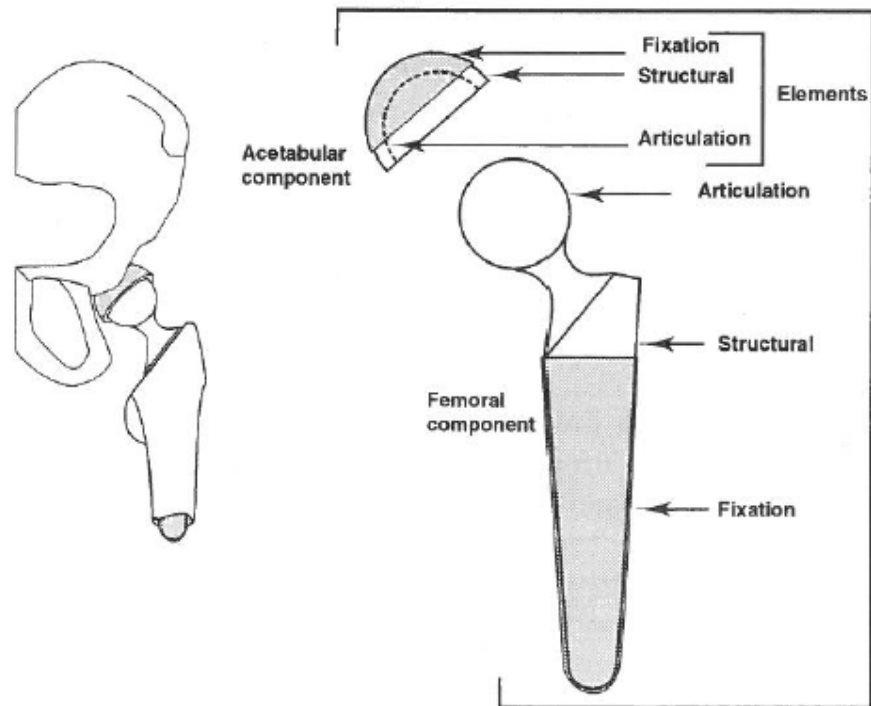


Figure 1-4. Generic total hip replacement device, showing components and elements (adapted from p.103, Black et al. 2007)

The articulating materials can be classified into hard-on-hard or hard-on-soft bearing couples. Hard-on-hard consists of two hard materials articulating against each other such as metal-on-metal, ceramic-on-ceramic and ceramic-on-metals whereas, a hard-on-soft bearings consist of a hard femoral head (ceramic or metal) articulating against a relatively softer material (Ultra High Molecular Weight Polyethylene, UHMWPE).

- Metal-on-Polyethylene (MoP)

In the late 1950's, John Charnley used a few polymers as acetabular components in combinations with a metal (stainless steel) femoral head (Charnley, 1961). Probably the most noteworthy polymer which he used was Polytetrafluoroethylene (PTFE). He initially chose this material for its low coefficient of friction which seemed appropriate for articulating components. However, PTFE had high wear rates and early failure occurred. Charnley then used UHMWPE for the acetabular cup articulating against a metal femoral head. The low-friction articulation has proved to be successful in elderly patients.

The UHMWPE currently used can have different levels of crosslinking and mode of sterilisation which influences its properties, and different design features such as; 1) thickness of the rim area and 2) the metal backing design which can influence the failure. Even though the effects of wear particles (discussed in Chapter 1.4) are well documented in the literature, this bearing combination is still a viable solution to restore hip joint function. To get a perspective of the

improvements since the 1950's and the confidence on the material, MoP designs are the most common bearing used in the United Kingdom (NICE, 2013).

- Ceramic-on-Polymer (CoP)

Ceramic on polymer operates on the same principle as a MoP. A hard femoral head articulates against a soft acetabular polymer. Since the wear of a polymer is related to the roughness of the counter-facing bearing (as discussed in Chapter 1.3), smooth surfaces are of importance for the joint replacement. Ceramics possess a great deal of resistance against scratching. For this reason, ceramics can be a good solution as an alternative to metal femoral heads which are more sensitive to scratching.

- Metal-on-Metal (MoM)

Overall, predominantly the metal alloys used for orthopaedic industry include cobalt-based and titanium-based. Stainless steel (MoM bearing couples) was utilized in the late 1920's (Gilbert, 2007). Cobalt (Co) and Chromium (Cr) are very good due to their hardness properties. It was later recognized that Molybdenum (Mo) had great properties to reduce pitting and corrosion. Currently, great interest exists in Co-Cr-Mo and Titanium ELI alloys (Ti-6Al-4V). When short and long term failures were linked to osteolysis due to Polyethylene particles, the interest of evaluating and testing of MoM re-emerged with the objective of using this bearing combination as an alternative to Polyethylene and a hard femoral head.

- Ceramic-on-ceramic (CoC)

Boutin (1971) introduced the first total hip replacement with the use of Alumina bearings in 1969. Since then, improvements were achieved in the late 1970's by reducing the grain size and better grain distribution and porosity of the Alumina (Boutin *et al.*, 1988). Zirconia was also developed as an articulating bearing in Total Hip Replacements (THR) (Rieger, 2001). A perceived disadvantage of ceramics is their susceptibility to fracture. However, current ceramics materials are made of mixed ceramics composites to maximize the properties such as fracture toughness. Modern ceramics are Hot Isostatically Pressed (HIPed) which reduces the size of the grains (Rieger, 2001). A CoC combination can offer a better lubrication regime as they have a higher wettability factor due to their hydrophilic (ionic) nature (Boutin *et al.*, 1988). Furthermore, due to their high hardness, ceramics can be polished to a higher degree than any other component available for joint prosthesis.

- Ceramic-on-Metal (CoM)

With the improvements generated on the manufacturing of the ceramics and metals, CoM can be coupled together. There are advantages from this combination due to the decrease of synergism from the combined adhesive and abrasive wear expected from MoM or CoC. The ceramic is hydrophilic, thus improving lubrication.

1.2.2. Design

1.2.3. Design considerations

The biomechanics and anatomy of the natural hip joint are key factors for designing the hip implants. The cup is intended to be implanted like the normal orientation of the acetabulum, at approximately 45° caudally and 15° anteriorly.

The designed features of modern hip components are developed on the basis that the femoral head will articulate within the inner surface of the acetabular cup. All designs and models (such as total hip replacement, bipolar, hip resurfacing, etc.) work on the principal concept that the load can be transmitted and motion is permitted while both components retain concentricity. These models are mostly designed on flawless anatomical parameters rather than the limitations from the surgical procedures and the inputs of adverse conditions.

The reasons which help generate low wear are the design features that promote the components to perform under mixed lubricated conditions. These features are high surface polish, high geometrical tolerances and good conformity. Due to the manufacturing process of the materials, it is easier to achieve all of these features on hard bearings. A ceramic component can be polished to a surface roughness (Ra) of approximately 0.001 µm and a metal to approximately 0.01 µm. The type of materials used is also a great factor to prevent low wear. Metals with high carbon content, ceramics with low grain size, and toughened polyethylene are preferred for low wear.

1.2.4. Head size

Large diameter bearings tend not to be used when articulating on polymers for several reasons. One of them is the concern of liner thickness with increasing bearing size. Additionally, larger head sizes equate to larger sliding distances and larger contact areas increase the polymer wear. Reducing the amount of material can induce high stresses on the liner and promote failure.

However, with metal-on-metal bearings, the wear rate decreases with increasing head size with well positioned prosthesis due to improved lubrication regimes (Silva *et al.*, 2005). Larger

bearings also reduce the rate of dislocation due to their conformity and increased jumping distance. The head and outer cup radius relationship is important to determine the frictional force at the acetabular fixation (Jin *et al.*, 2006).

1.2.5. Clearance

The space between the femoral head and acetabular cup is known as the clearance. For the purpose of consistency, when speaking about the clearance, it is referred to the diametral difference. Lower clearances will conform better due to the tight tolerances which keep the components close together without moving their matched centres of rotation substantially. Due to close conformity, the contact area is larger compared to a high clearance component. A high clearance couple will have a smaller contact area and higher contact stresses. Clearance has to be large enough to accommodate the variation in manufacturing dimensions.

1.2.6. Jumping distance

The jumping distance is the translation required for the head to migrate out of the cup, such that it is no longer in the adequate position and dislocation occurs. Due to the position and the geometry of the cup, there could be different jumping distances for different designs and head sizes.

1.2.7. Cup coverage

The cup coverage is the angular coverage provided by the design of the cup. On some designs, the cup coverage is decreased in order to increase the range of motion and avoid impingement of the neck against the rim of the cup.

1.3. Tribology

1.3.1. Contact mechanics

Contact in terms of tribology is defined by the real surfaces i.e. the contact of asperities. The contact mechanics between two surfaces is important as the geometry is an influential factor to consider. The basic interpretation of the hip prosthesis contact is defined by the articulating surfaces of the femoral head and the acetabular cup. In order to obtain a geometrical interpretation of this, the contact is dependent on the head diameter, and the cup diameter. With this information the equivalent radius can be calculated (Jin *et al.*, 2006).

1.3.2. Friction

Friction can be defined as the resistance of motion encountered by a load. For a joint replacement, one has to consider the coefficient of friction between the two interacting bodies. Even though the coefficient of friction between components is low, that is not an

indication of lower wear (McKellop *et al.*, 1981). A better understanding of the interaction of surfaces due to friction can be made via friction simulators. Brockett *et al.* (2007) demonstrated how the frictional factor for different coupled materials changes using newborn calf serum with different protein concentrations. The inverse relationship of protein concentration with hard bearings was demonstrated with MoM and CoC (Figure 1-5). The friction factor of CoC bearings decreases with decreasing the protein concentration in the serum. Thus, the lowest friction factor was obtained when water was used as a lubricant. However, the friction factor of MoM had the inverse relationship (Brockett *et al.*, 2007). Interestingly, the CoM couple behaved similarly as the CoC.

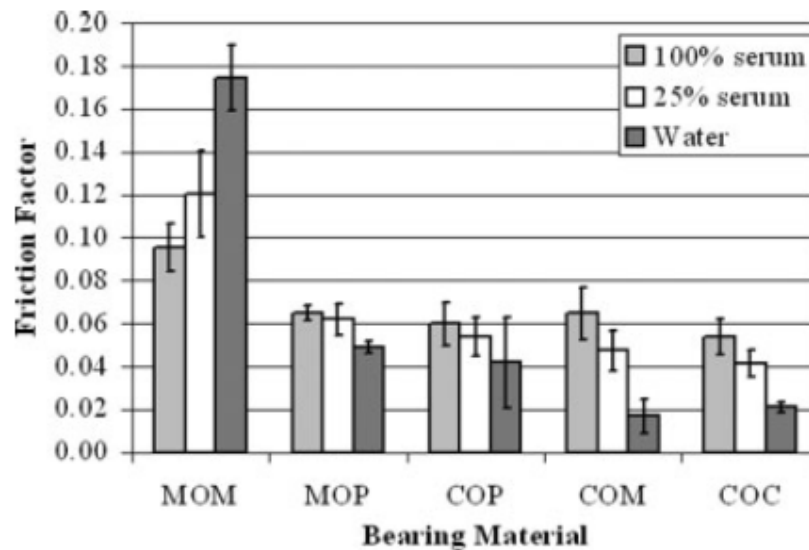


Figure 1-5. Effect of protein concentration upon friction factor, tested with 100 N swing phase load (Brockett *et al.*, 2007).

1.3.3. Lubrication

Lubrication is an effective mechanism to reduce friction and wear from two bodies which are in relative motion to each other (Hersey, 1935). In essence, the lubricant (solid, liquid or gas) separates the two surfaces. In order to understand the performance of the interfaces, a relationship is defined by the magnitude of the film thickness and roughness of the two surfaces (Johnson *et al.*, 1972). This is known as the specific film thickness or lambda ratio. With increasing specific film thickness, the interaction between the two surfaces decreases thus changing the lubrication regime. The lubrication regimes are defined by the lambda ratio as follows:

Fluid Film	$\Lambda > 3$
Mixed	$3 > \Lambda > 1$
Boundary	$1 > \Lambda$

Boundary lubrication is the point of high friction, where significant wear occurs due to the close interaction of the asperities. With the increase of the specific film thickness the coefficient of friction decreases, this area is known as mixed lubrication. Fluid film lubrication is when complete separation occurs and it is the point of lowest friction and wear. This work was originally carried out by Richard Stribeck in the 1900's. Stribeck's studies (such as 'Kugellager für beliebige Belastungen' and 'Die wesentlichen Eigenschaften der Gleit- und Rollenlager') of load and speed on sliding metal bearings demonstrated how there was high friction at low speeds, followed by the minimum friction when the bearing components were not in contact and finally increased in friction when the speed was increased (Jacobson, 2003).

This behaviour is normally plotted on a graph called the Stribeck diagram (Figure 1-6), where the use of dimensionless parameters such as the friction factor and Sommerfeld number (z) can be used to compare the effect on different variables (Jin *et al.*, 2006).

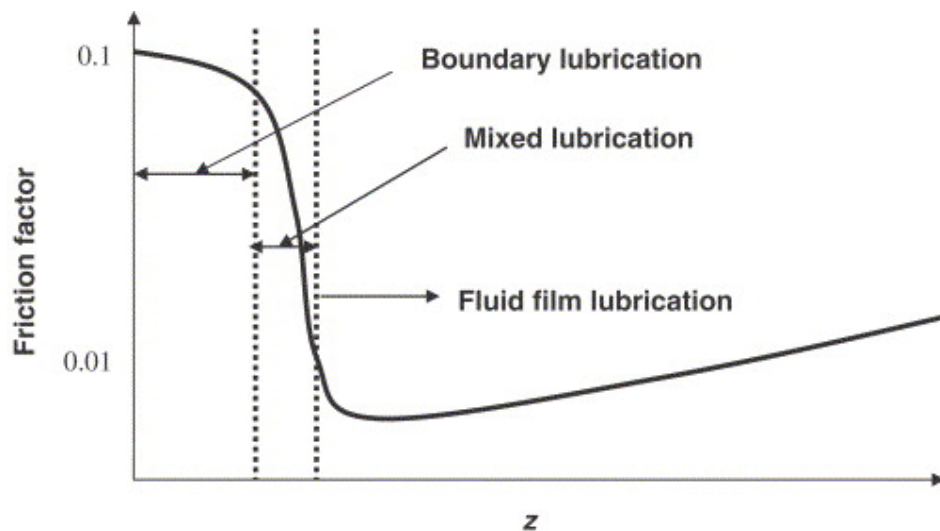


Figure 1-6. Stribeck diagram showing friction factor against Sommerfeld number and the lubrication regimens (Jin *et al.*, 2006).

1.3.4. Wear mechanisms

Wear can be defined as progressive damage, involving material loss or removal from the surface of a body due to a motion.

The wear mechanisms are distinguished by their mechanical, physical and chemical interaction, but all take into account the rough nature of the real surfaces and impact due to asperities. There are four major wear modes, adhesion, abrasion, surface fatigue and tribochemical reactions. However, these can occur in combination at one time, and lead to synergism.

- During adhesion, the real contact area of the asperities is very small, hence creating large pressure which make the asperities deform plastically. This can lead to a solid-phase welding, and transfer of material occurs from one surface to the other within the relative motion.
- Abrasion occurs when there is motion of materials with different local contacts and properties. The hard asperity penetrates the “softer” counter-face due to the load and removes the material (as “ploughing”) from the motion travelled. This type of mechanism not only can occur between two bodies, but also from third body particles present in the system. It can be detected by the track marks or grooves that appear on the surface.
- Surface fatigue is the mechanism where cyclic loading acts over a period of time. It can also occur in the absence of direct articulation between two surfaces. This type of wear mode is commonly observed as shallow pits.
- Tribochemical reactions occur when the surface of the material reacts with the environment it is in. With corrosive materials, an oxidation layer forms on the surface. In time this layer thickens and their products can be easily removed. This process repeats when the chemical reaction starts again.

In biomedical devices, wear can adversely alter the function of the device, and the wear particles can create adverse effects to the surrounding environment (Jin *et al.*, 2006).

1.4. Biological response to wear debris

A factor which still affects the longevity for the majority of the hip prosthesis is aseptic loosening. According to the report by NICE (2013), in the United Kingdom (UK), it is still the greatest factor influencing revision. Aseptic loosening leads to implant failure because the stability of the prosthesis is compromised. Thus, aseptic loosening is sometimes termed osteolysis due to the localized granulomatous reaction leading to revision (Armfield and Towers, 2007). However, the stability of the prosthesis should be evaluated to determine if it were caused by osteolysis.

The biological response is not necessarily the same for all the bearing material combinations.

- Polyethylene (PE) or Ultra High Molecular Weight Polyethylene (UHMWPE)

Histological examinations show that polyethylene particles are removed from the bearing surface due to abrasion and migrate to the pseudomembranes (Lerouge *et al.*, 1997). An example of the wear rate of a polymer *in vivo*, at ten years, was found to be 0.18 mm per year (Dowd *et al.*, 2000). Since UHMWPE is bio-inert, the system/organism is not able to deal with

the particulates, and end up diffusing around the joint (Elfick *et al.*, 2003). The macrophages which are present to degrade foreign material will start generating numerous cytokines and mediators (Ingham & Fisher 2000). In an *in vitro* study by Green *et al.* (1998), the polymer particles of 0.3 to 10 μm in size were found to induce cytokine activity more than other sizes. Furthermore, the discrete number of particles was found to influence the activity for different cytokines (Green *et al.*, 1998). The minimum wear rate of polyethylene which was correlated to osteolysis was found to be approximately 0.1 mm per year (Dowd *et al.*, 2000). Polyethylene debris larger than 5 to 10 μm has been found within giant cell (Lerouge *et al.*, 1997). The long term effects of this reaction causes bone resorption and compromises the stability of the prosthesis (Ingham & Fisher 2005).

- Metals

MoM articulation wear tend to generate smaller particles compared to MoP (Ingham & Fisher 2000). However, one has also to consider the number of particles. In the review by Ingham & Fisher (2000), metal particles sizes found *in vivo* can range from nano-meter size to hundreds of microns. Since the wear particles from MoM can be smaller, they can travel away from the periprosthetic tissue more easily. Furthermore, the accumulation of such small particles will have a greater surface area from which corrosion can occur (Ingham & Fisher 2000). Osteolysis due to metal debris does not seem to be of the same high level reported as polymer particles. However, there are linkages associated with the stimulation of macrophages (Ingham & Fisher 2000). Moreover, there are concerns to the changes to the tissue which are associated with the metal debris; such as pseudotumours, and cellular necrosis. In addition, patients may be hypersensitive to metal debris.

- Ceramics

The main concerns for previous ceramic-on-ceramic bearing designs were fractures. With recent development and improvements in manufacturing techniques, ceramics are now available with higher toughness properties. The size of ceramic particles that are generally found in modern ceramic materials are of a few microns in size and smaller (Yoon *et al.*, 1998, Hatton *et al.*, 2002, De Pasquale *et al.*, 2013). Hatton *et al.* (2002) demonstrated that at least two methods are required to identify the full spectrum of particles from THR. They evaluated periprosthetic tissue from ceramic bearings via SEM and TEM which demonstrated a bi-modal size of particles. The SEM gave a mean (\pm SD) particle size of $0.43 \pm 0.33 \mu\text{m}$, whilst the TEM gave a mean (\pm SD) of $24 \pm 19 \text{ nm}$. Other larger particles ($\geq 3 \mu\text{m}$) were observed but minimal in numbers compared to the nano-meter size (Hatton *et al.*, 2002).

Hatton *et al.* (2003) investigated the reactivity of ceramic particles on cells. They reported that high levels of particles (greater than 100:1 cell ratio) are required to produce significant levels of TNF- α . In their study, the variations of particle size influence the production of TNF- α as other studies with different materials (Green *et al.*, 1998).

Based on the surface examination from retrievals analysed by Dorlot *et al.* (1989) the wear rate was assessed to be of 0.025 μm per year. Given the complexity of a THR i.e. metal stem, ceramic bearings and, metal backing and bone cement (if used), it can be difficult to conclude what causes the osteolysis. An example of this is the histological evaluation of loosened ceramic prostheses by Lerouge *et al.* (1997), where bone particles cement were found to be in larger quantities than the ceramic particles.

There are some papers available where osteolysis was present with large numbers of ceramic particles (size less than 5 μm) in the osteolytic tissue (Nam *et al.*, 2007). The lack of papers available on revision of CoC due to osteolysis (demonstrating osteolytic tissue) could indicate that; 1) ceramic particles are less prominent for bone resorption, or 2) the levels/types of wear from ceramics are not sufficient to cause osteolysis (Esposito *et al.*, 2013).

The study by Yoon *et al.* (1998) is a good analysis and example of osteolysis detected on a ceramic THR, but also a large numbers of metal particles rather than ceramics were found in an area of osteolytic tissue. Thus, preceding studies claiming osteolysis based on the bearing combination should not be drawn to conclusion so likely based on a radiograph alone. Another case of osteolysis has been reported by Wirganowicz & Thomas (1997), where the numbers of Aluminium particles present were greater than any other. To note, they also noticed the osteolytic regions to be extensively stained with metal particles. In contrast there have been cases of loosening but with no evidence of osteolysis by Nevelös *et al.* (1993).

1.5. Implant position

1.5.1. Surgical approach

- Pre-op planning

Common practice before hip joint replacement surgery would be first to X-ray the joint of the patient and get either a diagnosis, or use that X-ray to plan the surgery. The x-ray serves as a good indicator of the acetabular cup and femoral head size which could be used. A minimum of two X-ray views are required, anteroposterior (AP) and lateral (Armfield and Towers, 2007).

The back of the acetabular cup prosthesis should ideally be completely covered by the acetabulum, preferably it spans between the teardrop and the superolateral margin of the

acetabulum (Barrack *et al.*, 2007). When using the template over the X-ray, it should be positioned at 45° inclination angle next to the lateral edge of the teardrop (Barrack *et al.*, 2007). The assessment of this should guide the surgeon in order to select the best component size which requires minimal removal of the subchondral bone (Barrack *et al.*, 2007).

Surgeons aim to place the cup component at an inclination of 45° and an anterversion of approximately 15° (Harris 1978, Nevelös *et al.*, 1993, Widmer & Zurfluh, 2004, Soong *et al.*, 2004). The bases of these particular angles are influenced by many factors, such as; the natural anatomy, hip prostheses designed range of motion and contact mechanics, factors influencing hip replacement dislocation and impingement, etc. (Dorlot *et al.*, 1989, Nevelös *et al.*, 1993, Soong *et al.*, 2004).

Intraoperative orientation is difficult to assess (Saxler *et al.*, 2004). Factors which influence the positioning and fixation are significantly based on the surgeon's experience, and the visualization during surgery. During surgery features are used to accurately position the components with respect to the anatomy of the patient (Harris, 1978, Armfield and Towers, 2007).

- Operating approach

There are a variety of operative approaches and some may have advantages depending on the examination and the history of the patient, however, most surgeons utilize the same approach based on their training and experience (Barrack *et al.*, 2007). The surgical procedure essentially consists of an incision on the skin, followed by further incisions on the muscles and retracting the muscles to expose the hip joint. Once the hip joint is exposed it is dislocated by levering the leg or cutting the femoral head. Drills (reamers) and broaches are used to prepare the capsule and femur to create enough space for the hip replacement components. The following approaches are described briefly as detailed by (McGann, 2007):

- Anterior approach

The anterior approach includes a dissection via the tensor fascia lata muscle, with one end just below the Anterior Superior Iliac Spine (ASIS). Further exposure to the hip capsule is dependent on the extent of dissection of the gluteus medius. To completely expose the hip capsule, the rectus femoris is then divided. For further exposure of the acetabulum, the inguinal ligament and sartorius origin can be released from the ASIS. The capsulotomy is then performed and the hip is prepared for dislocation.

- Anterior-lateral

The anterior-lateral approach provides limited exposure due to the limited dissection of the major muscles groups. The curvilinear incision is made between the gluteus medius and the tensor fascia lata. The advantage of this approach over the anterior is that it is considered less invasive on the abductor muscles (gluteus medius and minimus). The fascia is divided along the same skin incision, curvilinear and border with the gluteus maximus. The objective is to identify the border of the gluteus medius. The tensor can be retracted and flexion and external rotation of the hip improves the exposure to the anterior capsule. The hip capsule is dissected in a medial direction border with the gluteus minimus. The hip can be dislocated after the incision or excision of the capsule by externally rotating the femur.

- Direct lateral

The direct-lateral approach has a similar exposure to the hip capsule as the anterior-lateral. The advantage of this method is the preservation of the posterior soft tissues. The incision is through the anterior portion of the abductors, parallel to anterior border of the femoral shaft. The gluteus medius and vastus lateralis are elevated and retracted by cutting the trochanter region on which these are attached. The thigh is abducted prior to capsulotomy, and the dislocation is performed by externally rotating the leg. Problems have been associated with loss of abductor function with this approach. In cases where leg lengthening has occurred, the trochanteric side may not return to its original position. The extensile modification of the direct lateral has a deeper cut of the trochanteric region which contains the capsule attachment. This is an alternative method for soft tissue release.

Transtrochanteric:

This approach has the hip flexed between 30-45° (depending on intra or extra-capsular approach) and the incision is aligned with the fibres of the gluteus maximus muscle on the lateral side of the patient. Exposure of the hip capsule is made by a further incision on the anterior soft tissues (tensor fascia lata) and retracting the muscles. This type of approach facilitates exposure and helps improve soft tissue tension. Overall this method can be divided into intra-capsular or extra-capsular. In extra-capsular, the hip capsule is sacrificed to preserve the gluteus medius and minimus.

- Posterior and posterior-lateral

The posterior approach as the name suggest has good exposure to the posterior capsule. This approach is suited for isolated cases of the femur. The posterior-lateral has received many modifications which aim to relieve tension from the skin and increase exposure to the femur

and the acetabulum. The incision is made in the posterior direction at an angle of 45° down to the deep fascia. After the fascia is incised, the fascia is retracted anteriorly and posteriorly. Release of the gluteus maximus help relieve tension. The posterior approach is then performed. The knee is flexed 90° and the hip is internally rotated 30° and extended to facilitate access. The piriformis tendon is released to expose the posterior capsular of the gluteus minimus. The obturator externus is clamped and released. The inferior capsule is exposed by a lever (caudad). At this point the capsulotomy can be carried out, or a modified version used to preserve a portion of the capsule.

As it can be understood from the surgical approach, each, in theory can have advantages over another, but they all require incisions through the muscles and the hip capsule. The different approaches above provide different visualisation of the hip joint as the patient is rested in an adequate angle to create the incision. In some cases for better exposure, further dissection of soft tissues are performed or removed, like the hip capsulotomy (McGann, 2007). The visualisation of the joint capsule has been discussed to pose difficulties in assessing the orientation that the cup should have in the patient (Saxler *et al.*, 2004). This can influence where the contact area between the head and the cup lies. Furthermore, the type of approach has been considered to influence the preservation of soft tissue and the function on the muscles.

1.5.2. Clinical studies of hip prostheses

a) *Imaging for total hip replacement alignment*

X-rays are widely used for clinical studies to determine the position of the components, however, there can be inaccuracies during examination of the patient that lead to a different result. It is not unusual to find clinical studies where the examined implantation angles are beyond that which are considered appropriate (Saxler *et al.*, 2004, Widmer & Zurfluh, 2004, Soong *et al.*, 2004, Callanan *et al.*, 2011).

Prior to surgery, an important point to acknowledge when templating on a radiograph (i.e. AP), is that the femur should be internally rotated by approximately 15° to 20° to most accurately predict the stem size, neck length, offset and neck resection (Armfield and Towers, 2007). Inaccuracies in the preoperative planning based on malrotated radiographs can lead suboptimal information of the neck-shaft angle, femoral offset and limb length (Barrack *et al.*, 2007).

It is important to evaluate the position of the implant after surgery to determine if it is adequate and it is also used for comparison during follow-up. There are different terminologies (Murray, 1993) and methods for examining the implant such as; X-Ray, Computerised Tomography (CT) scan, fluoroscopy, or depending on the surgery, they may use Roentgen Stereophotogrammetric Analysis (RSA). It is up to the orthopaedic centre and facilities whether an X-ray or other means are used to evaluate the positioning. To note, a one plane radiograph cannot fully and accurately give the positioning of all the components inserted.

RSA is a good tool to determine the migration of the prosthesis and evaluation (Kärrholm, 2012) during the life time implanted. The probes that are implanted with the prosthesis are used to identify the position using x-rays. By examining the implant after certain periods, it can deduct if movement according to the previous location has occurred. The precision for measuring of this method can be highly accurate and detect translation and rotations up to two decimal places with a 95% confidence interval (Nieuwenhuijse *et al.*, 2012).

There are currently no methods available that measure the forces associated in a hip joint replacement which evaluate the positioning of both the head and the cup as individuals in patients *in situ*. Imaging methods as described above are widely used to orientate and determine the position, neck length and femoral offset. But as mentioned, there can be inaccuracies which lead to different outcomes. Mainly, the only feedback a surgeon has during surgery when deciding what design to use (i.e. neck length, Figure 1-7) and how to position it, is his or her experience.

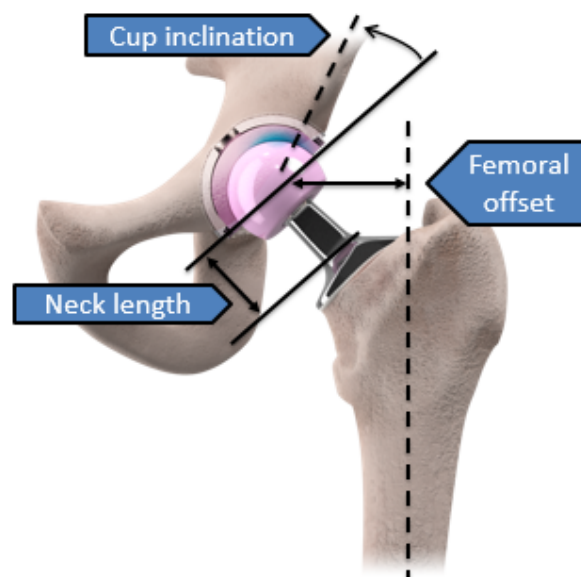


Figure 1-7. Schematic of different parameters to consider during hip joint replacement surgery.

b) *Centre of rotation (premorbid centre) and tissue tension*

For a functional and mechanically stable hip, two factors are important, these are the restoration of the centre of the normal hip as well as the soft tissue tension (Barrack *et al.*, 2007). The restoration of the centre of rotation is one of the primary goals in hip joint replacement (Barrack *et al.*, 2007). With adequate restoration of the hip centre, the lever for the abductor muscles is recreated. If the soft tissue is not appropriately tensioned, the body cannot generate adequate force and in the case of the abductor muscles the pelvis drops to the opposite side during single-leg stance (Barrack *et al.*, 2007). Another reason to restore the hip centre is to avoid impingement between the femur or the femoral component and the pelvis. In cases where there isn't adequate bone available, the surgeon can potentially leave and accept a high or medial hip centre (Barrack *et al.*, 2007). However, a high hip centre has disadvantages, and can lead to loosening (Yoder *et al.*, 1988).

c) *Femoral offset*

The femoral offset is defined as the perpendicular distance between the centre of rotation of the femoral head and longitudinal axis of the femur (McGrory *et al.*, 1995). The femoral offset is important to restore the soft tissue balance (Barrack *et al.*, 2007). One of the concepts for increasing the femoral offset is to decrease the abductor force required for walking and decrease the incidence of impingement (McGrory *et al.*, 1995). With insufficient offset, it may produce hip instability and tissue laxity (Barrack *et al.*, 2007). However, with higher offsets, there is a risk of out of plane bending moment applied on the femoral component (McGrory *et al.* 1995, Barrack *et al.*, 2007). This increases the rotational moment at the stem-bone interface and increase the risk of loosening. Modularity in the prosthesis can help give the correct adjustments to achieve the offset required.

With changes to the location of the femur in respect to the pelvis, consequential alterations can occur to the gait kinematics. Sariali *et al.* (2014) looked at the range of motion during walking in total hip arthroplasty. When evaluating the kinematics of gait, it is important to consider the motion not only of the femur but also the linkages of the whole leg i.e. the knee and the ankle in order to have a better representation of the alterations, if any. When analysing one parameter, such as the range of motion due to offset, one should also consider the other factors that could influence gait such as leg length inequalities. Sariali *et al.* (2014) and McGrory *et al.* (1995) results suggest that with an increased offset, a larger range of abduction occurs during the gait. By increasing the length offset, the lever can increase, in doing so, the isometric strength increases as measured by McGrory *et al.* (1995).

Pasquier *et al.* (2010) describe the various limitations from using a frontal plane radiograph to measure the femoral offset. Such limitations can be; the patient positioning, and also, the neck fixed in external rotation, and the distance between the X-ray tube and plate. Pasquier *et al.* (2010) describe in their study that a CT scan is more accurate to determine the femoral offset than with a single frontal radiograph.

d) *Leg lengthening*

Due to the changes in the anatomy created by the offset, leg length inequality could occur. Leg lengthening can occur when there is lack of preoperative analysis, inappropriate selection of components or insufficient care to restore the hip anatomy (Parvizi *et al.*, 2003). In other cases, lengthening occurs as a result of increasing the tissue tension. As the name suggest, the operated limb is longer than the other one. To get an idea of the range of limb length discrepancy, it can range from 20 to 70 mm (Parvizi *et al.*, 2003).

e) *Stem migration*

In context, years of clinical studies conclude that a patient who has undergone hip joint replacement whose prostheses continues to migrate “excessively” through the years, is very likely to require revision. It is common that components revised had high migration in the early stages after the operation (Pijls *et al.*, 2012). A high migration will probably result in loosening or lead to revision.

There are two techniques to measure migration of the stem via RSA as described by Wierer *et al.* (2013). It can either be measured at the centre of gravity or the migration of each probe attached to the stem. Wierer *et al.* (2013) describe that major advantage of measuring by the centre of gravity is that it is easier to interpret.

It is considered reasonable that stems migrate in the direction of the force applied i.e. vertical migration. However, the amount of migration per year can determine the probability of revision. According to the results from Kärrholm *et al.* (1994), migration of the cemented stems higher than 1.2 mm in two years have a higher probability of revision. The implants from this study with higher migration observed via the RSA assessment in the early stages of follow-up required revision.

An RSA study by Kiernan *et al.* (2013) on cemented stems showed regardless of their anteversion position (1° to 43°), all stems can migrate up to about 1 mm in the sagittal plane (downwards from the force being applied) at 10 years. To note, it appeared that the stems positioned at less than 10° anteversion (measured by CT scan) had the highest migration with a

mean of 3 mm at ten years in the same direction. Also, those stems positioned at less than 10° had the highest migration on the longitudinal plane (coronal), hence the highest rotational migration measured along this axis as well.

f) Cup migration

It can be postulated that cup migration occurs when it is not affixed appropriately and/or the forces exerted cause the migration in the direction of the applied force. This would make it comparable to the migrations observed on the stem. However, the rotation of the cup could occur partially when loading is applied to the non-bearing surfaces such as the edge/rim section. This can occur when there is laxity and the head moves away from the centre of rotation from the cup. This is difficult to interpret, because most studies related to cup migration, do not report rotation and the ones that do, don't explicitly elaborate on the rotation reference (Pijls *et al.*, 2012).

An RSA study by Nieuwenhuijse *et al.* (2012) endorses the need for cup migration assessment during the early stages to establish the performance post-operation. Their two year follow up results show that high sagittal rotation leads to device failure. The migration required to increase the risk of revision for cemented polymer cups is estimate to be 0.74 mm per year in the cranial translation. In comparison, at two years, well performing cups migrated (cranial plane) about 0.50 mm, and seem to plateau. Pijls *et al.* (2012) review concludes that a proximal migration of the cup larger than 1.00 mm in two years has less than 95% survivorship at 10 years. Nieuwenhuijse *et al.* (2012) results indicate good working prosthesis over 10 years with maximal migration of 3.57 mm. From these studies, it should be understood that good working prosthesis can migrate very small amounts.

One way to look at the cause of the migrations is that the components are not located in the correct location and one component is forcing another one to move. Another scenario is that the force applied overcomes the fixation of the component. Either way, these scenarios indicate an offset force caused by either soft tissue tension or a malposition.

1.5.3. Edge loading and stripe wear

Wear patterns formed under edge loading conditions are produced due to high stress concentrations. The outcome is loss of material and increase in surface roughness in ceramics bearings. Overall, the combinations of these outcomes prevent fluid film and mixed lubrication, thus the wear rate is increased.

a) *Rotational and translational malposition*

Each component (the cup and the head) can be malpositioned (or mal-orientated) as they both have 6 degrees of freedom. Translational malposition is when the cup and the head centres are not matching each other in any direction i.e. medially-laterally, anteriorly-posteriorly or superiorly-inferiorly. Rotational malposition is when the degree of rotation of the cup is not adequate for articulation and the contact area is reduced.

Translational malpositioning is defined if the centres of rotations of the head and /or the cup are not matched with the centre of rotation of the hip joint (Figure 1-8). One or both components may be malpositioned at any one time. Under such condition, edge loading may occur if the resultant forces around the joint change in magnitude and direction to cause separation of the centres of rotations of the femoral head and acetabular cup during an activity, causing the femoral head to slide towards the rim of the acetabular cup or change the location of the contact area. Due to conformity of the hip joint, under high load, the femoral head is located within the sphericity of the acetabular cup. So although malposition between the centre of rotations of the head and the cup exists, static X-rays of the hip joint will not detect such offset. In such scenarios where edge loading is driven by joint separation, it can only be detected under dynamic conditions where an activity is being performed. An example of a translational mismatch in clinical terms is an offset deficiency, where there isn't sufficient soft tissue tension to maintain the head within the cup. It is hypothesised, that these examples lead to edge loading due to the force imbalance when the head and the cup are implanted leading to change in the contact area away from the bearing surface (Fisher 2011). However edge loading is multifactorial and translational malposition covers only one aspect.

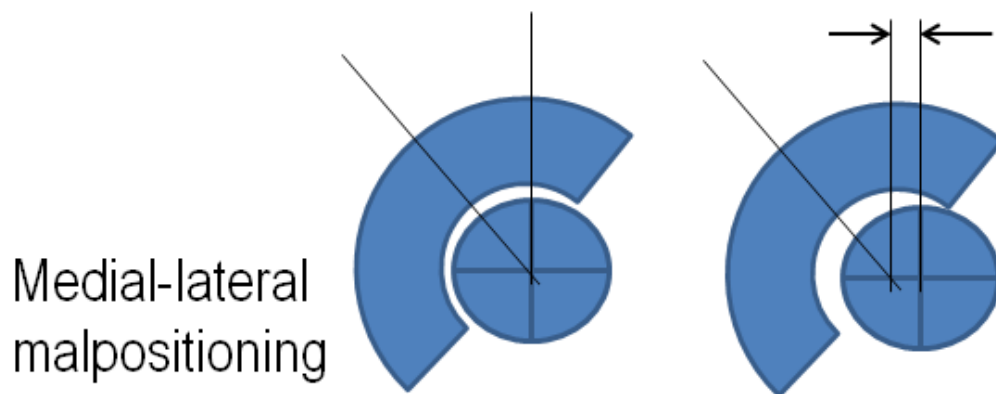


Figure 1-8. Schematic representing medial-lateral malposition.

As reviewed in Chapter 1.5.2, after implantation, the cup or the head can migrate away from its original position. This migration may occur such that it moves medially, anteriorly or inferiorly. The question regarding migration remains: does it migrate to restore the anatomical centre of rotation, or does it migrate creating adverse conditions?

Rotational malposition is defined when the cup orientation (Figure 1-9) is in such position that causes the contact area between the head and the cup to reach the rim of the acetabular cup during an activity. This can occur under steep inclination angle or excessive version of the acetabular cup. One of the factors leading to edge loading is the visualisation of the joint capsule as previously described in the surgical approach. The position of the cup has been linked to the increase in incidence of edge loading (Kwon *et al.*, 2012).

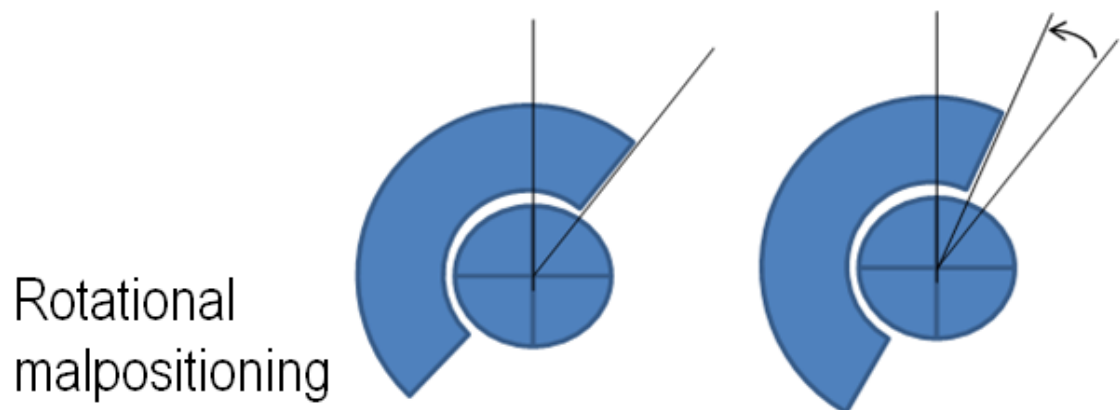


Figure 1-9. Schematic representing rotational malposition.

Another factor leading to edge loading is impingement. It is also important to note that shallow inclination angle of the acetabular cup may cause impingement of the femoral stem and acetabular cup. Impingement may also lead to separation or even subluxation of the femoral head leading to edge loading. This thesis does not consider separation and edge loading driven by component impingement.

Gross wear on ceramics due to a high inclination angle was proposed since the late 1980's (Boutin *et al.*, 1988), but there wasn't a wear study which could simulate it at the time. The idea of high stresses due to a high inclination angle have also been published at that time (Boutin *et al.*, 1988). Subluxation leading to gross wear on ceramics was possibly first observed and mentioned by Griss & Heimke (1981). At that time, other groups believed that gross wear only occurred after loosening (Boutin *et al.*, 1988). However, this wear mechanics was first described as stripe wear due to edge loading by Nevelos *et al.* (1999).

Several studies have shown stripe wear patterns and gross wear which occurred due to edge loading on the head due to contact with the rim of the cup (Boutin *et al.*, 1988, Dorlot, 1992,

Nevelos *et al.*, 1999, Nevelos *et al.*, 2000, Nevelos *et al.*, 2001, Walter *et al.*, 2004, Yamamoto *et al.*, 2005, Campbell *et al.*, 2006, Shishido *et al.*, 2006, Tateiwa *et al.*, 2007, De Haan *et al.*, 2008, Kwon *et al.*, 2010, Lombardi *et al.*, 2010, Matthies *et al.*, 2011, Affatato *et al.*, 2012, Esposito *et al.*, 2012, French *et al.*, 2012, Brandt *et al.*, 2013, Currier *et al.*, 2013, Korim *et al.*, 2014).

b) Retrievals related to edge loading

A limitation of retrieval analysis is that it is very difficult to account for all of the variables which lead to the failure of the prosthesis and map them correctly and chronologically. To properly examine retrievals, one also needs to consider both components i.e. the cup and the matching head.

Nevelos *et al.* 1999, Esposito *et al.* (2012) and Brandt *et al.* (2013) have shown that stripe wear in ceramic-on-ceramic bearings is not found on all the retrieval cases. Retrieval studies show that the stripe wear has grain pull out areas and thus makes the surface rougher (Nevelos *et al.* 1999). The surface roughness (Ra) over the stripe wear region can increase by 3 fold from its original unworn value (Clarke *et al.*, 2009). Similar cases were identified in earlier retrievals where gross wear was found (Griss & Heimke, 1981, Boutin *et al.*, 1988, Dorlot *et al.*, 1989). The Ra of the stripe wear from retrievals studies indicates it can be between 50-200 nm e.g. changing from its original of Ra of approximately 4 nm (Nevelos *et al.*, 1999, Tateiwa *et al.*, 2007, Clarke *et al.*, 2009). In addition, stripe wear has also been associated with higher maximum depth of valley value and negative surface skewness (Brandt *et al.*, 2013).

While these findings demonstrate that material has been removed and the surface is rougher in ceramic bearings, it has not shown applicability on how it further affects the wear in the hip simulator studies. These findings can be used to compare against simulator studies and determine if the same or similar results can be achieved from a specific method.

The location of the wear scar is dependent on many factors such as cup inclination, version and anteversion, level of malposition, soft tissue tension, and activity. The directionality, orientation and angle of the stripe wear can be defined from the angle of the cup i.e. inclination and anteversion where the edge loading occurs. However, the orientation of the stem and mechanical activity needs to be incorporated. So far, two stripe wear location areas seem to be predominant. These have been categorised by Esposito *et al.* (2012) as anterosuperior and posterior (i.e. edge loading on the front or back of the cup). However, different studies may give it another annotation depending on their evaluation (Walter *et al.*, 2004).

The influence of the cup positioning on the wear rate and stripe wear remains incomprehensible in the retrievals studies. Other factors, like the joint laxity can play a role on the occurrence of edge loading. Esposito *et al.* (2012) suggested that anteverision cup positioning play a significant role on the overall wear rate. However, the error of $\pm 5^\circ$ is significant in their evaluation. Their results do seem to indicate high wear rate at 10° anteverision though. In contrast, Brandt *et al.* (2013) suggests high wear rates when the angle was higher than 45° , although their results are not quantitative, and the anteverisions angles were not evaluated. A reason which could explain the variation in wear due to the same and different inclination and version angles of the cup found in retrievals is that these studies sometimes do not evaluate the full parameters of the cup position (inclination and version). Furthermore, the translational malposition of these components has not been evaluated. Thus, the severity of the wear has only been evaluated based on the rotational malposition.

Translational malposition medial-laterally has been reported to affect the wear severely on standard and high inclination angles (Nevelos *et al.*, 2000, Williams *et al.*, 2008). If a translational malposition or edge loading happened to be performed anteriorly-posteriorly, superiorly-inferiorly, it could also severely affect the wear as in previous studies. An increased offset from the centre of either the head or the cup which may not be detectable could increase the wear. During surgery the size and position of the component is templated against the radiograph. If both, the acetabular cup and femoral head are placed against the radiograph, this would suggest the components are concentric. However, often a femoral offset is used and one of the reasons is to decrease impingement (McGrory *et al.*, 1995); thus, exerting a force which means the head and the cup have a translational malposition. This is because the prosthesis is no longer in the matched centre, as one component is forcing another one in the direction of the offset applied.

A particle size characterisation study (of adverse conditions) from ceramic retrievals by Tipper *et al.* (2002) showed a bi-modal particle size distribution i.e. small particles in the nanometre scale region and larger particles in the micrometre scale. Since non adverse conditions do not show particles in the micrometre scale (see Chapter 1.6.3), this indicates that the larger particles could originate from the adverse conditions. Nam *et al.* (2007) case report study from a retrieved ceramic bearing (BIOLOX® forte), showed wear particles of less than $5 \mu\text{m}$ in size. Abundant particles were found at the regions of the osteolytic tissue, and osteolysis was the reason for revision. Since grain pull-out was observed on the bearing surface and on the edge, it is very likely that edge loading was one of the reasons for the larger particles. Even with low numbers of wear per year ($>2 \text{ mm}^3$ per year) from CoC retrievals, as studied by Esposito *et al.* (2013), it is evident that revision is multifactorial and edge wear is not the only cause.

The indication that edge loading occurs on ceramics is well documented because the stripe wear is notable on the retrievals. Edge loading has also been observed on MoM bearing couples, which gives a strong indication that edge loading is not material related but rather a combined result from the surgical procedure (leading to rotational malposition), joint laxity, subluxation, posture of the patient or activity.

c) *In vivo translation*

Subluxation of the femoral head in patients with ceramic THR has been proposed since the 80's by Griss & Heimke (1981). But a study or examination that could verify this *in vivo* was not available at that time.

A fluoroscopy examination is a technique that can be used to evaluate the prosthesis during a certain activity. The studies by Lombardi *et al.* (2000), Dennis *et al.* (2001), Glaser *et al.* (2008) and Glaser *et al.* (2010) focus on evaluating any separation occurring between the centre of the cup and the centre of the head during a patient's activity.

Dennis *et al.* (2001) first looked at abduction and adduction motion specifically. Their results were the first to show separation between the centres of rotation of the head and the cup. Certain limitations (i.e. error in measuring the separation) perhaps should be accounted when evaluating the results from these studies. Especially if considering the magnitude of separation as a primary factor for the evaluation of *in vitro* models. Nevertheless, their results indicate that unconstrained prostheses show the highest separation. Overall results do have a correlation where constrained prostheses show little to no separation as expected due to their designs. One major contribution to the wear mechanism of stripe wear is that they observed contact maintained between the femoral head and the acetabular cup as translation between the centres of rotation occurred (Dennis *et al.*, 2001). Thus the contact stress increased gradually as the contact area decreased during the translation, rather than a quick impact motion.

Results from Lombardi *et al.* (2000) identified higher levels of separation during leg lift-off for walking. One key point to incorporate into hip simulator methods or specification for assessing the performance of prostheses is that consideration should be taken to test the conditions which are more significant and rigorous. For example retrospectively, one movement/motion could have higher wear or damage in comparison to another which is less severe.

Subsequent studies from this group moved onto correlating sound and video for walking (Glaser *et al.*, 2008). In these studies, separation was observed during the stance phase on MoM, MoP and CoP components. Glaser *et al.* (2010) had a similar result where, the MoP

indicated a relative amount of separation during the stance phase, and also this was the maximum separation observed overall.

For MoM, the maximum separation was observed just before heel strike. It was indicated that MoM bearings had a distinctive separation pattern compared to other bearing combinations. A rapid decrease in separation was observed after heel strike, but it was mentioned that separation decreased after toe off as well.

The previous studies mentioned above resulted with a separation between 0 to 3 mm. The measurement is made from detecting the edges of the components which serve as a reference from the maximum and minimum displacement based on the geometry of the components. To consider, the error in the *in vitro* assessment when measuring a separation in a static condition was 0.5 mm. This means any reading of less than 1 mm may not be separation as the equipment and methodology was not accurate enough. Measurements during *in vivo* conditions would pose more challenges and the error could increase. Furthermore, this technique did not measure the travel direction nor considers the rotational aspect of the components.

More complex fluoroscopy techniques have been developed to determine THR kinematics (Tsai *et al.*, 2013). This is a method that applies two X-ray sources to evaluate the implant, and offer better accuracy to determine malpositioning. The method is similar to RSA however, no markers are used.

Digas *et al.* (2013) study indicated no displacement observed by the RSA technique. They evaluated polymer cups, and two types of motion; abduction and flexion. The flexion results should be reviewed carefully as the analysis was performed on steps increasing from 0° to 30°. Potentially weight was applied during the intervals, which would place the head back into the socket. However, the abduction movement alone only indicated medial translation of the head penetrating against the cup.

Tsai *et al.* (2014) did not detect a translation higher than 0.5 mm in any direction. Typically their translation values during gait were 0.2 mm. To consider, this was a study carried out with MoP, and hard bearings may indicate a different result as they are stiffer.

d) *Effect of the translational mismatch on the biomechanics*

A clinical example of a translational mismatch is when tissue tension has been applied in the form of a femoral offset. In this example a force is exerted in the direction of the femoral offset such that the head centre is not in a neutral position.

Changing the femoral offset could lead to alterations in motion. McGrory *et al.* (1995) identified that with higher femoral offset, there is a larger range of motion (lateral), and higher force can be exerted when abducting.

According to Sariali *et al.* (2014) femoral offset could alter the kinematic performance during the walking cycle. Even though this study does not take into account the leg length variable, it strengthens the concept of the variation of kinematics due to different anatomy. His study focused on the impact of increased or decreased femoral offset. Statistically it may show a decrease in adduction range, however, it is important to consider and understand at what point during the cycle this change is occurring. Total range of motion does not fully characterise the changes in kinematics and gait. It may be possible that the full extent of range of motion is performed during the whole cycle, but there can also be a decrease in certain sections which needs to be detected.

1.6. Wear of hip joint replacement bearings

Historically, hip joint replacements were evaluated on trial and error and success rate. As the technologies advanced, more consideration has been taken on the environment it is in, its design, the biocompatibility and wear from the components. To understand the wear mechanisms of the components, different hip simulators have been manufactured with the aim to replicate in vivo biomechanics.

1.6.1. Hip joint replacement biomechanics

a) *In vivo forces*

Walking is the predominant activity in our daily lives. Hence, a lot of focus and research has been generated in order to understand the fundamentals of this motion. The biomechanics of the natural hip joint and the walking cycle are key factors for designing hip implants, and a good indicator. However, it is good to consider and analyse the biomechanics after the prosthesis has been implanted. This, like the biomechanics of the natural hip, will more than likely create different populations which are based on the factors associated with the changes and the patient classification.

The vertical forces and maximum joint reaction force measured on hip prosthesis during the walking gait cycle by Bergmann *et al.* (2001) were roughly about the same result of 3 times body weight from those measured by force plates (Crowninshield *et al.*, 1978). Bergmann's *et al.* (2001) measurements indicated that the forces as is acting in the lateral direction on the femoral head are approximately 500 N throughout the stance phase, and decreasing slightly during the swing phase. The forces acting posteriorly-anteriorly were significantly lower

compared to the forces in the other directions, and fluctuated from negative to positive (posteriorly-anteriorly). The vertical force decreased to about the same force acting laterally during the swing phase. With this in mind, there is a possibility of the head translating towards the rim section of the cup, especially if the lateral force surpasses that of the vertical. Depending on the design of the cup, edge loading can occur when considering the change in geometry at the beginning of the rim section. One point to consider is that studies measuring forces *in vivo* via telemetry do not account for the related influence of the force acting due to malposition and soft tissue tensioning.

b) In vivo motions

Considering that the anatomy is changed after a THR, it is reasonable to assume a change can also occur in the kinematics and kinetics during the walking gait cycle. Factors to consider are leg length, femoral offset and, cup version (which could reduce range of motion due to impingement) and perhaps muscle strength. In Bennett's *et al.* (2008) study, this difference is clear. The group without THR had a maximum extension of -6.2° (SD ± 8.6) where the negative sign denominates extension, and the THR group had a maximum extension of $+6.3$, where the positive sign indicates to be in the flexion region. Hence no extension was observed. This doesn't indicate that the leg doesn't extend, it just means it doesn't extend as much. One factor to consider in this study is that clarification of the reference point at which zero flexion was obtained for comparison against other studies is important. A similar case was observed for the abduction where patients with THR had about half the range in comparison to the non-THR group.

Small differences have also been detected to occur due to the surgical approach used (Glaser, Dennis, *et al.*, 2008). These changes are seen on the variance by groups and maximum motion in comparison to other surgical approaches. These differences are suspected to be due to the size of incision and incised muscle groups. Glaser *et al.* (2008) demonstrated larger variance in the walking gait cycle in comparison with minimally invasive approaches and range of motion as detailed in Table 1-3.

Tsai *et al.* (2014) evaluated MoP THR using dual fluoroscopy imaging system to measure the gait kinematics. Their results also showed no extension, but interestingly, no adduction and no internal rotation during the walking gait cycle either. The range of motion is however similar to the other study by (Bennett *et al.*, 2008). Tsai *et al.* (2014) obtained a range (\pm SD) of $38.9^\circ \pm 6.4^\circ$, $9.0^\circ \pm 3.3^\circ$, and $10.5^\circ \pm 4.9^\circ$ for flexion/extension, adduction/abduction and internal/external rotation respectively.

In contrast, Bennett's *et al.* (2008) study of MoP THR, showed a significant difference in the hip rotation with the use of capture cameras and markers. Their results ranged between 0° and 20° externally (Bennett *et al.*, 2008), where Tsai *et al.* (2014) resulted externally between 12° and 35°.

Table 1-3. Nominal range of motion from total hip replacement gait studies

Study group	Reference	Method	Nominal range (°) ±SD			Comments
			F/E	ABD/ADD	I/E rotation	
Tsai	Unknown	RSA	38.9 ±6.4	9.0 ±3.3	10.5 ±4.9	No extension
Glaser (PL)			40	15	15	
Glaser (PL-MIS)	Supine	Camera	25	7	10	No extension
Glaser (AL-MIS)			15	8	15	No extension
Bennett (Group 1)			37.3 ±7.1	7.8 ±2.7	16	No extension, and no internal rotation
Bennett (Group 2)			32.7 ±7.0	7.9 ±4.2	16	No extension, and no internal rotation
Bennett (Group 3)			33.6 ±6.0	6.8 ±2.2	16	No extension, and no internal rotation
Bennett (Group 4)	Unknown	Camera	35.1 ±7.0	6.9 ±2.2	16	No extension, and no internal rotation
Bennett (Group 5)			30.4 ±6.4	6.3 ±2.6	16	No extension, and no internal rotation
Bennett (No THA)			45.9 ±2.6	12.7 ±2.4	16	No internal rotation

F/E = Flexion / Extension, ABD/ADD = Abduction / Adduction, I/E = Internal / External, PL = Post Lateral, AL = Anterior Lateral, MIS = Mini Incision Surgery

Either the reference points are different, or the fluoroscopy imaging system neglects soft tissue which may impact the camera's system. Regardless, both have a similar range of rotation. Both studies also showed a small reduction in the nominal range of adduction occurring during the swing phase in comparison to the natural hip.

If the motions found by Tsai *et al.* (2014) are the most accurate motions of patients with joint replacements, certain changes may need to be considered on the kinematics used in the laboratories for *in vitro* studies. If the walking cycle is required to be replicated by *in vitro* laboratories, the kinematics measured *in vivo* need to be considered. Also it would be good to

classify walking cycles that are affected by the position of the implant such as leg lengthening, centre of rotation, femoral offset, etc.

When analysing the gait motions, the internal-external rotation does not seem to be as easily defined in comparison to the flexion because it does not look like a single continuous stroke (Bennett *et al.*, 2008, Glaser *et al.*, 2008, Tsai *et al.*, 2014). Perhaps the most noticeable change occurs just before toe off and heel strike where there appears to be a common indication that it rotates externally. The abduction and adduction motion is slightly similar to the rotation variation, such that with patient variability, it is difficult to account for distinctive motions and extremes that stand out at particular points. However studies indicate that maximum adduction appears to be at toe off (Bennett *et al.*, 2008, Glaser *et al.*, 2008 Tsai *et al.*, 2014). With this in mind, for *in vitro* studies, it is easier to simplify the motion in a single sinusoidal wave which represents that of *in vivo* motions.

A common result from gait analysis studies and measured forces is that the data is generally summarised. By compiling the average data, one could overlook at instances which may be more significant. For example, it is commonly known that the walking cycle has a double peak force and a trough in between. If edge loading occurs *in vivo* during the swing phase when the load is dropped sufficiently for the femoral head to translate away, the number of occurrences can be obscured when averaging the results.

1.6.2. *In vitro* hip simulator studies

a) Factors

There are many factors that need to be considered for analysing and comparing the results from hip experimental simulators studies, some of these are:

- Number of rotating axis (flexion/abduction/rotation)
- Acting unit for rotation (which component moves relative to the other)
- Delivery of force applied and acting axis (i.e. of simplified joint reaction force and direction loading)
- Degrees of rotation (path and velocity)
- Loading profile; i.e. maximum load (peak force applied), minimum load (swing phase force applied), acceleration and frequency, etc.
- Bearing fixtures and contact area (inclination angle, edge loading or concentricity, and clamping method)
- Lubricant (friction factor and type of fluid regime)
- Running in or steady state phase (time of measuring intervals)
- Bearing design and material (surface roughness, clearance, diameter, and rim geometry)

In the following sections, selected studies are described where different factors were considered to affect the wear results.

b) Influence of kinematics

The motion and path executed on hip simulators are mainly influenced by *in vivo* physiology from gait cycle studies. However, not all hip simulators may have the capability to perform all the motions as in the body due to the design complexity, and increased cost. Barbour *et al.* (1999) developed a wear path for a two axis simulator, consisting of flexion/extension and internal/external rotation, to represent the physiological walking cycle. This was achieved by introducing 90 degree phase lag between the flexion/extension and internal/external rotation (Figure 1-10), thus the wear path remained elliptical in shape as that shown for a three axis simulator. This means that during the swing phase it is mainly internally rotating, and at stance phase (or vertically loaded), it is alternating between external and internal rotation. In contrast to the ISO14242-1 guidelines for hip simulator testing and gait analysis, the loading is applied slightly earlier before heel strike (ISO14242-1, 2014).

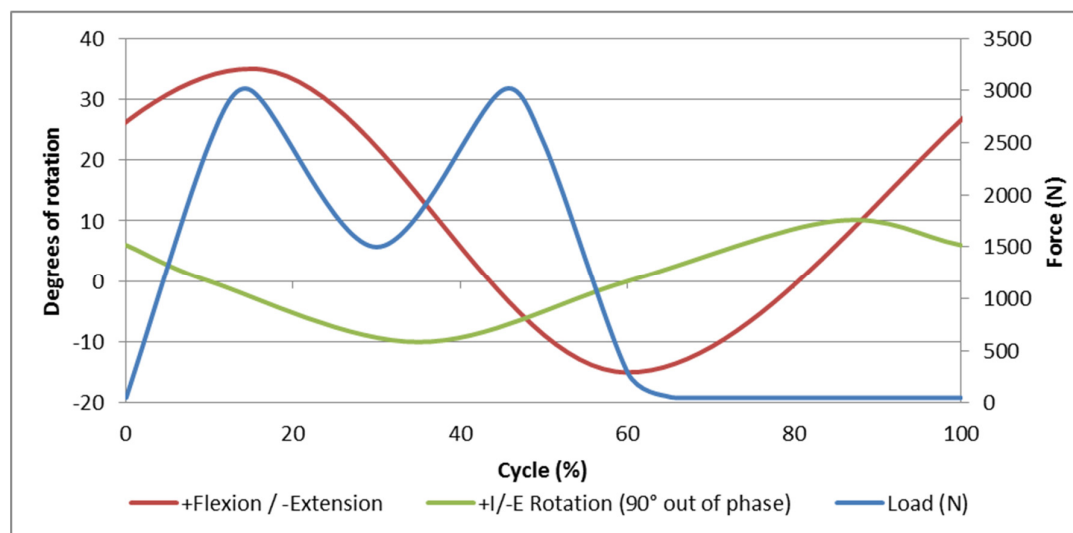


Figure 1-10. Kinematics on the Leeds Mark II Anatomical Hip Simulator

A study by Firkins *et al.* (2001) compared the difference of a two and a three axis simulator with metal bearings. The path used in the two axis simulator was based on that developed by Barbour *et al.* (1999). The path for the three axis simulator was based on a physiological motion. Their results showed that higher wear was obtained in the initial and steady state phases from the two axis simulator. It was believed that the difference in results was due to the alterations in the wear path, where the two axis simulator had a more eccentric path shape (Firkins *et al.*, 2001). One factor which at the time was not considered to influence the wear is the minimum load applied during the swing phase. Other factors which may have influenced the difference were the articulation, contact area and third body particles if present. They noted in their topographical analysis deeper scratches and higher surface

roughness (0.1-1.0 μm) in the results from the two axis simulator. The slight changes from the path and position of the cup could have influenced where the bearings articulated.

Williams et al., (2006) showed that, a high swing phase load gave higher bedding in wear on MoM bearings in comparison to a lower swing phase load. Their results are in agreement with their increase in coefficient of friction from a high swing phase load (280 N) to a lower (100 N) one; their coefficient of friction was 0.171 and 0.129 respectively. Interestingly, the high swing phase load did not show significant difference in the steady state, which may imply that the coefficient of friction decreased due to a better lubrication regime.

An *in vitro* study by Oliveira *et al.* (2011) which compared the two kinematic cycles of the ISO14242 Part 1 and Part 3, indicated that Part 3 was a more vigorous test due to the difference in surface damage from the components used (UHMWPE and stainless steel). It is perhaps then the much greater difference in abduction/adduction which causes the greater surface damage. In comparison, the Part 3 has 35° more in the abduction/adduction motion. The speed at which this change must occur is also quicker, thus it can influence the wear. Comparing Part 1, the abduction/adduction has 15 degrees during loading. If Part 3 has the same loading pattern, and considering the motion, it has over 46 degrees where the load is applied which is significantly more. Another point to mention however on their study is that the result on the femoral heads doesn't show much change unlike they show on the polymer, hence perhaps the larger multidirectional motion has a greater effect on the surface roughness. This study however is missing key factors that should be investigated. Such as; wear assessment by weight, repeatability of the machine and, fatigue and creep due to the loads applied on the polymer.

The kinematics can also affect the breakdown of the fluid layer. Other studies where the input was changed to a Stop-Dwell-Start (SDS) motion for a walking cycle breaks the fluid layer and maintains the bearings in contact via loading (Hadley *et al.*, 2014). In the SDS cycle, after the dwell cycle, one walking cycle is executed and then stop again for another dwell period under load. This type of kinematic and like jogging testing (Bowsher and Shelton, 2001) aim to increase the wear rate via different inputs.

c) *Wear of hip joint replacements*

- Lubrication

Diluted bovine serum is widely used) for *in vitro* hip replacement testing, and this has been accepted due to the representative friction and conditions as that of synovial fluid and hip joints (Scholes and Unsworth, 2006). The effect of the protein concentration on UHMWPE has

been widely documented and studies suggest increase wear with the increase dilution of the bovine serum (Liao *et al.*, 1999, Saikko, 2003, Tateiwa *et al.*, 2006, John, 2010). However, other lubricants or lack of lubricant can give different results (Derbyshire *et al.* 1994, Bigsby *et al.* 1997). Nevelos *et al.* (2001) tested the ceramic-on-ceramic bearings under dry conditions and observed relatively higher wear than when tested with new-born calf serum as lubricant. They also tested diluted serum (25%), Gelofusine® (a gelatin-based protein solution) and water. Their results indicated lower wear rates with water which can be due to the lower friction as reported by Brockett *et al.* (2007) on a pendulum friction simulator.

- Surface of the bearing

The surface roughness is considered to affect the wear as the peaks of the asperities and hard contact points from valleys on the surfaces can act as the main local points that remove material. Wang *et al.* (1998) demonstrated that surface roughness can impact the wear in hard-on-soft bearings, however, no significant change in wear was found with the femoral heads of a lower surface roughness (Ra) of less than 0.05 μm . Another factor to consider though is the level of activity. Bowsher & Shelton (2001) induced damage to femoral heads to a surface roughness (Ra) of 0.38 μm , and wear increased dramatically under simulated jogging conditions. With regards to hard bearings, Chan *et al.* (1999) analysed the wear of MoM with the increase of surface roughness based on relatively similar clearances (ranging from 81 to 107 μm). The total volumetric wear was higher with increased surface roughness.

- Bearing size (MoM)

The wear of an articulating bearing in dry conditions is considered to be proportional to the sliding distance. Smith *et al.* (2001) demonstrated no evidence of mixed lubrication in their smaller (16 to 22.225 mm) bearings during articulation in the hip simulator. Thus, the wear increased with the increased bearing size under the boundary conditions. They also tested a larger bearing (28 mm) which generated less wear. This was explained due to the evidence of mixed lubrication since at occasions the surfaces were separated by the lubricant (Smith *et al.* 2001). The smaller bearings did not show bedding in unlike the large bearing size of 28 mm. However, the steady state wear values of both small bearings are larger than the bedding in of the bigger bearing. The increase of wear from 4.9 $\text{mm}^3/10^6$ cycles to 6.3 $\text{mm}^3/10^6$ cycles demonstrates the effect in increased bearing size within the boundary conditions.

A similar study was carried out by Bowsher *et al.* (2005), where three bearing sizes (28, 40 and 56 mm) were tested. Their tests ran for 3 million cycles where the values of steady state started to decrease with increasing bearing size. However, all three bearings types had

different clearances. The smaller (28 mm) bearing had a clearance of 84 μm , and the 40 and 56 mm bearings had approximately three times that clearance (240 and 280 μm respectively). Therefore if only considering the clearance of over 240 μm for the two bearing sizes a small decrease is observed on the steady wear with increasing the bearing size.

Affatato *et al.* (2006) reported a decrease in wear with increasing head size. They tested 28, 36 and 54 mm bearings. However, the larger prosthesis had twice the clearance (200 μm) in relation to the two smaller prostheses of 28 and 36 mm (90 μm and 105 μm , respectively). Nevertheless, the same correlation was found with the increased diameter size.

Leslie *et al.* (2008) tested different surface replacement diameters and found that larger bearings (55 mm diameter) reached the steady state quicker than smaller ones (39 mm). Hence, larger amounts of wear were acquired during the bedding in phase on the smaller bearings for the same test conditions. The steady state wear for both bearing sizes after the bedding-in reached the same value in this study.

Al-Hajjar *et al.* (2012) also reported a decrease of mean wear rates with increasing the head diameter from 28 to 36 mm. The clearances used for these two bearing sizes were similar. The 28 mm bearings had a mean clearance of 40 μm and the 36 mm bearing had a mean of 45 μm (Table 4-1).

A summary which encapsulates the results from the above studies is on Table 1-4. To note, the information extracted from these studies is purposely categorised with the same clearance within the study for comparison of different bearing sizes. These studies indicate that when the bearing is operating in a mixed lubrication, the wear decreases in comparison to boundary lubrication. However, with increased head diameter the wear can decrease further due to better lubrication leading to fluid film conditions which can occur in hip simulators (Dowson *et al.*, 2000). This is highlighted more on the bedding in phase as the steady state figures are relatively close. On the other hand, if the components are operating in the boundary conditions, the increase of head size increases wear due larger sliding distances when articulating (Smith *et al.*, 2001).

The increase of head size of a polymer couple is not advisable because the articulation of these would be in the boundary lubrication regime and as observed by Smith *et al.* (2001), the increase of such bearing increases the wear (Clarke *et al.*, 1996). In contrast the CoC articulation behaves like MoM due to the hard bearing material.

Table 1-4. *In vitro* wear of MoM joint replacement with increased head size

Author (Year)	Clearance (μm)	Bearing diameter (mm)	Bedding in (mm^3/Mc)	Steady state (mm^3/Mc)	Comment
Smith <i>et al.</i> (2001)	60	16	N/a	4.85	Decreased bedding in and steady state wear with increasing bearing size
		22	N/a	6.30	
		28	1.62	0.54	
Bowsher <i>et al.</i> (2005)	240 280	40	N/a	0.39	Decreased steady state wear with increasing bearing size
		56	N/a	0.32	
Affatato <i>et al.</i> (2006)	90 105	28	2.21	0.33	Decreased wear with increasing bearing size
		36	0.85	0.28	
Leslie <i>et al.</i> (2008)	120	39	2.58	0.10	Decreased bedding in with increasing bearing size
		55	1.15	0.09	
Al Hajjar <i>et al.</i> (2012)	45	28	N/a	0.99	Decreased wear with increasing bearing size
		36	N/a	0.35	

- Clearance (MoM)

The work by Chan *et al.* (1999) demonstrates how the increase in clearance affects the wear for the 28 mm bearings tested. They had three types of bearing materials, wrought with low carbon, wrought with high carbon and cast with high carbon content. In their analysis, when this groups are clustered together without much relative change of the surface roughness (5 to 10 nm), the total volumetric wear increases with increasing clearance. It can also be seen by material category that based on the means small increments occur due to increase in clearance.

Scholes *et al.* (2001) reported lower steady state wear with the increase of clearance for a 28 mm diameter bearing. However a significant difference was not found for either the bedding in or the steady state.

Dowson *et al.* (2004) also compared large bearing components (55 mm) and small (36 mm) with different clearances. It was evident from this study that a trend exists, where the increased clearance increased the bedding in wear. To note, this is only occurs when the lubrication is operating on the mixed lubrication regime.

Angadji *et al.* (2007) tested the same size bearings with different clearances under different conditions. The conditions were reduced load for walking, jogging and standard walking. Their bedding wear for two of their conditions (reduced load and jogging) indicated that increasing the clearance generated larger wear. However it is difficult to assess a pattern under their normal walking conditions, and the data suggest the opposite to the other studies. The steady

state data for standard walking conditions is split into three sections. It can be argued that in the first and second section, the increase in clearance generated larger wear. However, overall the normal walking conditions showed a lot of scatter and it may be arguable that more points are required to come to a conclusion.

A summary which encapsulates the results from the above studies is on Table 1-5. To note, the information extracted from these studies was purposely categorised with the same bearing diameter within the study for comparison of different clearances.

As it has been pointed out in the last two sections, MoM wear is sensitive to the geometry and lubrication conditions and previous studies have addressed these factors with hip simulator testing (Kretzer *et al.*, 2009). However, these studies were carried out with can be considered as optimal testing conditions. Thus, these trends (Figure 1-11) apply only under optimal testing conditions and may not reflect the full spectrum of *in vivo* cases.

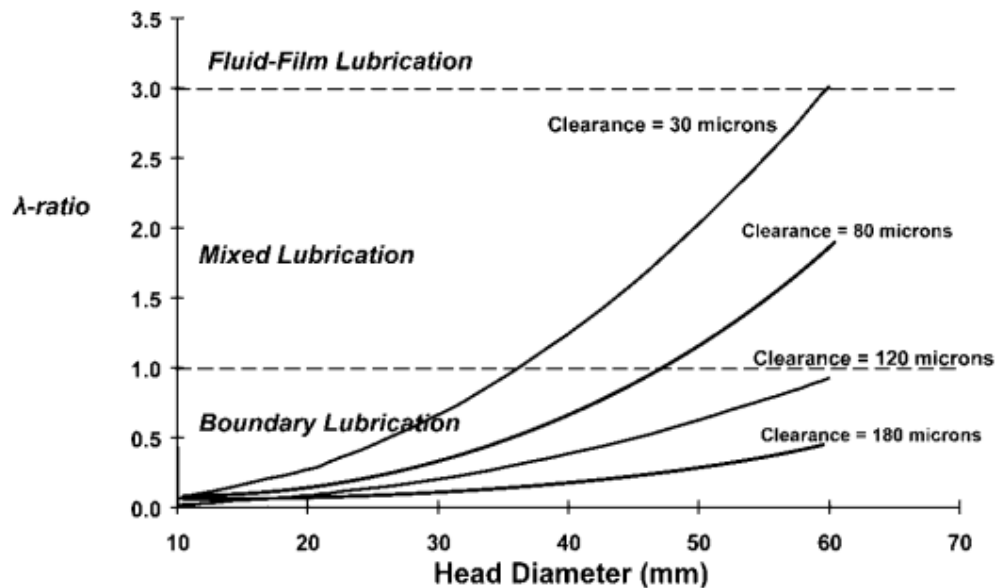


Figure 1-11. Summary graph to elaborate on how a favourable film-thickness-to-surface-roughness ratio (lambda ratio) is desirable in order to maintain low friction between the articulating surfaces for MoM studies under optimal testing conditions. Figure 1 from Silva *et al.*, 2005.

Table 1-5. Wear of MoM joint replacement with increased clearance *in vitro*

Author (Year)	Bearing diameter (mm)	Clearance (μm)	Bedding in (mm^3/Mc)	Steady state (mm^3/Mc)	Comment
Chan <i>et al.</i> (1999)	28	57	0.21	0.06	Increased wear with increased clearance
		65	0.24	0.07	
		100	0.76	0.11	
Scholes <i>et al.</i> (2001)	28	44	0.69	0.09	No significant increase of wear with increased clearance
		80	0.82	0.25	
Dowson <i>et al.</i> (2004)	36	105	2.32	N/a	Increased wear with increased clearance
		124	2.81	N/a	
		143	3.51	N/a	
	55	83-129	0.76	0.09	
	54	254-307	3.28	0.17	
Angadji <i>et al.</i> (2007)	48 (reduced walking)	100	3.94	0.25	Increased wear with increased clearance
		150	5.77	0.32	
		200	5.07	0.33	
		300	5.71	0.31	
	48 (jogging)	100	3.58	N/a	Increased wear with increased clearance
		150	5.10	N/a	
		200	7.06	N/a	
		300	6.74	N/a	
	48 (normal walking, steady state section #3)	100	2.11	0.19	Decreased wear with increased clearance
		150	2.57	0.15	
		200	0.33	0.19	
		300	1.18	0.33	

- Material

Perhaps the first step for differentiating the materials is by soft or hard materials. Soft materials like polymers are easily deformed and operate in the boundary lubrication despite high surface finish on the opposite bearing (Scholes and Unsworth, 2000). This means that wear from these are relatively linear, however, the increased area due to creep and wear of the specific material play a role on the subsequent amount of wear due to increased contact area. Scholes *et al.* (2001) studied the wear comparison of MoM's and MoP under the same conditions, which demonstrated the polymer wears more and have a steady state wear

throughout unlike the metals. To consider, the metal head used on the polymer were scratched which may account for the higher wear in comparison to the other studies. Hard materials on the other hand have an initial bedding-in (or running-in) wear rate under standard testing conditions and after, the wear rate decreases to what is commonly known as steady state (Chan *et al.*, 1999, Nevelos *et al.*, 2001, Vassiliou *et al.*, 2006). The decrease in wear after the first measurement point would indicate a better fluid film performance created after the initial wear-in period. However if the lubrication is disrupted after the initial bedding in, this can lead to increase wear. Some methodologies have been developed creating this type of condition and sometimes they are referred to adverse conditions. The adverse conditions will be covered in Section 1.6.3.

Metal bearings can be manufactured via different processes which influence their properties. Chan *et al.* (1999) did not see any significant difference between wrought with low carbon, wrought with high carbon and cast with high carbon content in their analysis for the same size bearings. However, the comparison was not controlled for surface roughness and clearance.

Another type of hard-on-hard bearing such as ceramic-on-metal can be employed and may reduce wear on the basis that wear through adhesion should be eliminated. Firkins *et al.* (2001a) tested CoM couples and found reduced wear in comparison to MoM bearings. It was thought that one of the reasons for the decrease in wear was the high surface finish of the ceramic head which did not change during testing. Furthermore, the reduction of adhesive wear can play a role in the synergism of the overall wear. They reported no sign of bedding in the CoM wear unlike the MoM bearings. CoM bearings under different swing phase loading conditions have been reported not to be as critical as in MoM (Williams *et al.*, 2007).

Ceramic materials overall have demonstrated low wear rates under standards testing conditions and in some cases very difficult to determine the wear or show significant difference between different materials (Nevelos *et al.* 2001, Smith and Unsworth, 2001). Modern ceramics have reduced grain sizes that to reduce the wear and fracture via improved manufacturing processes. Nevelos *et al.* (2001) tested the difference from a non-HIPed and HIPed ceramics bearings. They demonstrated lower wear on the HIPed, but wasn't significant. One of the potential factors influencing the low wear of ceramics may be due to the low friction and fluid film lubrication (Scholes and Unsworth 2000 and Brockett *et al.* 2007).

1.6.3. *In vitro* malposition and adverse conditions

a) *Rotational malposition*

The inclination angle of the cup is an important subject of study for hip joint replacements and has been the interest of study for many laboratories. The three main reasons considered for evaluating different cup inclination angles are that; 1) radiographs show a variation of inclination angles in patients, 2) theoretically, changing the cup inclination angle changes the contact area and thus affects the wear, and 3) it is important to understand and replicate the wear mechanisms as found in retrievals. What needs to be considered when evaluating results from different studies is that there is a variety of designs, the contact area due to geometry cannot be assumed equal for all and the hip joint simulator design can influence the location of the contact area. Therefore, it is expected to have variability between different laboratories and studies. Overall, the *in vitro* testing of different cup inclination angles indicates that the material can influence the results.

Ceramic bearings do not seem to be affected by the cup inclination angle when tested in a hip joint simulator under a walking gait cycle. Nevelos *et al.* (2001) tested ceramic bearings with different cup inclination angles (45° and 60°) and their results indicated that the wear did not increase with the increased cup inclination angle. Affatato *et al.* (2004) also tested various angles (23°, 45° and 63°) with alumina bearings and there was no correlation found between the wear and cup inclination angle. More recent studies by Al-Hajjar *et al.* (2010) demonstrate the same with third generation (BIOLOX® delta) of Alumina Matrix Composite (AMC) HIPed between a 55° and a 65° cup inclination angle. Similar testing demonstrates the same results for CoC and MoP (Halma *et al.*, 2014).

In contrast metals have indicated that the cup inclination angle can affect the wear when tested under a standard walking cycle. The study by Williams *et al.* (2008) demonstrated that a higher cup angle affects the wear rate in metal-on-metal bearings. Increasing the cup inclination angle from 45° to 55° resulted in an increase on the bedding-in wear (approx. $1 \text{ mm}^3/10^6$ cycles higher for the 55° cup angle) and on the steady state wear by approximately $1 \text{ mm}^3/10^6$ cycles (Williams *et al.*, 2008). Also, surface replacements studies demonstrated an increase on the wear under a steeper angle (Leslie *et al.*, 2009). Furthermore, when different heads sizes were tested, the results indicate that a smaller head size can be more susceptible to edge contact, leading to higher wear under a steeper cup inclination angle (Al-Hajjar *et al.*, 2012). The wear difference between a 28 mm and a 36 mm head under a steep inclination angle from Al-Hajjar *et al.* (2012) was due to smaller contact area creating higher stresses. This reinforces how the bearing design can play a role on the wear.

Angadji *et al.* (2009) also tested metal bearings with different inclination angles. The study resulted in small increase in wear on the components with the higher inclination angle (positioned at 60°) than the lower ones (35°). The steady state difference between the two angles was 1.5 mm³/10⁶ cycles. The study shows no difference in the bedding in and in the transition phase for all the components. A difference was only found at the steady state. If the bedding-in (up to ~0.6 x 10⁶ cycles) wear from the 60° cup angle is removed from the analysis, the results could be interpreted differently. The wear from these does not seem to go through a transition zone unlike the other angles (35° and 50°). If the mean wear of the 60° cups is taken from 0.6 x 10⁶ cycles onwards, it results in 1.8 mm³/10⁶ cycles. In comparison, the steady state wear was 1.7 mm³/10⁶ cycles, which is hardly any difference. Hence it may be reasonable to assume that their high inclination angles do not go through a transition phase and keeps wearing more due to the smaller contact area and high stresses i.e. proximity to the rim area.

The difference on the wear due to an increased cup inclination angle for ceramic-on-ceramic (Nevelos *et al.*, 2001, Affatato *et al.*, 2004, Al-Hajjar *et al.*, 2010) and metal-on-metal (Williams *et al.*, 2008, Angadji *et al.*, 2009, Al-Hajjar *et al.*, 2012)) bearings under standard conditions may be due to the sensitivity of the contact area (Williams *et al.*, 2008). Which implies the change in stress is sufficient to cause an effect on the wear. Furthermore, an influential factor could be the material properties as the ceramics are harder and tougher (Table 1-6).

Table 1-6. Comparison of material properties for metal and ceramic THR bearings

Bearing material	Young's modulus (GPa)	Hardness, HV1 (GPa)	Source
Ceramics			
AMC (BIOLOX [®] Delta)	358	19	CeramTec, 2014
Metals			
CoCrMo	230	4	Gilbert, 2007 Sahin <i>et al.</i> , 2011

b) Microseparation simulation (translational malposition)

After several attempts with different conditions (Nevelos *et al.*, 2001, Nevelos *et al.*, 2001), Nevelos *et al.* (2000) managed to replicate the wear scar as found on some ceramics heads from retrieval studies (Nevelos *et al.*, 1999, Nevelos *et al.*, 2001). These adverse conditions were produced by displacing the centres of rotation between the head and the cup via a force generated by a spring in the medial-lateral direction. This method was termed microseparation (Figure 1-12). This microseparation produced edge loading during the swing phase of the cycle, which meant the head articulated away from the spherical region and onto the contours of the rim of the cup. In this method, the cup was translated when the swing phase load was sufficiently low such that the spring forced the cup away. The microseparation developed on

the Leeds Mark II hip simulator created a dynamic displacement which was kept constant at approximately 0.5 mm. From these studies, it was learned that; 1) edge loading conditions resulted in higher wear and replicated the stripe wear as *in vivo*, 2) the severity of the wear was dependant on the swing phase load (Stewart *et al.*, 2001).

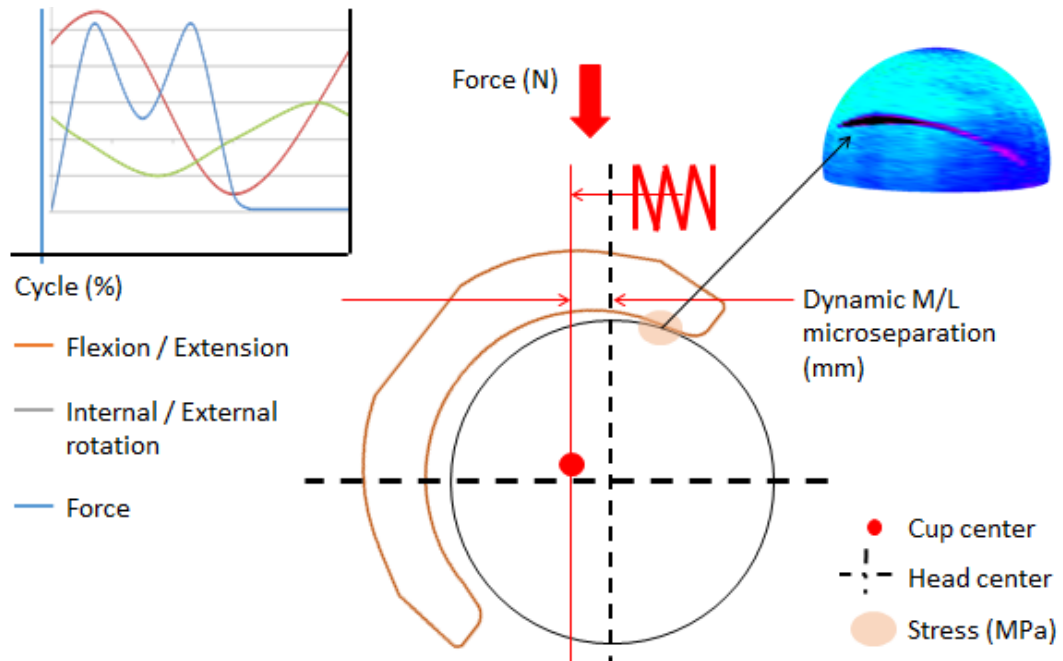


Figure 1-12. Schematic of the test methodology to apply edge loading with a dynamic microseparation.

The microseparation methodology has been adapted in other laboratories (Manaka *et al.*, 2004, Williams *et al.*, 2011) and equipment but certain dissimilarities exist between some studies. The dissimilarities vary from the minimum and maximum load employed, others use a negative force to produce a vertical distraction, and changes to the magnitude of microseparation tested. While others studies only apply edge loading in a different manner in shock type of devices which are very different to hip simulators (Uribe *et al.*, 2013).

Microseparation has been increased to up to 2 mm (Clarke *et al.*, 2009) and other studies have applied different magnitudes of microseparation (Schroeder *et al.*, 2014) to evaluate ceramics under edge loading but the studies suggest the same, increased wear and stripe wear on the heads that has a higher surface roughness. Ceramics are not the only material tested under edge loading conditions.

Translating the microseparation methodology onto another type of simulator may not always result in the same results and increased wear. Williams *et al.* (2003) tested polymer liners articulating against ceramic heads and the study resulted in a decrease in wear rate under microseparation conditions when compared to standard conditions. To note, the methodology to replicate edge loading was different due to the design of the hip simulator as a negative

force was applied on the head fixture to displace the head away from the cup by approximately 0.5 mm. This study didn't measure the medial-lateral load applied thus the severity of edge loading cannot be compared to the Leeds II Hip Simulator. However based on the results, it can be proposed lower loading on the rim of the cup due to the retraction of the head and less severe than the Leeds II Hip Simulator.

Polymer samples would have a different effect under edge loading due to the difference in modulus when tested against a metal or ceramic head. It is important to consider the effects of edge loading on polymer materials as under edge loading, high stresses can deform the rim of the polyethylene liners (Partridge *et al.*, 2017), and retrievals have reported cracking in the rim area of the polymer (French *et al.*, 2012).

Like the simulator design, there can be many variables that can alter the results. The positioning of the femoral and acetabular component in the hip simulator can alter the results of the test, such as the position of the wear scar. The tilt on the stem can alter the location of the stripe wear on the head. In the study by Stewart *et al.* (2001), the wear scar was more noticeable located on the top/polar section of the head. Al-Hajjar *et al.*, (2014) changed the orientation (anteversion) of the cup holder 30°. Their results changed the orientation of the stripe wear. Retrieval studies have indicated variability in the location and orientation of the stripe wear (Esposito *et al.*, 2012), hence the component position and activity of a patient can influence the location of the stripe wear as found *in vitro*.

c) *Wear particle size*

Stewart *et al.* (2001) found that under adverse conditions not only was the wear rate significantly increased for ceramics, but the distribution of the particle size increased and was comparable to *in vivo* (Hatton *et al.*, 2002). Under edge loading the particle size ranged from 10 nm to 1 µm (Stewart *et al.*, 2001). Tipper *et al.* (2002) used SEM and TEM methods to analyse the distribution and came to the conclusion that wear particles with adverse conditions had a bi-modal distribution. Since micro scale particles are not found in non-adverse testing conditions for ceramics, it was implied that larger particles originate from the adverse conditions, when the head strikes/contacts the rim of the cup. Unlike ceramics, MoM wear debris under edge loading did not result in a bi-modal distribution, but a higher size distribution was found when compared to non-adverse conditions (Leslie *et al.*, 2009). There can be different ways to replicate edge loading and various parameters could influence the results. When analysing and comparing the wear particles under edge loading conditions, the severity of edge loading needs to be considered, as it may impact on the size of the particle and the distribution. For example, the force applied on the rim while under edge loading could

generate different results. However, current studies demonstrate that adverse conditions (edge loading) generate a higher particle size distribution for hard-on hard bearings.

d) Effect of rotational malposition in combination with microseparation

Hard-on-hard bearings have shown to increase the wear when tested under edge loading conditions. However, as the wear can increase due to an increased cup inclination angle, it is also important to understand the effect of the cup inclination angle while under microseparation conditions. The studies carried out by Williams *et al.* (2008) and Leslie *et al.* (2009) demonstrated that on MoM the cup angle alone can have an effect on wear, and both of these studies conclude that, when a high inclination angle was tested in combination with edge loading, the wear increases further. These previous studies did not test high versus low angle exclusively with microseparation, but the wear rates were higher for a high cup inclination angle and microseparation conditions. A further study by Al-Hajjar *et al.* (2013) concluded that the cup inclination angle did not affect the wear rate while under microseparation conditions for 28 and 36 mm MoM bearings.

Overall, it can be assumed that metal bearings are more sensitive to cup angles. Alternatively, CoC seem to behave differently and appear not to be affected when tested under a different cup inclination angle (Al-Hajjar *et al.*, 2010), and other studies indicate the same when tested under standard conditions such the study by Nevelos *et al.* (2001) and Affatato *et al.* (2004). There are factors to consider when dealing with translational malpositioning, such as the design, in particular the rim, and the actual conditions during the testing.

During most of the adverse testing conditions carried out at the Leeds laboratory, the experiment was set-up to have as an input, a dynamic separation of approximately 0.5 mm medial-laterally. If the cup/head translates the same amount for different cup inclinations angles, it can be deduced that it does not impact the wear outcome even though the contact mechanics are different due to angle.

1.7. Rationale

Pre-clinical testing is required to determine and reduce the risk of hip joint replacement failures. There are many factors that need to be considered for the testing of hip joint replacements, and these include the surgical delivery in the form of implant positioning, the activity and patient variability. Edge loading has been identified as one of the factors leading to the revision of hard-on-hard bearing implants, mainly metal-on-metal (Kwon *et al.*, 2010). In ceramic-on-ceramic bearings, edge loading has been previously identified in retrievals by a stripe wear on the femoral heads and rim damage on the acetabular cup. Previous testing methodologies for edge loading applied a dynamic microseparation to displace the cup and create a contact between the head and the rim of the cup in a hip joint simulator (Nevelos *et al.*, 2000). These studies led to higher wear for hard-on-hard bearings, however the input was controlled to a specific dynamic separation of 0.5 mm in the medial-lateral axis. When testing under a fixed displacement controlled input, the individual evaluation of other parameters such as the cup inclination angle was not possible due to the constraints of the test methodology. The influences of edge loading are multiple and overlapping and hard to measure *in vivo*. Therefore, a method is required which can encompass the variables for surgical malposition in order to understand the relationship of wear due to translational malposition and edge loading.

Current practice of standard testing in hip joint simulators is to aim to set-up the head and cup components concentric for certain reasons; 1) to allow a transfer of load and rotation at the same time, 2) to test the bearing surface only, 3) to ensure the wear is consistent, 4) to ensure the wear testing consistency between different facilities, 5) for wear measurement points, the components need to be extracted and then re-setup, thus aiming to set in the same location (ISO14242-1, 2014). Therefore the set-up is bearing designed and testing consistency driven. The purpose of the standard is to assess the wear performance of the bearing surfaces of the head and the cup under one average and simplified activity with one set-up (i.e. cup inclination angle, cup version angle, tilt). In reality, a variation of the cup inclination (and version) angle occurs during surgical delivery (Callanan *et al.*, 2011), with variations in the contact area of the cup and variations in the load transfer/kinematics, i.e. biomechanics due to activities (Bergmann *et al.*, 2001). Thus multiple testing combinations should be explored related to patient surgical delivery, patients' anatomy and biomechanics that can influence the wear.

1.8. Aims and objectives

The principal aim of this study was to develop a testing methodology where different factors leading to the occurrence of edge loading can be evaluated individually to understand the severity.

The aim of this study was achieved by completing the following objectives:

- To determine the influence of different levels of **translational malposition** on the occurrence and magnitude of dynamic separation conditions, severity of edge loading conditions and the level of wear of ceramic-on-ceramic (BIOLOX[®] delta) bearings in total hip replacement.
- To determine the influence of **rotational malposition** on the occurrence and magnitude of dynamic separation conditions, severity of edge loading conditions and the level of wear of ceramic-on-ceramic (BIOLOX[®] delta) bearings in total hip replacement.
- To determine the influence of magnitude of **the joint reaction force** on the occurrence and magnitude of dynamic separation conditions, severity of edge loading conditions and the level of wear of ceramic-on-ceramic (BIOLOX[®] delta) bearings in total hip replacement. This is achieved by modifying **the swing phase load**.
- To determine the influence of the **medial-lateral force applied relative to the translational mismatch** on the occurrence and magnitude of dynamic separation conditions, severity of edge loading conditions and the level of wear of ceramic-on-ceramic (BIOLOX[®] delta) bearings in total hip replacement. This is achieved by modifying the **spring constant**.

1.9. Outline of studies

The studies were carried out in with different phases. Phase 1 and 2 which relate the function of the mechanical aspects and which are not wear related were termed biomechanical studies.

- Phase 1 in these studies provided a wider variation of test parameters (n=3).
- Phases 2 in these studies were selected conditions from Phase 1. New samples were tested (n=6).
- Wear studies: The data gathered from Phase 1 and 2 was compared against the wear studies. New samples were tested (n=6).

Key measurements were derived from the output signals (Figure 1-13).

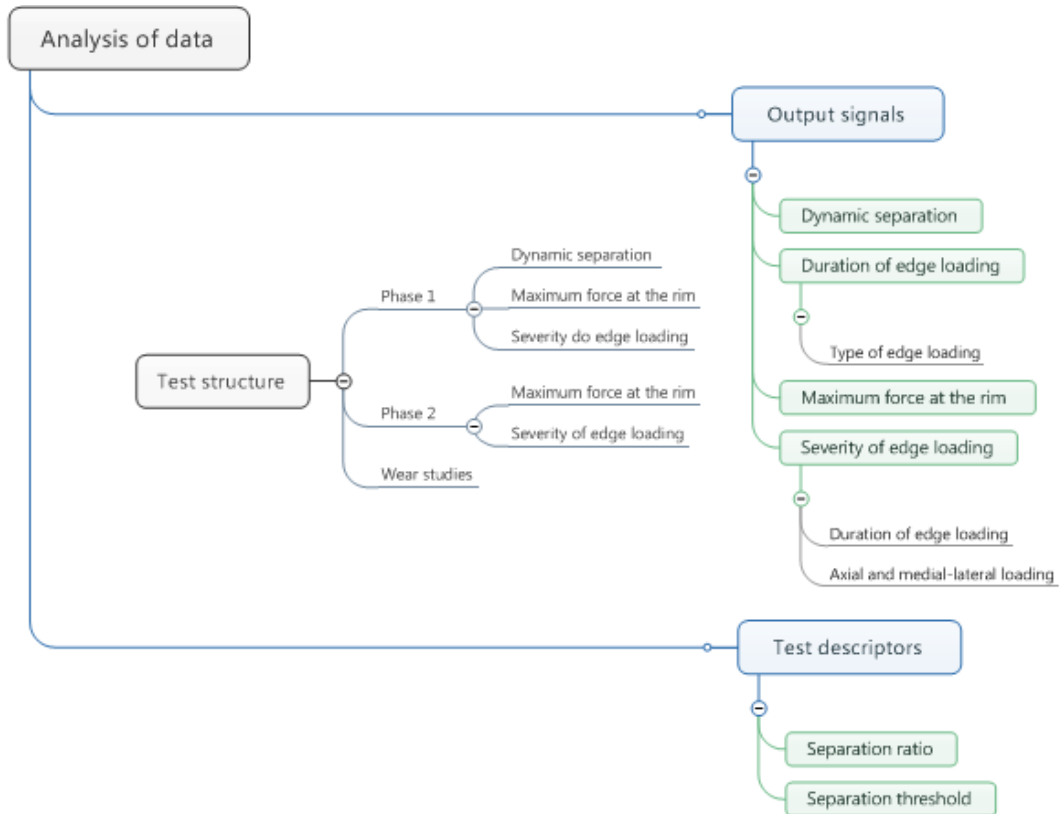


Figure 1-13. Schematic of the analysis of data and the test structure.

Details of the parameters tested in the studies are expanded in Table 1-7.

Table 1-7. Matrix of hip simulator test conditions

Hip simulator study	Variable	Magnitude			
Translational malposition	Mismatch (mm)	1	2	3	4
Rotational malposition	Cup inclination angle (°)		45	55	65
Joint reaction force	Swing phase load (N)			50 - 500	
Medial-lateral force	Spring constant (N/mm)		50	100	200

1.10. Hypothesis and research questions

Hypothesis: The combinations and magnitudes of the translational and rotational component positioning influence the severity of edge loading and wear.

Research questions:

- What is the effect of the different magnitudes and combinations of translational and rotational malpositioning on the severity of edge loading, magnitude of microseparation, load acting on the rim of the cup, the severity of edge loading and wear?
- How does the increase in medial-lateral translational mismatch affect the wear rate on different angles?
- At what point does the amount of medial-lateral translational mismatch dramatically influence the wear with a steep cup inclinations angle?
- Does the time spent on the rim of the cup with increased medial-lateral translational mismatch affect the wear?
- Does the increase in axial force while under a translational mismatch increase the severity of edge loading?
- Does the increase in axial and medial-lateral force increase the severity of edge loading?
- What is the effect of the increased force to create medial-lateral separation on the wear?

2. Methodology

2.1. Materials

Ceramic-on-ceramic (CoC) bearings (DePuy Synthes Joint Reconstruction) of 36 mm in diameter (Figure 2-1) were used through-out all the hip joint simulator studies. This material is the fourth generation ceramics, Alumina Matrix Composite (AMC) also commercially known as BIOLOX[®] delta (CeramTec, Germany). This material contains mainly Aluminium Oxide, with added Zirconium Oxide and other mixed oxides. Unlike other ceramics commercially available, this material has a small grain size (Aluminium Oxides) of less than 0.6 μm . Further properties are found in Table 2-1. The liners were manufactured to fit the PINNACLE[®] design, where the cup was taper locked on the 56 mm diameter. The cup was neutral and the head had a +5.0 mm offset. The mean clearance of these bearings was 90 μm .



Figure 2-1. AMC Ceramic bearings (BIOLOX[®] delta).

Table 2-1. Properties of BIOLOX[®] delta adapted from the scientific information and performance data, CeramTec (2014).

Variable	Unit	Average	Variance
Aluminium Oxide	Volume (%)	81.6	0.17
Zirconium Oxide	Volume (%)	17	0.1
Other oxides	Volume (%)	1.4	0.01
Density	g/mm^3	0.00437	0.01
Grain size (Aluminium Oxide)	μm	0.56	0.036
4 point bending strength	MPa	1384	67
Young's modulus	GPa	358	1
Fracture toughness	$\text{MPa m}^{1/2}$	6.5	0.3
Hardness (HV1)	GPa	19	-

2.2. Hip joint simulator

2.2.1. Leeds Mark II Physiological Anatomical Hip Joint Wear Simulator

The Leeds II hydraulic hip joint simulator is six station testing equipment with a five-axis machine allowing five degrees of freedom, flexion/extension ($+30^\circ$ to -15°), internal/external rotation ($+10^\circ$ to -10°), medial-lateral translation (0 to approximately 5 mm), anterior-posterior translation (0 to approximately 5 mm) and a vertical load (50 N to approximately 3000 N). The vertical load is applied via the pressure pump and the servo valve which was linked to all six stations. This simulator has been used extensively for over a decade (Nevelos *et al.*, 2000, Firkins *et al.*, 2001b, Stewart *et al.*, 2003, Al-Hajjar *et al.*, 2013).

2.2.2. Fixtures

The femoral head was positioned so that its centre of rotation matched the centre of rotation of the hip simulator. The stem was held in place with bone cement (poly methyl methacrylate, PMMA) in a metallic holder (Figure 2-2). The femoral head was taper locked on a stainless steel stem (C-STEM™ AMT, DePuy Synthes, UK) with 12/14 taper. The head was aligned to a mark on the stem, thus the orientation was kept the same after head removal and re-assembly during measurement points. The stem fixture was mounted firmly in the hip simulator. Silicon was used to seal any remaining gaps which could lead to lubricant leakage.



A



B

Figure 2-2. C-STEM™ AMT (A) and, ceramic head mounted in the stem fixture with bone cement (B).

The acetabular cup was inserted in a 56 mm titanium shell (PINNACLE®, DePuy Synthes, UK) which was held in place using bone cement in a cup fixture (Figure 2-3). The assembly was also positioned such that the loading was transmitted via the centre of the cup. The cup was aligned to a mark on the metal shell, thus the orientation was kept the same after cup removal during measurement points. The cup fixture was mounted in the simulator and held in place so that it can rest on top of the femoral head. The bearing setup of the cup station allows it to maintain concentricity during kinematics.



Figure 2-3. PINNACLE® shell (A) and, ceramic liner inserter in the cup fixture (B).

As the hip simulator applies the force in the vertical axis, different types of cup fixtures were used which allow the cup to be at a higher inclination angle relative to the force vector (Figure 2-4). Bergmann's *et al.* (2001) work describes the resultant joint reaction force with an approximated 10° shift on the frontal plane at peak force, thus a cup fixture potted at 35° equates to *in vivo* cup inclination angles of 45° relative to the joint reaction force acting anatomically (Williams *et al.*, 2008).



Figure 2-4. Two designs of cup the fixtures, top is 65° and bottom is 45° inclination angle.

2.2.3. Kinematics

Flexion and extension were controlled via the hydraulic motor, which applied the same level of motion to all the stations at any one time. The flexion and extension motion was applied to the stem, while the internal and external rotation was applied to the cup. The hip simulator was run at 1 Hz and the input profiles are displayed in Figure 2-5. Vertical loading was applied and controlled by a single feedback loop station. All hydraulic input was controlled by ProSim (Simulator Solutions, UK) software from an input profile file.

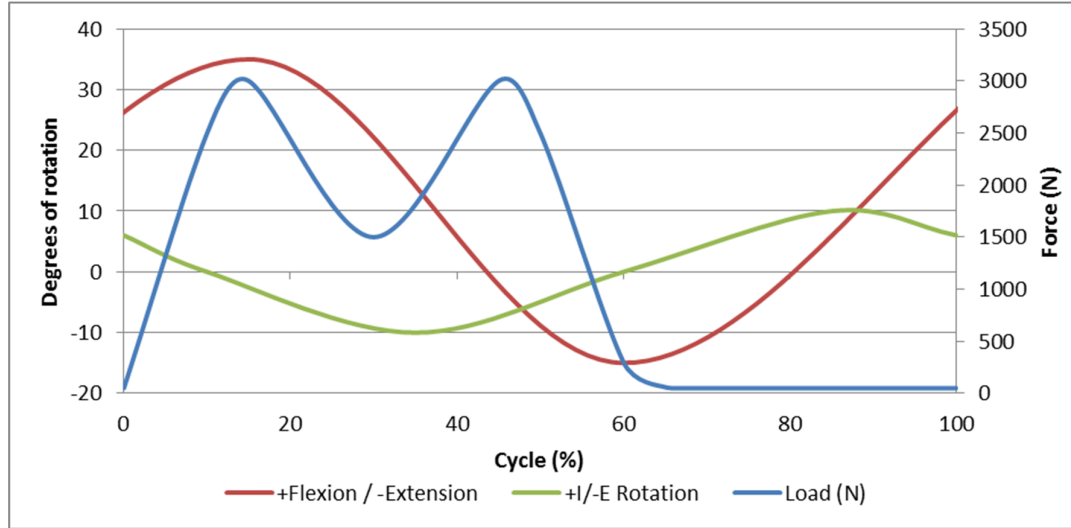


Figure 2-5. Schematic of the inputs in the Leeds Hip Joint Simulator.

2.2.4. Medial-lateral component translational mismatch

In order to define what a medial-lateral component translational mismatch is, first it is important to define the starting position of the test samples.

Definitions:

Axially aligned

The centre of the femoral head and the centre of the acetabular cup lie in close proximity of each other when a load is applied on the cup in the hip simulator. This is dependent on the design of the samples, the actual sphericity tolerance and the actual bearing clearance. Determining the actual centre point of either of the test samples and during assembly is beyond the capabilities of the current study and not within the scope of these studies. However to continue this work, it is first necessary to interpret what is 'axially aligned' and clarify its meaning. The definition of axially aligned for the purposes of this work is when the head and the cup centres are in close proximity of each other, such that they are axially aligned due to loading applied in the vertical axis. When the components are axially aligned,

this was considered as the centre of the assembly (head and cup) and it was measured relative to a reference plane in the medial-lateral axis. During the test, the point where the head and the cup were axially aligned was first measured relative to a reference plane in the equipment (Figure 2-6). Then a mismatch was applied relative to the reference plane medial-laterally.

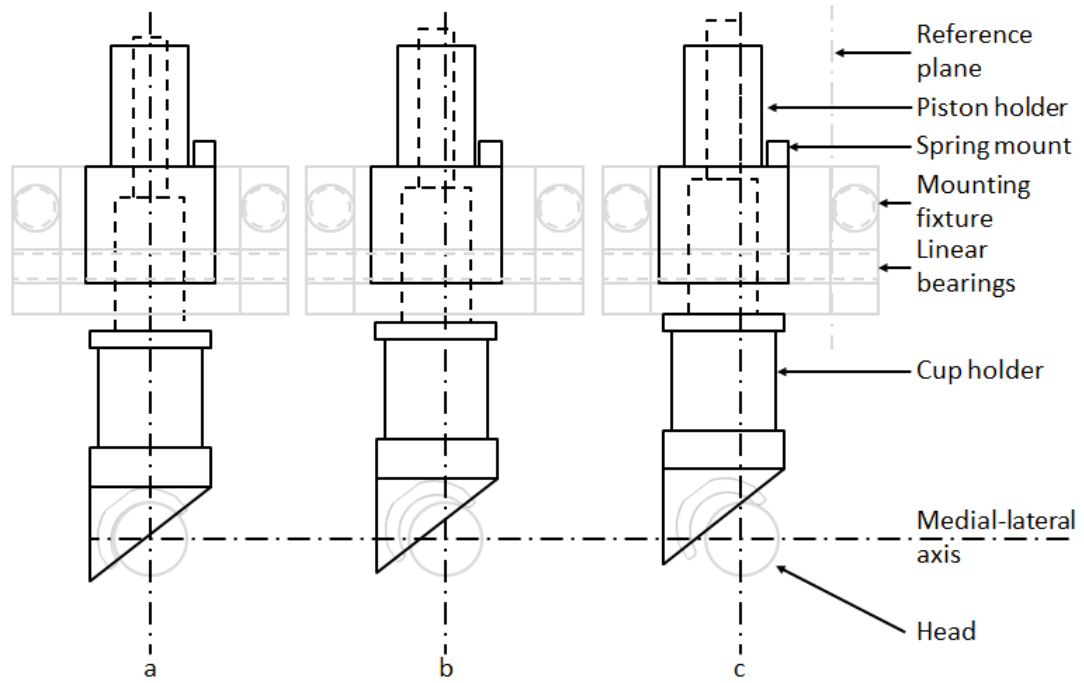


Figure 2-6. Schematic of the cup holder and mounting fixture at different points a) axially aligned, b) and c) with a displacement in the medial-lateral axis away from the reference plane.

Translational mismatch

The translational mismatch was the distance between the centres of rotations of the femoral head and of the acetabular cup measured in the medial-lateral axis during the set-up of components and without any vertical load applied (Figure 2-7). This mismatch was applied with a spring which translated the cup medially (away) from the head, this also introduced a superior translation due to the sphericity of the components and due to the cup version and inclination angle. The mismatch is not dependent of the cup holder weight, a check is performed to ensure when a mismatch is applied that the spring is in contact with the cup holder. When a high vertical load was applied, the spring compressed and the cup 'returned' to the centre of the assembly (Figure 2-7). During dynamic separation, the cup translated away from the centre of the head and the contact area between the components (head and cup) translated away from the bearing surface towards the rim of the cup while retaining contact. Previous studies did not apply a translational mismatch input, instead an input of 0.5 mm dynamic microseparation was applied and maintained consistent throughout the test (Nevelos *et al.*, 2000, Stewart *et al.*, 2003, Al-Hajjar *et al.*, 2013).

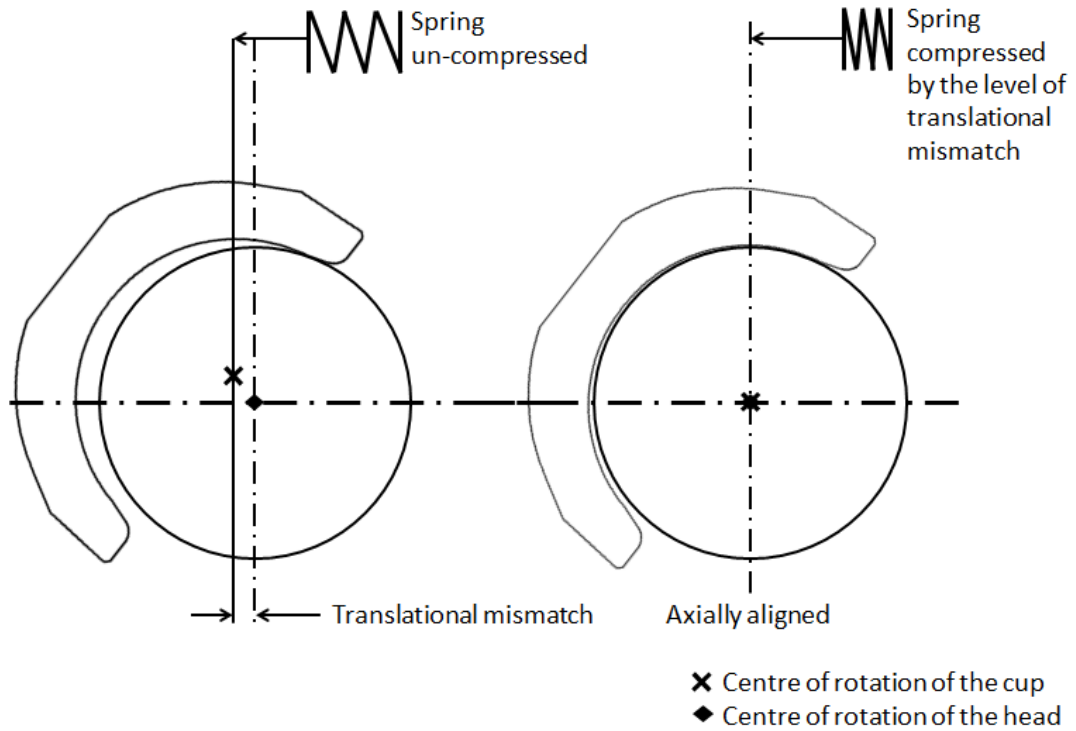


Figure 2-7. Schematic of the medial-lateral component translational mismatch input between the head and cup centre and without a vertical load applied on the cup, and axially aligned when a load is applied.

An external Linear Variable Differential Transformer (LVDT) was used to routinely check during the wear studies the cup holder displacement of the stations (Figure 2-8). The LVDT has a working range of 10 mm (-5 and +5 mm). The cup holder displacement is not the dynamic separation, please see definition of dynamic separation in Section 2.3.5. During test it was compressed sufficiently until operating around the mid-point and checked that it can cover the maximum displacement. An oscilloscope (Tektronix, USA) was used to visualise and measure the cup holder displacement. Readings were taken at different intervals on every station to monitor the displacement of the individual stations.

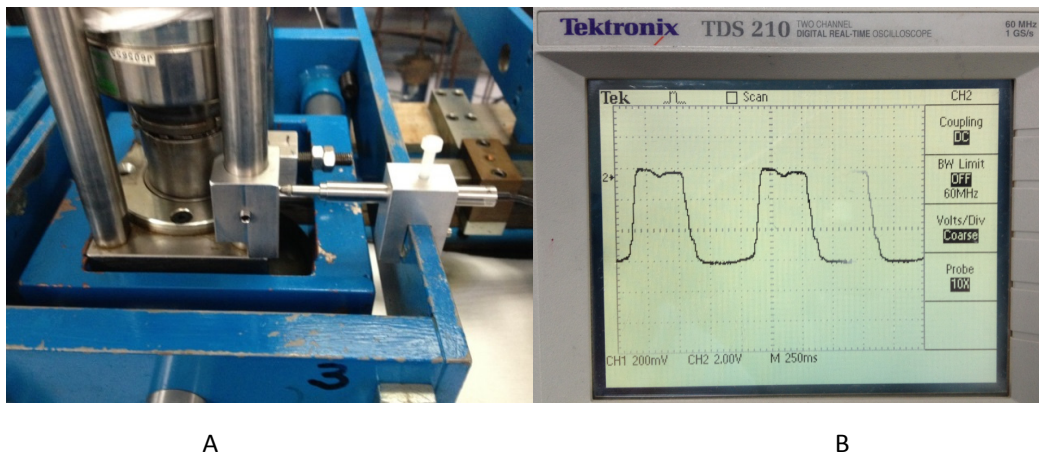


Figure 2-8. LVDT set-up for routine check (A), and visualisation of the cup holder displacement in an oscilloscope (B).

Edge loading

The definition of edge loading is when there is a contact between bearing surface of the femoral head and the rim (or chamfer area) of the acetabular cup while a load is present and transmitted between the two components. The contact area under this scenario tends to be smaller as evaluated in previous studies by Mak *et al.*, (2002) and Hua *et al.*, (2014) and thus the stress increases. Edge loading occurs when the relative displacement of either the head or the cup which is greater than the clearance of the test samples, or when the contact area has migrated away from the bearing surface of the cup without any measurable displacement between the components.

Springs

The springs used to apply the input mismatch on each station on the hip joint simulator have relative small geometrical differences at the end of the coils which differ from station to station. The springs were manufactured with closed ends and ground (Figure 2-9). Thus the geometry is dependent on how much material was machined off and overall individual finish. This variation affects the compressive force required to grip properly before the springs are fully supported by the active coils. The details of the variability from the springs can be found in Appendix A. The approximate distance (\pm SD) required to grip the springs of 100 N/mm was 0.30 ± 0.20 mm.



Figure 2-9. Photograph of a spring used in these studies to illustrating geometrical-end finish.

2.2.5. Monitoring and Data Acquisition System (MDAS)

To acquire, measure and analyse the displacements and loads during dynamic conditions, two independent vertical load cells (type RLC 500 kg, with an accuracy of ± 50 N) from the ProSim software (Simulator Solution, UK), along with two independent LVDTs (D6/0500A-L10, with an

accuracy of ± 0.01 mm) were fitted in two of the stations of the Leeds II hip simulator (Figure 2-10). Six independent sub-miniature compression load cells (type RSL0856, with an accuracy of ± 10 N) were also fitted in each of the six stations to measure the force applied via the spring. The signals from the six sub-miniature load cells, the two vertical load cells, and the two LVDT were sent to a transducer amplifier (Type DR7AC) and processed via a DAQ card (NI USB-6210). All signals were analysed and managed in a LabView (NI Instruments, Germany) program, designated as Monitoring and Data Acquisition System (MDAS). One hundred points per sec were taken for each cycle (1 Hz) on each sensor.

Use of equipment in studies:

The studies were mainly split into two biomechanical studies and a wear study.

The biomechanical studies had two phases:

Phase 1 used only station #3 of the Leeds II hip simulator and the dynamic separation, maximum force at the rim and severity of edge loading were calculated from the output signals measured from the MDAS.

Phase 2 used all six stations from the Leeds II hip simulator. Each station was used separately where the LVDT was swapped on each occasion and the maximum force at the rim and the severity of edge loading were calculated from output signals measured from the MDAS.

The wear studies used all six stations of the Leeds II hip simulator and the use of the MDAS equipment is laid out in Figure 2-10. The cup holder displacement was only measured during the wear studies. An LVDT was placed in close proximity to the position of the spring, see Figure 2-8.

Where applicable, test descriptors are the ratios of the input parameters. These are then compared to the output measurements.

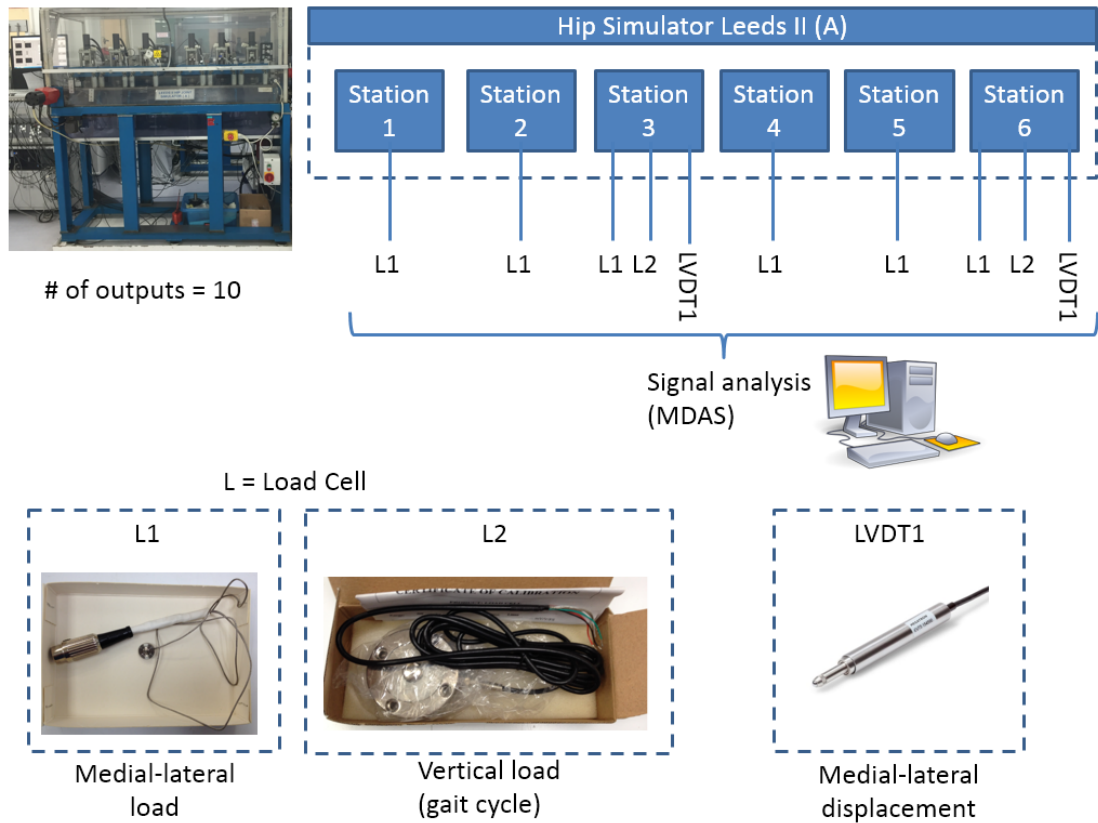


Figure 2-10. Diagram of the Monitoring and Data Acquisition System (MDAS) for the Leeds II (A) Hip Joint Simulator.

2.2.6. Lubrication

New-born calf serum, Gibco® (Life Technologies, New Zealand), diluted to 25% concentration (with 74.97% deionized water and 0.03% Sodium Azide) was used as a lubricant. The protein content was approximately 15 g/L. Sufficient lubricant (500 ml) was poured into the gaiter, ensuring it covered the articulating surfaces when in operation (Figure 2-11). The test cells were topped up with water when necessary due to water evaporation. Care was taken to ensure the articulating surfaces were under constant lubrication. During wear studies, the lubricant was changed approximately every 330,000 cycles (every four days). For each change of lubricant, the test cells were cleaned to remove any particulates and protein deposits via various steps and multiple washes. During the serum change, care was taken to remove protein deposits from the gaiter and surroundings.



Figure 2-11. Leeds Hip Simulator with lubricant serum applied on the stations

Once the serum was extracted and frozen, depending on the stage of the test, it was either disposed or stored.

2.3. Measurements

2.3.1. Gravimetric wear analysis

The wear of the test components was assessed gravimetrically every million cycles. The test components were removed manually with care from the hip simulator with the use of in-house extraction devices and procedures. Test specimens were cleaned and prepared for weighing.

- Cleaning and preparation for weighing

The test components were cleaned via a series of steps aimed at removing lubricant deposits and prepping for weighing. At the end of the cleaning process the test specimens were placed in a weighing laboratory. Care was taken to ensure the beakers and equipment used were cleaned accordingly beforehand.

- Weighing

The components were weighed in a temperature and humidity controlled laboratory; $21\pm 1^\circ\text{C}$ and $45\pm 5\%$ Relative Humidity (RH) after being left in the weighing room for 24 hours. All components were weighed with Mettler Toledo XP205 balance (Mettler-Toledo International, Switzerland, 0.01 mg readability). Test specimens were weighted five times and an average weight was determined. For sets with values outside the ± 0.05 mg range, the weighing was repeated until consistent values were measured within this tolerance. A control sample of the same material and same dimension was kept in the weighing laboratory to reference and normalise the results against. Cumulative wear volume was calculated using the weight loss and density of the materials (Equation 1). The density of the BIOLOX[®] delta (0.00437 g/mm^3) was obtained from the scientific information and performance data (CeramTec, 2014).

Equation 1.
$$Volume = \frac{Weight}{Density}$$

2.3.2. Clearance measurements

The clearances were obtained by subtracting the diameter of the head from the diameter of the cup before each test. A Coordinate Measuring Machine (CMM) Legex 322 (Kemco, UK) was used to measure the diameter and the form of the components. Twenty five measurement points were made for each component using the 'measure a sphere' option. One point was taken at the pole, a ring of 10 points at approximately 20° latitude and a ring of 14 points at approximately 110° latitude.

2.3.3. Volumetric wear analysis

Three dimensional reconstruction (cloud points) of the test specimens was generated using the CMM at every one million cycles. The heads and the cups were positioned accordingly to the alignment mark. The head was mounted firmly on a spigot (Figure 2-12), and the cup was held on the CMM measuring table held in place with plasticine. A 3 mm diameter stylus was used to take 72 traces with 5 degrees between each trace. Each trace had several points (167) with 0.2 mm spacing (pitch) between each point. When measuring the heads, each trace started at the pole and finished 3 mm below the equator. When measuring the cups, each trace started at the trough and finished at the rim. The length of the trace for cups from the trough across into the rim section was 22 mm.

The data was exported to 'Sphere Profiler' software (RedLux, UK) to determine the wear volume and depth of the scar. The wear on the heads was evaluated on each reconstructed surface at every one million cycles. At each interval, the nominal radius was calculated from the selected unworn surface area. The cups were analysed using a script which compared two files, the unworn (reference cup) surface data and the worn surface data. The wear volume of the heads and the cups was calculated by selecting all the worn area until it was of approximate level to the nominal radius of the sample and subtracting it from the nominal radius.

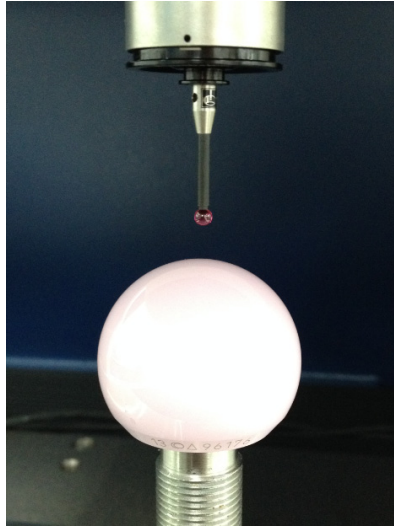


Figure 2-12. CMM and ceramic head set-up

2.3.4. Surface topography analysis

A two-dimensional contacting profilometer (Form Talysurf series, Taylor-Hobson, UK) was used to assess the surface of the test specimens. Measurements were taken before and after the completion of the test (3 million cycles). Three pre-test 19 mm traces were taken on the acetabular cup and the femoral head specimens in relation to the alignment mark. Traces P1 and P2 were normal to each other and traced at the pole (Figure 2-13). The third trace (P3) on the head was carried out by rotating the component 90°, such that the alignment mark was positioned normal to the 90° axis. The cup had the equivalent three traces as the head. The third trace on the cup was taken by rotating the cup approximately 45°. Before each measurement the stylus was “crested” either on the pole of the head or the trough of the cup to find the midpoint of the x and y axis.

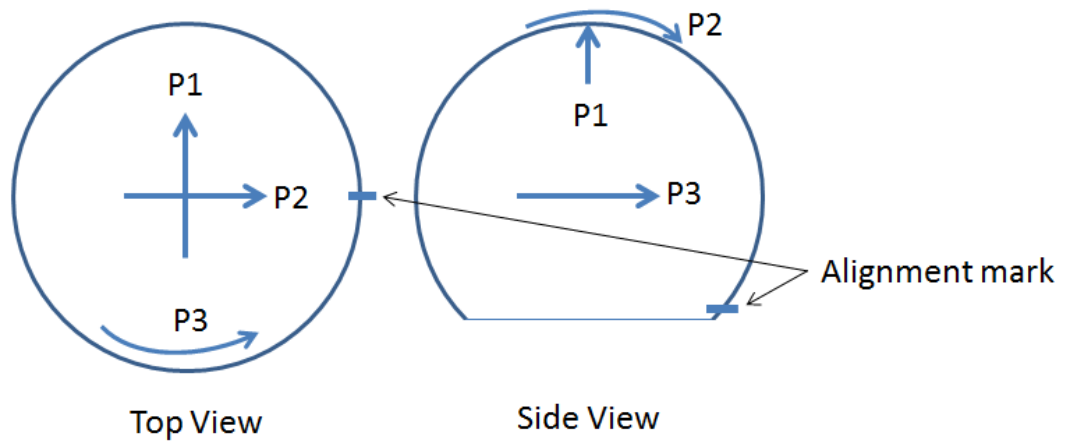


Figure 2-13. Schematic of the three traces performed on the heads before testing.

Two 19 mm traces were taken after the test on the heads; one trace across the pole (P1) and one trace along the longitudinal direction of the stripe wear (P2) as shown in Figure 2-14.

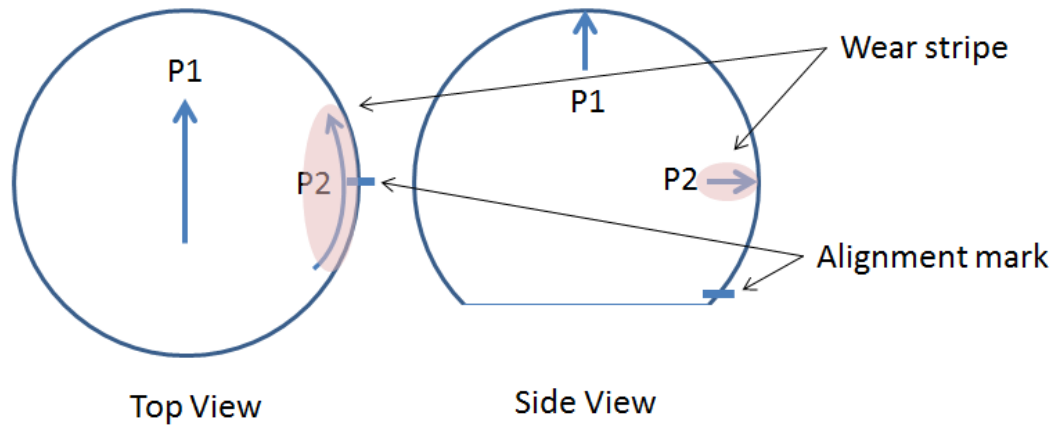


Figure 2-14. Schematic of the two traces performed on the heads after testing.

Surface roughness (R_a), skewness (R_{sk}), and the maximum peak to valley height (R_z) were calculated. R_a is universally recognised as an international parameter for roughness and it is the arithmetic mean of absolute departures of the roughness profile from the mean line. R_{sk} is the measure of symmetry of the profile about the mean line. The two parameters chosen (R_a and R_{sk}) determined the roughness of the surface with indication to the amplitude of the asperities. R_z is the mean peak to valley height, which is the sum of R_p (height of peak), and R_v (height of the valley). The data was analysed using least squares arc with Gaussian filter and a 0.08 mm cut off (30:1 bandwidth). The analysis was done with TalyMap Universal 3.1 Taylor Hobson software Mountains™ and the form removed.

2.3.5. Dynamic separation

Effect of the input mismatch on the cup displacement due to the tilt of the cup holder

The cup holder can translate medial-laterally due to the bearings of each test station. The medial-lateral springs employed to apply a force are not directly aligned along the axis of the head and the cup centre. A high force applied by the spring while an axial force is present tilts the cup holder from the neutral axis (Figure 2-15). The LVDT was positioned above the bearing level to measure the dynamic separation, thus the tilt of the cup holder was measured as a displacement medial-laterally as well. The details of the tilt of the cup holder measured due to a mismatch applied via a spring while under cyclic loading can be found in Appendix B.

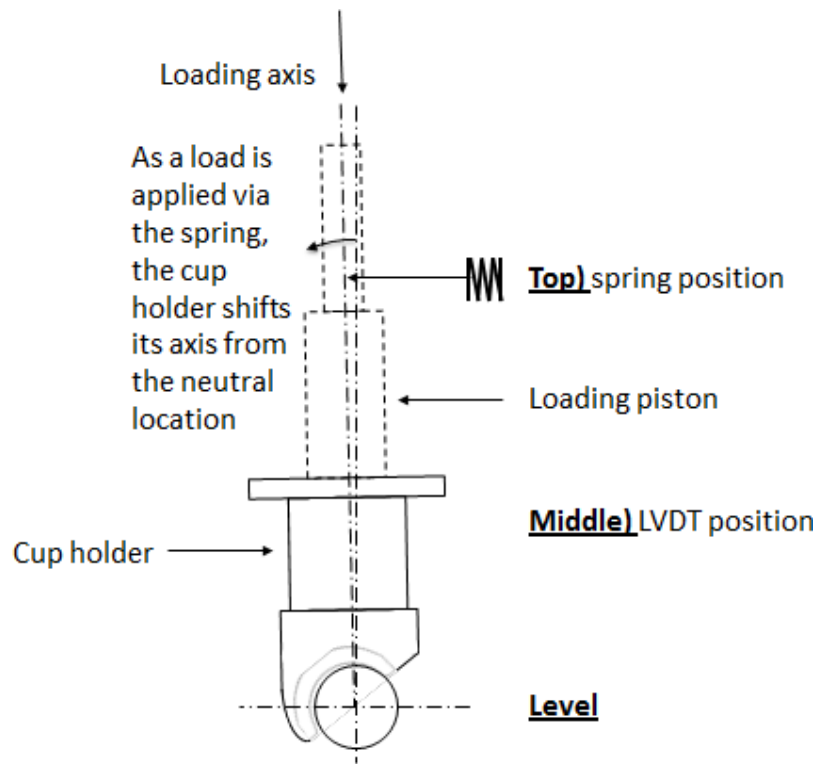


Figure 2-15. Schematic illustrating the tilt on the cup holder due to the position of the spring applying a force at a different position than that of the head and cup centre.

During the set-up the centre of the assembly under a vertical force was measured when the spring was not employed. When a spring was introduced, the new centre of the assembly during cyclic loading was recorded. A calibration was run to determine the difference between the assembly centres relative to a reference plane with and without a spring during cyclic loading. In summary, the results from the Appendix B demonstrates that with the increase of the translational mismatch, the tilt of the cup holder increases due to the force applied, where $F = \text{mismatch} \times \text{spring rate}$ (Figure 2-16).

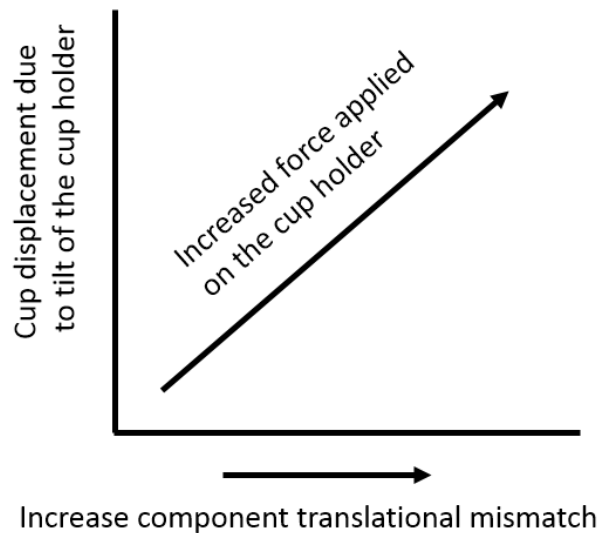


Figure 2-16. Schematic illustrating the effect of the translational mismatch on the cup holder displacement medial-laterally during cyclic loading.

Dynamic separation calculation

The result of the spring's position and force acting medial-laterally alters the behaviour of the system by tilting the cup holder and the assembly centre point termed axially aligned (head and cup assembly point) when a spring was introduced (Figure 2-15). The value corresponding to the change of the centre assembly position due to the amount of force/mismatch acting on the cup holder when a spring was employed was termed 'tilt calibration'. The 'dynamic separation' was the maximum displacement away from the axially aligned conditions (without a spring) minus the 'tilt calibration' determined from the conditions of the test during cyclic loading with a spring (Figure 2-17). The dynamic separation was measured via an LVDT placed in the middle section of the cup holder (as shown in Figure 2-15), above the test samples.

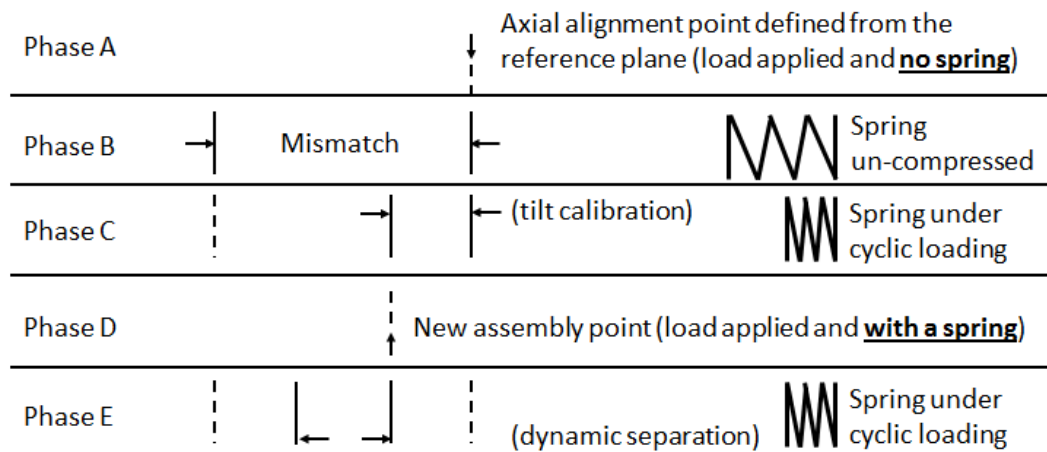


Figure 2-17. Schematic illustrating the mismatch, the tilt calibration and dynamic separation during cyclic and axially aligned conditions. In order to calculate the dynamic separation, first the axial alignment point was defined (Phase A), then a mismatch was applied (Phase B), the tilt calibration was measured (Phase C), this defined the assembly point (Phase D) and the dynamic separation was calculated (Phase E).

Budget of uncertainty

During the swing phase load, the MDAS recorded a M-L displacement which varied depending on the magnitude of the mismatch and once the tilt effect was accounted, the dynamic separation was calculated. During the double peak load of the cycle, a M-L displacement was also measured, which varied depending on the magnitude of the translational mismatch and the magnitude of the swing phase load. The system itself (cup holder and flexion tray) has a relative movement which corresponds to the loading and motion of the cycle. This displacement measured in the M-L direction during the double peak load of the cycle was considered as the 'budget of uncertainty'. The magnitude of the budget of uncertainty varied with the inputs of the cycle, but overall an average of 0.35 mm of M-L displacement can be accounted for, during the double peak load of the cycle. The budget of uncertainty was not used to calculate the dynamic separation, it is simply a measure of the magnitude of displacement that the system has which can imply not sensitive for magnitudes below 0.4 mm.

2.3.6. Duration of edge loading

The MDAS was used to overlay the displacement and loading output from the conditions tested. The duration of edge loading was measured from the point considered as the start of the cup separation from the suggested displacement away from the head and cup assembly point until the point considered as relocation from the suggested decrease in displacement (Figure 2-18). The beginning of the separation 't₀' as the force decreases from 3000 N. The end of separation was dependant on the type of condition and it was termed 't'. An example of the output displacement can be seen in Figure 2-19. The data was compensated from the reference point as described in Section 2.3.5.

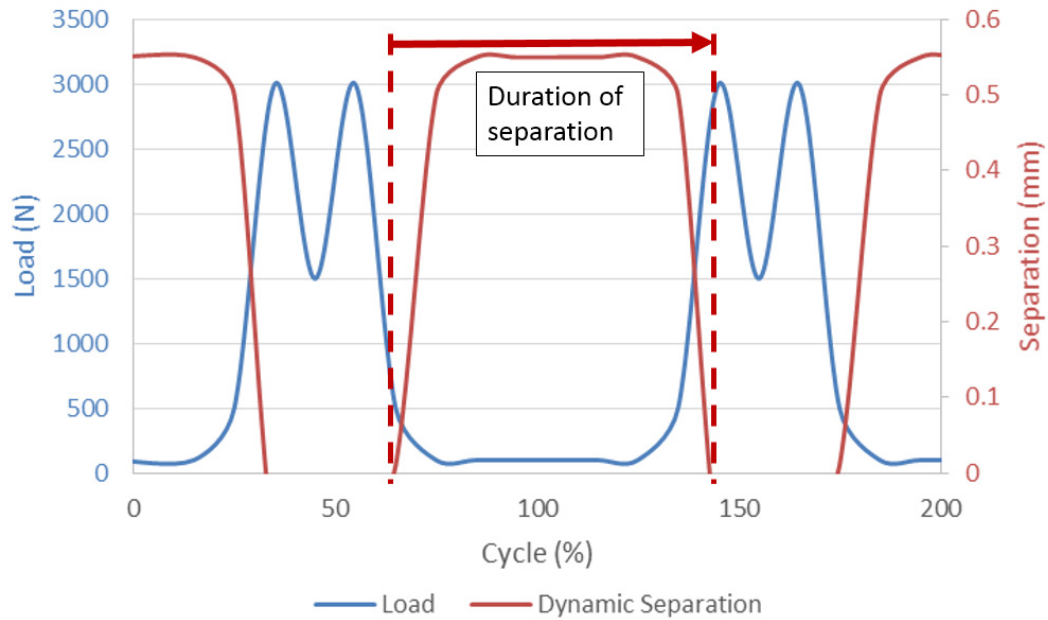


Figure 2-18. Schematic of the duration of edge loading from a load and dynamic separation curves.

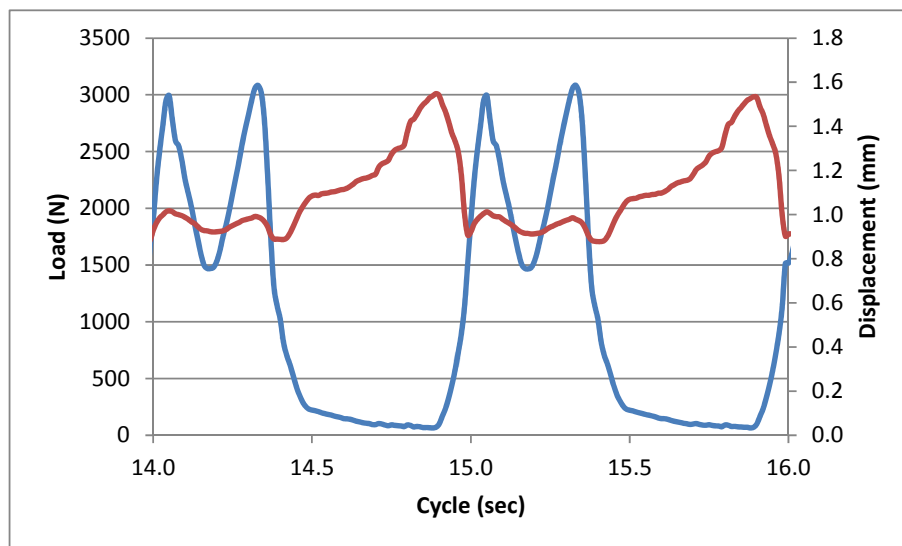


Figure 2-19. Example of raw output force (blue) and displacement (red) data under a translational mismatch. The zero point of the displacement indicates when the head and the cup were axially aligned.

2.3.7. Maximum vertical force under of edge loading

The MDAS was used to overlay the separation and loading profiles from the conditions tested. The maximum vertical force under edge loading was obtained by firstly detecting the point considered as relocation from the suggested decrease in displacement and secondly by taking a reading of the load profile at 0.1 mm from the head and cup assembly point as described in Figure 2-20.

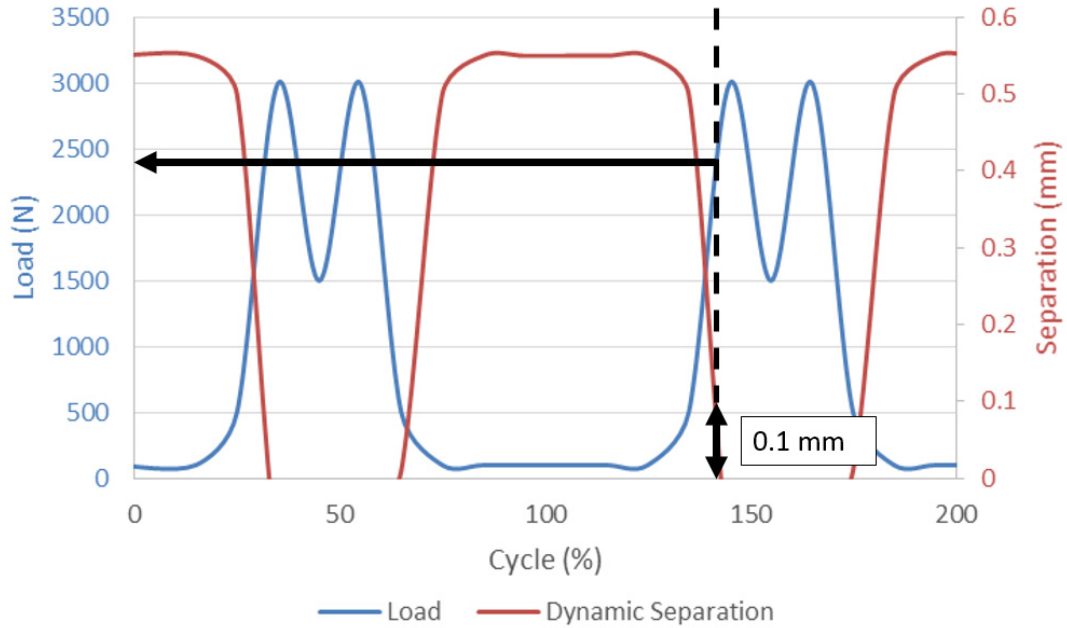


Figure 2-20. Schematic of the measured maximum vertical force under edge loading from a load and dynamic separation profile.

2.3.8. Severity of edge loading

The severity of edge loading is time during the cycle where the head is in contact with the rim (duration of separation) and the magnitude of the forces applied (Equation 2). The severity of edge loading was calculated from the output $F(x)$ and $F(y)$ loads from each condition. It was measured by taking the beginning (t_0) and end point (t) of the edge loading condition and evaluating the area under the axial (F_y) and medial-lateral (F_x) load curve between ' t_0 ' and ' t ' (Figure 2-21). The MDAS was used to acquire the magnitude of the vertical and medial-lateral loading during the conditions tested. An example of the axial and medial-lateral load output is shown in Figure 2-22.

$$\text{Equation 2. } \textit{Severity of Edge Loading} = \int_{t_0}^t F_x dt + \int_{t_0}^t F_y dt$$

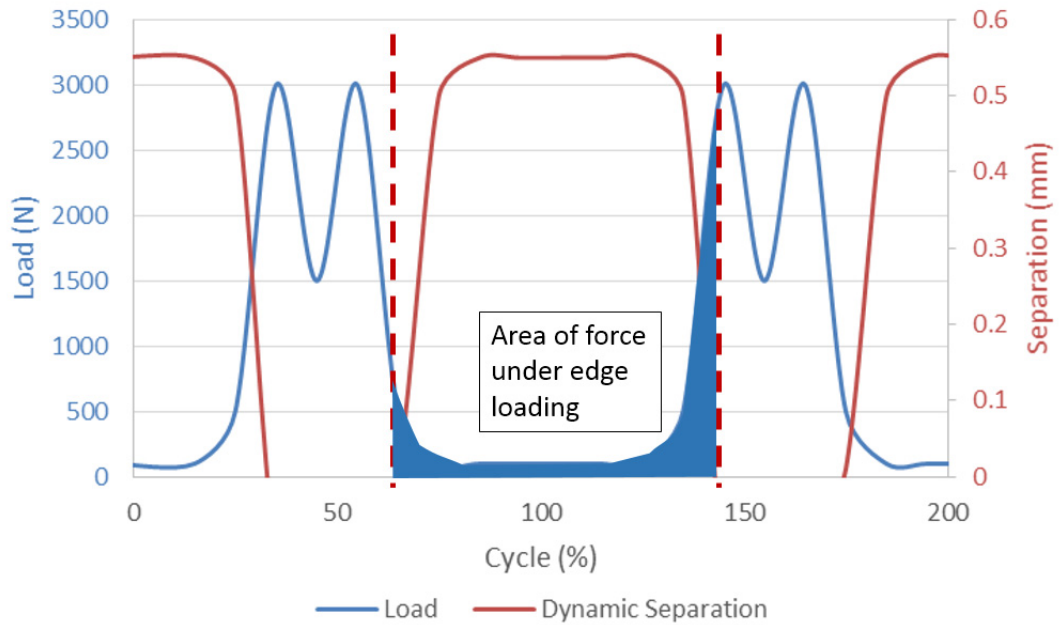


Figure 2-21. Schematic of the evaluation of the severity of edge loading from the load and separation curves.

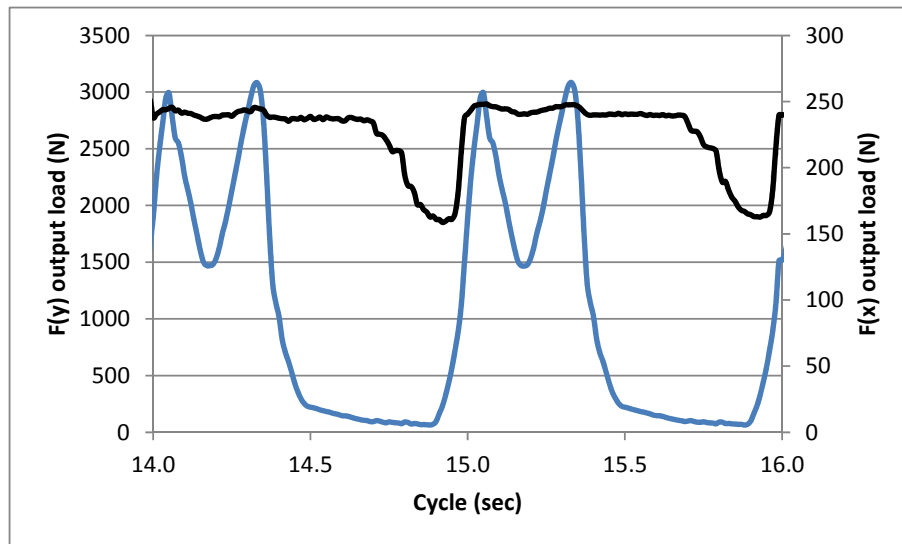


Figure 2-22. Example of output axial (F_y , in blue) and medial-lateral (F_x , in black) force data under a translational mismatch.

3. The Combined Effect of the Mismatch between the Head and Cup Centres and the Cup Inclination Angle on the Occurrence and Severity of Edge Loading and Wear in Ceramic-on-ceramic Hip Joint Replacements

3.1. Introduction

Clinically, the inclination and version angles of the acetabular cup have been found to vary (Callanan *et al.*, 2011). In some cases, inclination angle in excess of 55 degrees have been reported. Retrieval studies have shown wear mechanisms and increased wear associated with edge loading (Nevelos *et al.*, 1999, Walter *et al.*, 2004, Yamamoto *et al.*, 2005, Lusty *et al.*, 2007, Tateiwa *et al.*, 2007, Affatato *et al.*, 2012, Esposito *et al.*, 2012, Brandt *et al.*, 2013, Korim *et al.*, 2014). Testing of ceramic-on-ceramic hip replacements bearings under standard gait conditions and a steep cup inclination angle condition did not recreated stripe wear on the heads (Nevelos *et al.*, 2001). A test method developed by Nevelos *et al.* (2000) reproduced this wear mechanism on ceramic-on-ceramic bearings. This *in vitro* condition was termed microseparation, where the heads slides over the rim of the cup during the gait cycle causing edge loading at heel strike and producing clinically relevant wear mechanisms. The magnitude of the separation under this condition was pre-determined. Thus, the tests were set with a 0.5 mm dynamic separation operating between head and the cup centres. Additionally, it was demonstrated that under microseparation, the edge loading also produced a stripe wear on the heads as found in retrievals (Nevelos *et al.*, 2000). This demonstrated that under edge loading the wear rates increased and the particle distribution of the wear debris produced by the ceramic-on-ceramic was similar to that found clinically (Tipper *et al.*, 2002, Hatton *et al.*, 2002).

There are numerous studies linking the wear particles, predominately the long term effect of polyethylene particles, leading to failure of a joint replacement (Ingham & Fisher, 2000, Elfick *et al.*, 2003, Ingham & Fisher, 2005). The patient, surgical positioning and activity variability that could influence the severity of edge loading and amount of wear needs to be better explored, since excessive wear can lead to revision surgery. Therefore it is important to understand under what conditions can a prosthesis operate effectively and under what conditions it will not (Fisher, 2012) and therefore create a strategy for the improvement in the longevity of the prosthesis and patient outcomes.

Clinically, a mismatch in the centres of rotation of the femoral head and the acetabular cup can occur due to many reasons. Post-surgery, stem or cup migrations occur, thus the relative centres between the head and the cup have changed. Studies have shown that *in vivo*

migrations of either the cup or the stem for patients after surgery which do not indicate to be at risk of loosening tend to be about 0.5 mm per year up to about 4 mm (refer to Chapter 1.5.2). Commonly during surgery of total hip joint replacement, the cup is initially set, then the head is inserted afterwards. During this process, the centre of the cup defines the centre of the replacement hip joint, i.e. the central point from which the leg joint rotates (Figure 3-1). Medialisation of the joint centre may occur as the cup is fixated into the bone via impaction to enable adequate coverage of the external surface of the shell and sufficient fixation with the bone. Clinical medialisation can contribute to a change in the cup centre in the medial, posterior and superior position when following the neutral axis of the acetabulum. When the head is inserted, the approximation of setting the neutral centre of rotation of the head exactly where the cup centre is without any tension or laxity, is very difficult. Commonly, to reduce risk of dislocation, tension is applied to the joint, an example can be with the use of a large femoral neck. This implies, the centre of rotation of the head relative to the cup is not neutral and a mismatch between the relative centres of the two components exist (Figure 3-2). This mismatch can be in the medial-lateral, anterior-posterior and superior-inferior direction.



Figure 3-1. Schematic of the acetabular cup and femoral head conforming to each other at the hip joint centre set by the cup position.



Figure 3-2. Schematic of a total hip joint replacement where a translational mismatch is present between the centre of the head and the centre of the cup.

A strategy to account for the surgical positioning can be the concept of the testing methodology outlined in Chapter 2.2.4, where it considers the head and the cup centre as two individual components thus each have a centre. The rationale behind this concept was developed from how the components of the hip joint replacements are placed in the body during surgery. This study explored the surgical scenarios of a mismatch between the head and cup in the medial-lateral axis. Specifically, when there was no compensation for tensioning of the joint; such as excessive cup reaming (cup medialisation), head offset deficiency and insufficient neck length (head lateralisation).

This chapter explores the hypothesis that the head and cup centre mismatch, the cup angle and the combination of the mismatch and cup angle influence both, the biomechanics and tribology. Different levels of mismatches were applied between the head and cup centre (1, 2, 3, and 4 mm) in the medial-lateral direction and the cup angle modified was the inclination angle (45°, 55°, and 65°). The outcomes of the test were the evaluation of the parameters which influence the wear under these testing conditions. These were the level of dynamic separation, the maximum load under edge loading and the severity of edge loading. From the results, selected conditions were chosen to evaluate the wear. These were, 2, 3 and 4 mm translational mismatches with a 45° and 65° cup inclination angle.

3.2. Aim

The first aim of this study was to determine how the level of medial-lateral component translational mismatch between the head and cup centres for different cup inclination angles for ceramic-on-ceramic (BIOLOX® delta) bearings affect the biomechanics, such as; the relative level of displacement between the components and the relative forces acting on the bearings during the cycle. The second aim was to determine how the level of the medial-lateral component translational mismatch between the head and cup centre under different cup inclination angles for ceramic-on-ceramic (BIOLOX® delta) bearings affects the wear.

3.3. Methodology of the study

This study was split into two sections:

Section 1. Biomechanical study

Phase 1: A broad biomechanical study to evaluate; 1) the magnitude of dynamic separation, 2) the magnitude of the force acting under edge loading, and 3) the time during the cycle the head spends on the rim of the cup (duration of edge loading) under four levels of medial-lateral component translational mismatch between the head and cup centre (1, 2, 3 and 4 mm), and each level of translational mismatch was coupled with a cup inclination angle equivalent *in vivo* to 45°, 55° and 65°, equating to 12 conditions in total.

Phase 2: A limited biomechanical matrix study to evaluate; 1) the magnitude of the force acting under edge loading, and 2) the time during the cycle the head spends on the rim of the cup (duration of edge loading) under a combination of medial-lateral component translational mismatches and rotational malposition. The six selected test conditions were:

- A 2 mm translational mismatch under 45° and 65° cup inclination angle
- A 3 mm translational mismatch under 45° and 65° cup inclination angle
- A 4 mm translational mismatch under 45° and 65° cup inclination angle

Section 2. Wear study

A limited wear matrix study to determine the influence of edge loading due to translational mismatches and rotational malposition on the wear of ceramic-on-ceramic (BIOLOX® delta). The selected test conditions were the same as those selected on Phase 2 of the biomechanical study. These were: 2, 3 and 4 mm medial-lateral component translational mismatch for 45° and 65° cup inclination angles, equating to 6 conditions in total.

3.4. Biomechanical study Phase 1: Evaluation of the biomechanics under a medial-lateral component translational mismatch between the head and the cup for different cup inclination angles

3.4.1. Aim

The aim of this study was to determine how the variables associated with component positioning can influence the occurrence and severity of edge loading. This was determined by assessing; 1) the magnitude of dynamic separation, 2) the magnitude of the forces between the head and the rim of the cup acting under edge loading, 3) the time during the cycle the head spends on the rim of the cup (duration of edge loading). The variables associated with component positioning were as follows; medial-lateral component translational mismatch between the head and cup centres and the acetabular cup inclination angle.

3.4.2. Methodology

Station number three of the Leeds Mark II Physiological Anatomical Hip Joint Wear Simulator was used, and the methodology described in Chapter 2 was followed. The bearing material used was BIOLOX® delta as detailed in Chapter 2.1. Three cup inclination angles for the acetabular cup were chosen, these were 45°, 55° and 65° relative to the joint force vector. A translational mismatch was applied at the start of the test to the hip simulator. This was achieved by moving the cup in the medial direction away from the femoral head centre by 1, 2, 3 and 4 mm (Figure 3-3). This equates to 12 different conditions considered for this study in total, and for each condition 3 samples were employed. One station was used to evaluate each condition. The details of the test are described in Table 3-1. Mean values and $\pm 95\%$ Confidence Intervals (CI) were determined and statistical analysis (one way ANOVA) completed (significance taken at $p < 0.05$).

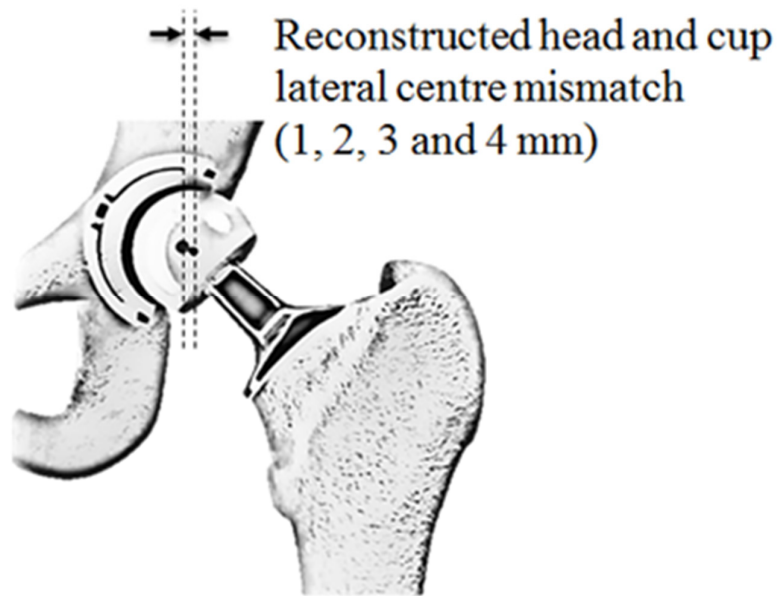


Figure 3-3. Schematic representing the hip simulator testing conditions with reconstructed head and cup medial-lateral centre mismatch.

Table 3-1. Details of the biomechanical study for the evaluation of the medial-lateral component translational mismatch in a hip joint simulator.

Study	Details (Unit)	Input
Biomechanical study	Equipment	Six-station Leeds Mark II (A)
	Materials	Ceramic-on-ceramic (BIOLOX® delta)
	Design	PINNACLE®
	Head size diameter (mm)	36
	Frequency (Hz)	1
	Loading profile	Paul walking cycle (twin peak load)
	Max peak force (N)	3000
	Trough load (N)	1500
	Swing phase load (N)	50
	Motion profile	Leeds walking cycle (Barbour <i>et al.</i> , 1999)
	Flexion / Extension (°) of the head	+30 / -15
	Internal / External rotation (°) of the cup	+10 / -10
	Stem anterversion angle (°)	20
	Cup version angle (°)	0
	Translational mismatch (mm)	1, 2, 3 and 4
	Spring constant (N/mm)	100
	Number of total bearings tested	3
	Cup inclination angle (°)	45, 55 and 65
	Cycles completed	240
	Station used (#)	3

3.4.3. Results

The outputs from this study were: the magnitude of separation, the maximum vertical force under edge loading, the maximum and minimum medial-lateral force, the type of edge loading and the severity of edge loading for different levels of head and cup centre mismatches and cup inclination angles.

The magnitude of the dynamic separation increased steadily as the level of translational mismatch between the femoral head and acetabular cup increased from 1 to 4 mm ($p < 0.01$) for all cup inclination angles (Figure 3-4). The dynamic separation was found to increase significantly ($p < 0.01$) due to the increased cup inclination angle and due to the combined interaction with the translational mismatch (Table 3-2). When the translational mismatch was greater than 1 mm, an increase in dynamic separation was observed when the cup inclination angle increased from 45° to 55° to 65° for each specific translational mismatch condition. The highest dynamic separation was observed under a translational mismatch of 4 mm with a cup inclination angle of 55° and 65°.

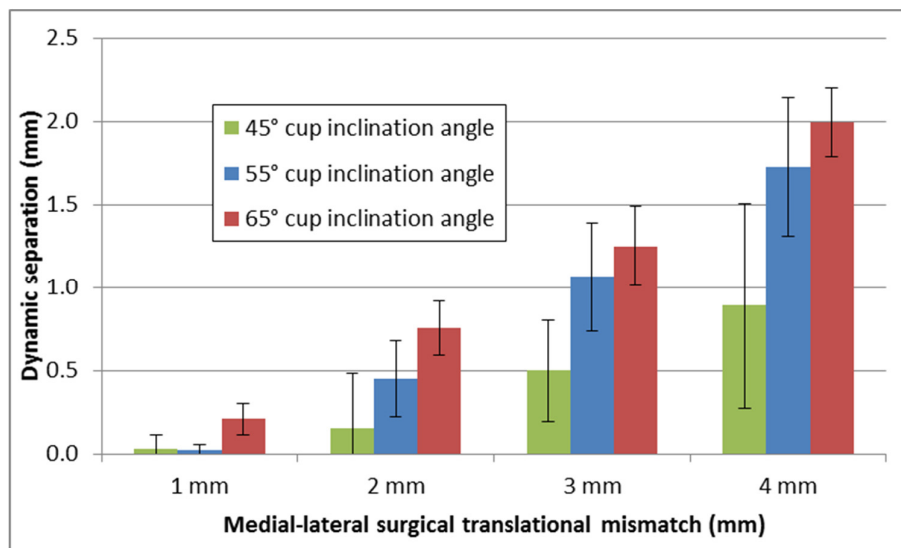


Figure 3-4. Mean ($n=3$, $\pm 95\%$ CI) dynamic separation of 36 mm ceramic-on-ceramic (BIOLOX® delta) bearings under 1, 2, 3 and 4 mm translational mismatch conditions for three cup inclination angle conditions, 45°, 55° and 65°.

Increasing the level of translational mismatch increased ($p < 0.01$) the maximum force during edge loading for all the cup inclination angles (Figure 3-5). The maximum force during edge loading was found to increase significantly ($p < 0.01$) due to the increased cup inclination angle and due to the combined interaction with the translational mismatch (Table 3-3). The maximum force during edge loading occurred when the cup inclination angle was increased to 65°, and a large translational mismatch (i.e. 3-4 mm) was applied.

Table 3-2. Two-way ANOVA with Tukey analysis for the dynamic separation under a 1, 2, 3 and 4 mm translational mismatch and 45°, 55° and 65° cup inclination angle for n = 3.

Two-way analysis	Variable		p	
	Mismatch		0.00	
	Inclination		0.00	
	Mismatch*Inclination		0.00	
Tukey analysis	Variable (inclination)		Comparison	p
	45°		55°	0.00
			65°	0.00
	55°		65°	0.00
	Variable (mismatch)		Comparison	p
	1 mm		2 mm	0.00
			3 mm	0.00
			4 mm	0.00
	2 mm		3 mm	0.00
			4 mm	0.00
3 mm		4 mm	0.00	

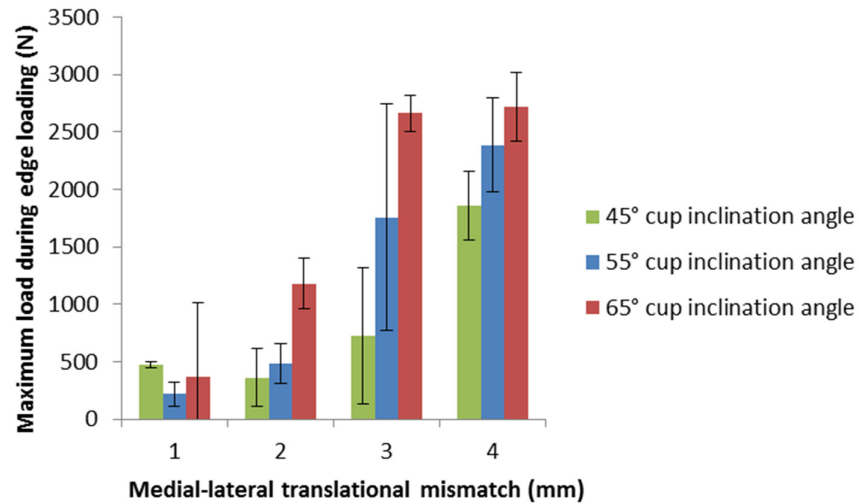


Figure 3-5. Mean (n=3, ±95% CI) maximum load recorded at 0.1 mm separation during edge loading at different component positions including acetabular cup and femoral head translational mismatch.

Table 3-3. Two-way ANOVA with Tukey analysis for the maximum force during edge loading under a 1, 2, 3 and 4 mm translational mismatch and 45°, 55° and 65° cup inclination angle for n = 3.

Two-way analysis	Variable	p	
	Mismatch	0.00	
	Inclination	0.00	
	Mismatch*Inclination	0.00	
Tukey analysis	Variable (inclination)	Comparison	p
	45°	55°	0.00
		65°	0.00
	55°	65°	0.00
		Variable (mismatch)	Comparison
	1 mm	2 mm	0.00
		3 mm	0.00
		4 mm	0.00
	2 mm	3 mm	0.00
		4 mm	0.00
3 mm	4 mm	0.00	

The maximum medial-lateral load occurred during the double peak load of the cycle, and the minimum medial-lateral load occurred during the swing phase load (Figure 3-6). The maximum medial-lateral load increased for all the cup inclination angles when a higher level of translational mismatch was employed. Overall, across all the cup inclination angles, the operating maximum medial-lateral load under cyclic conditions was the same while under the same level of translational mismatch. Only under the conditions of a 4 mm translational mismatch and 65° cup inclination angle, a decrease (roughly 100 N) in maximum medial-lateral load was observed in comparison to the 45° and 55° cup inclination angles.

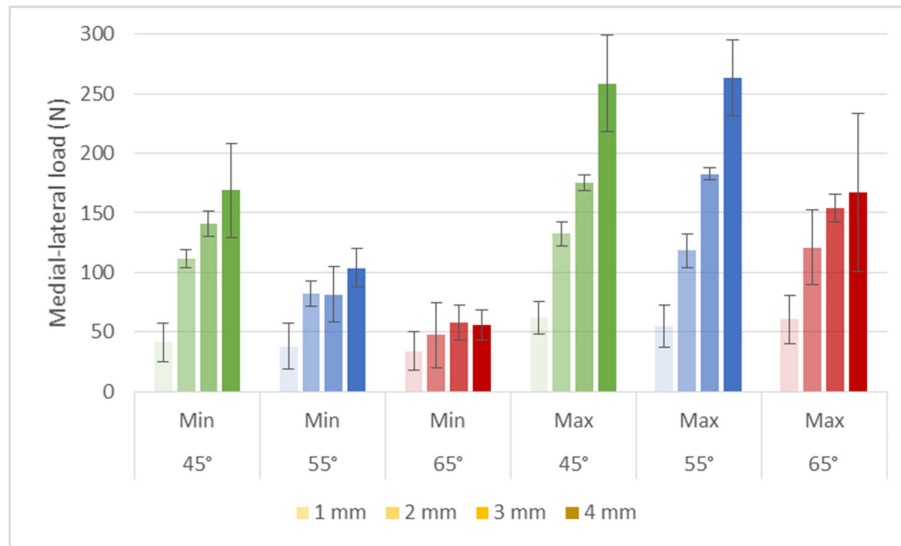


Figure 3-6. Mean minimum and maximum medial-lateral load (n=3, $\pm 95\%$ CI) of 36 mm ceramic-on-ceramic (BIOLOX® delta) bearings under 1, 2, 3 and 4 mm translational mismatch conditions (color coded and shaded against increased in translational mismatch) for three cup inclination angle conditions, 45° (green), 55° (blue) and 65° (red).

The extended coverage of the cup inclination angle created a resistance to separation away from the head and this was identified on minimum medial-lateral load across the different cup inclination angles. Thus, a higher medial-lateral force was observed during the swing phase load under lower cup inclination angles for larger levels of translational mismatches (i.e. 2-3 mm).

Different types of edge loading were observed. Under low levels of medial-lateral component translational mismatch, the cup relocated in a single action (Figure 3-7) as the vertical load increased. This type of edge loading was consistent for all the levels of translational mismatches under a 45° and 55° cup inclination angles.

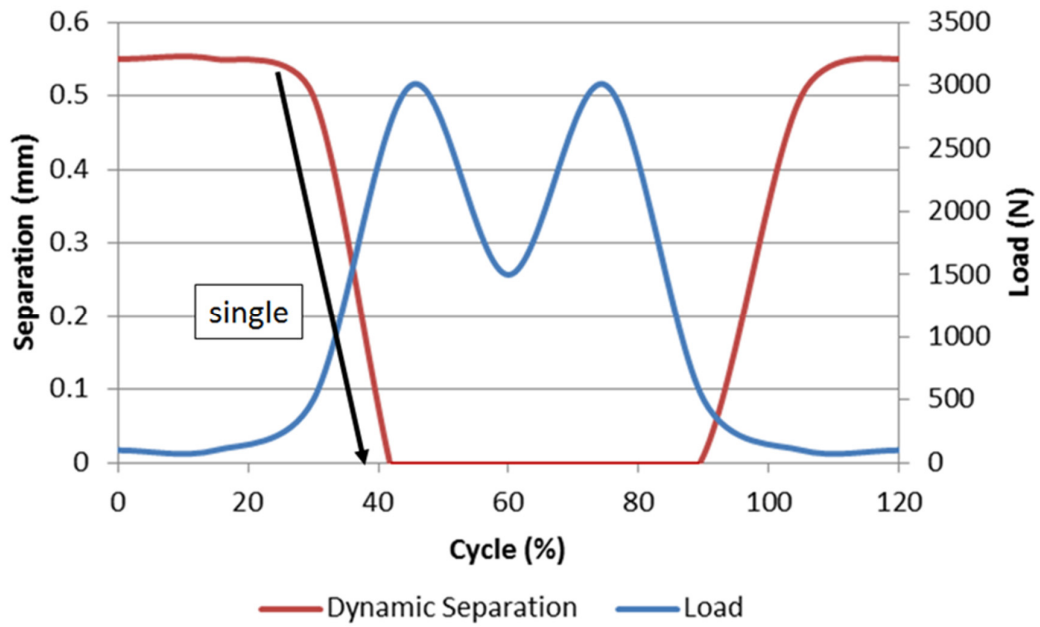


Figure 3-7. Schematic representing the relocation of the cup into the head in a single action.

The results under a cup inclination angle of 65° demonstrated that as the level of translational mismatch was increased, it delayed the point at which the cup relocated, and under certain conditions, interrupted (Figure 3-8) the “relocation” such that it either appeared to; relocate under the second peak load of the cycle, or it did not appear to relocate back to the assembly centre during the entire cycle, or relocated under the first peak but kept the cup holder tilted such that it appears as not concentric and then the second peak forced the cup holder back even further. All samples under a 4 mm translational mismatch and 65° cup inclination angle exhibited an interrupted relocation.

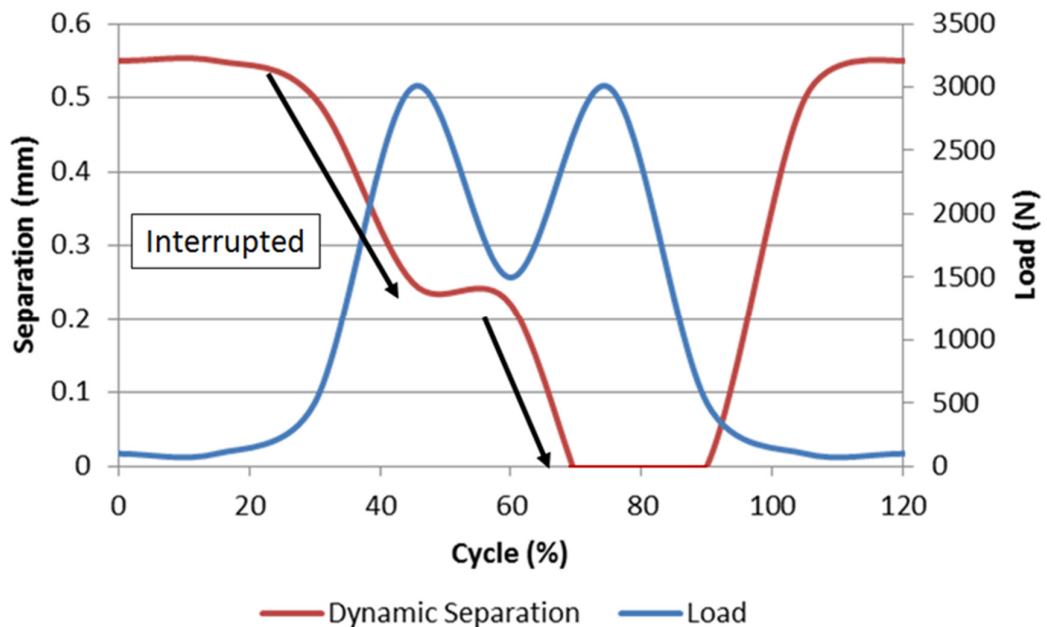


Figure 3-8. Schematic representing an interrupted edge loading condition.

The severity of edge loading was found to increase significantly ($p < 0.01$) due to the translational mismatch and the cup inclination angle and the interaction between each other (Figure 3-9). Three cases were identified as not statistically significant. These were between 1 and 2 mm translational mismatch, between 3 and 4 mm translational mismatch, and between the 45° and 55° cup inclination angles (Table 3-4).

The severity of edge loading increased under all the cup inclination angle conditions when larger level of translational mismatches (i.e. 2-4 mm) were employed. Under a 45° and 55° cup inclination angle the increase in severity of edge loading with the increased translational mismatch was steady (roughly 50-125 Ns). A large increase in the severity of edge loading (roughly 500 Ns) occurred only from a 2 to 3 mm translational mismatch with a cup inclination angle of 65°. This increase was found significant ($p < 0.01$) only between the 1 and 4 mm, and 2 and 4 mm translational mismatch conditions for the 65° cup inclination angle. The highest severity of edge loading values were found only while under a 3 and 4 mm translational mismatch and a 65° cup inclination angle conditions, where an interrupted relocation was observed, such that the rim of the cup was in contact with the head after the first peak load of the cycle. A significant difference was found in the severity of edge loading between the 45° and 65° and between the 55° and 65° cup inclination angles under a 4 mm translational mismatch ($p < 0.01$ and $p < 0.01$, respectively).

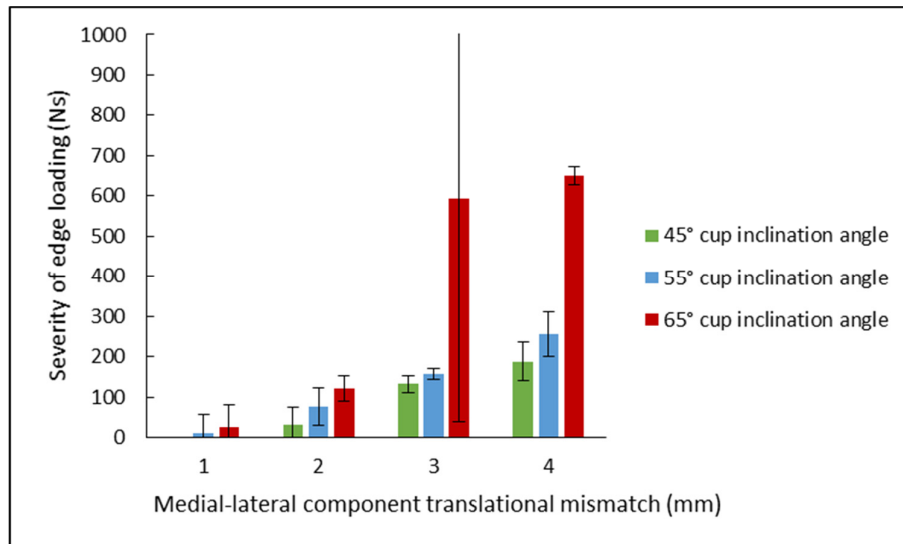


Figure 3-9. Mean ($n=3$, $\pm 95\%$ CI) severity of edge loading of 36 mm ceramic-on-ceramic (BIOLOX® delta) bearings under 1, 2, 3 and 4 mm translational mismatch conditions for three cup inclination angle conditions, 45°, 55° and 65°.

Table 3-4. Two-way ANOVA with Tukey analysis for the severity of edge loading under a 1, 2, 3 and 4 mm translational mismatch and 45°, 55° and 65° cup inclination angle for n = 3.

Two-way analysis	Variable	p	
	Mismatch	0.00	
	Inclination	0.00	
	Mismatch*Inclination	0.00	
Tukey analysis	Variable (inclination)	Comparison	p
	45°	55°	0.38
		65°	0.00
	55°	65°	0.00
	Variable (mismatch)	Comparison	p
	1 mm	2 mm	0.19
		3 mm	0.00
		4 mm	0.00
	2 mm	3 mm	0.00
		4 mm	0.00
3 mm	4 mm	0.14	

The biomechanical study indicated a big discrepancy in the severity of edge loading under a 3 mm translational mismatch and a 65° cup inclination angle to that of 45° and 55° cup inclination angle. This was because interrupted relocation was observed under 65° on two out of three samples while under a 3 mm translational mismatch. Hence the 95% confidence interval was large for this condition.

3.5. Biomechanical study Phase 2: Evaluation of severity of edge loading for specific testing conditions under a medial-lateral component translational mismatch between the head and the cup centre

3.5.1. Aim

The aim of this study was to determine how the variables associated with component positioning can influence severity of edge loading (refer to Chapter 2.3.8). This was determined by assessing; 1) the magnitude of the forces acting under edge loading, and 2) the time during the cycle the head spends on the rim of the cup (duration of edge loading). The variables associated with component positioning were as follows; medial-lateral component translational mismatch between the head and cup centres and the acetabular cup inclination angle.

3.5.2. Methodology

The six station Leeds Mark II Physiological Anatomical Hip Joint Wear Simulator was used, and the methodology described in Chapter 2 was followed. The bearing material used was BIOLOX® delta as detailed in Chapter 2.1. Six testing conditions were chosen for this study. Two cup inclination angles for the acetabular cup, these were 45° and 65° relative to the joint force vector. A translational mismatch was applied at the start of the test to the hip simulator. This was achieved by moving the cup in the medial direction away from the femoral head centre by 2, 3 and 4 mm (Figure 3-10). This equates to 6 different conditions considered for this study in total, and for each condition 6 samples were employed. All six stations were used for this study, however only one station at a time per sample. The details of the test are described in Table 3-5. Mean values and $\pm 95\%$ Confidence Intervals (CI) were determined and statistical analysis (one way ANOVA) completed (significance taken at $p < 0.05$).

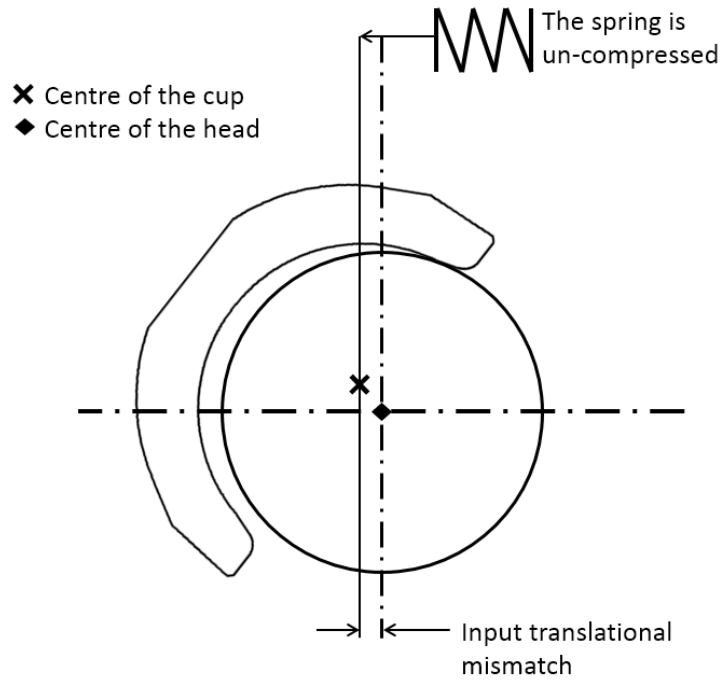


Figure 3-10. Schematic of the input translational mismatch between the centre of the head and the centre of the cup in the Hip Joint Simulator.

Table 3-5. Details of the biomechanical study for the evaluation of the severity of edge loading under selective medial-lateral component translational mismatch conditions.

Study	Details (Unit)	Input
Biomechanical study	Equipment	Six-station Leeds Mark II (A)
	Materials	Ceramic-on-ceramic (BIOLOX® delta)
	Design	PINNACLE®
	Head size diameter (mm)	36
	Frequency (Hz)	1
	Loading profile	Paul walking cycle (twin peak load)
	Max peak force (N)	3300
	Trough load (N)	1500
	Swing phase load (N)	50
	Motion profile	Leeds walking cycle (Barbour <i>et al.</i> , 1999)
	Flexion / Extension (°) of the head	+30 / -15
	Internal / External rotation (°) of the cup	+10 / -10
	Stem anterversion angle (°)	20
	Cup version angle (°)	0
	Translational mismatch (mm)	2, 3 and 4
	Spring constant (N/mm)	100
	Number of total bearings tested	6
	Cup inclination angle (°)	45 and 65
	Cycles completed	900
	Stations used (#)	1, 2, 3, 4, 5, 6

3.5.3. Results

The severity of edge loading increased for all the cup inclination angle conditions as the translational mismatch increased from 2 to 3 to 4 mm (Figure 3-11). The mean ($\pm 95\%$ CI) severity of edge loading for the 45° cup inclination angle was 32 \pm 8, 79 \pm 16 and 167 \pm 25 Ns under a 2, 3 and 4 mm translational mismatch respectively. The severity of edge loading for the 65° cup inclination angle was 123 \pm 41, 243 \pm 159 and 624 \pm 169 Ns under a 2, 3 and 4 mm translational mismatch respectively. The results from the 45° cup inclination angle were lower ($p < 0.01$, $p = 0.05$ and $p < 0.01$) for each comparative translational mismatch (2, 3 and 4 mm respectively) than the 65° cup inclination angle conditions.

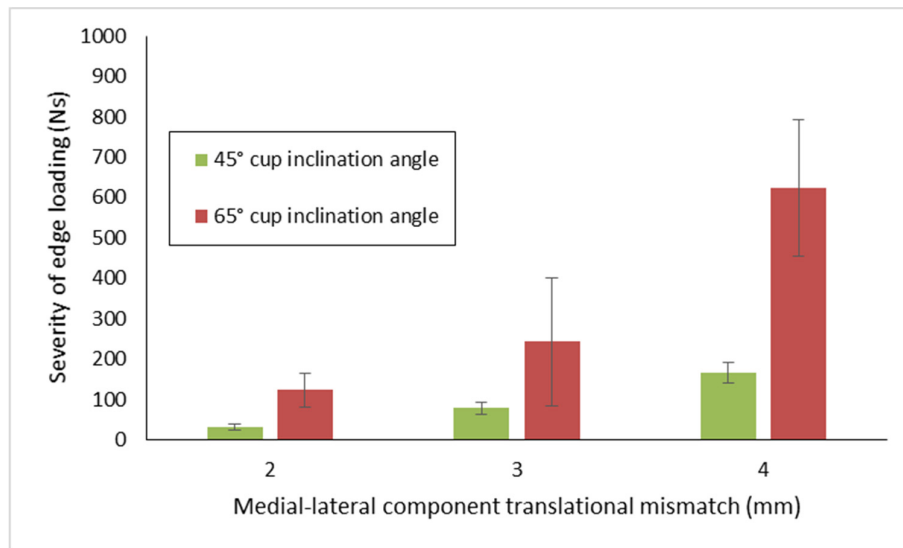


Figure 3-11. Mean ($n=6$, $\pm 95\%$ CI) severity of edge loading of 36 mm ceramic-on-ceramic (BIOLOX® delta) bearings under 2, 3 and 4 mm translational mismatch conditions for two cup inclination angle conditions, 45° and 65°.

3.6. The wear of 36 mm CoC (BIOLOX® delta) under edge loading due to a medial-lateral component translational mismatch of 2, 3 and 4 mm for a 45° and 65° cup inclination angle

3.6.1. Aim

The aim of this study was to determine the wear and damage of CoC under edge loading due to a medial-lateral component translational mismatch and rotational malposition by evaluating different cup inclination angles.

3.6.2. Methodology

The methodology for the wear study was described in Chapter 2. The bearing material used was BIOLOX® delta as detailed in Chapter 2.1. Two inclination angles for the acetabular cup were chosen. The inclination angles used were 45° and 65° relative to the joint force vector. The inclination angle at 45° was referred to as “standard”, and the higher inclination of 65° was referred to as “steep” (rotational malposition). A translational mismatch was applied at the start of each test to the hip simulator. This was achieved by moving the cup in the medial direction away from the femoral head centre by 2, 3 and 4 mm (Figure 3-12).

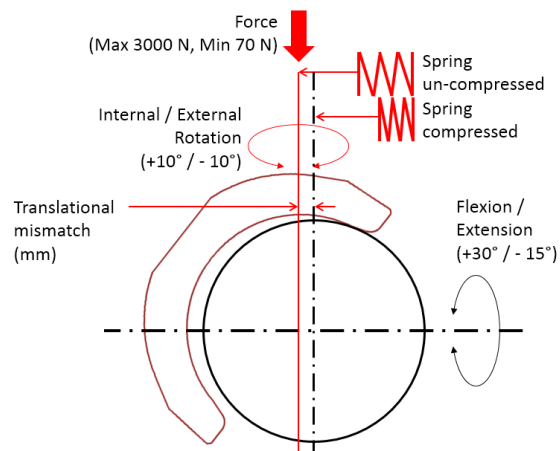


Figure 3-12. Schematic of the inputs on the Hip Joint Simulator.

The test was run for 3 million cycles for each condition (n=6 per condition). The test stations were alternated between standard and steep angles, such that after the completion of the first 3 million cycles, the stations were changed by swapping the inclination angle on each station and new test samples were inserted. Details of the inputs for the test are described in Table 3-6. The first few cycles (approximately 30 minutes) were run without any translational mismatch to ensure a good performance of the equipment e.g. check the bone cement and fixtures hold without any malfunction. Afterwards, the cycle count was reset. A translational mismatch was applied to all the stations. During intermissions i.e. either at serum change or at a measurement point (one million cycles), the fixtures and mounts were checked to ensure that no change occurred to the input translational mismatch. Checks on the hip simulator were done daily for good performance. Mean values and $\pm 95\%$ Confidence Intervals (CI) were determined and statistical analysis (one way ANOVA) completed (significance taken at $p < 0.05$).

Table 3-6. Details of the medial-lateral component translational mismatch wear study under 2, 3 and 4 mm.

Study	Details (Unit)	Input		
Wear study	Equipment	Six-station Leeds Mark II (A)		
	Materials	Ceramic-on-ceramic (BIOLOX® delta)		
	Design	PINNACLE®		
	Head size diameter (mm)	36		
	Frequency (Hz)	1		
	Loading profile	Paul walking cycle (twin peak load)		
	Max peak force (N)	3000		
	Trough load (N)	1500		
	Swing phase load (N)	50		
	Motion profile	Leeds walking cycle (Barbour <i>et al.</i> , 1999)		
	Flexion / Extension (°) of the head	+30 / -15		
	Internal / External rotation (°) of the cup	+10 / -10		
	Stem anterversion angle (°)	20		
	Cup version angle (°)	0		
	Translational mismatch (mm)	2, 3 and 4		
	Spring constant (N/mm)	100		
	Number of total bearings tested	36		
	Cup inclination angle (°)	45 and 65		
	Cycles completed	3 x 10 ⁶	3 x 10 ⁶	
	Station 1 inclination angle (°)	45	65	
	Station 2 inclination angle (°)	65	45	
Station 3 inclination angle (°)	45	65		
Station 4 inclination angle (°)	65	45		
Station 5 inclination angle (°)	45	65		
Station 6 inclination angle (°)	65	45		

3.6.3. Results

The outputs from the study were the wear from the ceramic bearings, the scar depth on the femoral heads, the change in surface roughness and volumetric assessment of the heads and cups via the CMM due to edge loading under a 2, 3 and 4 mm translational mismatch for a 45° and 65° cup inclination angles.

The total displacement of the cup holder during routine checks measured using the LVDT did not show a difference between the standard and the steep inclination angle under a 2 mm translational mismatch (Figure 3-13), and no significant difference was found between the means ($p=0.11$).

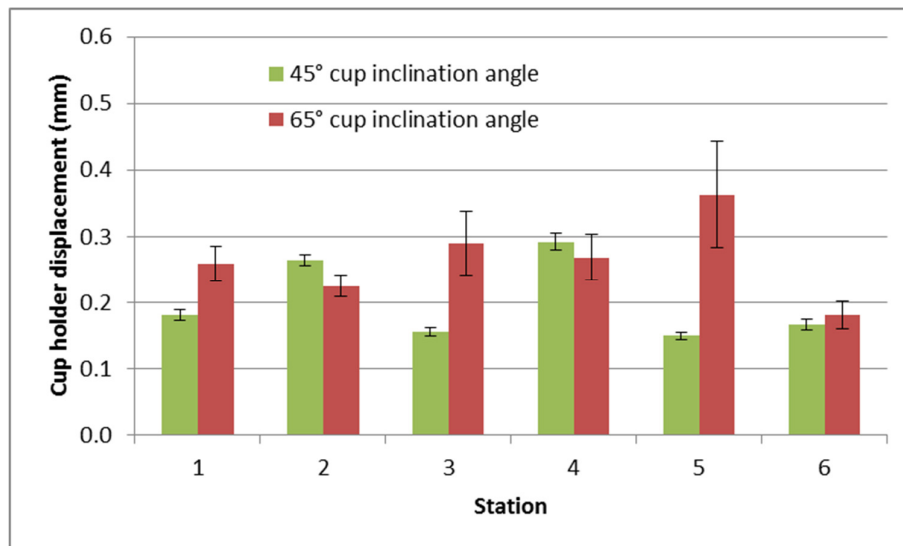


Figure 3-13. Average displacement of the cup holder ($\pm 95\%$ CI) for standard and steep inclination angles under a 2 mm translational mismatch.

The total displacement of the cup holder during routine checks measured using the LVDT was different between the standard and the steep inclination angle under a 3 mm translational mismatch (Figure 3-14), and a significant difference was found between the means ($p<0.01$).

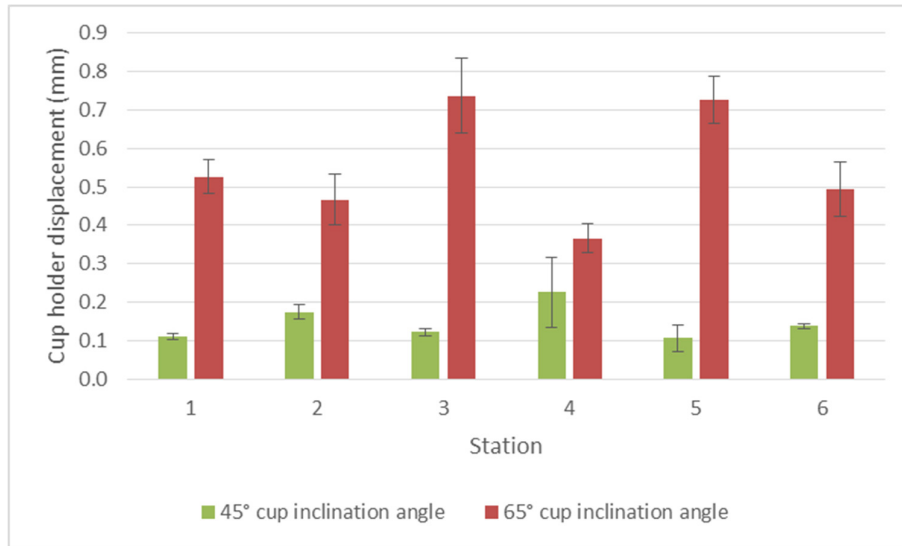


Figure 3-14. Average displacement of the cup holder ($\pm 95\%$ CI) for standard and steep inclination angles under a 3 mm translational mismatch.

The total displacement of the cup holder during routine checks measured using the LVDT was different between the standard and the steep inclination angle under a 4 mm translational mismatch (Figure 3-15), and a significant difference was found between the means ($p < 0.01$).

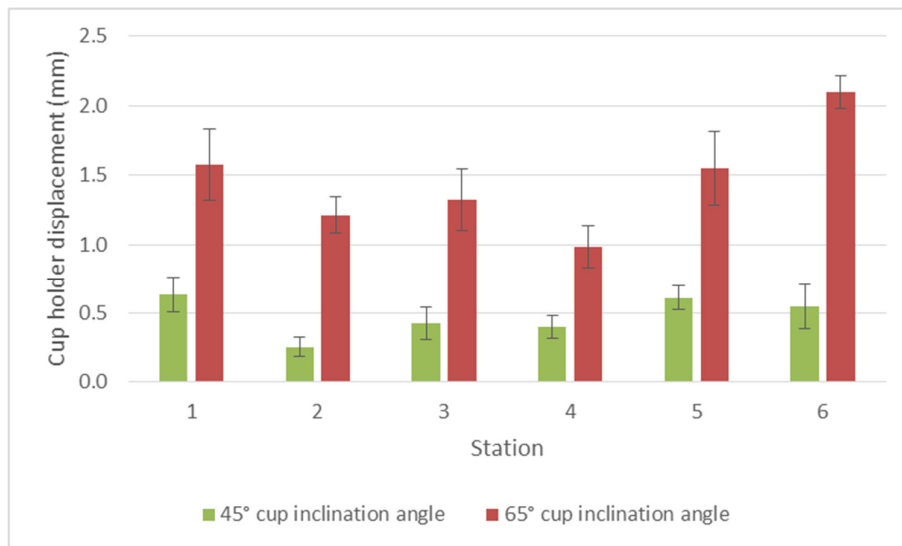


Figure 3-15. Average displacement of the cup holder ($\pm 95\%$ CI) for standard and steep inclination angles under a 4 mm translational mismatch.

The cumulative wear volume for each station under a 2 mm translational mismatch is shown in Figure 3-16. The wear rate on the femoral heads and the acetabular cups were consistent at every interval apart from two occasions; an increase in the wear rate on station #1 with a 65° cup inclinational angle at 1 million cycles, and a decrease in the wear rate on station #3 with a 65° cup inclination angle at 3 million cycles. This increase and drop could perhaps be explained by the observed increased cup holder displacement on station #1 after 1 million cycles (from 0.19 to 0.26 and 0.29 mm) and the decrease at 2 million cycles on station #3 from the LVDT unit. After three million cycles of testing, the mean wear rate under the standard cup inclination angle condition was $0.07 \pm 0.04 \text{ mm}^3/10^6 \text{ cycles}$ and the mean wear rate under the steep cup inclination angle was $0.14 \pm 0.05 \text{ mm}^3/10^6 \text{ cycles}$ (Figure 3-17). The wear rate for the steeper angle under a 2 mm translational mismatch was significantly higher ($p=0.02$) than the wear under the standard angle condition.

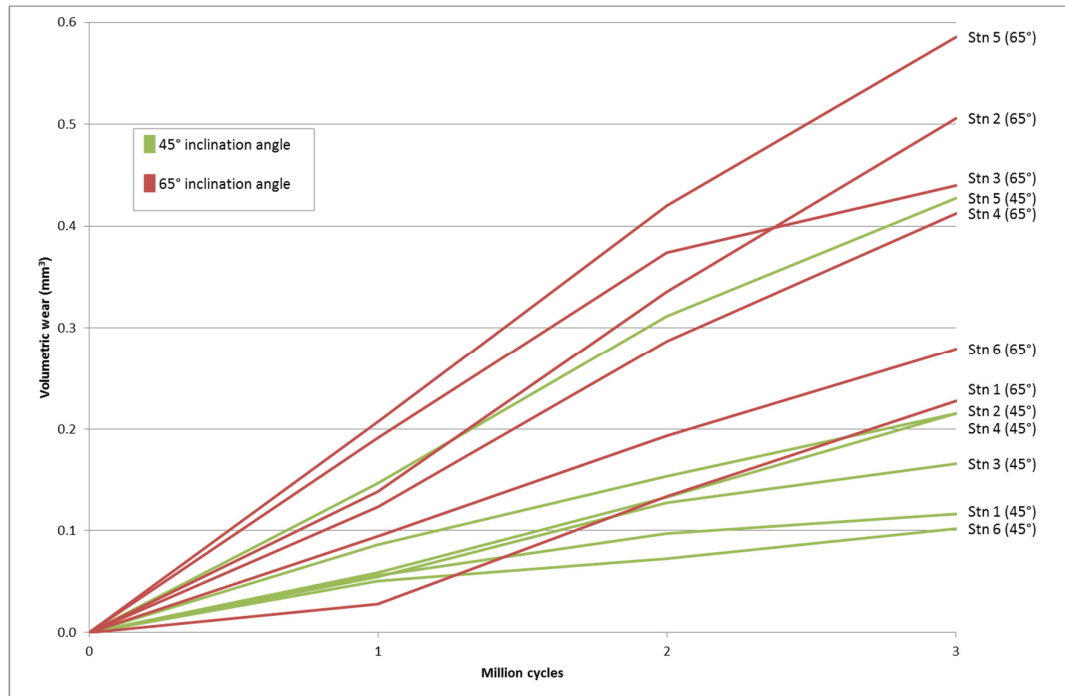


Figure 3-16. Individual volumetric wear for standard (45°) and steep (65°) cup inclination angles under 2 mm medial-lateral component translational mismatch. Stn = Station.

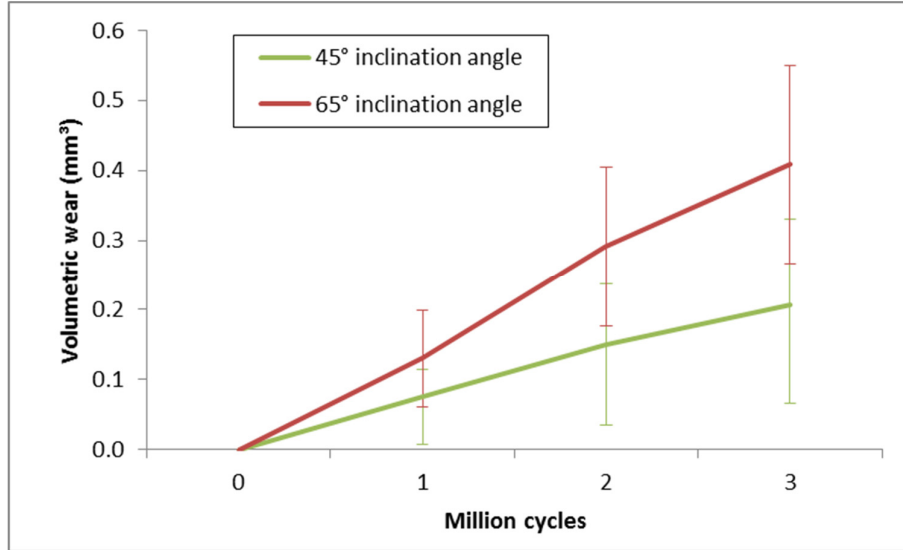


Figure 3-17. Mean ($n=6$, $\pm 95\%$ CI) wear rates for standard (45°) and steep (65°) inclination angles under 2 mm medial-lateral component translational mismatch.

The individual wear from all the stations under a 3 mm translational mismatch is shown in Figure 3-18. The wear rate on the femoral heads and the acetabular cups was consistent at every interval apart from two occasions; a decrease in wear rate on station #3 with a 65° cup inclination angle at 2 million cycles, and an increase in wear rate on station #5 with a 65° cup inclination angle at 3 million cycles. After three million cycles of testing, the mean wear rate under the standard cup inclination angle condition was $0.11 \pm 0.02 \text{ mm}^3/10^6 \text{ cycles}$ and the wear rate under the steep cup inclination angle was $0.30 \pm 0.16 \text{ mm}^3/10^6 \text{ cycles}$ (Figure 3-19). The wear rate for the steeper angle under a 3 mm translational mismatch was significantly higher ($p=0.02$) than the wear under the standard angle condition.

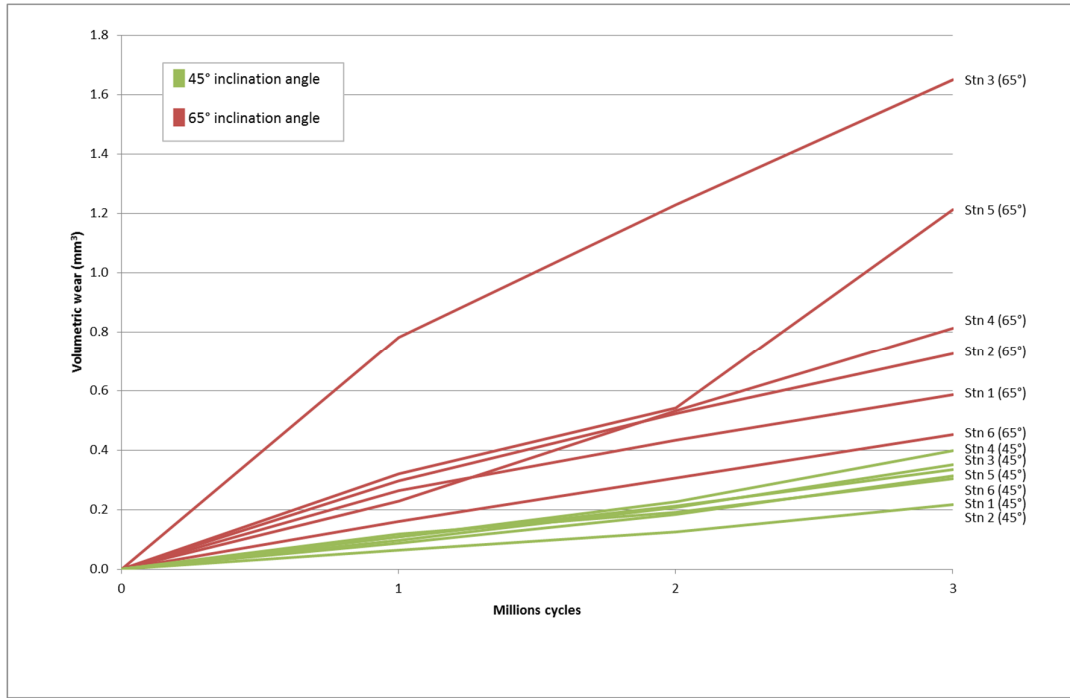


Figure 3-18. Individual volumetric wear for standard (green) and steep (red) cup inclination angles under 3 mm medial-lateral component translational mismatch. Stn = Station.

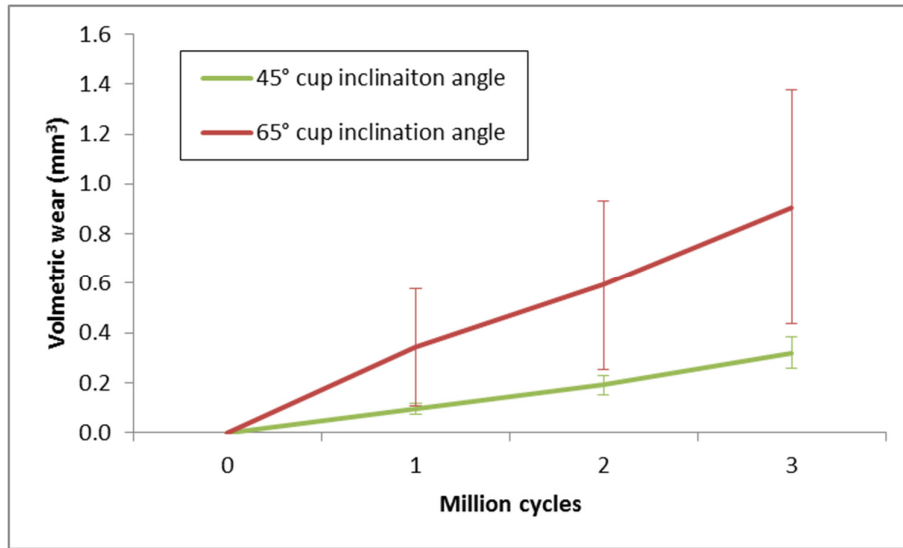


Figure 3-19. Mean (n=6, ±95% CI) wear rates for standard and steep inclination angles under 3 mm medial-lateral component translational mismatch.

The individual wear from all the stations under a 4 mm translational mismatch is shown in Figure 3-20. The wear rate on the femoral heads and the acetabular cups was consistent at every interval apart from a decrease in the wear after the first million cycles for the steep conditions. After three million cycles of testing, the mean wear rate under the standard cup inclination angle condition was $0.32 \pm 0.04 \text{ mm}^3/10^6 \text{ cycles}$ and the wear rate under the steep cup inclination angle was $1.01 \pm 0.17 \text{ mm}^3/10^6 \text{ cycles}$ (Figure 3-21). The wear rate for the steeper angle under a 4 mm translational mismatch was significantly higher ($p < 0.01$) than the wear under the standard angle condition.

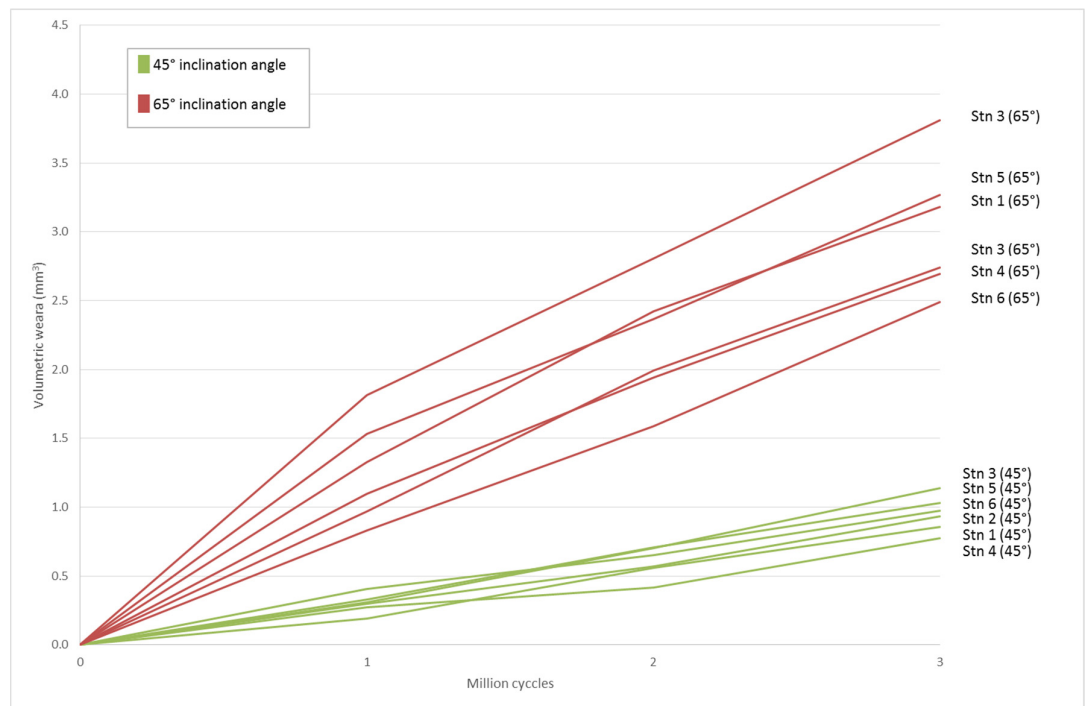


Figure 3-20. Individual volumetric wear for standard (green) and steep (red) inclination angles under 4 mm medial-lateral component translational mismatch. Stn = Station.

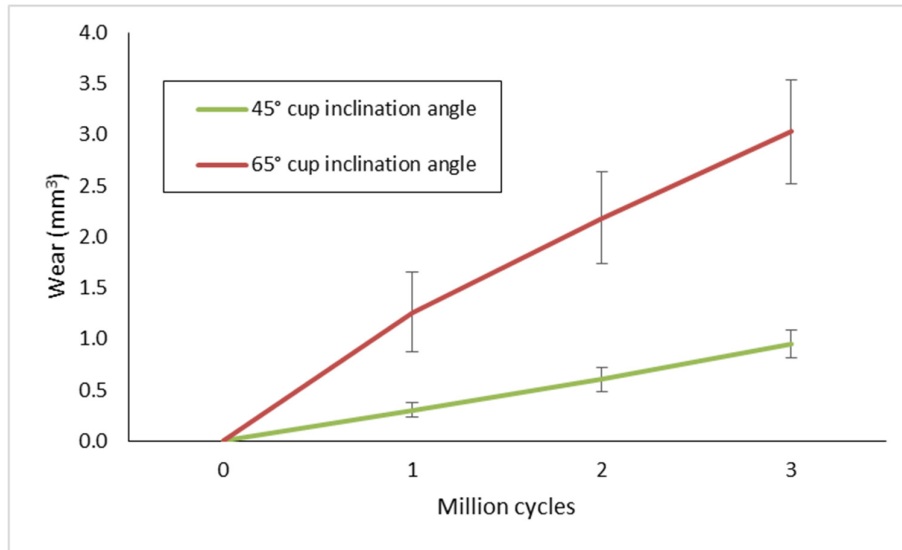


Figure 3-21. Mean (n=6, ±95% CI) wear rates for standard and steep inclination angles under 4 mm medial-lateral component translational mismatch.

The wear results from these studies indicate that, as the input translational mismatch was increased, the wear rate increased (Figure 3-22). Overall, the 65° cup inclination angles had a higher wear rate than that of the 45° cup inclination angle for any given translational mismatch, and as the translational mismatch increased the wear difference between that of 45° and 65° became larger.

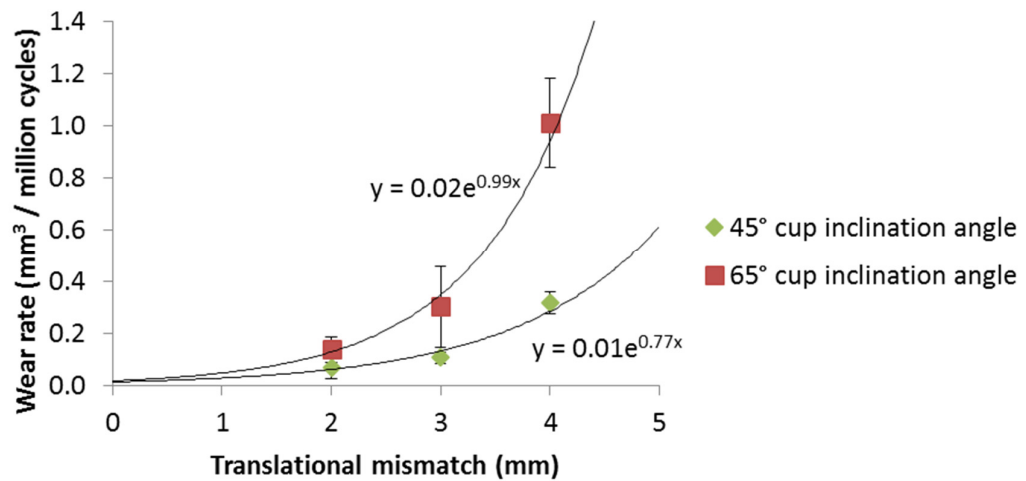


Figure 3-22. Mean (n=6, ±95% CI) wear rate of 36 mm ceramic-on-ceramic (BIOLOX® delta) bearings under 2, 3 and 4 mm translational mismatch conditions with a cup inclination angle conditions of 45° and 65°.

The stripe wear location was found to be similar within the standard group and within the steep cup inclination angles group under a 2 mm translational mismatch. A representation of the CMM data after 3 million cycles analysed is shown in Figure 3-23. The steep cup inclinations angles caused the edge loading on the heads to be at a higher point closer to the pole of the head than the cups with the standard inclination angle.

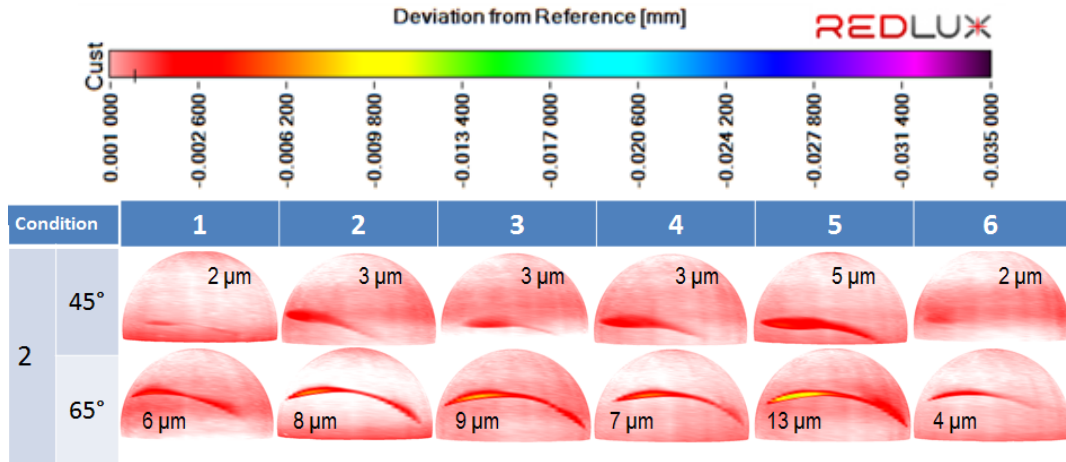


Figure 3-23. Visualisation of the heads tested under a 2 mm medial-lateral component translational mismatch via RedLux software after 3 million cycles. The maximum depth of the scar is labelled beside each head accordingly.

The stripe wear location was found to be similar within the standard cup inclination group under a 3 mm translational mismatch (Figure 3-24). The steep cup inclinations angles caused the edge loading on the heads to be at a higher point closer to the pole of the head than the cups with the standard inclination angle. Head #3, with a steep cup inclination angle, had the highest level of penetration towards the right side of the wear scar and was different in comparison to all the other samples.

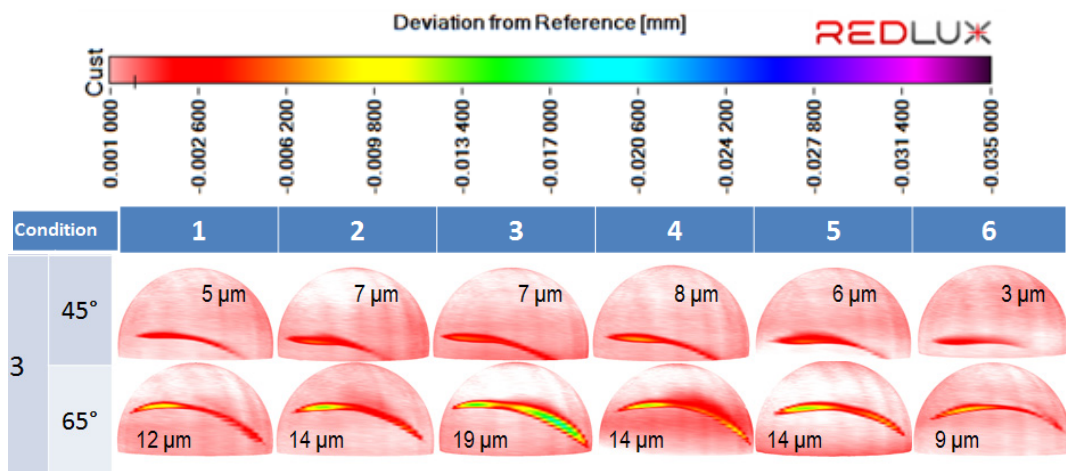


Figure 3-24. Visualisation of the heads under a 3 mm medial-lateral component translational mismatch via RedLux software after 3 million cycles. The maximum depth of the scar is aligned to each head accordingly.

The stripe wear location was found to be similar within the standard group and within the steep cup inclination angles group under a 4 mm translational mismatch. A representation of the CMM data after 3 million cycles analysed is shown in Figure 3-25. The steep cup inclinations angles caused the edge loading on the heads to be at a higher point closer to the pole of the head than the cups with the standard inclination angle.

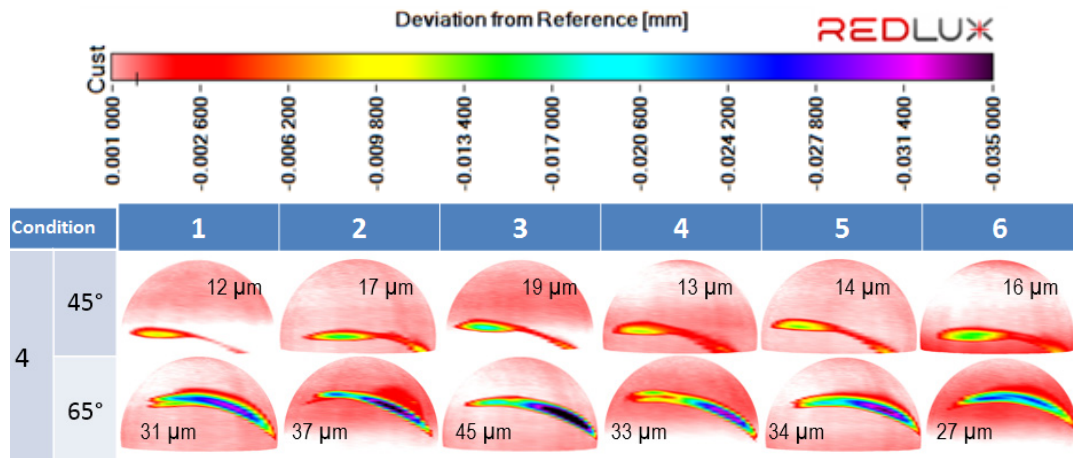


Figure 3-25. Visualisation of the heads under a 4 mm medial-lateral component translational mismatch via RedLux software after 3 million cycles. The maximum depth of the scar is aligned to each head accordingly.

The scar depth increased for all the cup inclination angle conditions as the translational mismatch increased from 2 to 3 to 4 mm (Figure 3-26). The mean scar penetration under a 2 mm translational mismatch on the heads due to edge loading between the standard ($2.9 \pm 0.8 \mu\text{m}$) and steep ($7.6 \pm 3.1 \mu\text{m}$) cup inclination angle conditions was found to be significantly greater under the steep conditions ($p=0.01$) after 3 million cycles. The mean scar penetration under a 3 mm translational mismatch of the heads due to edge loading between the standard ($6 \pm 1.8 \mu\text{m}$) and steep ($13 \pm 3.2 \mu\text{m}$) inclination angle was found to be significantly greater ($p<0.01$) after 3 million cycles. The mean scar penetration under a 4 mm translational mismatch of the heads due to edge loading between the standard ($15 \pm 2.6 \mu\text{m}$) and steep ($35 \pm 6.6 \mu\text{m}$) inclination angle was found to be significantly greater ($p<0.01$) after 3 million cycles.

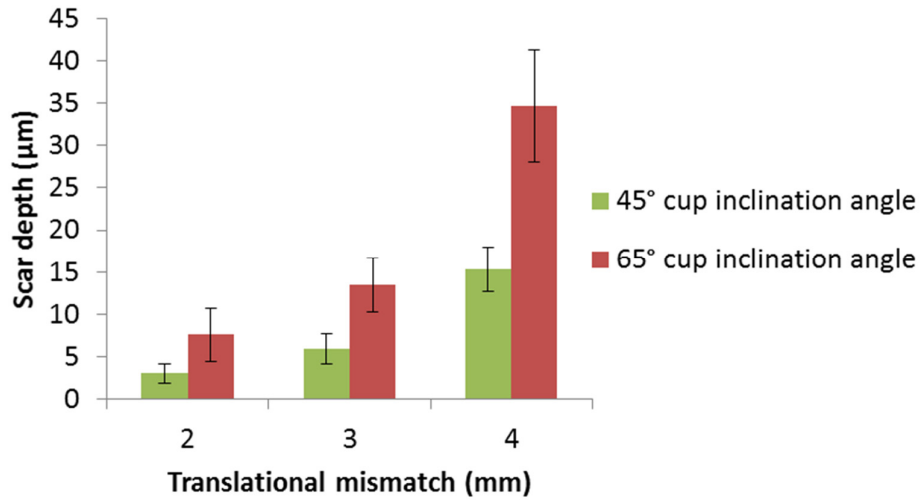


Figure 3-26. Mean ($n=6$, $\pm 95\%$ CI) maximum scar penetration after 3 million cycles under a 2, 3 and 4 mm medial-lateral component translational mismatch conditions for standard (45°) and steep (65°) cup inclination angles.

Post-test, no change in surface roughness (Ra) was observed on the pole region (P1 tested) of the heads under a 2 mm translational mismatch (Figure 3-27). The surface roughness increased where the wear stripe was located (P2 tested) to 11 ± 1 nm from 6 ± 1 nm. No significant difference ($p=0.73$) was found between the standard and steep inclination angles.

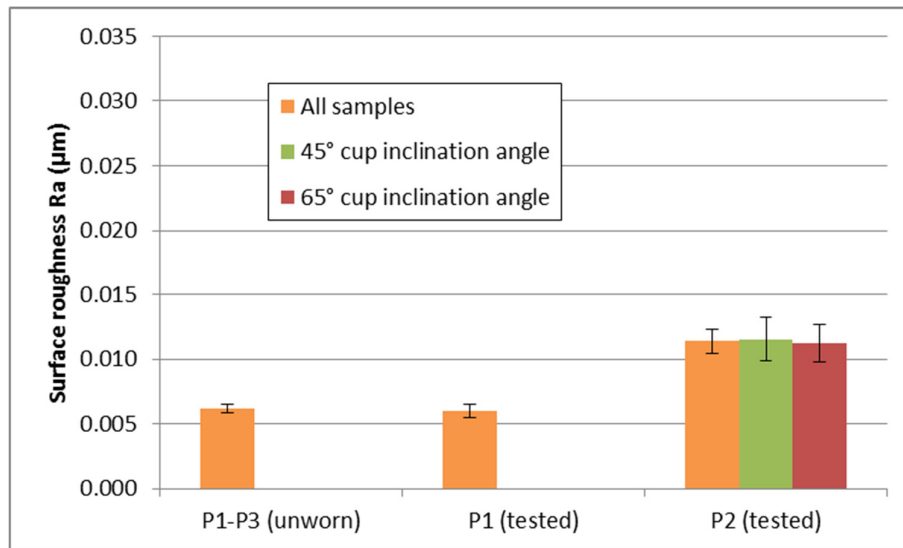


Figure 3-27. Mean surface roughness (Ra) for unworn head samples (P1-P3), and post-test at the pole (P1), and the wear scar (P2) under 2 mm medial-lateral component translational mismatch for standard (45°, $n=6$) and steep (65°, $n=6$) cup inclination angles.

Post-test, a small increase on the surface roughness (Ra) was observed from the one trace at the pole region (P1 tested) of the heads under a 3 mm translational mismatch (Figure 3-28) in comparison to the three traces (P1, P2 and P3) at pre-test. The surface roughness also increased where the wear stripe was located (P2 tested) to 17 ± 3 nm. No significant difference was found between the standard and steep inclination angles ($p=0.68$).

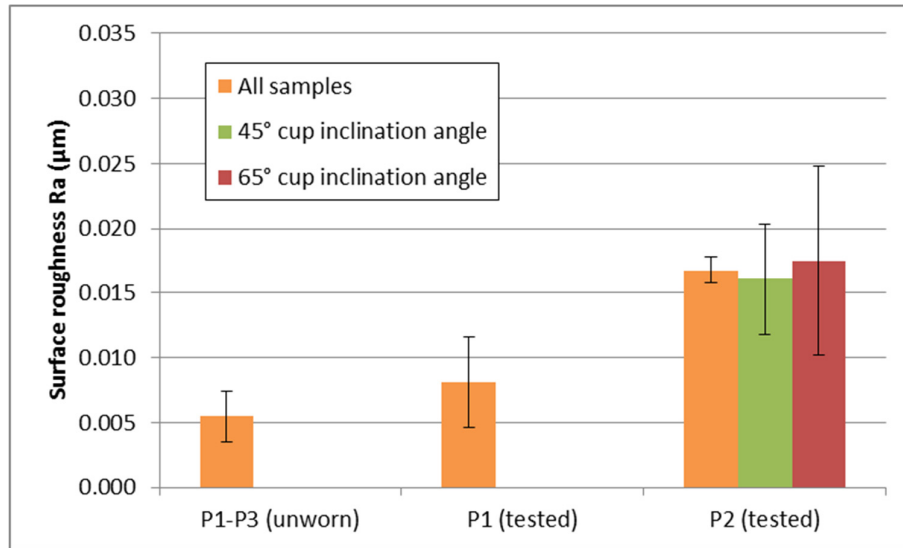


Figure 3-28. Mean surface roughness (Ra) for unworn head samples (P1-P3), and post-test at the pole (P1), and the wear scar (P2) under 3 mm medial-lateral component translational mismatch for standard (45°, n=6) and steep (65°, n=6) cup inclination angles.

Post-test, the surface roughness increased at the wear stripe location (P2 tested) to 18 ± 4 nm (Figure 3-29). No significant difference was found between the standard and steep inclination angles ($p=0.66$).

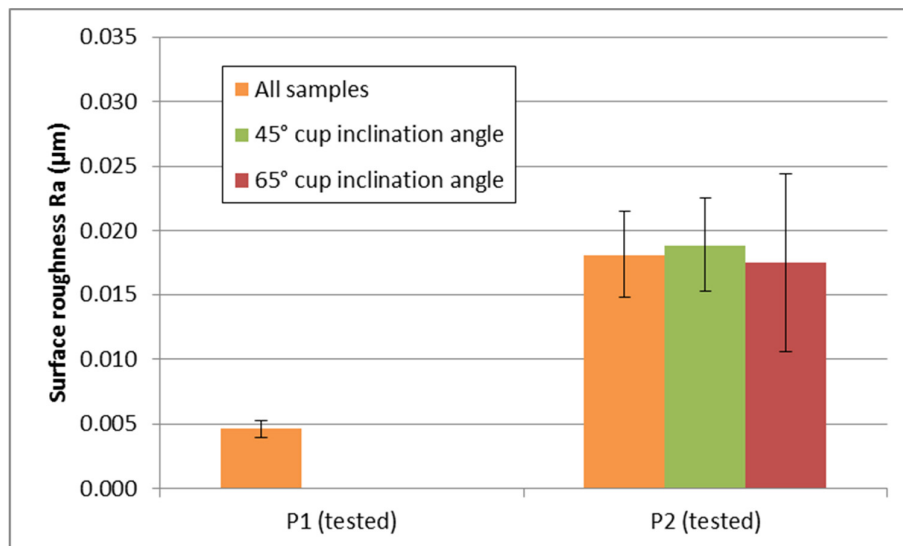


Figure 3-29. Mean (n=6, $\pm 95\%$ CI) surface roughness (Ra) for head samples post-test at the pole 'P1 (tested)', and the wear scar 'P2 (tested)' under 4 mm medial-lateral component translational mismatch for standard (45°) and steep (65°) cup inclination angles.

Volumetric wear assessment via the CMM

The mean calculated volumetric wear rate of the heads under a 2 mm translational mismatch via the surface analysis was $0.02 \pm 0.02 \text{ mm}^3/10^6$ cycles for the standard angles and $0.05 \pm 0.03 \text{ mm}^3/10^6$ cycles for the steep angles. This was similar to the gravimetric results which were $0.03 \pm 0.02 \text{ mm}^3/10^6$ cycles and $0.06 \pm 0.02 \text{ mm}^3/10^6$ cycles for the standard and steep inclination angles respectively. The volumetric wear calculated on the cups via the surface analysis was found to be lower than when measured gravimetrically, and in some cases with low wear, unable to acquire a value. However, a similar pattern between the stations was seen on the severity of wear as that measured gravimetrically and via CMM analysis.

The mean calculated volumetric wear rate of the heads under a 3 mm translational mismatch via the surface analysis was $0.03 \pm 0.01 \text{ mm}^3/10^6$ cycles for the standard angles and $0.11 \pm 0.07 \text{ mm}^3/10^6$ cycles for the steep angles. This was similar to the gravimetric results which were $0.05 \pm 0.01 \text{ mm}^3/10^6$ cycles and $0.14 \pm 0.08 \text{ mm}^3/10^6$ cycles for the standard and steep inclination angles respectively. The calculated volumetric wear rate on the cups via the surface analysis was $0.03 \pm 0.08 \text{ mm}^3/10^6$ cycles for the standard angles and $0.12 \pm 0.17 \text{ mm}^3/10^6$ cycles for the steep angles. This was also similar to the gravimetric results which were $0.06 \pm 0.03 \text{ mm}^3/10^6$ cycles and $0.16 \pm 0.23 \text{ mm}^3/10^6$ cycles for the standard and steep inclination angles respectively.

The mean calculated volumetric wear rate of the heads under a 4 mm translational mismatch via the surface analysis was $0.11 \pm 0.09 \text{ mm}^3/10^6$ cycles for the standard angles and $0.51 \pm 0.23 \text{ mm}^3/10^6$ cycles for the steep angles. This was similar to the gravimetric results which were $0.14 \pm 0.07 \text{ mm}^3/10^6$ cycles and $0.49 \pm 0.26 \text{ mm}^3/10^6$ cycles for the standard and steep inclination angles respectively. The cups were unable to be compared between the gravimetric results and the CMM analysis as pre-test measurements were not available.

3.7. Discussion

3.7.1. Dynamic separation

A simplified axial loading is used for most *in vitro* testing of hip joint replacement bearings. Early studies which investigated the wear under a single loading axis (joint reaction force) and a high cup inclination angle were not able to replicate stripe wear (edge loading) on ceramic-on-ceramic because the contact area does not shift significantly towards the rim region of the cup (Nevelos *et al.*, 2001). Nevelos *et al.*, (2001) demonstrated that the cup inclination angle under such test condition didn't affect the wear. Similar studies where the cup inclination angle was evaluated under the same test conditions indicate no difference between the cup inclination angles tested (Affatato *et al.*, 2004, Halma *et al.*, 2014) for ceramic-on-ceramic. These testing conditions are not the appropriate way to evaluate a surgical scenario and clinical delivery such as the cup inclination angle, as the outcome of the test is driven by the direction of the load which does not incorporate the multifactorial complexity of edge loading.

Previous studies at the University of Leeds, used a protocol termed microseparation to replicate the edge loading wear mechanisms. This protocol used a pre-determined level of dynamic separation which was kept constant throughout the test (i.e. an output of approximately 0.5 mm of dynamic separation). This meant the same level of dynamic separation was applied to the different parameters of the test, which yielded a similar level of severity of edge loading as it was a semi-control edge loading output. Thus, studies under this protocol were not able to differentiate the wear outcome of CoC bearings for different parameters such as the cup inclination angle or bearing diameter (Al-Hajjar *et al.*, 2010, Al-Hajjar *et al.*, 2012). This study however employs a translational mismatch as an input parameter and thus the dynamic separation is not controlled. Furthermore, the level of separation under certain conditions were greater than 0.5 mm and the maximum dynamic separation measured was 2 mm.

The same principle to replicate edge loading applies to this methodology, the contact area shifts towards the rim due to the dynamic separation, causing a higher stress as the contact area becomes smaller and the stripe wear indicating the area of contact develops on the head. With a controlled level of dynamic separation, the contact area and stress can be predominately similar when testing different conditions such as the head or cup inclination angle. This may explain why previous tests under a controlled dynamic separation for ceramic-on-ceramic and metal-on-metal indicated no difference in wear for different test conditions (Al-Hajjar *et al.*, 2010, Al-Hajjar *et al.*, 2012). Other studies where there was no dynamic separation present and results were different between the cup inclination angles, the increase

in wear can be explained based on the smaller contact due to the higher cup inclination angle leading to a higher stress (Williams *et al.*, 2008, Leslie *et al.*, 2009, Al-Hajjar *et al.*, 2012).

The magnitudes of dynamic separation obtained in this study under different head and cup centre mismatches and different cup inclination angle conditions, were of similar range of magnitudes as those measured by other studies from clinical assessment (Lombardi *et al.*, 2000, Tsai *et al.*, 2014). The maximum separation found by Tsai *et al.* (2014) was 0.4 mm, and the maximum separation found by Lombardi *et al.* (2000) was 3.0 mm. In this study different levels of dynamic separation were observed in the hip joint simulator depending on the input conditions of the test. The results from this study ranged from 0 to 2 mm of dynamic separation.

While the maximum separation observed clinically may serve as a point for comparison with this study, it is not likely that every patient fits under the same maximum level of separation as differences can be expected from patient to patient, from different activities and from different surgical deliveries, thus very complex. Different levels of separation have been observed for different activities, and different materials, ranging from 0-3 mm in the medial-lateral, anterior-posterior and superior-inferior direction (Lombardi *et al.*, 2000, Dennis *et al.*, 2001, Glaser *et al.*, 2008, Glaser *et al.*, 2010 and Tsai *et al.*, 2014).

Under lower levels of dynamic separation (less than 0.5 mm for a 45° cup inclination angle), edge loading was also observed with a stripe wear on the heads. This is an indication that clinically, a large dynamic separation is not required for edge loading to occur. Clinically, edge contact, due to high cup inclination angle is thought to be a driver for increased wear (De Haan *et al.*, 2008). However edge loading can occur clinically with various cup inclination angles (Esposito *et al.*, 2012). Several studies (refer to Chapter 1.6.3) have addresses only the effect of the cup inclination angle, while not considering the other factors or establishing a testing methodology which addresses the variability.

The low cup inclination angle in this study was thought to create a resistance to separation due to the spherical shape of the cup (Figure 3-30). A high cup inclination angle provided less coverage than a low cup inclination angle in the direction of the spring force applied. Hence why larger dynamic separations were observed for the 65° cup inclination angle in comparison to the 45° and 55° cup inclination angle, when comparing against the same level of translational mismatch (Figure 3-4). The resistance to separation due to the higher coverage can be assessed by evaluating the medial-lateral load measured during the swing phase of the cycle (Chapter 3.7.4). The minimum medial-lateral load increasing from the 65° to the 45° cup inclination angle (Figure 3-6) could explain the increase in resistance to separation.

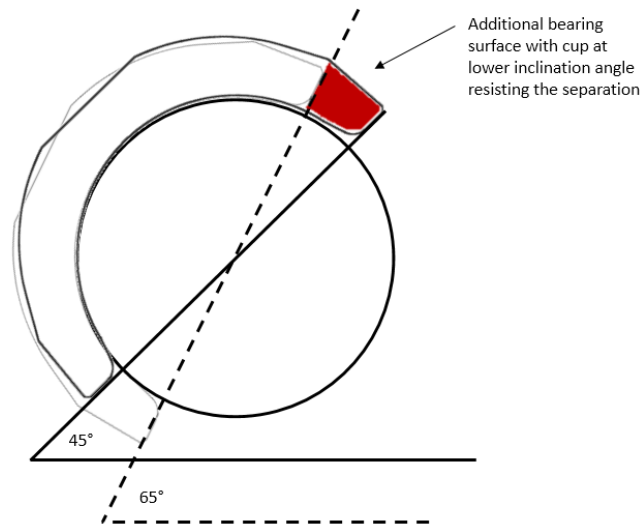


Figure 3-30. Schematic showing the acetabular cup at two inclination angle conditions highlighting the additional bearing surface with the cup at lower inclination angle which aids in the resistance of the separation due to medial-lateral force from the component translational mismatch.

3.7.2. Wear correlations

This study sets out to utilise the factors which influence the wear to generate a predictive tool for the variation of conditions that can be applied in a hip joint simulator which reflect *in vivo* conditions. Thus, the outputs of the biomechanical studies are discussed below to assess its influence as a predictive wear tool. The capability to predict the wear from simple changes to a system is encouraging for the evaluation of hip joint replacements. This test method could serve as a baseline for future and better wear predictors for different materials under more complex scenarios.

The study was split into two biomechanical phases. In Phase 1 (n=3) where only one station was used, the dynamic separation, maximum force at the rim and severity of edge loading were evaluated. In Phase 2 (n=6) where all six stations were employed, the severity of edge loading was only evaluated.

When the translational mismatch was increased, it resulted in a larger dynamic separation, and also higher wear. When these two outputs are plotted together (Figure 3-31) a strong positive power correlation was found ($R^2=0.95$). Previous studies of a set cup holder displacement of 0.5 mm resulted in $0.2 \text{ mm}^3/10^6$ cycles (Al-Hajjar *et al.*, 2013). The previous studies with a 0.5 mm cup holder displacement roughly equate to about 0.5 mm dynamic separation. The wear study from Al-Hajjar, *et al.*, (2013) was similar to the results of this study for a 0.5 mm dynamic separation for a 65° cup inclination angle. Hence the correlation indicates that for 45° and 65° cup inclination angle the wear would result in about $0.1 \text{ mm}^3/10^6$ cycles.

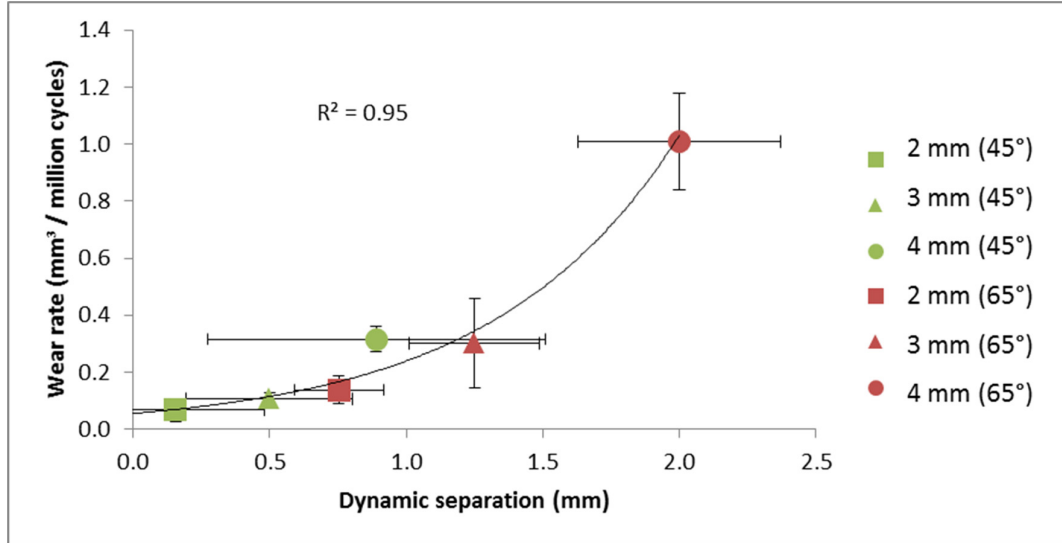


Figure 3-31. Mean wear rate ($\pm 95\%$ CI, n=6) of 36 mm ceramic-on-ceramic (BIOLOX® delta) bearings against the mean dynamic separation ($\pm 95\%$ CI, n=3) under 2, 3 and 4 mm translational mismatch conditions with a cup inclination angle conditions of 45° and 65°.

The increase in translational mismatch resulted in a higher force during edge loading and higher wear, when the means of these two are correlated with each other, a positive correlation was found ($R^2=0.85$), but there was a discrepancy of roughly $0.7 \text{ mm}^3/10^6 \text{ cycles}$ in the wear between the 3 and 4 mm translational mismatches under a 65° cup inclination angle (Figure 3-32). This was due to the larger duration of edge loading from the 4 mm condition as indicated by the severity of edge loading (Figure 3-9, p. 79).

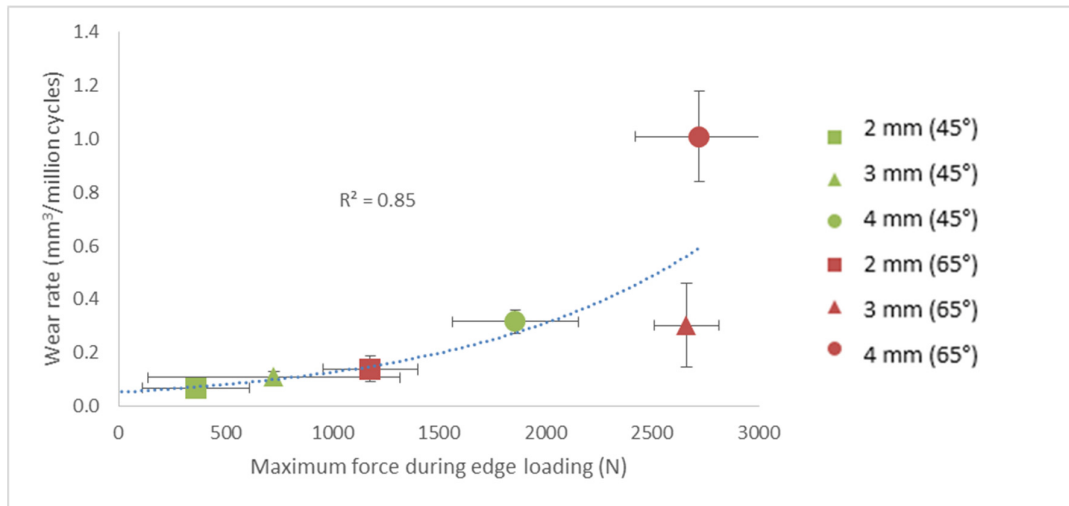


Figure 3-32. Mean wear rate ($\pm 95\%$ CI, n=6) of 36 mm ceramic-on-ceramic (BIOLOX® delta) bearings against the maximum force under edge loading ($\pm 95\%$ CI, n=3) under 2, 3 and 4 mm translational mismatch conditions with a cup inclination angle conditions of 45° and 65°.

A good positive correlation was also found between the severity of edge loading and the wear rate (Figure 3-33). During the Phase 1 of the biomechanics study under a 3 mm translational mismatch and 65° cup inclination angle there was one sample which had single type of relocation thus, the CL was very high and the mean from three samples was large due to the two samples with interrupted relocation. A larger sample number (n=6) was obtained from Phase 2 of the biomechanics study and all the stations were utilised to incorporate the variability.

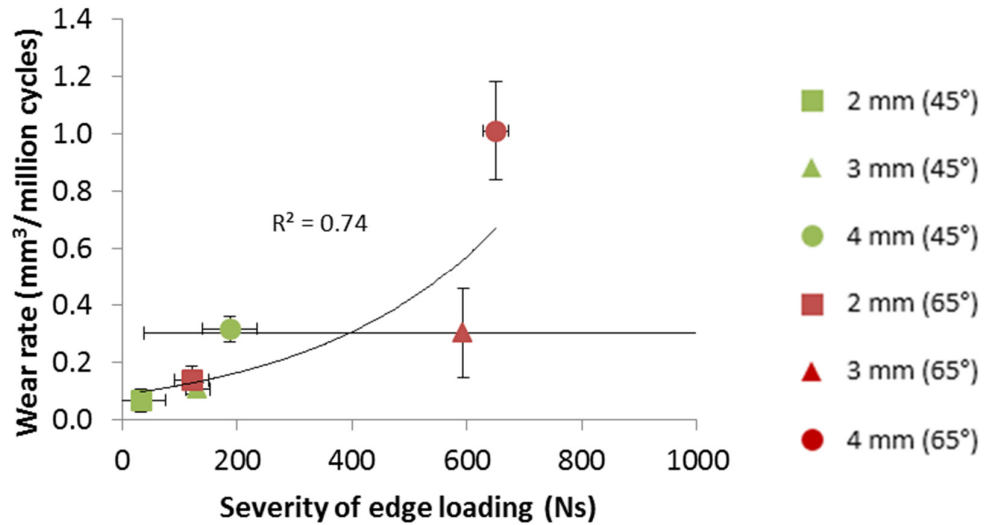


Figure 3-33. Mean wear rate ($\pm 95\%$ CI, n=6) of 36 mm ceramic-on-ceramic (BIOLOX® delta) bearings against the severity of edge loading ($\pm 95\%$ CI, n=3) under 2, 3 and 4 mm translational mismatch conditions with a cup inclination angle conditions of 45° and 65°.

The results from the Phase 2 aligned better with the wear study (Figure 3-34) and a higher correlation was found ($R^2=0.98$). During the wear study under a 3 mm translational mismatch and 65° cup inclination angle, station #3 had interrupted relocation throughout the test, whereas, station #4 and #5 had occasional interrupted relocation. Thus, the mean from the Phase 1 biomechanics study based on three samples did not encapsulate fully the variability from six stations during the wear study. These results indicate that the 3 mm translational mismatch was the threshold between for higher wear due to interrupted relocation and the longer time spent under edge loading.

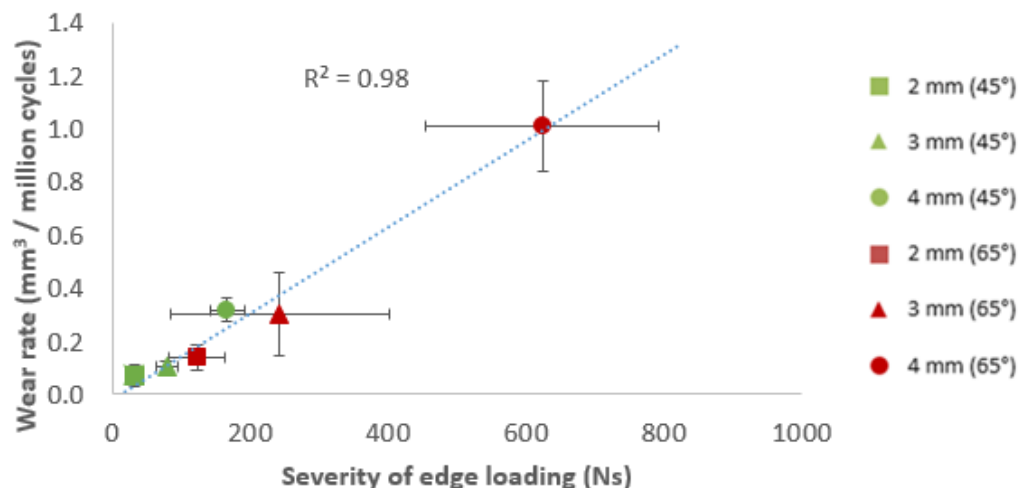


Figure 3-34. Mean wear rate ($\pm 95\%$ CI, $n=6$) of 36 mm ceramic-on-ceramic (BIOLOX® delta) bearings against the severity of edge loading ($\pm 95\%$ CI, $n=6$) under 2, 3 and 4 mm translational mismatch conditions with a cup inclination angle conditions of 45° and 65°.

The high correlation between the severity of edge loading and the wear indicates this type of evaluation considers the greatest factors driving the wear for these test conditions. Previous studies that evaluated the geometrical parameters such as the head diameter, clearance have led to an understanding to how the lubrication changes and higher or lower wear can be expected. However, those previous studies elaborate on the trends under optimal testing conditions. In this methodology, the lubrication is compromised by initiating contact between the rim of the cup and the head, thus the trends may no longer be applicable. Hence why a high correlation between the time and loading on the rim can be associated with the higher wear.

In regards to the type of wear mechanics occurring during edge loading when the rim of the cup is in contact with the head, as the head and the cup are the same material with equal hardness properties, adhesive wear could be considered as the driving wear mechanism. It can be hypothesised that the asperity points undergo fatigue due to the high contact stresses and the bond between the micro-particles break leading to removal of material.

The change in geometry in the rim of the cup and the increase in depth of the wear scar of the heads confirms the contact between the two components. It is difficult to account the influence of the bovine serum lubricant on the wear, but it is reasonable to assume boundary lubrication during edge loading from these testing conditions. This type of ceramic material has high hydrophilic properties which would decrease the probability of dry conditions, and also to consider the test cell is completely submerged with lubricant.

Previous wear equations for polyethylene consider the sliding distance, the contact area, the hardness difference, the type of lubrication and the level of cross shear to predict the wear (Liu *et al.*, 2012). This is the first time the profile (curve) from the loading cycle is utilised to quantify the severity of wear in an *in vitro* model. Other factors to consider and include with regards to the severity of edge loading could be, the contact area and the hardness, as the change of these two will impact the wear under a translational mismatch condition.

3.7.3. Maximum vertical force under edge loading

It is important to consider the maximum loading conditions during an activity as an input parameter of an *in vitro* testing protocol. The maximum load recorded for walking is approximately 3 times body weight (Bergmann *et al.*, 2001). This magnitude and condition has been used extensively for the evaluation of hip joint replacement bearing designs and materials. However, patient to patient variation and different activities means the magnitude and direction of loading differs. Thus, in order to understand the variation in the severity of wear it is important to have a testing protocol where the magnitude of loading differs.

Increasing the level of the translational mismatch resulted in an increase of the maximum vertical force applied under edge loading conditions (Figure 3-5, p. 75). This was due to the force provided by the spring in the medial-lateral direction. The higher level of translational mismatch, the higher the force exerted on the cup medial-laterally (Figure 3-6, p. 77). Hooke's Law states the force ' F ' required to compress a spring is proportional to the distance ' x ' and the spring constant ' K ', Equation 3. Hence, under a higher level of translational mismatch (in this case ' x ') the duration of edge loading was prolonged due to the higher medial-lateral force applied on the cup. Only until a sufficient vertical load was applied to overcome the medial-lateral force, the cup relocated back towards the centre of the head.

Equation 3.
$$F = kx$$

The increase in maximum vertical force under edge loading due to the increase in cup inclination angle (Figure 3-5, p. 75) was considered to be influenced by the magnitude of the dynamic separation. A higher cup inclination angle had a larger separation away from the centre of the head (Figure 3-4, p. 74), thus the amount of distance required for the cup to relocate back towards the centre of the head was greater than a lower cup inclination angles. This increased distance between the head and the cup centres in the medial-lateral direction was thought to delay the point when the cup relocates, thus increase the maximum vertical load under edge loading.

It is difficult to determine the magnitude of the force under edge loading *in vivo* and the circumstances which lead to edge loading. Finite element models have evaluated the increased contact pressure and torque under specific conditions where the rim is in contact with the head (Mak *et al.*, 2002, Liu *et al.*, 2013). However, currently there isn't a study where edge loading has been isolated *in vivo* and the force acting on the rim evaluated for a patient with a hip joint replacement.

3.7.4. Medial-lateral load

The cup inclination angle was thought to play a role on the resistance for separation. A way to capture this resistance is by evaluating the medial-lateral load. The minimum medial-lateral load consistently occurred during the maximum separation (swing phase cycle of the profile), i.e. the low vertical loading period. The minimum medial-lateral load for the 45° cup inclination angle increased from around 50 to 150 N as the translational mismatch increased (1-4 mm). In contrast, the minimum medial-lateral load for the 65° cup inclination angle plateaus around 50 N. The 55° cup inclination angle sits between the two conditions (45° and 65° cup inclination angles). The lower force measured for the 65° in comparison to the 45° cup inclination angle, is an indication that the spring is not fully compressed. This correlates with the higher separation observed for the 65° in comparison to the 45° cup inclination angle. Furthermore, the higher force measured for the 45° in comparison to the 65° cup inclination angle is an indication of the higher resistance against separation.

Different types of edge loading were observed during the biomechanical studies. The test condition under a 4 mm translational mismatch and 65° cup inclination angle caused an interrupted relocation. The medial-lateral force provides evidence of the different type of relocation exhibited in contrast with the rest of the conditions tested. The maximum medial-lateral force occurred during the double peak loading of the cycle profile while the head and the cup were conforming to each other along the centres of rotations, i.e. a sufficient force was applied vertically to relocate the cup with the head. The maximum medial-lateral force for 45° and 55° increased with the increased translational mismatches (Figure 3-6, p. 77). Under low levels of translational mismatches (1-3 mm) the maximum medial-lateral force also increased under a 65° cup inclination angle for the increased translational mismatch. However, under a 4 mm translational mismatch, the medial-lateral force for the 65° did not increase as much as the 45° and 55° cup inclination angles. The lower medial-lateral force under a 4 mm translational mismatch and 65° cup inclination angle was an indication that the spring was not fully compressed during the double peak loading. Thus, a separation may exist between the cup and the head. The wear scar on the heads from this condition indicates edge loading was present for a longer period which correlates with head not relocating after the first peak load

(Figure 3-25, p. 94). An alternative explanation for the lower medial-lateral load for this condition could be that the cup holder was tilted during the double peak loading which also leads to higher wear due to edge contact with the rim of the cup.

In vivo, many conditions can lead to stripe wear. The force exerted by the input translational mismatch in this study shifted the contact area towards the rim of the cup as indicated by 2 mm translational mismatch under a 45° cup inclination angle. During gait the magnitude and direction of the force can produce a shift of the location of the contact area between the head and the cup such that edge contact occurs without any separation between the centres of the head and the cup. Studies from *in vivo* measurement of the medial-lateral load during walking conditions indicate to operate between 100 and 500 N acting in the medial direction, i.e. the head forced against the cup (Bergmann *et al.*, 2001). This may be an indication of varied levels of soft tissue tension in the joint after the hip joint replacement surgery, or differences in loading due to patient variability (i.e. gait, weight, anatomy etc.) While the direction and magnitude of force from Bergamnn's (2001) results may not align with this study, it can be postulated that the magnitude of the force could change the contact area towards the rim of the cup for patients with a low cup inclination angle and edge contact may occur under these conditions leading to higher wear.

3.7.5. Type of edge loading

Previous *in vitro* studies that replicate edge loading conditions either employ a spring to create a medial-lateral displacement (Nevelos *et al.*, 2000) or a negative force to create a subluxation type (Williams *et al.*, 2003) in hip joint simulators, but these only applied low force during edge loading i.e. edge loading only during the swing phase load which is a low force profile input (50-300 N). Currently there isn't a study for hip joint replacement testing that has evaluated the wear under edge loading under high forces acting on the rim. Thus, this is the first time this wear mechanism has been noted *in vitro*. The hip joint simulator is a physical unit where inputs are set to represent *in vivo* scenarios. This study does not associate the clinical scenario where a large translational mismatch and a high cup inclination angle will result with this specific type of wear mechanism i.e. interrupted relocation for a walking cycle. The reason for the interrupted relocation may be due to a variety of factors, such as but not exclusively; the rate at which the first loading peak was applied and the maximum force, the tilt caused on the cup holder due to the input translational mismatch, the friction in the cup holder unit which allows the translational displacement (medial-lateral bearings), and the design of the cup. Only during interrupted relocation scenarios squeaking was heard which seemed to originate from the ceramic bearings. The literature indicates that squeaking can occur when ceramic bearings are used but is not exclusive to an activity (Sexton *et al.*, 2011). The reason for squeaking *in vivo* is

not fully understood, but it is reasonable to accept that squeaking can originate from the high friction and high stresses even when a lubricant is employed.

3.7.6. Severity of edge loading

The evaluation of the severity of edge loading considers the duration of separation between the centres of the head and the cup. During the migration of the contact area as the cup translates away from the head, it is likely that hard on hard contact occurs in the form of boundary or mixed lubrication. An important parameter is the instance at which migration begins and when it ends. During edge loading, the force acting on the rim is another important parameter to interpret the severity. Thus, the vertical and medial-lateral force measured during edge loading along with the duration, give a good correlation with the wear. For these studies, the flexion motion was of the same magnitude throughout. It would be ideal to consider the motion such as the translation of the cup relative to the head and the head rotation along the severity of the wear. However, it is necessary to first separate the independent relationship between the translation and the wear during edge loading.

During gait, it is difficult to predict the duration of edge loading and the force on the rim of the cup. The cup inclination angle and the activity would influence the duration of edge loading (Xijin *et al.*, 2016). Walter *et al.*, (2004) postulated some scenarios leading to edge loading from their retrievals studies. Chair rising or step climbing was linked to posterior edge loading. However, the direction of the load, magnitude and cup orientation play a role on the occurrence and migration of the contact area towards the rim of the cup.

The severity of edge loading could be a link of fractured ceramic components *in vivo*. Currently, the incidence of fracture has decreased since the introduction of the 4th generation of composite ceramics known as BIOLOX[®] delta (Massin *et al.*, 2014). However, previously ceramics were known to fracture more frequently (Griss and Heimke, 1981). Steward *et al.*, (2003) tested ceramic-on-ceramic couples under edge loading conditions. Their methodology involved only a displacement measure for separation ranging from 0.5-1.0 mm. Within this magnitude, severe edge loading conditions, such as interrupted relocation could have occurred as the time and force under edge loading were not measured and neither was the translational mismatch input. During their study, one of their samples fractured during testing. Therefore, severe edge loading conditions may be the reason as to why that sample failed.

3.7.7. Wear under a translational mismatch

The wear results from these studies indicate that, as the input translational mismatch was increased, the wear rate increased (Figure 3-22, p. 92). Overall, the 65° cup inclination angles had a higher wear rate than that of the 45° cup inclination angle for any given translational

mismatch, and as the translational mismatch increased the wear difference between that of 45° and 65° became larger. Previous studies of CoC under edge loading demonstrate that the wear rate will increase compared to standard conditions (Stewart *et al.*, 2001). Furthermore, previous studies that compared different cup inclination angles for CoC under edge loading conditions did not show a difference on the wear (Al-Hajjar *et al.*, 2010). The conditions on which they were tested however were of the same magnitude of dynamic separation, whereas, in this test the dynamic separation was an output of the test. Currently, there isn't a wear study which has generated high wear rates for hip joint replacements greater than 0.3 mm³/10⁶ cycles for BIOLOX® delta ceramic coupled bearings. In contrast, retrievals show a variation of wear rates (ranges from 0-7.2 mm³/year) for CoC (Esposito *et al.*, 2012). These retrievals studies with signs of edge loading have shown a correlation between the length of the wear scar on the heads and the total wear volume. A better correlation however, may be that of the depth of the scar and the wear.

Higher wear rates were measured under a 4 mm translational mismatch and a 65° cup inclination angle. This type of condition resulted in an interrupted relocation, and the evidence can be seen on the maximum penetration on the heads which was towards the right-end side (Figure 3-25), indicating the head is extending on the profile cycle of the hip simulator. For every translational mismatch conditions, the maximum penetration on the heads was always higher for the 65° cup inclination angle than the 45°. Thus the maximum depth of the scar was a good indication of the wear comparison between the cup inclination angles. The wear scar with the maximum depth was measured under a 4 mm translational mismatch and a 65° cup inclination angle.

It may be postulated that the interrupted relocation is another test condition entirely and if it didn't occur the wear projection with the increase of the translational mismatch for the 65° cup inclination angle may be more aligned along the 45° cup inclination angle curve (Figure 3-22). One could expect based on the biomechanical study (dynamic separation, max force on the rim and severity of edge loading) indicated by the 55° cup inclination angle that the degree of wear for the 65° cup inclination angle condition would be higher than the 45° cup inclination angle if the interrupted relocation was not present.

This study indicated that the test conditions change the way the ceramic bearings wear as time progresses. Some previous edge loading testing simulation for ceramic-on-ceramic did not demonstrate a bedding-in wear phase for the first million cycles of testing (Al-Hajjar *et al.*, 2013). However, other studies with previous ceramic material generations (BIOLOX® forte) do indicate a bedding in phase (Stewart *et al.*, 2001). In contrast, metal-on-metal tested under

edge loading conditions has not demonstrated higher wear during bedding-in than the steady state wear (Al-Hajjar *et al.*, 2012). In this study, there was no bedding-in wear associated with a lower translational mismatch and any of the 45° cup inclination angle test conditions. However, the wear under a translational mismatch of 4 mm and a cup inclination angle of 65° exhibited a bedding-in phase which had higher (0.38 mm³) wear than the steady state phase.

Post-wear test, the wear scar of the heads always had a higher surface roughness compared to pre-worn, this increase was from 0.005 µm up to 0.020 µm. The surface roughness seemed to increase when a larger translational mismatch was applied. However, there was no difference seen between the two types of inclination angles for each type of translational mismatch. It is difficult to account how does the increase in surface roughness affects the tribology of the test. For more plastic materials, it has the potential to increase the wear in the form of an abrasive wear mechanism. For this test scenario it could increase the frictional torque, however the test conditions indicate that the input translational mismatch can also factor an increase in the frictional torque between the bearings (Al-Hajjar *et al.*, 2015).

3.7.8. Limitations

This study sets out to evaluate the dynamic separation, however, it can be challenging determining the exact value. The hip test cell or system (cup holder, flexion tray, stem, etc.) itself moves, and the input conditions of the test alter the behaviour of the system. Thus, a budget of uncertainty was calculated to account for all the different scenarios. As an average the system had a maximum uncertainty value of 0.35 mm of medial-lateral displacement. Thus, it is reasonable to consider this value as the maximum error from the dynamic separation calculated.

Another challenge was defining the point where the head and the cup were axially aligned as various aspects need to be considered; such as the clearance between the components, the displacement associated with the force applied to the head, stem, and flexion tray during dynamic conditions. The identification of the head and cup assembly centre is important as it aids defining the maximum displacement between the centre of the head and the cup. It also affects the maximum force measured under edge loading, as the protocol sets a reading of the force at 0.1 mm from the assembly centre point. It also affects the severity of edge loading calculated as defining the two key points in time, initial displacement and the assembly point contributes to the magnitude of the severity of edge loading.

Different methodologies can be used to evaluate the dynamic separation, the maximum force during edge loading and the severity of edge loading. However, during this study all the evaluations were consistent for all the conditions for consistency in the results. Through the

process of defining a methodology for the assessment, it was found that regardless of the evaluation employed, the same pattern was found for different evaluations.

This methodology did not consider the effect of the vertical mismatch due the medial-lateral translational mismatch input. The input translational mismatch causes a superior displacement due to the geometry of the cup during dynamic separation, but this was not measured at any stage of the test (i.e. either at the input set-up or during cyclic loading). The vertical mismatch can be estimated by calculating the geometries of the components and set a virtual mismatch, but the principle of the method was to maintain a constant medial-lateral translational mismatch.

Another limitation in this study was associated with the test equipment which can influence the severity of edge loading and wear. An example of this is the maximum joint reaction force applied to the specimens (i.e. the double peak load). During the 3 mm translational mismatch (Chapter 3.6) a decrease in the peak loading occurred during the testing (Figure 3-35). The peak load kept decreasing as the test progressed, and at the end it was substantially low (approximately 2300 N). The output signal from the hip joint simulator indicated the rate at which the load was applied was slower, and also not reaching the desired peak load. This could have impacted the capacity of the cup to relocate back to its original position, hence affecting the severity of edge loading and the wear.

The loading profile can also affect the magnitude of the dynamic separation. During routine calibration and testing readings, station #6 was found to have a higher swing phase load (approximately 100 N higher than the input) during the wear study (Chapter 3.6). The swing phase load acts as a resistance against separation and a higher swing phase load can lead to a lower dynamic separation. Chapter 4 evaluates the effect of the swing phase load under a translational mismatch.

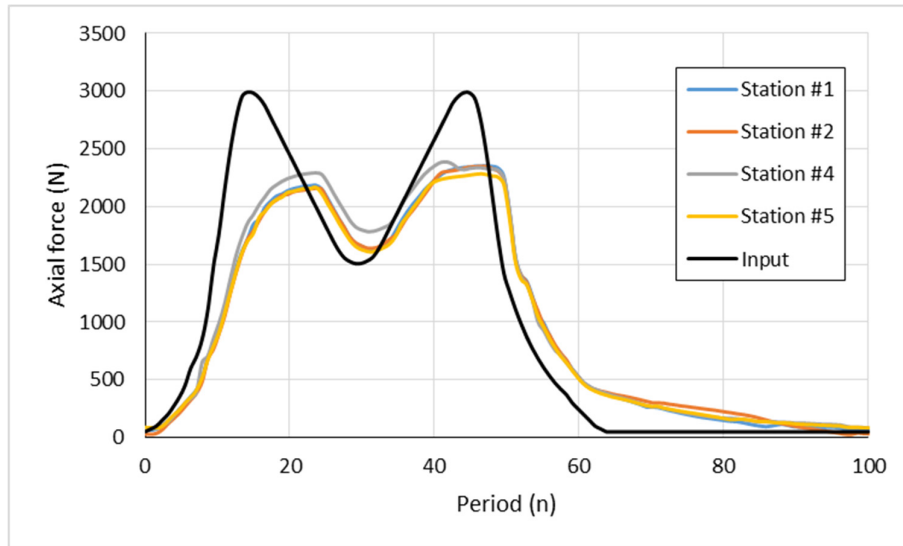


Figure 3-35. Input (in black) and output (Stn #1, #2, #4 and #5') readings from the Leeds II Hip Joint Simulator during the wear study under a 3 mm translational mismatch and 65° inclination angle condition.

3.8. Conclusion

An *in vitro* test method was developed to represent a translational mismatch between the centres of the head and the cup clinically as an input. Thus, the outcome is dependent on the variables associated with the positioning such as the level of translational mismatch and the cup inclination. The level of translational mismatch influenced the force exerted on the cup. This force results in two scenarios, firstly, it changes the contact area between the head and the cup, and under a low joint reaction force it allows the cup to translate away from the head centre. The results indicated that when a translational mismatch was employed as an input test variable, the magnitude of dynamic separation, the duration and magnitude of the forces under edge loading are affected when different cup inclination angles are employed. As the translational mismatch increased the severity of edge loading increased and resulted in higher wear rates under these kinematic conditions. The cup inclination angle of 45° exhibited greater resistance to separation due to the extended coverage angle, and when tested under low levels of translational mismatch resulted in the lower wear compared to the 65° cup inclination angle due to the lower time spent on the rim and lower forces under edge loading.

4. The Influence of the Swing Phase Load on the Occurrence and Severity of Edge Loading and Wear for Ceramic-on-ceramic Total Hip Replacement under Variations of Component Positioning

4.1. Introduction

Clinical data indicates a surgical variation with regards to the positioning of the acetabular cup (inclination angle) in a patient. Callanan *et al.* (2011) indicated that about 50% of the population in their study were within the cup orientation target considered appropriate (30° - 45° cup inclination angle). Pre-clinical testing indicates that this target orientation may work well in patients when only considering the wear of the bearing surface of the hip joint replacement components as defined in the international testing standards (ISO14242-1). However, the current international testing standards are not developed to consider a wider set of conditions and evaluate the performance of the hip joint replacements, and incorporate the variability of the wear mechanisms and failures as indicated by retrievals studies (Nevelos *et al.*, 1999). Many studies have been carried out to understand the behaviour of hip joint replacements under adverse conditions (described in Chapter 1.6.3). However a platform to evaluate adverse conditions is still yet to be adopted as part of regulatory requirements for hip joint replacement testing.

Edge loading condition is recognised as one of the factors leading to the failure of the implant. Several studies have demonstrated increase in wear due to such conditions which are not exhibited by conventional testing standards (ISO14242-1). In Chapter 3, a translational mismatch between the centre of rotation of the head and the cup was applied during a standard walking cycle as a platform to incorporate edge loading in a test. The results demonstrated how the level of translational mismatch applied in combination with the cup inclination angle affected the biomechanics and wear. The tests conditions have defined inputs which are controlled in the hip simulator in order to replicate edge loading by displacing the cup away from the head and creating a contact between the head and the rim of the cup. One of the inputs, was the defined swing phase load. This is a simulated reaction force applied to the acetabular cup in one axis. The load profile applied to the cup comes from a standardised double peak load to represent walking. The *in vivo* forces that the hip joint replacements experience during walking are not always the same and Bergmann *et al.* (2001) data indicate that the swing phase load vary from patient to patient during walking conditions. Thus, clinically it is necessary to consider different magnitudes of forces during edge loading, and experimentally it is necessary to better understand the associated load input profile effect while applying a translational mismatch to replicate edge loading.

4.2. Aim

The first aim of this study was to determine how the swing phase load influences the biomechanics of ceramic-on-ceramic (BIOLOX® delta) bearings when a medial-lateral component translational mismatch between the head and cup centre was applied and different cup inclination angles were employed. The second aim was to determine how the swing phase load affects the wear of ceramic-on-ceramic (BIOLOX® delta) bearings when a medial-lateral component translational mismatch between the head and cup centre was applied under a single cup inclination angle.

4.3. Methodology of the study

This study was split into two sections:

Section 1. Biomechanical study

Phase 1: A broad biomechanical study to evaluate the influence of the swing phase load on; 1) the magnitude of dynamic separation, 2) the relationship of the input conditions against the output dynamic separation, 3) the magnitude of the force acting under edge loading, and 4) the time during the cycle the head spends on the rim of the cup (duration of edge loading) under four levels of medial-lateral component translational mismatch between the head and cup centre (1, 2, 3 and 4 mm), where each translational mismatch was coupled with a cup inclination angle equivalent *in vivo* to 45°, 55° and 65°. For each of the 12 conditions, a swing phase load ranging from 50 to 450 N was employed, equating to 132 conditions in total. Three samples were used in total per condition.

Phase 2: A limited biomechanical matrix study to evaluate; 1) the magnitude of the force acting under edge loading, and 2) the time during the cycle the head spends on the rim of the cup (duration of edge loading) under a medial-lateral component translational mismatch and a single cup inclination angle for two swing phase load conditions. Six samples were used in total per condition. The two selected test conditions were:

- A 4 mm translational mismatch under a 65° cup inclination angle with a swing phase load of 150 N
- A 4 mm translational mismatch under a 65° cup inclination angle with a swing phase load of 300 N

Section 2. Wear study

A limited wear study to determine the influence of edge loading due a translational mismatch and a single cup inclination angle on the wear of ceramic-on-ceramic (BIOLOX® delta). The selected test conditions were the same as those selected on Phase 2 of the biomechanical study. These were: 4 mm medial-lateral component translational mismatch for 65° cup inclination angles under a 150 and 300 N swing phase load, equating to 2 conditions in total.

4.4. Biomechanical study Phase 1. Evaluation of the biomechanics for different swing phase loads under variations in translational mismatch and cup inclination angle

4.4.1. Aim

The aim of this study was to determine how the swing phase load influences the occurrence and severity of edge loading. This was measured by assessing; 1) the magnitude of dynamic separation, 2) the relationship of the input conditions against the output dynamic separation, 3) the magnitude of the forces acting under edge loading, 4) the time during the cycle the head spends on the rim of the cup (duration of edge loading). The variables associated with component implant positioning were as follows; medial-lateral component translational mismatch between the head and cup centres and the acetabular cup inclination angle.

4.4.2. Methodology

Station number three of the Leeds Mark II Physiological Anatomical Hip Joint Wear Simulator was used, and the methodology described in Chapter 2 was followed. The bearing material used was BIOLOX® delta as detailed in Chapter 2.1. Three cup inclination angles were chosen, which were 45°, 55° and 65° relative to the *in vivo* joint force vector. A translational mismatch was applied at the start of the test to the hip simulator. This was achieved by moving the cup in the medial direction away from the femoral head centre by 1, 2, 3 and 4 mm. For each of these conditions a swing phase load of 50 to 450 N was employed as described in Table 4-1. This equated to 132 conditions, and for each condition 3 samples were employed. One station was used to evaluate each condition. The details of the test are described in Table 4-1. Mean values and $\pm 95\%$ Confidence Intervals (CI) were determined and statistical analysis (one way ANOVA) completed (significance taken at $p < 0.05$).

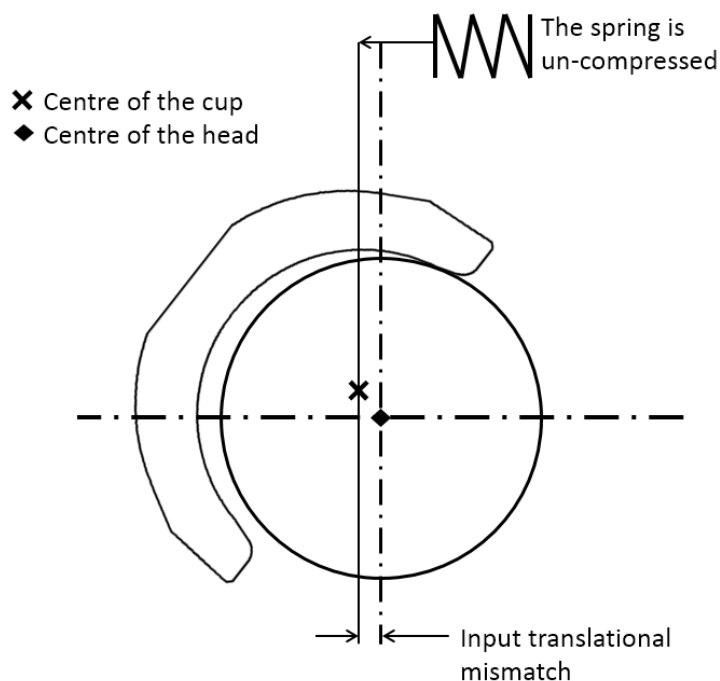


Figure 4-1. Schematic of the input translational mismatch between the centre of the head and the centre of the cup in the Hip Joint Simulator.

Table 4-1. Details of the biomechanical study for the evaluation of different swing phase loads under a translational mismatch in a hip joint simulator.

Study	Details (Unit)	Input
Biomechanical study	Equipment	Six-station Leeds Mark II (A)
	Materials	Ceramic-on-ceramic (BIOLOX® delta)
	Design	PINNACLE®
	Head size diameter (mm)	36
	Frequency (Hz)	1
	Loading profile	Based on Paul's walking cycle (twin peak load)
	Max peak force (N)	3000
	Trough load (N)	1500
	Swing phase load (N)	50, 75, 100, 125, 150, 175, 200, 250, 300, 350, and 450
	Motion profile	Leeds walking cycle (Barbour <i>et al.</i> , 1999)
	Flexion / Extension (°) of the head	+30 / -15
	Internal / External rotation (°) of the cup	+10 / -10
	Stem anterversion angle (°)	20
	Cup version angle (°)	0
	Translational mismatch (mm)	1, 2, 3 and 4
	Spring constant (N/mm)	100
	Number of total bearings tested	3
	Cup inclination angle (°)	45, 55 and 65
	Cycles completed	240
	Station used (#)	3

4.4.3. Results

The outputs from the tests were: the magnitude of separation, the ratio of the input test conditions against the dynamic separation, the type of edge loading and the severity of edge loading for different magnitudes of swing phase loads under different levels of translational mismatches and different cup inclination angles.

Under a translational mismatch of 1 mm, hardly any dynamic separation was observed for all the three cup inclination angles (45°, 55° and 65°), Figure 4-2. A small (less than 0.35 mm) dynamic separation was observed for the 65° cup inclination angle under a low swing phase load (50 N).

When the translational mismatch was increased to 2 mm, different levels of dynamic separation were observed for the three cup inclination angles through the different swing phase load conditions (Figure 4-2). The largest dynamic separation was detected under the 65° cup inclination angle, followed by the 55° and finally the 45° cup inclination angle under a low swing phase load (50 N). As the swing phase load increased, the dynamic separation decreased for all the cup inclination angles, until no separation was detected.

Larger levels of dynamic separation resulted from the 3 mm translational mismatch for all the cup inclination angles under low swing phase load (50 N) conditions (Figure 4-2). The 45° cup inclination angle had no noticeable dynamic separation under higher than 70 N swing phase load conditions. The dynamic separation for the 55° and 65° cup inclination angles decreased to about 0.25 mm under higher swing phase load conditions of 200 N.

Under 4 mm of translational mismatch, higher levels of dynamic separation were observed for all the cup inclination angles under low swing phase load conditions (50 N), Figure 4-2. Some dynamic separation was evident for slightly higher swing phase load conditions (roughly 150 N) for all cup inclination angles. Under the conditions of 250 N swing phase load, a relative displacement was measured, however, it was thought that it is not dynamic separation but rather movement of the overall components. These displacements were noticeably lower than 0.5 mm in comparison to the larger levels of dynamic separation.

Overall, the increase in swing phase load impeded and decreased the dynamic separation.

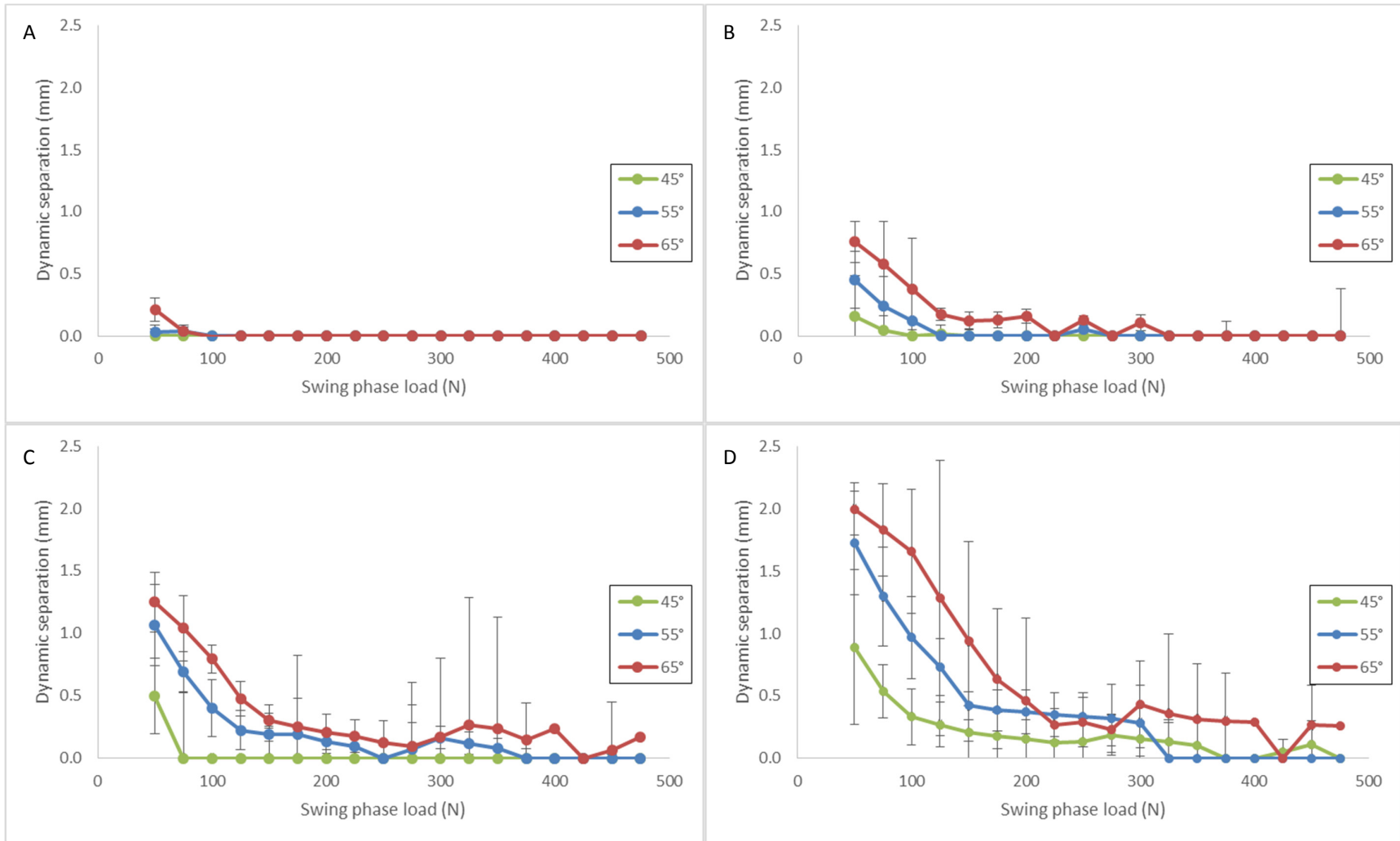


Figure 4-2. Mean ($n=3$, $\pm 95\%$ CI) dynamic separation for 36 mm ceramic-on-ceramic (BIOLOX® delta) bearings under 1, 2, 3 and 4 mm translational mismatch conditions (A, B, C and D respectively) with a cup inclination angle of 45°, 55° and 65°.

Separation ratio

The Separation Ratio (SR) is the relationship between the input translational mismatch and input swing phase load in the hip joint simulator which produces an output dynamic separation. A dynamic separation occurs due to the spring effect, the magnitude of the force applied by the spring (i.e. translational mismatch) and the swing phase load applied in the hip joint simulator. In Chapter 3 the effect of the input translational mismatch on the dynamic separation was evaluated. It indicated that the higher cup inclination angle and higher translational mismatch gave higher dynamic separation (refer to Chapter 3.4.3 Figure 3-4, p. 74). This study evaluates the effect of the input swing phase load on the dynamic separation. Thus, the SR is an evaluation tool to analyse the cause and effect from the inputs in the hip joint simulator for multiple conditions. The SR is the relationship of the inputs in the hip joint simulator for dynamic separation (i.e. translational mismatch times the spring constant) and input of the resistance against dynamic separation (i.e. the minimum swing phase load) during cyclic loading, Equation 4.

$$\text{Separation Ratio (SR)} = \frac{\text{translational mismatch (spring constant)}}{\text{minimum swing phase load}} \quad \text{..... Equation 4.}$$

For example, as the separation ratio increases, the magnitude of the dynamic separation increases due to the greater force applied to translate the cup away from the head (Figure 4-3) relative to the resistance of the system.

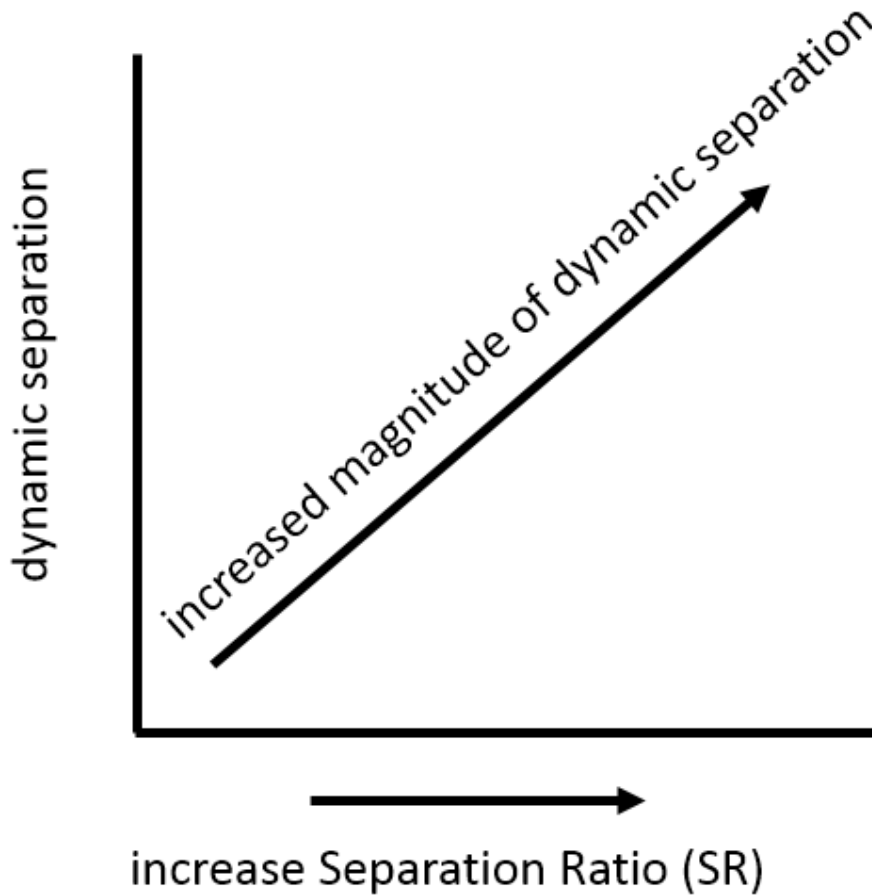


Figure 4-3. Schematic of Separation Ratio (SR) versus the dynamic separation.

Separation threshold

In the same manner that the separation ratio elaborates on the capacity for dynamic separation, the inverse relationship of the input separation ratio elaborates on the threshold point where the separation is no longer present under different conditions. The Separation Threshold (ST) is the relationship of the capacity to resist the dynamic separation (i.e. the minimum swing phase load) and the capacity to overcome the point where the dynamic separation is no longer present during cyclic loading, Equation 5.

$$Separation\ Threshold\ (ST) = \frac{minimum\ swing\ phase\ load}{translational\ mismatch\ (spring\ constant)} \dots\dots\dots Equation\ 5.$$

For example, if you increase the separation threshold you decrease the capacity of dynamic separation to occur, i.e. the point where the swing phase load is too high for separation to occur Figure 4-4.

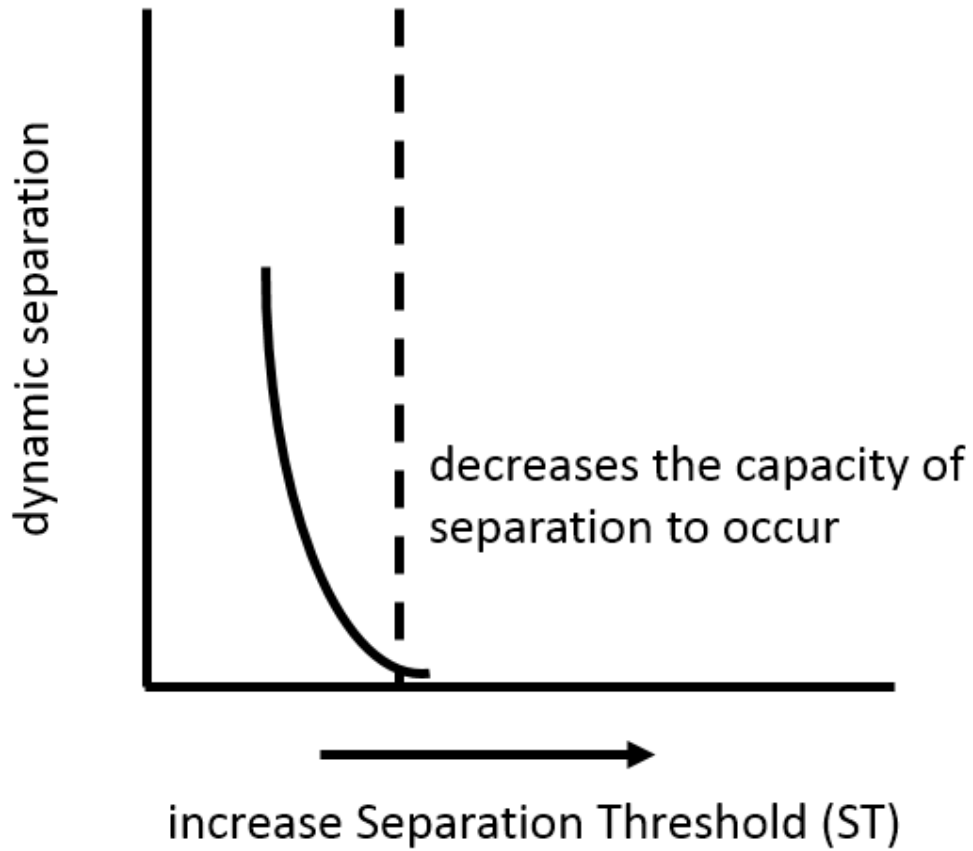


Figure 4-4. Schematic of Separation Threshold (ST) versus the dynamic separation.

A positive linear correlation was observed between the separation ratio and the dynamic separation for the three cup inclination angle (45°, 55° and 65°) conditions (Figure 4-5). As the separation ratio increased for all the cup inclination angle conditions (45°, 55° and 65°), the dynamic separation also increased. The 65° cup inclination angles had the highest dynamic separation for a specific separation ratio. The 45° cup inclination angle had the highest dynamic separation for a specific separation ratio, and the 55° fell in between the two 45° and 65° cup inclination angle.

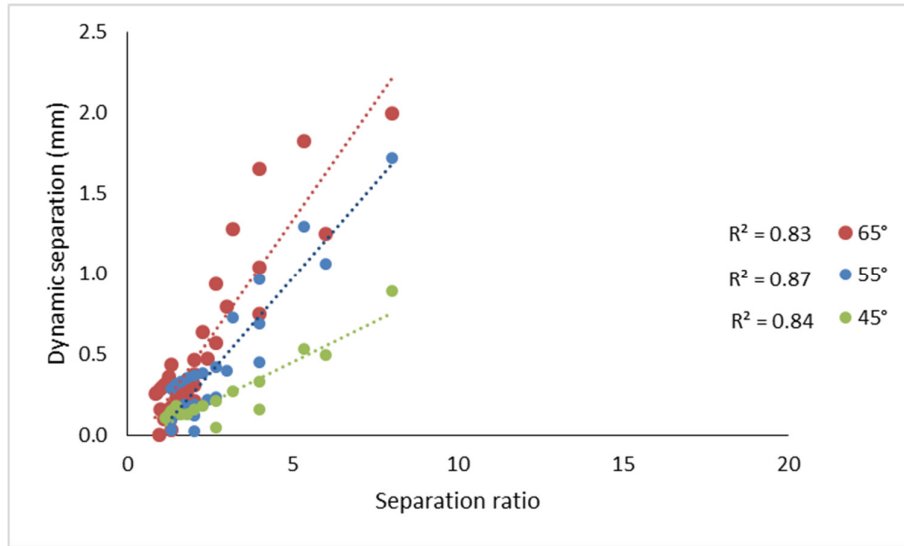


Figure 4-5. Dynamic separation against separation ratio for 1, 2, 3 and 4 mm translational mismatches grouped per inclination angle of 45° (green), 55° (blue) and 65° (red) for different swing phase loads conditions.

Overall, as the separation threshold increased for all the cup inclination angle conditions (45°, 55° and 65°), the dynamic separation decreased (Figure 4-6). A trend (power correlation) was found between separation threshold and the increase in the cup inclination angle, such that the capacity for the dynamic separation to occur increased as cup inclination angle increased from 45° to 55° to 65°.

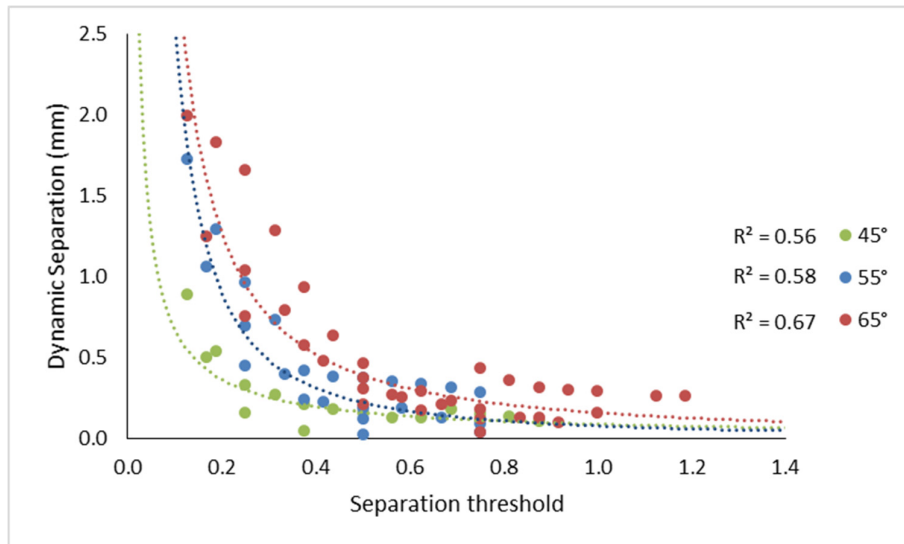


Figure 4-6. Dynamic separation against separation threshold for 1, 2, 3 and 4 mm translational mismatches grouped per inclination angle of 45° (green), 55° (blue) and 65° (red) for different swing phase loads conditions.

Different types of edge loading conditions were observed. Under low levels of component translational mismatch, the cup relocated in a single action as the vertical load increased. As the swing phase load increased the separation decreased and at certain conditions, no separation was detected.

Only under a cup inclination angle of 65° there was evidence of interrupted relocation for the 3 and 4 mm mismatch. However, as the swing phase load increased for this test condition, the type of relocation changed from interrupted to single type.

Thus, overall three observations were seen; no separation, single relocation, and interrupted edge loading. These were dependent on the cup inclination angles, the levels of component translational mismatch and the swing phase load (Figure 4-7). For a different representation of data see Appendix A, page 217.

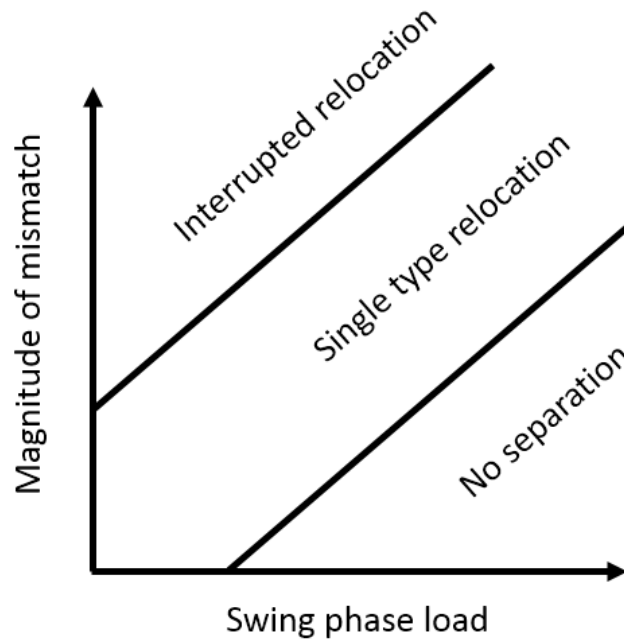


Figure 4-7. Schematic for the type of edge loading and the variables affecting it.

Low severity of edge loading (<50 Ns) was obtained for all the cup inclination angles under a 1 mm translational mismatch with a low swing phase load (Figure 4-8). The magnitude of the severity of edge loading decreased to zero once the swing phase load increased to about 100-150 N. There was no separation detected leading to edge loading under the 45° cup inclination angle under any of the swing phase load conditions.

The severity of edge loading increased for the 55° and 65° cup inclination angle under a 2 mm translational mismatch, while no difference was observed for the 45° angle in comparison to the

1 mm translational mismatch (Figure 4-8). The 55° cup inclination increased the severity of edge loading to 75 Ns under a low swing phase load, and steadily decreased as the swing phase load was increased. The severity of edge loading increased to 120 Ns as the cup inclination angle increased to 65° under a low swing phase load, and steadily decreased as the swing phase load was increased.

Under a 3 mm translational mismatch and a 65° cup inclination angle, an increase in the severity of edge loading was observed from 120 to 600 Ns under a low swing phase load (50 N), Figure 4-8. The severity of edge loading dropped towards 150 Ns under a swing phase load of 150 N.

The other two cup inclination angles (45° and 55°) had a similar severity of edge loading under the 3 mm translational mismatch and a low swing phase load. When the swing phase load increased under these conditions, the severity of edge loading decreased steadily towards zero when the swing phase load was reaching 450 N.

Under a 4 mm translational mismatch and low swing phase load (50-200 N) the severity of edge loading for the 65° cup inclination angle was higher than 650 Ns (Figure 4-8). When the swing phase load was increased to 175 N the severity decreased to less than 300 Ns and remained around that level for higher swing phase load conditions.

The severity of edge loading results from the 55° cup inclination angle under a 4 mm translational mismatch and a low swing phase load were 400 Ns lower than the 65° cup inclination angle. A decrease in the severity of edge loading of 100 Ns occurred at the 150 N swing phase load conditions.

The severity of edge loading results from the 45° cup inclination angle under a 4 mm translational mismatch and a low swing phase load were overall lower than the 55° cup inclination angle conditions. However, the decrease in the severity of edge loading occurred earlier at 100 N swing phase loading.

The severity of edge loading is the resulted time and load when the head is in contact with the rim of the cup. The increase in swing phase load condition decreases the possibility of contact with the rim, hence the severity (Ns) decreased when the swing phase load increased.

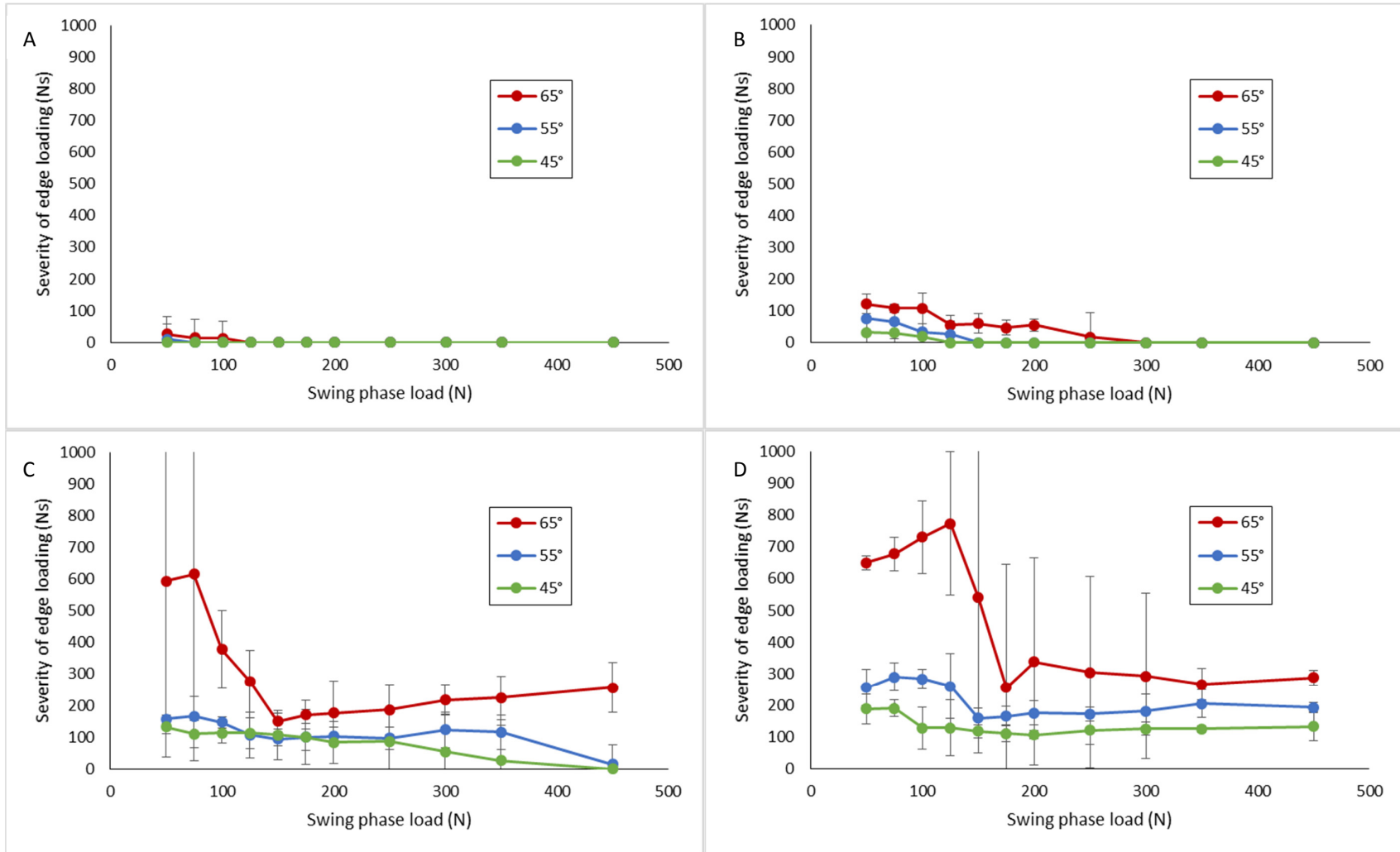


Figure 4-8. Mean ($n=3$, $\pm 95\%$ CI) severity of edge loading for 36 mm ceramic-on-ceramic (BIOLOX® delta) bearings under 1, 2, 3 and 4 mm translational mismatch conditions (A, B, C and D respectively) with a cup inclination angle of 45°, 55° and 65° for different swing phase load conditions.

4.5. Biomechanical study Phase 2. Evaluation of severity of edge loading of specific swing phase load conditions under a translational mismatch

4.5.1. Aim & methodology

This study (Biomechanical study Phase 2) only investigated two swing phase load conditions, where the maximum force and under edge loading and the severity of edge loading were evaluated. In this study the samples size was increased to six and all six stations were used. The two conditions applied were; 150 and 300 N swing phase load, were only one cup inclination angle and one translational mismatch was applied (Table 4-2). The data from Chapter 3, Phase 2 with a 70 N swing phase load (i.e. 4 mm translational mismatch and 65° cup inclination angle) was used to compare against the two swing phase load conditions evaluated in this study.

Table 4-2. Details of the biomechanical study for the evaluation of the severity of edge loading for selective swing phase load conditions under a translational mismatch.

Study	Details (Unit)	Input
Biomechanical study	Equipment	Six-station Leeds Mark II (A)
	Materials	Ceramic-on-ceramic (BIOLOX® delta)
	Design	PINNACLE®
	Head size diameter (mm)	36
	Frequency (Hz)	1
	Loading profile	Paul walking cycle (twin peak load)
	Max peak force (N)	3300
	Trough load (N)	1500
	Swing phase load (N)	150, 300
	Motion profile	Leeds walking cycle (Barbour <i>et al.</i> , 1999)
	Flexion / Extension (°) of the head	+30 / -15
	Internal / External rotation (°) of the cup	+10 / -10
	Stem anterversion angle (°)	20
	Cup version angle (°)	0
	Translational mismatch (mm)	4
	Spring constant (N/mm)	100
	Number of total bearings tested	6
	Cup inclination angle (°)	65
	Cycles completed	900
	Stations used (#)	1, 2, 3, 4, 5, 6

4.5.2. Results

The maximum force under edge loading for the 70 and 150 N swing phase load resulted in a similar range of approximately 2900 N (Figure 4-9). The 70 N swing phase load resulted 2947 ± 136 N and the 150 N swing phase load resulted in 2891 ± 198 N. The test condition under 300 N swing phase load resulted in a decrease in the maximum force under edge loading (536 ± 232 N), and was found significantly different to the lower swing phase loads ($p < 0.01$).

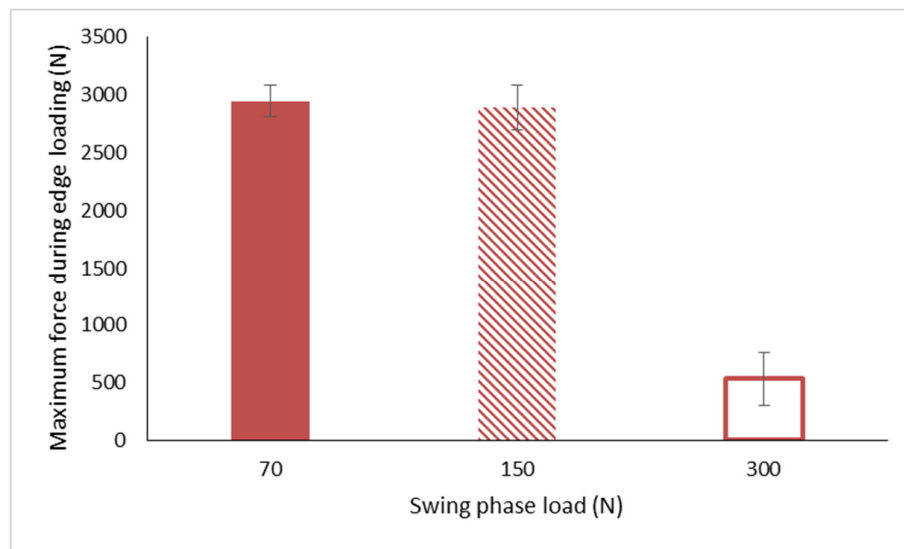


Figure 4-9. Mean ($n=6$, $\pm 95\%$ CI) maximum force under edge loading for 36 mm ceramic-on-ceramic (BIOLOX® delta) bearings under 4 mm translational mismatch conditions with a cup inclination angle of 65° for three swing phase loads (70, 150 and 300 N).

The severity of edge loading for the 150 and 300 N swing phase load was plotted in Figure 4-10, in addition, the severity of edge loading from the 70 N swing phase load (refer to Chapter 3.5.3) with the relevant condition (4 mm translational mismatch and 65° cup inclination) angle was added for comparison. The severity of edge loading decreased as the swing phase load increased from 150 to 300 N under a 4 mm translational mismatch for a 65° cup inclination angle. The mean ($\pm 95\%$ CI) severity of edge loading was 598 ± 277 Ns and 230 ± 48 Ns for the 150 and 300 N swing phase load respectively. The severity of edge loading under the 300 N swing phase load was found statistical significant ($p < 0.01$) when compared to the 70 and 150 N swing phase load.

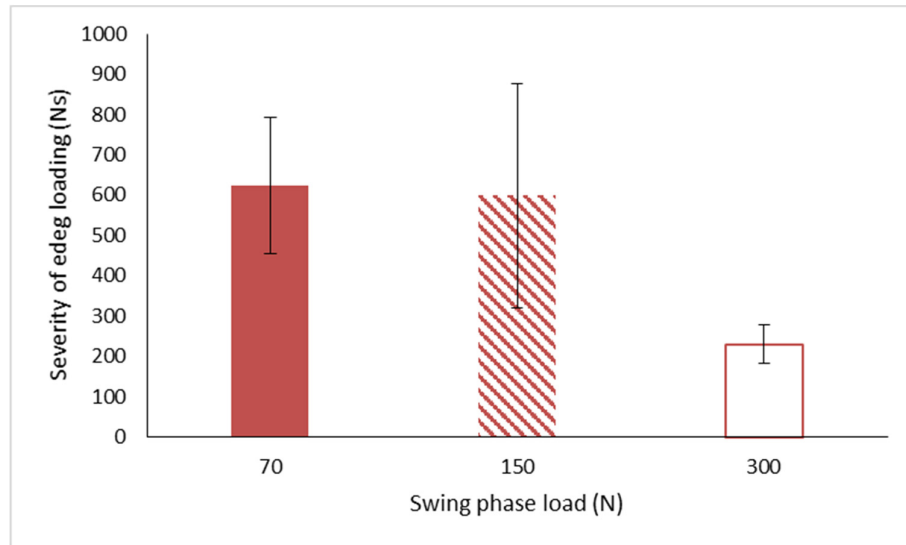


Figure 4-10. Mean ($n=6$, $\pm 95\%$ CI) severity of edge loading for 36 mm ceramic-on-ceramic (BIOLOX® delta) bearings under 4 mm translational mismatch conditions with a cup inclination angle of 65° for three swing phase loads (70, 150 and 300 N).

4.6. The wear of 36 mm CoC (BIOLOX® delta) under edge loading due to a medial-lateral component translational mismatch of 4 mm for 150 N and 300 N swing phase load with a cup inclination of 65°

4.6.1. Aim

The aim of this study was to determine the wear and damage of CoC under edge loading due to a medial-lateral component translational mismatch with swing phase loads of 150 and 300 N.

4.6.2. Methodology

The six-station Leeds Mark II Physiological Anatomical Hip Joint Wear Simulator was used, and the methodology described in Chapter 2 was followed. The bearing used was BIOLOX® delta as detailed in Chapter 2.1. A 65° cup inclination angle relative to the *in vivo* joint force vector was chosen for this study. A translational mismatch was applied at the start of the test to the hip simulator. This was achieved by moving the cup in the medial direction away from the femoral head centre by 4 mm (Figure 4-11). This mismatch was maintained constant and regular checks were performed for consistency.

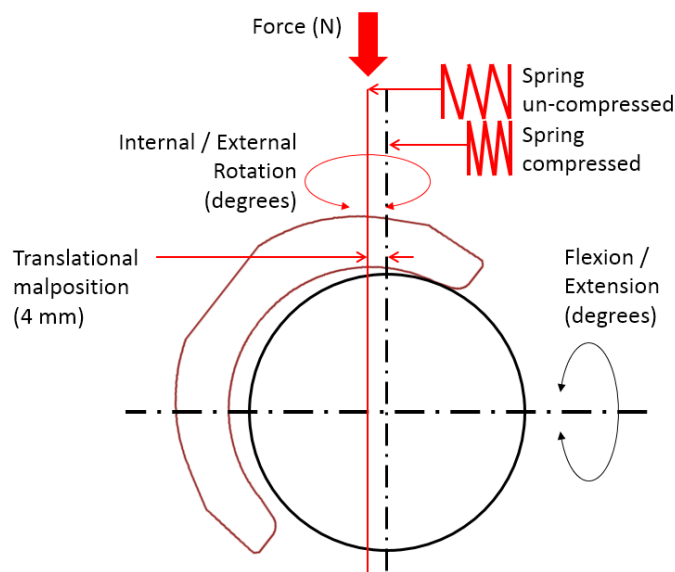


Figure 4-11. Schematic of the 4 mm translational mismatch input on the Hip Simulator.

The test was run for 3 million cycles (n=6). Details of the inputs for the test are described in Table 4-3. The first few cycles (approximately 30 minutes) were run without any translational mismatch to ensure a good performance of the equipment e.g. check the bone cement and fixtures hold without any malfunction. Afterwards, the cycle count was reset. A 4 mm translational mismatch was applied to all the stations. During the swing phase i.e. the low load phase (150 and 300 N), the spring forced the cup away. When the load was increased, the spring was compressed. As a routine check, an LVDT was employed to measure the displacement of the cup holder where the spring was placed. During intermissions i.e. either at serum change or at a measurement point (one million cycles), the fixtures and mounts were checked to ensure that no change occurred to the input mismatch. Checks on the hip simulator were done daily for good performance. Mean values and $\pm 95\%$ CI were determined and statistical analysis (one way ANOVA) completed (significance taken at $p < 0.05$).

Table 4-3. Details of the swing phase load wear study under a translational mismatch.

Study	Details (Unit)	Input
Wear study	Equipment	Leeds II (A)
	Materials	Ceramic-on-ceramic (BIOLOX® delta)
	Design	PINNACLE®
	Head size diameter (mm)	36
	Frequency (Hz)	1
	Loading profile	Paul walking cycle (twin peak load)
	Max twin peak force (N)	3000
	Trough peak load (N)	1500
	Swing phase load (N)	150 and 300
	Motion profile	Leeds walking cycle (Barbour <i>et al.</i> , 1999)
	Flexion / Extension (°) of the head	+30 / -15
	Internal / External rotation (°) of the cup	+10 / -10
	Stem anteverision angle (°)	20
	Cup version angle (°)	0
	Translational mismatch (mm)	4
	Spring constant (N/mm)	100
	Number of total bearings tested	12
	Cup inclination angle (°)	65
	Cycles completed	3×10^6

4.6.3. Results

The outputs from the study were the wear from the ceramic bearings, the scar depth on the femoral heads, the change in surface roughness and volumetric assessment of the heads via the CMM due to edge loading on a 4 mm translational mismatch for 65° cup inclination angles under a 150 and 300 N swing phase load.

The total displacement of the cup holder during routine checks for the 150 N swing phase load condition measured using the LVDT indicated some variation (CV = 33%) between the stations (Figure 4-12).

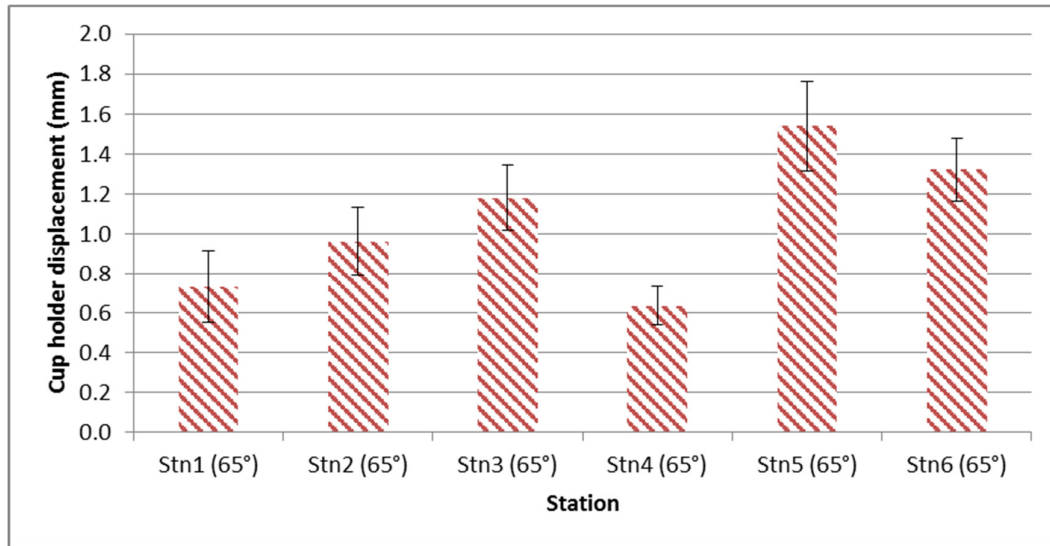


Figure 4-12. Average displacement of the cup holder ($\pm 95\%$ CI) for 65° inclination angles under a 4 mm translational mismatch and 150 N swing phase load.

The total displacement of the cup holder during routine checks for the 300 N swing phase load condition measured using the LVDT indicated to range between 0.1 - 0.2 mm for all the stations.

The individual wear for the 150 N swing phase load from all the stations is shown in Figure 4-13. The wear rates on the femoral heads and the acetabular cups were consistent at every interval apart from a decrease in the wear after the first million cycles for most stations. The stem from station #1 broke at the neck during the wear study at 1.18 million cycles. The test was continued without station #1 until a new stem was cemented, thus this specific station only reached 2.33 million cycles. The wear rate for station #1 was divided for the specific number of cycles and added to the cohort of the wear study.

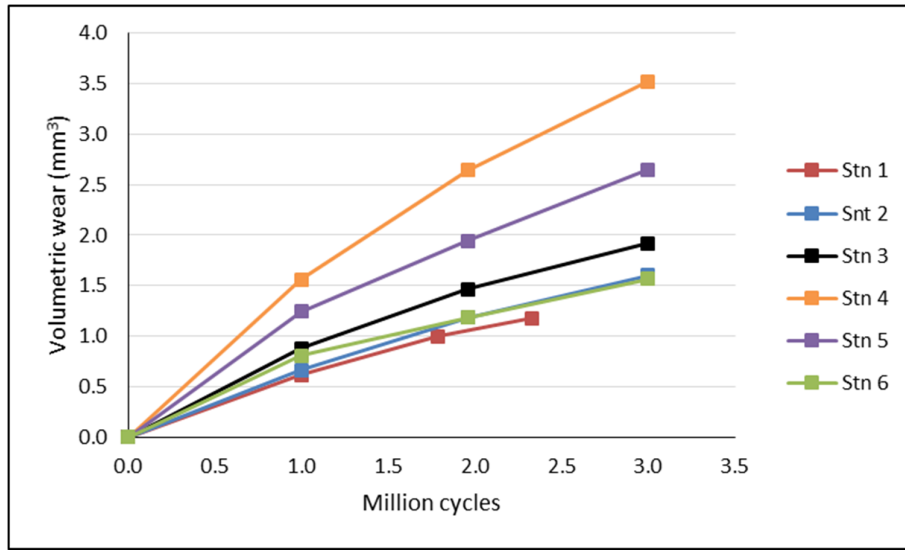


Figure 4-13. Individual volumetric wear under 4 mm translational mismatch for 65° cup inclination angle and 150 N swing phase load. Stn = Station.

The individual wear for the 300 N swing phase load from all the stations is shown in Figure 4-14. The wear rates on the femoral heads and the acetabular cups were consistent at every interval. Only station #4 and #5 indicated a higher wear rate (an extra 0.12 mm³/10⁶ cycles) throughout the test in comparison to the rest of the cohort.

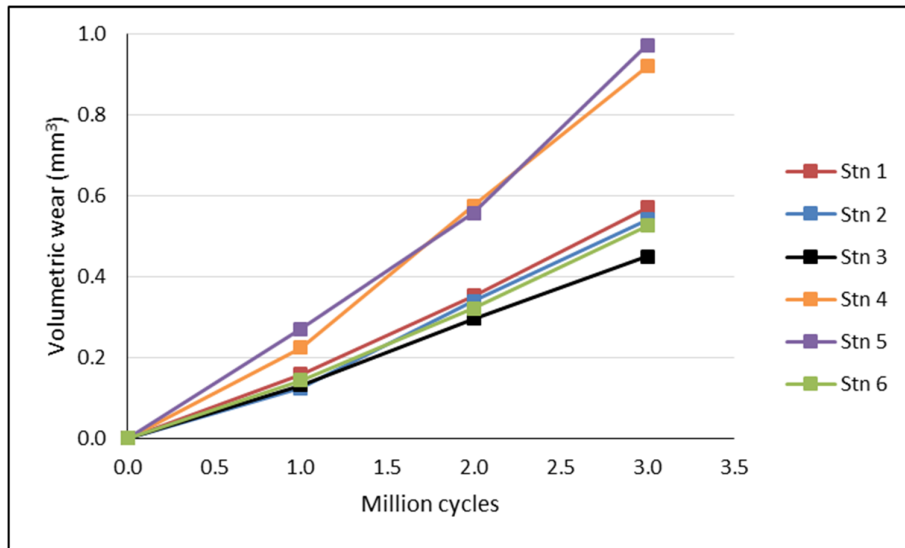


Figure 4-14. Individual volumetric wear under 4 mm translational mismatch for 65° cup inclination angle and 300 N swing phase load. Stn = Station.

After three million cycles of testing, the mean wear rate was $0.71 \pm 0.27 \text{ mm}^3/10^6 \text{ cycles}$ and $0.22 \pm 0.08 \text{ mm}^3/10^6 \text{ cycles}$ for the 150 and 300 N swing phase load respectively (Figure 4-15). A significant difference was found between the wear rates for the 150 and 300 N swing phase load testing conditions ($p < 0.01$).

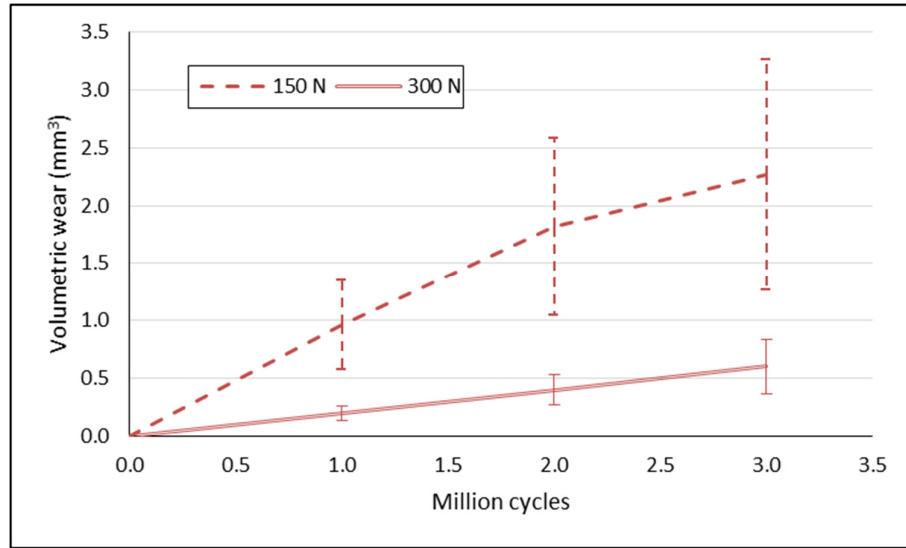


Figure 4-15 Mean ($n=6$, $\pm 95\%$ CI) wear rates for 150 and 300 N swing phase load under a 4 mm translational mismatch and 65° inclination angle.

A representation of the damage seen on the surface of the head after 3 million cycles for the 150 N swing phase load condition is shown in Figure 4-16. The point of maximum penetration in the stripe wear area was similar between the stations, apart from sample #4 which indicated an equal level of depth towards the right side of the wear scar, unlike the rest of the samples which had the maximum depth on the left hand side.

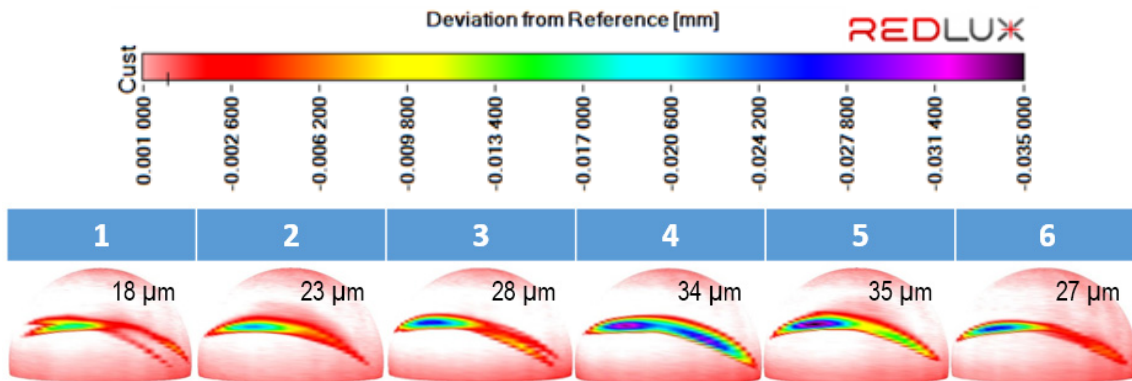


Figure 4-16. Visualisation of surface of the heads under a 4 mm translational mismatch and 150 N swing phase load via RedLux software at the end of the wear test. The maximum depth of the scar is aligned to each head accordingly.

A representation of the damage seen on the surface of the head after 3 million cycles for the 300 N swing phase load condition is shown in Figure 4-17. The point of maximum penetration in the stripe wear was similar for all the stations.

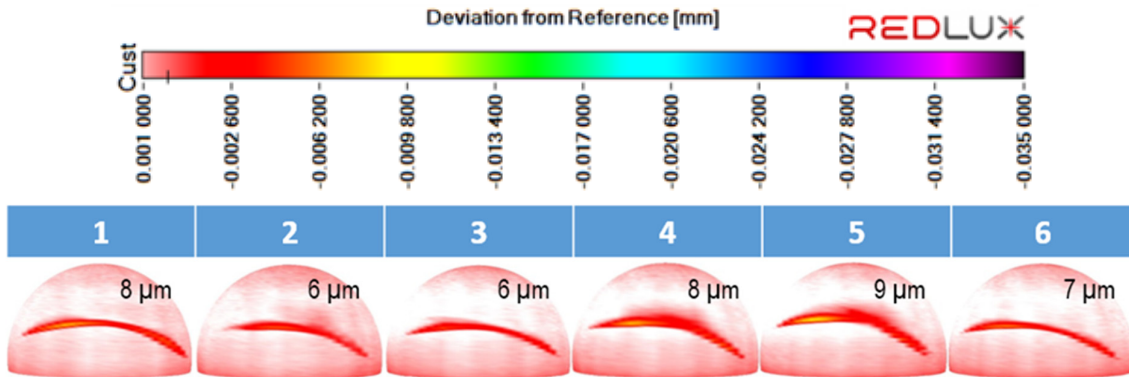


Figure 4-17. Visualisation of the heads under a 4 mm translational mismatch and 300 N swing phase load via RedLux software after 3 million cycles. The maximum depth of the scar is aligned to each head accordingly.

The mean scar penetration of the heads due to edge loading was $27.4 \pm 6.6 \mu\text{m}$ and $7.3 \pm 1.4 \mu\text{m}$ after 3 million cycles for the 150 and 300 N swing phase loads respectively (Figure 4-18). A significant difference was found between the 150 and 300 N swing phase load ($p < 0.01$).

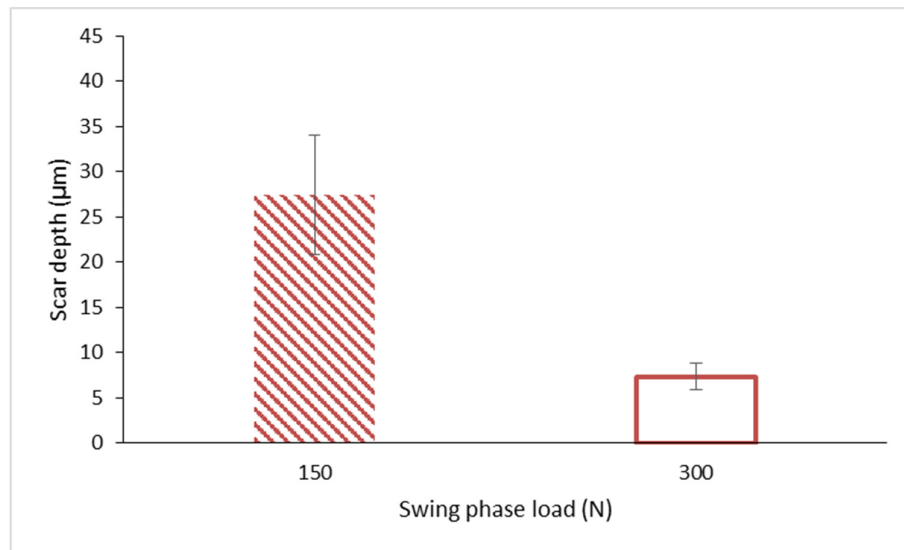


Figure 4-18. Mean ($n=6$, $\pm 95\%$ CI) maximum scar penetration after 3 million cycles under 150 and 300 N swing phase loads and a 4 mm translational mismatch condition with a 65° cup inclination angle.

Post-test, no change in surface roughness (Ra) was observed on the pole region (P1 tested) of the heads under the 150 and 300 N swing phase load (Figure 4-19). The surface roughness increased where the wear stripe was located 'P2 (tested)' from 5 ± 2 nm to 12 ± 3 nm for all the samples tested (i.e. 150 and 300 N swing phase load). The heads tested under 150 N swing phase load indicated to have a lower surface roughness than when tested under 300 N swing phase load at the wear stripe. A significant difference was found between the 150 and 300 N swing phase load ($p < 0.01$) at the wear stripe location 'P2 (tested)'.

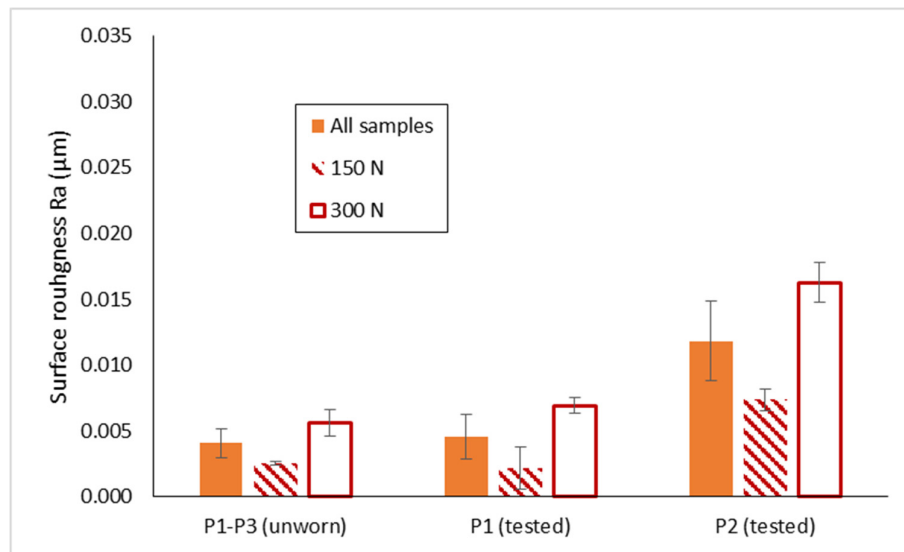


Figure 4-19. Mean ($n=6$, $\pm 95\%$ CI) surface roughness (Ra) for head samples post-test at the pole 'P1 (tested)', and the wear scar 'P2 (tested)' under 4 mm translational mismatch and 65° cup inclination angle for 150 and 300 N swing phase load compared against the pre-test 'P1-P3 (unworn)'.

Volumetric wear assessment via the CMM

The mean volumetric wear rate of the heads under a 4 mm translational mismatch with a 65° cup inclination angle and 150 N swing phase load condition calculated via the surface analysis was 0.28 ± 0.15 $\text{mm}^3/10^6$ cycles. This was similar to the gravimetric results which was 0.36 ± 0.12 $\text{mm}^3/10^6$ cycles.

The mean volumetric wear rate of the heads under a 4 mm translational mismatch with a 65° cup inclination angle and 300 N swing phase load condition calculated via the surface analysis 0.05 ± 0.02 $\text{mm}^3/10^6$ cycles. This was similar to the gravimetric results which was 0.08 ± 0.03 $\text{mm}^3/10^6$ cycles.

4.7. Discussion

4.7.1. Dynamic separation

Most of the *in vitro* testing in hip joint simulators is carried out using a simplified axial load to replicate the joint reaction force of the *in vivo* conditions. The magnitude and profile of the force has been considered to affect the wear of hip joint replacements materials such as metal-on-metal bearings under standard testing conditions (Williams *et al.*, 2006). When employing a translational mismatch to replicate edge loading in a hip joint simulator in Chapter 3, the magnitude of swing phase load was considered to affect the dynamic separation, severity of edge loading and wear. In Chapter 3, the swing phase load was set as a constant input and maintained within the capabilities of the equipment to match across all the stations.

The swing phase load has previously been considered as a test variable under microseparation conditions by Stewart *et al.* (2001). Their work demonstrated how increasing the swing phase load decreased the wear under microseparation conditions. In their study, the wear was associated with the level of 'separation', where "mild separation", with an input swing phase load of 400 N resulted in lower wear rate (less than $0.6 \text{ mm}^3/10^6$ cycles) in comparison to "severe separation", with an input swing phase load of 50 N which resulted in higher wear rate (approximately $1.25 \text{ mm}^3/10^6$ cycles for steady state) for ceramic-on-ceramic bearings BIOLOX® forte (HIPed third generation alumina ceramic). However, in their study the input translational mismatch was not controlled and the cup holder displacement varied from 0.2 to 0.5 mm. Thus, their wear study needs to be carefully considered, as the data in this chapter indicates that a dynamic separation 0.2 to 0.5 mm for a 45° cup inclination can be produced by different levels of mismatches and different swing phase loads. For a dynamic separation up to 0.5 mm, a translational mismatch of 2-4 mm and a swing phase load of 50-300 N can be considered as an input. The severity of edge loading under these condition however can vary, thus giving different wear results. The dynamic separation in the biomechanical study section of this chapter was evaluated with a controlled input translational mismatch and controlled input swing phase load. Under these controlled inputs, the results gave a clear indication that the increased swing phase load decreased the dynamic separation (Figure 4-2). And the reason for these results is due to the resistance created by the increased swing phase load which opposes the spring to un-compress.

The dynamic separation results from a 150 and 300 N swing phase load indicated a similar pattern as those of 70 N. The translational mismatch influenced the level of dynamic separation and was in alignment with the previous studies in Chapter 3 which demonstrated that a higher translational mismatch resulted in a greater dynamic separation, and the cup inclination angle influenced the

resistance to separation as shown in Figure 4-20 and Figure 4-21 for the 150 and 300 N swing phase load. Under higher swing phase loads the dynamic separation was lower and this was consistent across all the translational mismatches and the cup inclination angles. As the swing phase load increased to 300 N, in some cases, there was no evidence of a dynamic separation.

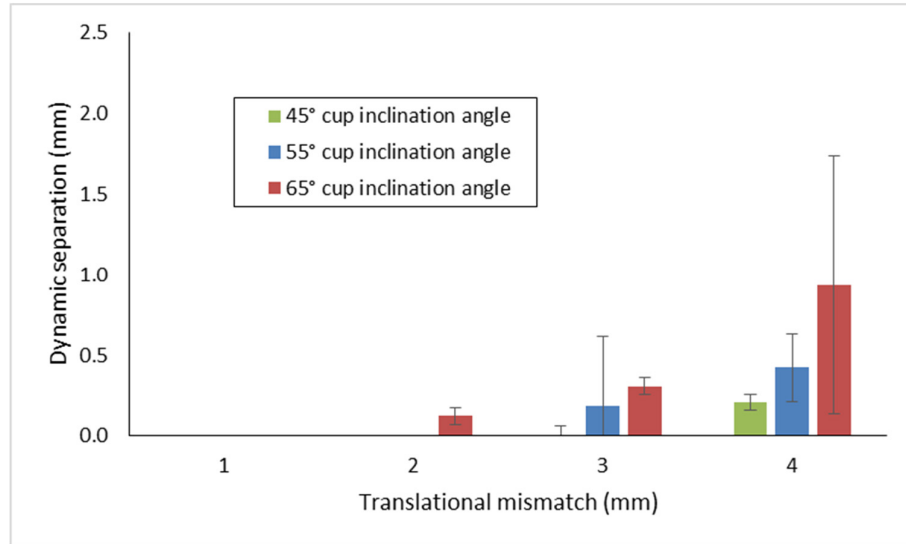


Figure 4-20. Mean ($n=3$, $\pm 95\%$ CI) dynamic separation for 36 mm ceramic-on-ceramic (BIOLOX® delta) bearings under variations in translational mismatch and cup inclination angle for a 150 N swing phase load conditions.

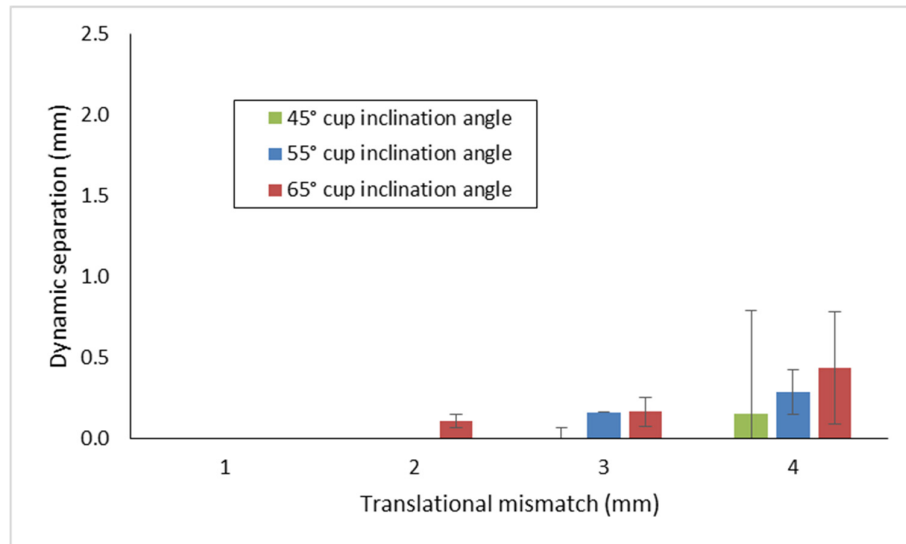


Figure 4-21. Mean ($n=3$, $\pm 95\%$ CI) dynamic separation for 36 mm ceramic-on-ceramic (BIOLOX® delta) bearings under variations in translational mismatch and cup inclination angle for a 300 N swing phase load conditions.

In Chapter 3, higher swing phase loads of over 100 N were noted during wear testing even though the swing phase load was set to 70 N and different magnitudes of cup holder displacement were also noted across the stations (Figure 3-15). The biomechanical study in this chapter has demonstrated how the increase in the swing phase load for specific inclination angle, for example a 65° cup inclination angle, can affect the resultant dynamic separation for different translational mismatches (Figure 4-22).

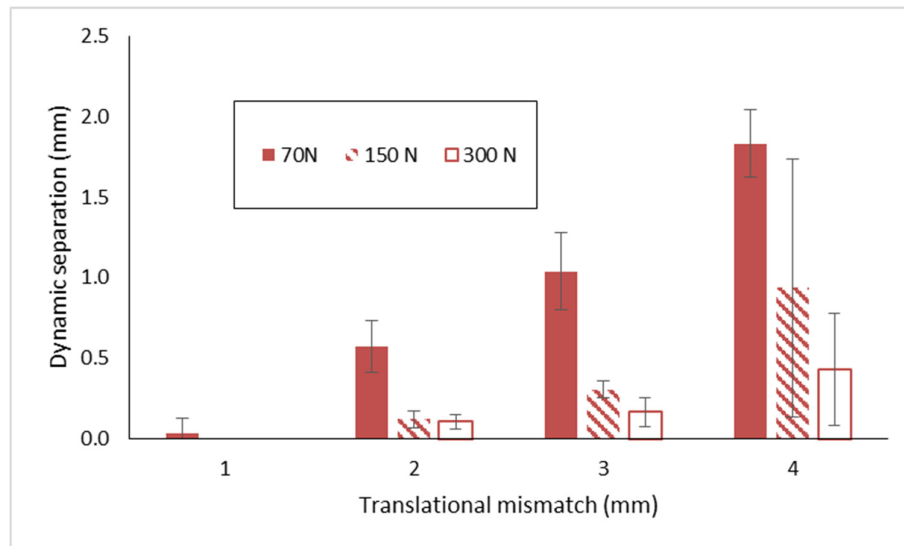


Figure 4-22. Mean ($n=3$, $\pm 95\%$ CI) dynamic separation for 36 mm ceramic-on-ceramic (BIOLOX® delta) bearings under 1, 2, 3 and 4 mm translational mismatch with a cup inclination angle of 65° for three swing phase load conditions (70, 150 and 300 N).

Current gait analyses that have measured *in vivo* separation of hip joint replacements, have not measured the actual forces experienced by the hip replacements (Komistek *et al.*, 2002). These studies only employed force plates and calculated the forces from inverse kinematics. Thus, the actual conditions and forces for edge loading and separation are not clinically available. A very complex set-up would be required to measure the forces during gait and the separation at the same time, and even then the component positioning needs to be also considered. The *in vivo* dynamic separation measurements which are found to range from 0-3 mm do not indicate to relate directly to an activity or the associated component positioning (Lombardi *et al.*, 2000). This study shows how different cup inclination angles can have the same level of dynamic separation depending on their kinematic conditions.

To improve a hip joint replacement through *in vitro* testing, many conditions have to be considered. However it is not realistic to test every single condition. Thus, an approach where the effects of different parameters and the combinations of these parameters on the occurrence and severity of edge loading using short term tests would be a viable solution. Then certain conditions would be

chosen to investigate the tribological performance of hip replacement bearings. The dynamic separation varied across different test conditions as indicated by the biomechanical study when the translational mismatch, cup inclination angle and swing phase load were set as independent parameters. However, the translational mismatch and swing phase load can be grouped as a ratio to determine the effect on the dynamic separation. This creates a relationship described in this chapter as the separation ratio.

The input separation ratio provided a way to analyse and compare the cup inclination angle effect on the magnitude of the dynamic separation for multiple conditions. As expected the 65° cup inclination angle resulted in a greater dynamic separation for different translational mismatches and multiple swing phase loads, hence why the dynamic separation linear correlation against the separation ratio for the 65° cup inclination angle was steeper in comparison to the 45° and 55° (Figure 4-5). Multiple iterations of translational mismatches and an input swing phase loads can be applied for a particular cup angle, thus by calculating the separation ratio beforehand the expected dynamic separation can be approximated.

In the other hand, the relationship between the separation threshold and the dynamic separation gave an indication of the input swing phase load required for dynamic separation to occur for the different cup inclination angles (Figure 4-6). If the threshold separation is lower than 0.3, a dynamic separation (greater than 0.5 mm) can be expected for a 45°, 55° and 65° cup inclination angle. This 0.3 threshold can be achieved under combinations of different translational mismatches and swing phase loads. Furthermore, the results demonstrate that a 65° cup inclination angle requires a higher separation threshold point to avoid dynamic separation in comparison to the 45° and 55° cup inclination angle because there is less resistance provided by 65° coverage angle.

The separation ratio and separation threshold predicts the expected dynamic separation for different input conditions. One can also consider the output loads to create trends against the actual dynamic separation for multiple conditions. Another way to evaluate the dynamic separation is to analyse the differences in the output M-L load (i.e. the maximum M-L load minus the minimum M-L load) for different conditions, such that when a difference in the M-L load is present, it indicates the spring is not fully compressed and this results in a separation between the centre of the cup and the centre of the head. Thus, a larger difference in the M-L indicates a larger separation. The same concept can be used to evaluate the threshold point for dynamic separation. One can use the output swing phase load for multiple conditions and detect under what swing phase load there is no difference present in the M-L load, indicating no dynamic separation present.

4.7.2. Wear correlations

Previously, in Chapter 3.6, the wear rate for a swing phase load of 70 N under a translational mismatch of 4 mm and a cup inclination angle of 65° indicated to be the highest wear rate ($1.01 \pm 0.17 \text{ mm}^3/10^6 \text{ cycles}$) condition. When considering this set of conditions (translational mismatch and cup inclination angle) and increase the swing phase load, the results demonstrate that under a higher swing phase loads the wear rate decreases (Figure 4-23). The wear rate under a 300 N swing phase loads was found statistically significant ($p < 0.01$) in comparison to the 70 and 150 N swing phase load test condition.

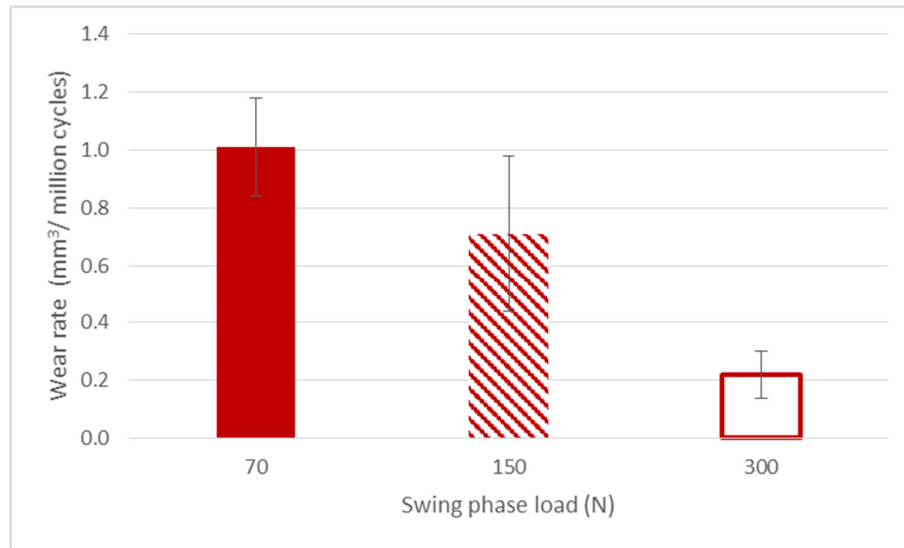


Figure 4-23. Mean ($n=6$, $\pm 95\%$ CI) wear rate for 36 mm ceramic-on-ceramic (BIOLOX® delta) bearings under 4 mm translational mismatch with a cup inclination angle of 65° and three swing phase loads (70, 150 and 300 N) conditions.

This result highlighted how the slight change in the swing phase load could have affected the wear results in the previous studies (Chapter 3) where a 70 N swing phase load was set as an input. In this hip simulator, it is difficult to control each station at a specific swing phase load, specifically at low forces of less than 200 N. Thus, a higher wear may result from the stations under a lower swing phase load and a lower wear may result from stations with a higher swing phase load. The swing phase load measured during the wear testing of 2, 3 and 4 mm translational mismatches for 45° and 65° cup inclination angle ranged from 25-170 N, however the load was always re-adjusted to best fit to a 50 N swing phase load. The standard deviation of the wear rate of these tested samples may incorporate to certain extent the variability of the swing phase load.

In Chapter 3.4, different levels of dynamic separation were obtained from Phase 1 of the biomechanical study. The selected conditions to investigate the tribological performance in Chapter 3.6 were a translational mismatch of 2, 3 and 4 mm with a cup inclination angle of 45° and 65°, all under a swing phase load of 70 N. In this Chapter, only two conditions were selected to

investigate the tribological performance. These were a swing phase load of 150 and 300 N under a translational mismatch of 4 mm and a cup inclination angle of 65°. When the dynamic separation and wear test results from Chapter 3 and 4 are plotted against each other, the results indicate a positive correlation ($R^2 = 0.71$), Figure 4-24. One could conclude that with the increase in dynamic separation, the wear rate increases. However that may only be true for these test conditions and the specifics of the load profile. To be more specific, the duration of edge loading and force acting while the head is in contact with the rim gave a better description of the relationship between the increase wear and the *in vitro* conditions.

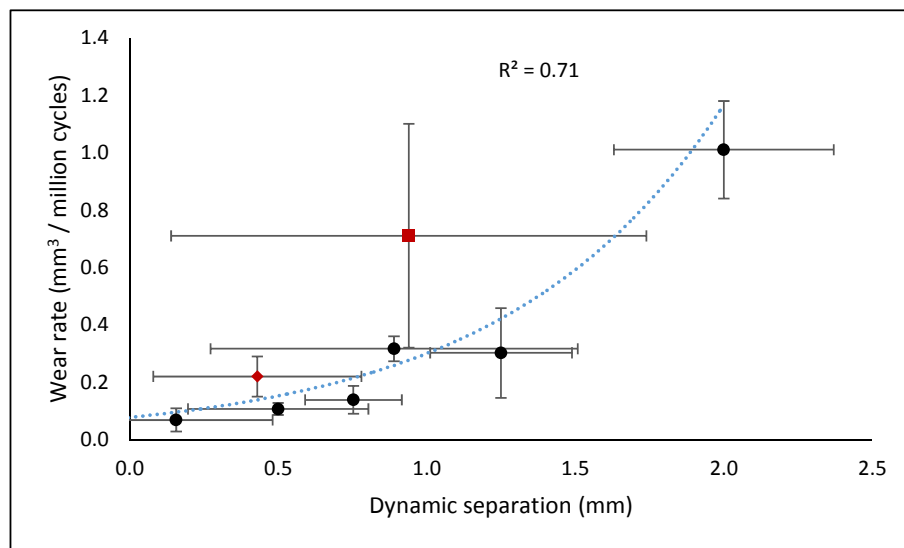


Figure 4-24. Mean ($n=3$, $\pm 95\%$ CI) dynamic separation against mean ($n=6$, $\pm 95\%$ CI) wear rate for 36 mm ceramic-on-ceramic (BIOLOX® delta) bearings under 2, 3 and 4 mm translational mismatches with a cup inclination angle of 45° and 65° under 70 N swing phase load (black circles), and 150 N (red square) and 300 N (red diamond) swing phase loads under a 4 mm translational mismatch and 65° cup inclination angle.

Previously in Chapter 3, the severity of edge loading (Ns) indicated to be a good analysis to compare the wear rate for different conditions. Plotting the two swing phase load conditions from the wear study tested in this chapter, along with the 70 N swing phase load under a 4 mm translational mismatch and 65° cup inclination angle indicates a positive power correlation ($R^2 = 0.97$) against the severity of edge loading (Figure 4-25). Furthermore, when plotting the 150 and 300 N swing phase load conditions along with previous wear studies from Chapter 3 (i.e. 2, 3 and 4 mm translational mismatch, and 45° and 65° cup inclination angle under a 70 N swing phase load), the severity of edge loading correlates positively ($R^2 = 0.93$) with the wear rates (Figure 4-26).

It is interesting to note that a severity of edge loading of approximately 200 Ns had a similar wear rate for a 300 N swing phase load under a 4 mm translational mismatch and a 65° cup inclination angle, and for a 45° under a 4 mm translational mismatch with a 70 N swing phase load condition.

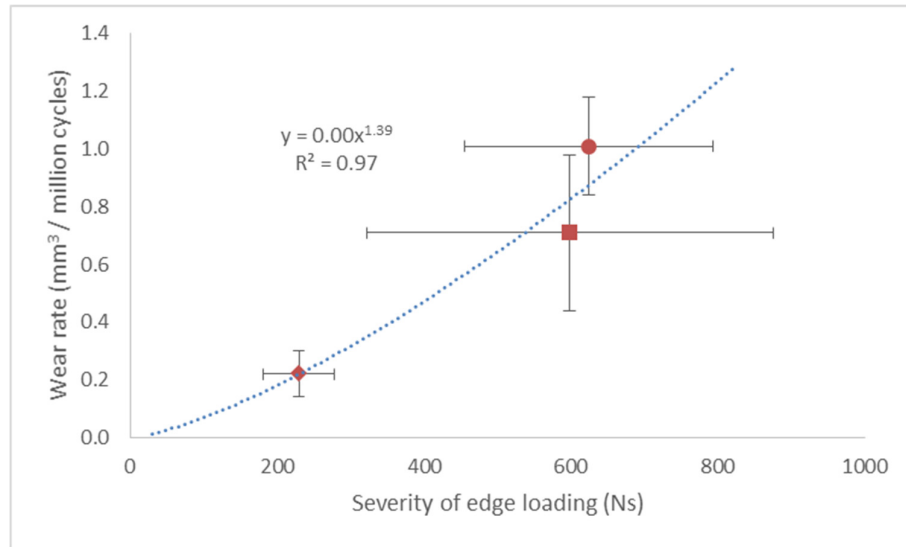


Figure 4-25. Mean ($n=6$, $\pm 95\%$ CI) severity of edge loading against mean ($n=6$, $\pm 95\%$ CI) wear rate for 36 mm ceramic-on-ceramic (BIOLOX® delta) bearings under 4 mm translational mismatch with a cup inclination angle of 65° for 70 (circle), 150 (square) and 300 (diamond) swing phase loads.

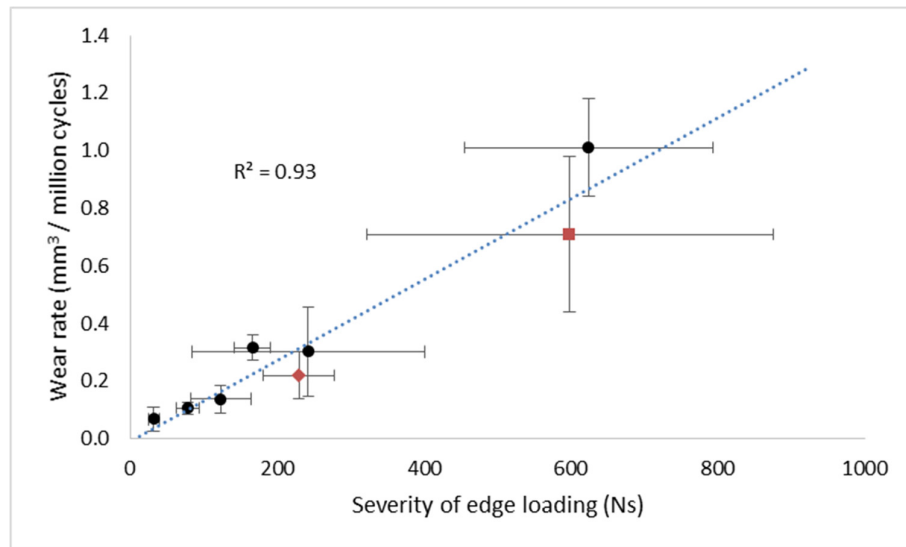


Figure 4-26. Mean ($n=6$, $\pm 95\%$ CI) severity of edge loading against mean ($n=6$, $\pm 95\%$ CI) wear rate for 36 mm ceramic-on-ceramic (BIOLOX® delta) bearings under 2, 3 and 4 mm translational mismatches with a cup inclination angle of 45° and 65° under 70 N swing phase load (black circles), and 150 N (red square) and 300 N (red diamond) swing phase loads under a 4 mm translational mismatch and 65° cup inclination angle.

4.7.3. *In vivo* biomechanics

The clinical studies that measured separation in patients with THRs (such as those by Lombardi *et al.* (2000), Dennis *et al.* (2001), Glaser *et al.* (2008), Glaser *et al.* (2010) and Tsai *et al.* (2014)) did not measure the forces during gait, thus it is difficult to conclude that increasing the dynamic separation would increase the wear for *in vivo* conditions based on these experimental studies. On the other hand, clinical studies that measured the forces during gait such as those by Bergman *et al.*, did not measure dynamic separation. The results from this experimental study indicate the relative medial and axial force required for dynamic separation to occur during a particular gait profile. Theoretically, from a loading perspective a mismatch of the centre of the head in the lateral direction away from the centre of the cup creates a loading on the head in the lateral direction as represented in the experimental study. However, in the clinical scenario it is uncertain how the translational mismatch affects the gait and forces leading to edge loading or whether a lateral load would decrease during dynamic separation at the swing phase as observed in the experimental study. The loads during gait created by the muscles and ligaments increase the complexity of interpreting and understanding the forces created by the relative mismatches of the femoral head and acetabular component. Currently there isn't a study which determines specifically why separation and edge loading occurs, however, separation and edge loading are multifactorial which increases the difficulty to understand the clinical scenario.

Edge loading as an *in vitro* test method needs to consider the variability in patients. The swing phase load is a parameter that can be changed and controlled in a hip joint simulator. In practice, altering the swing phase load resulted in different edge loading scenarios and different wear rates. Clinically, the swing phase load of patients has been shown to vary (Bergmann *et al.*, Hip 98). Bergman *et al.* (2001) suggests that patients have a range of swing phase loads while walking. Their results in the axial direction range from -20 to 300 N, and most of the patients have approximately 150 N. The magnitude of the load measured from Bergmann's studies are of relevance for *in vitro* testing which consider more than one load vector during gait and the variability in loading for different activities. This study has demonstrated that applying a load in another direction changes the contact area, and in turn leads to higher wear due to edge loading. In conditions where the vertical load does not drop below 300 N during gait, the occurrence of edge loading could be lower *in vivo*, however as demonstrated by the medial-lateral force applied in this experimental study, the magnitude of the load play a role on the severity of edge loading. Thus, the different magnitudes and direction of forces that patient's exhibit must play a role on the diversity and severity of edge loading leading to different scenarios of stripe wear as observed in retrievals.

Clinically, an increase in soft tissue tension in a patient during surgery in the form of an increased neck length of the stem could lead to increased joint reaction force during the swing phase load as the two components are “forced against each other”. This may be one of the variables affecting the ranges of forces in the swing phase load observed by Bergmann’s studies.

Based on this study, the magnitude and direction of the measured *in vivo* forces could potentially be used to determine the occurrence of edge loading in patients. For example, if a patient has a cup inclination angle set at 55° or 65° and if the minimum vertical compressive load is 100 N during the swing phase load of the walking cycle, edge loading, based on the separation threshold leading to a dynamic separation greater than 0.5 mm, can occur if a lateral force on the head is greater than 300 N. Another scenario could be when a relative force is present while the foot is grounded on the floor, for example a vertical compressive load of 300 N, edge loading can occur with lateral force on the head of 600 N, resulting in a separation threshold of 0.5, in which case for a 65° cup inclination angle it could result in a dynamic separation of approximately 0.4 mm. Thus, the magnitudes and forces can be predictors of dynamic separation for a variety of activities. Another way to predict the occurrence of edge loading could be by evaluating the contact mechanics from activities when depicting the direction of the forces in a virtual THR model (Hua *et al.*, 2016).

A surgical parameter that is not considered in the variability of this *in vitro* testing methodology is the hip joint centre set during surgery which affects the loading due to the strength of the patient’s muscles during gait and the forces acting due to the increased moment arm (Delp and Maloney, 1993) and (Sariali *et al.*, 2014). Future *in vitro* methodologies may require a sophisticated model which relates the surgical factors accurately and the interactions between the joint centre of the patient, the gait, and the reconstructed head and cup centre interaction proposed in this study to determine the risk of increase wear or failure.

4.7.4. Type of edge loading

As previously observed in Chapter 3, the magnitude of the translational mismatch affected the outcome of the test i.e. when the translational mismatch was increased from 2 to 3 and 4 mm for a 65° cup inclination angle, an interrupted relocation was observed. In this chapter the biomechanical study indicated the prevalence of the interrupted relocation. The interrupted relocation was only observed under a 3 mm translational mismatch with a swing phase load of 50 to 125 N and under a 4 mm translational mismatch with a swing phase load of 50 to 175 N for a 65° cup inclination angle. The high confidence intervals in the severity of edge loading under the 3 mm translational mismatch and low swing phase load (50 - 75 N) indicated that the interrupted relocation was not consistent

(Figure 4-8). In contrast, under a 4 mm translational mismatch, the prevalence of an interrupted relocation decreased as the swing phase load increased to 125 N and onwards (Figure 4-8).

When the severity of edge loading was higher than 400 Ns it essentially indicated that an interrupted relocation was present. This is an interpretation since the loading cycle was the same for all the conditions tested and the severity of edge loading was only seen to increase substantially when an interrupted relocation occurred. When interrupted edge loading occurred, the severity of edge loading increased to approximately 600 Ns.

While the biomechanical study gave an indication of the type of edge loading and the severity of edge loading, the low number of samples tested in Phase 1 with a single station did not accurately represent the long term test and station variability. When the sample numbers were increased to six in Phase 2, and each station was used independently, a better representation was obtained. For instance the high confidence intervals for the 300 N swing phase load decreased from ± 261 Ns to ± 48 Ns (from $n=3$ to $n=6$). The wear results correlated better with the severity when Phase 2 was used which gave a better representation of the severity of edge loading and smaller wear variance within that group condition.

The evidence of interrupted relocation can be seen on the wear scars of the heads, as the location of the high scar depth aligns with the point in time of maximum loading. During the wear test, stations #4 and #5 indicated by the separation profile and severity of edge loading indicated the prevalence of interrupted relocation (Figure 4-16). These two samples resulted in higher scar depth overall due the higher forces acting during edge loading and with some levels of damage visible on the right hand side of the head indicating the point the cup relocating back into the head. These two samples also had the higher wear rate in comparison to the rest of the cohort, resulting in nearly double the wear rate. Excluding the station #4 and #5, the mean wear rate (\pm SD) for three million cycles the 150 N swing phase load under a translational mismatch of 4 mm and a cup inclination angle of 65° equates to $0.6 \pm 0.1 \text{ mm}^3/10^6$ cycles and for station #4 and #5 only, resulted in $1.0 \pm 0.2 \text{ mm}^3/10^6$ cycles.

The results from the biomechanical study (Phase 2) from the 150 N swing phase load could be split between the samples without interrupted relocation resulting in a mean value of 330 Ns, and the samples with interrupted relocation, resulting in a mean value of 733 Ns. This data can be plotted against the wear study where the samples from the 150 N swing phase load with higher evidence of interrupted relocation having a deeper wear scar predominately on the right hand side as discussed above. The results indicate a better ($R^2=0.96$) correlation between the severity of edge loading and wear when splitting the magnitude of the severity of edge loading against type of edge loading condition (Figure 4-27).

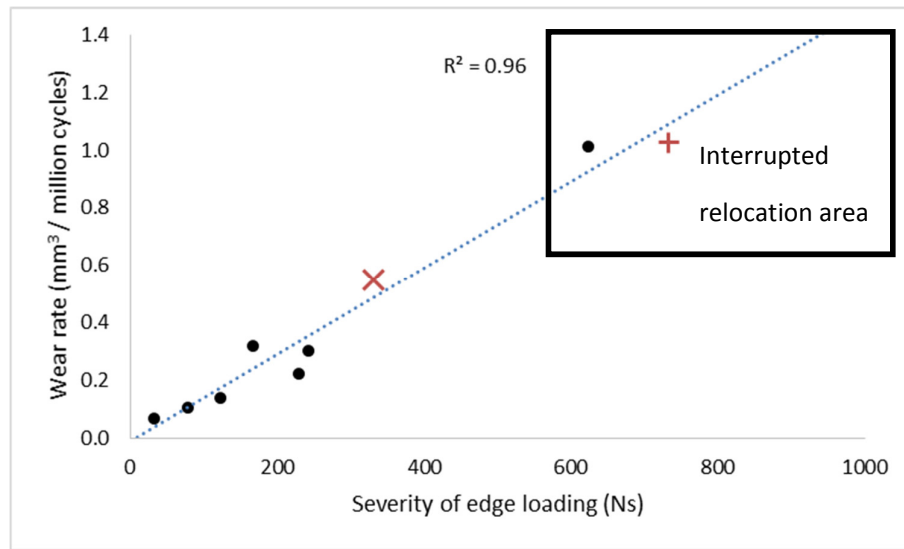


Figure 4-27. Mean ($n=6$, $\pm 95\%$ CI) severity of edge loading against mean ($n=6$, $\pm 95\%$ CI) wear rate for 36 mm ceramic-on-ceramic (BIOLOX® delta) bearings adapted from Figure 4-26 were the 150 N swing phase load under a 4 mm translational mismatch with a cup inclination angle of 65° is split with interrupted relocation (red '+') and with-out interrupted relocation (red 'x'). All other conditions from Figure 4-26 remain the same (black circles).

The dynamic separation alone cannot be used as an indication of edge loading. There can be scenarios when the separation is very small or when no dynamic separation is detected. The change in contact area without the presence of dynamic separation is another factor leading to edge loading. By applying a high medial-lateral load and a high swing phase load, the contact area between the head and the cup can shift towards the rim, thus edge loading can be present. However, there will be a threshold point where the axial load is far greater for the contact area to shift towards the bearing surface or for dynamic separation to occur. It is estimated that with a separation threshold of 1.5, there is no dynamic separation present for any of the tested conditions (Figure 4-6). The wear test results indicate that under low levels of dynamic separation (less than 0.5 mm) with a high swing phase load (300 N), edge loading can still occur when a high medial-force is present, and the scar on the heads is evidence of the contact between the head and the rim of the cup during kinematic conditions.

Squeaking in this study was heard during conditions with interrupted relocation. During the biomechanical study (Phase 1 and 2), squeaking did not consistently occur for all the conditions tested which exhibited interrupted relocation. During the wear test under 150 N swing phase load condition, where interrupted relocation was observed continuously, squeaking was intermittent and it would occur at periods for a considerable length of time, and at other periods not heard at all. These tests conditions with interrupted relocation may be generating higher friction due to the higher forces exerted at the rim and due to lubrication deprivation. The higher friction as reported by Brockett *et al.*, (2013) during squeaking may explain why hard-on-hard bearing squeak *in vivo*. The

reason as to why squeaking was heard in these simulator studies cannot be concluded. However, the associated large translational mismatch that was applied in the hip simulator which resulted in squeaking is not thought to be representative of a clinical scenario but rather equipment related.

4.7.5. Severity of edge loading

Each test condition can have a different scenario and displacement behaviour due to the load exerted on the testing components and the fixtures and the assemblies on which movement occurs and load is transmitted. The methodology (Chapter 2.3.8) describes the severity of edge loading as the duration the heads is in contact with the rim and the cumulative forces (axial and medial-lateral) acting between the head and the cup. To determine the point in time where the head is in contact with the rim, the dynamic separation for a specific testing condition was evaluated. When large separations occur due to large levels of translational mismatches and low swing phase load conditions, it is easy to detect the point defined as the start of separation. However, under high swing phase loads and large translational mismatches, detecting the start of separation is not easily identifiable. Under these conditions it is difficult to determine if the displacement measured is a dynamic separation of the head centre and the cup centre, or just bending in the system due to the magnitude of the loads being applied. The magnitudes of displacement are very small under these conditions and in the order of 0.2 mm. Thus, for these test conditions the start of the severity of edge loading was thought to be the point of maximum displacement. This means the severity of edge loading is potentially overestimated if the displacement observed is not separation. This may explain the rise in the severity of edge loading for a 3 mm translational mismatch and a 65° cup inclination angle from a swing phase load of 150 N onwards (rise from 150 Ns to 256 Ns). Whereas in other conditions the severity of edge loading notably decreased as the swing phase load increased. However, a stripe wear was observed during wear testing on the heads under a 300 N swing phase load condition and a 4 mm translational mismatch (Chapter 4.6) indicating edge loading was present. The stripe wear indicates that edge loading occurred during the swing phase load and the head relocated at heel strike as the maximum depth of the scar lies on the left hand side of the head (maximum flexion).

Whether edge loading *in vivo* occurs when no dynamic separation is present or not, a determining parameter is the severity of edge loading i.e. the magnitude of the force under edge loading. If edge loading was caused due to impingement it could also be assumed that the contact force and duration of edge loading would determine the severity as a comparative analysis. Currently there is no clinical evidence that measures the kinematics under edge loading, however the evidence of the wear scars indicate a variation in location and shape (Esposito *et al.*, 2012) thus one can assume different levels

of severities for different patients for different activities. Changing the swing phase loads test conditions in the simulator gave different magnitudes of wear scars depths.

In this chapter, the maximum load at the rim was not evaluated due to the increased number of conditions and the higher correlation of the severity of edge loading with the wear. Furthermore, the test conditions evaluated and chosen for the wear studies indicated interrupted relocation which was previously shown in Chapter 3 (Figure 3-5) not to correlate well with the wear as it does not capture the time and forces under edge loading. While the maximum force applied at the rim during edge loading holds useful information it has limitations related to detecting the maximum point of load before the cup relocates back in the head.

The surface roughness was unexpectedly different after the wear test even though different levels of severity of edge loading were applied in the test. The surface roughness of the 300 N swing phase load condition tested under a translational mismatch of 4 mm with a cup inclination angle of 65° was to be lower by 9 nm, than that tested under 150 N swing phase load. However the severity of edge loading indicated to be higher for the 150 N in comparison to the 300 N swing phase load test conditions. While the surface roughness of the 150 N swing phase load increased, it was also lower than that of similar conditions with a 70 N swing phase load and expected to be of a higher surface roughness due to the higher severity of edge loading being applied. Furthermore, the six samples were all in agreement with a small standard deviation between the samples indicating it wasn't a selected few with a low surface roughness or influences due to the location selected to do the analysis. It may be possible that some damage to the tip of the stylus that was not picked up during check and calibration of the equipment which could influence the results. However, a relative lower surface roughness was also found for the 150 N at pre-test in comparison to the 300 N swing phase load conditions. Overall the differences are very small when analysing in the nanoscale, but not found conclusively why they are different.

A neck fracture occurred on one of the stations during the wear testing of the 150 N swing phase load condition under a 4 mm translational mismatch and a cup inclination angle of 65°. The reason due to failure is unknown. However it can be postulated that the severity of offset loading that the stem may have encountered in this test is higher due the incidence of interrupted relocation (where a maximum force of up to 3 kN) and the separation generate a higher moment on the neck.

4.7.6. Limitations

While this testing methodology can compare the severity of wear due to edge loading for different designs, the damage to the rim based on the magnitude of the forces, the fatigue limit of the material, etc., it has certain limitations which need to be consider and firstly, it does not replicate

exactly what happens *in vivo*. However, it provides a testing platform where the risk of the implant failure can be assessed.

Secondly, the capacity to measure the severity of edge loading when no or little dynamic separation is present may not be the best approach, and considering the forces (axial and medial-lateral) during the swing phase load can provide useful information to compare among other testing conditions. Another way to assess the severity of edge loading is to evaluate the medial-lateral load. During high swing phase load conditions and large levels of translational mismatches the medial-lateral load did not decrease during the swing phase load, indicating the cup was relatively concentric with the head. However there can be scenarios where the wear increases due to edge loading, thus difficult to determine an accurate severity value.

Two samples out of the 300 N swing phase load wear test indicated a consistently higher wear rate in comparison to the rest of the cohort (Figure 4-14). Reasons for these may be due to a single or contribution of factors, such as; the distance required for the spring to grip leading to a higher translational mismatch, the input translational mismatch leading to higher forces, the friction on the cup holder test cell allowing medial-lateral separation, the operating minimum swing phase load, or another factor from the hip simulator that has not been thought of yet.

As previously mentioned in Chapter 3.7.8 the output load profile may not follow the peak input profile adequately at all times, and this was also noted for the minimum swing phase load (Figure 3-35). The output profile indicated that for low swing phase loads (<150 N), the minimum load was generally reached towards the end of the cycle i.e. near the 90% of the cycle. Under a high swing phase load (300 N) the output profile indicated a better match to the input than when a low swing phase load (50 N) was applied Figure 4-28. There are a number of differences that need to be considered in terms of methodology and comparison against other testing conditions. The input profile curve for all the testing was set with a 300 N swing phase load. Within the ProSim (Simulator Solutions, UK) software the minimum swing phase load was modified based on the load curve. This produces a different input curve profile which compensates for the change in the minimum load. This causes a change in terms the magnitude of the load applied when comparing different swing phase loads conditions at the same point of the cycle. For example the point in the cycle when the load increases where the input load reaches 500 N is different for different swing phase loads conditions. Thus, the point at which separation occurs and the point where the cup relocates are inherently different for different swing phase loads conditions as the input load would be different for certain points in the cycle.

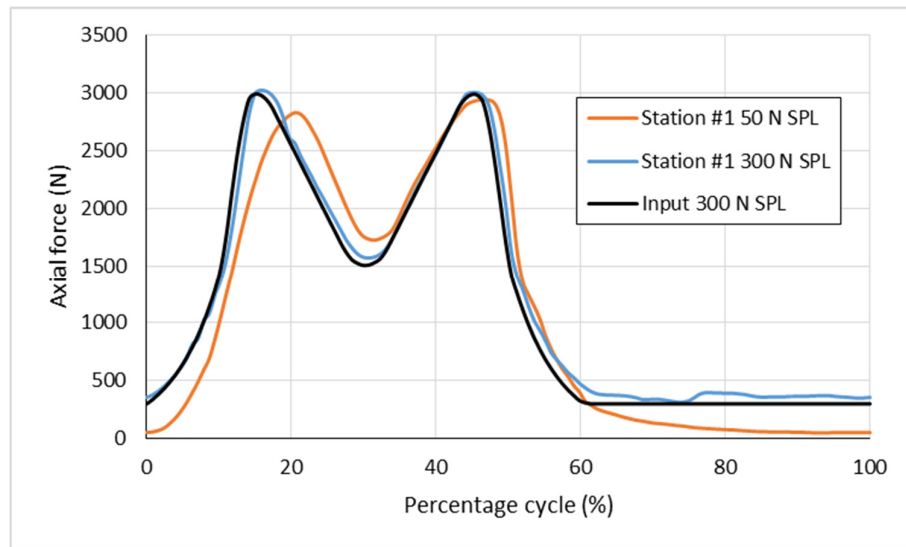


Figure 4-28. Input (black) for a 300 N swing phase load, and outputs for a 50 N swing phase load (orange) and 300 N swing phase load (blue) readings from the Leeds II Hip Joint Simulator during wear study under a 4 mm translational mismatch and a 65° inclination angle condition.

In this hip simulator the cup rotates along the version plane. This provides the internal-external rotation ($\pm 10^\circ$) acting on the head. The rotation of the cup away from the '0' position may contribute to an increased resistance of separation. During the swing phase load the cup rotates up to 10° where a greater coverage is exerted which may support the cup from translating away. However the resistance that could be provided by the cup rotation (version) was not measured and compared to when there would be no rotation, and a separate study would need to be carried out to determine the difference if any difference found. Previous studies, where the cup version was changed under edge loading (0.5 mm fixed dynamic microseparation) for CoC indicated the how this affected the location and orientation of the stripe wear on the head (Al-Hajjar *et al.*, 2014).

While the separation ratio and separation threshold serve as an evaluation to analyse input and outputs, it is not an exact evaluation as the direction of the forces acting on the system are not in the same plane i.e. axial load and medial-lateral load. The exact contribution due to the different direction on which the load is applied has not been considered, and this may shift the values. However, since the same methodology was applied throughout all the conditions, it serves as a comparison for different cup inclination angles when considering all test conditions.

The medial-lateral spring used in this study was kept at 100 N/mm to compare with previous studies under the same conditions and levels of dynamic separation. However the magnitude of the spring constant has no relation to *in vivo* conditions as the laxity value when dynamic separation occurs *in vivo* is not well understood. This may oppose a restriction on the magnitude of the medial-lateral loading resulted from a mismatch between the head and cup experienced *in vivo*. The magnitude of

force resulted from a mismatch between the head and the cup *in vivo* is unknown. Soft tissue may not exhibit tensioning for the levels of mismatches applied in this study. However the relative nature of increased or decreased tensioning is not understood experimentally.

4.8. Conclusion

An *in vitro* test method was developed to screen multiple conditions and evaluate the severity and relationships for component positioning for a set of kinematic conditions. The magnitude of the swing phase load affected the dynamic separation and severity of edge loading when a translation mismatch was employed to replicate edge loading conditions. The results indicated that increasing the swing phase load decreased the dynamic separation and severity of edge loading. The wear studies confirm that under a lower severity of edge loading due to an increased swing phase load the wear decreases. There wasn't a clear representation found of the *in vivo* conditions when applying a translational mismatch in a hip joint simulator while also controlling the swing phase load. However, the two parameters provide a test framework to independently evaluate edge loading for multiple conditions.

5. The Influence of the Spring Stiffness on the Occurrence and Severity of Edge Loading and Wear for Ceramic-on-ceramic Total Hip Replacement under Variations of Component Positioning *in vitro*

5.1. Introduction

The *in vitro* requirements to mimic and replicate edge loading associated with a translational mismatch between the centres of rotation of the head and the cup from a patient with a hip joint replacement are complex due to the interaction of the theoretical 'residual forces' due to the translational mismatch, the forces applied on the hip replacement due to the gait, and the interaction of the soft tissue tension which may also play a role. Previous studies (Chapter 3 and 4) evaluated one aspect, which was only the role of the translational mismatch. However, to only apply a 'resultant force' due to the mismatch in a hip joint simulator is not straight forward as the soft tissue tension and kinematics interaction are not de-coupled and their individual influences are unknown. Edge loading can be applied by using a spring which is a physical unit that is responsive to one variable (i.e. the translational mismatch) thus only able to evaluate the 'resultant force' in a controlled manner with a specific gait.

Considering that edge loading is multifactorial, it can be replicated in a hip simulator by others means and with higher capabilities such as with a multi-axis hip joint simulator with displacement and/or load controlled capable of changing the contact area between the bearings. However the Leeds II Hip Joint Simulator does not have a multi-axis displacement or load controlled capabilities built in. With this limitation the spring serves as a mechanism to replicate edge loading however the significance of the spring is subject of debate when simulating an *in vivo* scenario due to the reasons mentioned earlier.

One point to keep in mind is that retrievals studies show evidence of edge loading and a test methodology replicating a wear mechanism needs to be robust enough where the factors associated with the test are understood, demonstrate repeatable results and maintain sufficient criteria as the cases exhibited *in vivo*. Previous studies used a 100 N/mm spring constant which enabled the displacement of the cup holder in the hip simulator test cell (Nevelos *et al.*, 2000). While there are no studies indicating the selection of this particular spring constant, the spring itself is a physical unit that only reacts to the system around it. With this in mind, in the previous Chapters (3 and 4), the magnitude of the dynamic separation, severity of edge loading and wear were affected by the

translational mismatch and swing phase load applied. The extent of these variables are only known for one spring stiffness, and it is unknown if the relationship and magnitudes hold for different spring constants. In practice, a higher spring stiffness should generate a higher force and a larger dynamic separation. Currently the 100 N/mm spring constant hold as the only reference (results from Chapter 3 and 4) and a higher and a lower spring constant will be introduced to evaluate its effect when testing under a translational mismatch and compare against the previous data.

5.2. Aim

The aim of this study was to determine the effect of the spring stiffness on the magnitude of dynamic separation, severity of edge loading and wear of ceramic-on-ceramic (BIOLOX® delta) bearings under variations in component positioning in a hip joint simulator.

5.3. Methodology

This study was split into two sections:

Section 1. Biomechanical study

Phase 1: A broad biomechanical study to evaluate the influence of the spring stiffness on; 1) the magnitude of dynamic separation, 2) the magnitude of the force acting under edge loading, and 3) the time during the cycle the head spends on the rim of the cup (duration of edge loading) under four levels of medial-lateral component translational mismatch between the head and cup centre (1, 2, 3 and 4 mm). Each translational mismatch was coupled with a cup inclination angle equivalent *in vivo* to 45°, 55° and 65°, and each condition was tested under different swing phase loads, ranging from 50 to 450 N. Three spring stiffness were evaluated, these were 50, 100 and 200 N/mm. The total number of conditions tested when incorporating these two spring stiffness equate to 396 conditions. Three samples were used in total per condition.

Phase 2: A limited biomechanical matrix study to evaluate; 1) the magnitude of the force acting under edge loading, and 2) the time during the cycle the head spends on the rim of the cup (duration of edge loading) under a medial-lateral component translational mismatch and a single cup inclination and a single swing phase load condition and two spring stiffness. Six samples were used in total per condition. The two selected conditions were:

- A 4 mm translational mismatch under a 65° cup inclination angle with a swing phase load of 70 N, and a spring stiffness of 50 N/mm
- A 4 mm translational mismatch under a 65° cup inclination angle with a swing phase load of 70 N, and a spring stiffness of 200 N/mm

Section 2. Wear study

A limited wear study to determine the influence of edge loading due a translational mismatch and a single cup inclination angle on the wear of ceramic-on-ceramic (BIOLOX® delta). The selected test conditions were those selected on Phase 2 of the biomechanical study. These were: 4 mm medial-lateral component translational mismatch for 65° cup inclination angles under a 70 N swing phase load, and a spring stiffness of 50 and 200 N/mm, equating to 2 conditions in total.

5.4. Biomechanical study Phase 1. Evaluation of the biomechanics for different spring constants under variations in translational mismatch and cup inclination angle

5.4.1. Aim

The aim of this study was to determine how the spring constant (spring rate) influences the occurrence and severity of edge loading. This was measured by assessing; 1) the magnitude of dynamic separation, 2) the magnitude of the forces acting under edge loading, 3) the time during the cycle the head spends on the rim of the cup (duration of edge loading). The variables associated with component implant positioning were as follows; medial-lateral component translational mismatch between the head and cup centres and the acetabular cup inclination angle.

5.4.2. Methodology

Station number three of the Leeds Mark II Physiological Anatomical Hip Joint Wear Simulator was used, and the methodology described in Chapter 2 was followed. Further analysis was carried out as described in Chapter 4.4. The bearing material used was BIOLOX® delta as detailed in Chapter 2.1. Three cup inclination angles for the acetabular cup were chosen, these were 45°, 55° and 65° relative to the joint force vector. A translational mismatch was applied at the start of the test to the hip simulator as Figure 5-1. This was achieved by moving the cup in the medial direction away from the femoral head centre by 1, 2, 3 and 4 mm. For each of these conditions a swing phase load of 50 to 450 N was employed. Two different springs were employed to apply the translational mismatch (Table 5-1). This equated to 264 conditions, and for each condition 3 samples were employed. Further details of the test are described in Table 5-1. Mean values and $\pm 95\%$ Confidence Intervals (CI) were determined and statistical analysis (one way ANOVA) completed (significance taken at $p < 0.05$).

The data from Chapter 4, Phase 1 with a 100 N/mm spring constant (i.e. 1, 2, 3 and 4 mm translational mismatch with a 45°, 55° and 65° cup inclination angle for different swing phase load conditions) was used to compare against the two spring constant evaluated in this study.

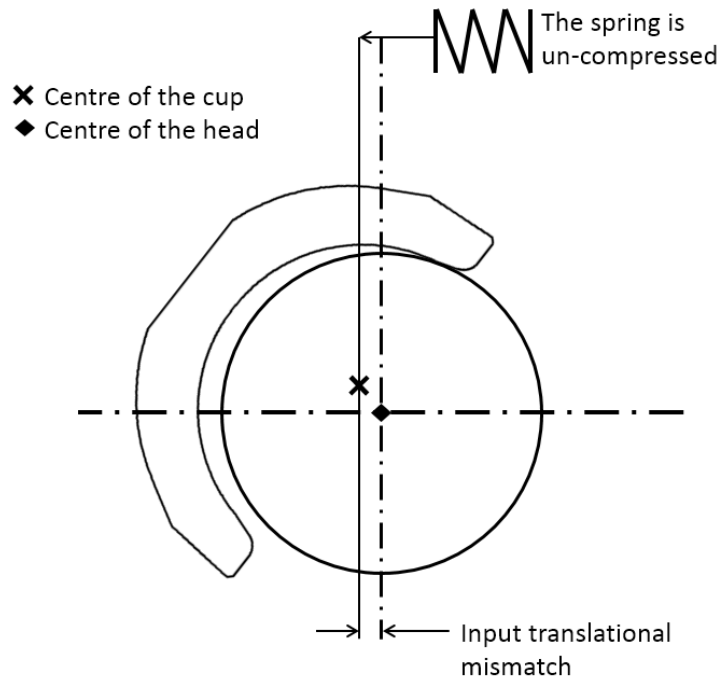


Figure 5-1. Schematic of the input translational mismatch applied with a spring between the centre of the head and the centre of the cup in the Hip Joint Simulator while no load is applied.

Table 5-1. Details of the biomechanical study for the evaluation of different spring constants under a translational mismatch in a hip joint simulator.

Study	Details (Unit)	Input
Biomechanical study	Equipment	Six-station Leeds Mark II (A)
	Materials	Ceramic-on-ceramic (BIOLOX® delta)
	Design	PINNACLE®
	Head size diameter (mm)	36
	Frequency (Hz)	1
	Loading profile	Based on Paul walking cycle (twin peak load)
	Max peak force (N)	3000
	Trough load (N)	1500
	Swing phase load (N)	50, 75, 100, 125, 150, 175, 200, 250, 300, 350, and 450
	Motion profile	Leeds walking cycle (Barbour <i>et al.</i> , 1999)
	Flexion / Extension (°) of the head	+30 / -15
	Internal / External rotation (°) of the cup	+10 / -10
	Stem anterversion angle (°)	20
	Cup version angle (°)	0
	Translational mismatch (mm)	1, 2, 3 and 4
	Spring constant (N/mm)	50, 100 and 200
	Number of total bearings tested	3
	Cup inclination angle (°)	45, 55 and 65
	Cycles completed	240
	Station used (#)	3

5.4.3. Results

The outputs from the tests were split into the three spring constant (50, 100 and 200/mm), first detailing the magnitude of separation and the severity of edge loading for each spring constant under different levels of translational mismatches and different cup inclination angles and different magnitudes of swing phase loads, followed by collectively analysis of the three springs on the input test conditions against the dynamic separation and the type of edge loading.

Spring constant of 50 N/mm

Under a translational mismatch of 1 mm, hardly any dynamic separation was measured for all the three cup inclination angles (45°, 55° and 65°) under a spring constant of 50 N/mm (Figure 5-2, A).

Under a translational mismatch of 2 mm, a small dynamic separation (0.7 mm) was observed only for the 65° cup inclination angle while under low swing phase loads conditions (less than 150N), and there was no evidence of any dynamic separation for the 45° and 55° when tested under a 50 N/mm spring rate (Figure 5-2, B).

Under a translational mismatch of 3 mm, there was no evidence of a dynamic separation for 45° cup inclination angle and a 50 N/mm spring rate, however the 55° and 65° cup inclination angle indicated dynamic separation for low swing phase loads conditions (approximately 75 N), Figure 5-2, C. Under the 55° and 65° cup inclination angles, as the swing phase load increased, the dynamic separation decreased. Larger dynamic separation resulted from the 65° cup inclination angle conditions in comparison to the 55° cup inclination angle for the same swing phase load condition.

Under a translational mismatch of 4 mm, larger magnitudes of dynamic separation were observed for all the cup inclination angles (45°, 55° and 65°) under low swing phase load conditions for a 50 N/mm spring rate (Figure 5-2, D). The dynamic separation increased as the cup inclination angle increased from 45° to 55° to 65°. In contrast, the dynamic separation indicated to decrease for all the cup inclination angles as the swing phase load increased.

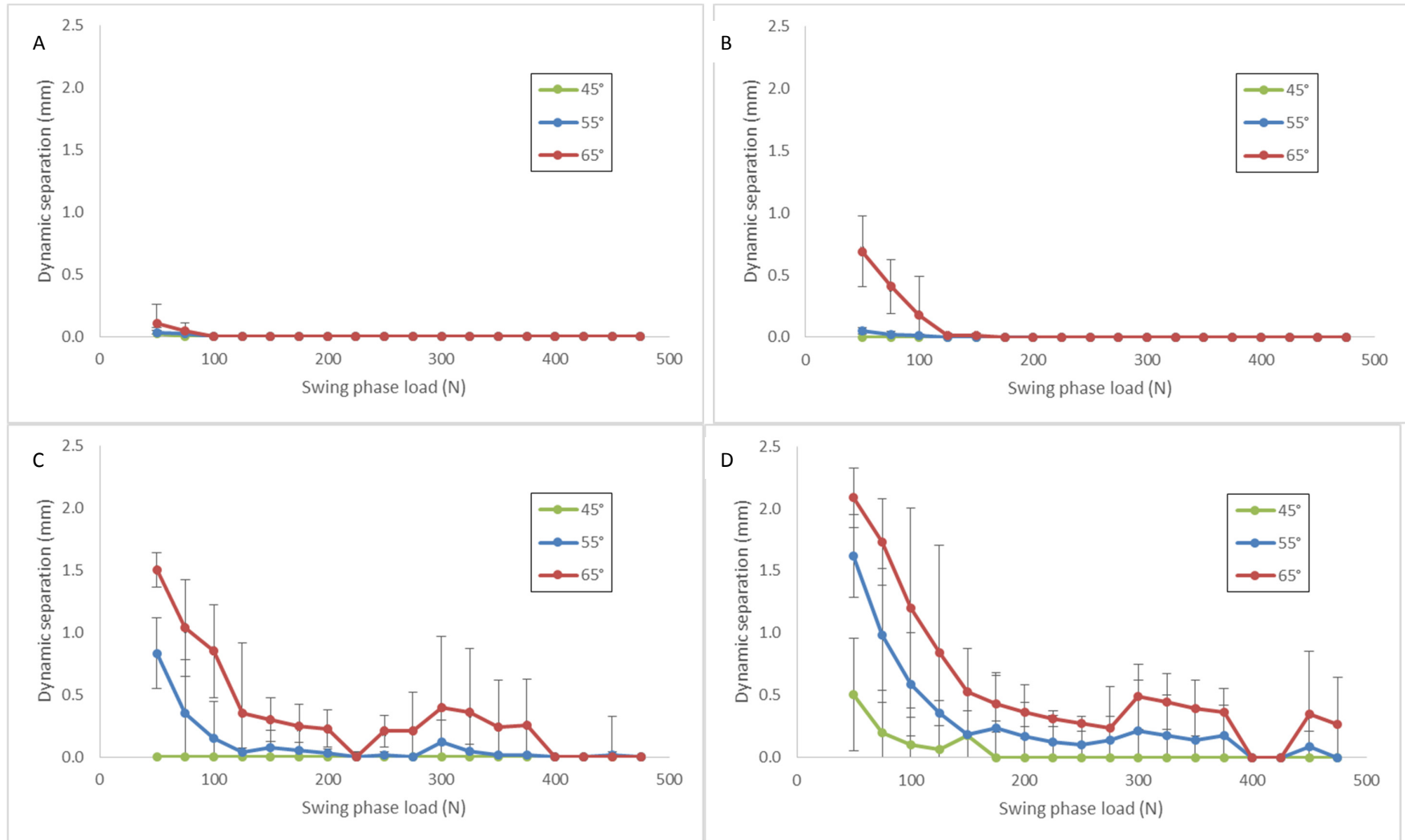


Figure 5-2. Mean ($n=3$, $\pm 95\%$ CI) dynamic separation for 36 mm ceramic-on-ceramic (BIOLOX® delta) bearings under 1, 2, 3 and 4 mm translational mismatch conditions (A, B, C and D respectively) with a cup inclination angle of 45°, 55° and 65° and a spring stiffness of 50 N/mm.

The severity of edge loading for a 50 N/mm spring constant under a 1 mm translational mismatch for different cup inclination angles and different swing phase loads is plotted in Figure 5-3. There is little to no dynamic separation detected leading to edge loading for all the conditions. A mean ($\pm 95\%$ CI) value of 3 ± 14 Ns was measured for the 65° cup inclination angle under a 50 N swing phase load. Thus, practically there was no measurable severity of edge loading for any of the cup inclination angles (45° , 55° and 65°) under a 1 mm translational mismatch and a 50 N/mm spring constant.

The severity of edge loading increased for low swing phase loads conditions under a 2 mm translational mismatch with a 65° cup inclination angle and a 50 N/mm spring constant (Figure 5-3). However, the 45° and 55° cup inclination angles did not indicate any increase in the severity of edge loading for any swing phase load.

A mean ($\pm 95\%$ CI) value of 4 ± 19 Ns was measured for the 55° cup inclination angle under a 50 N swing phase load. Higher magnitudes of severity of edge loading were measured under a 3 mm translational mismatch for a 50 N/mm spring constant (Figure 5-3). The 65° cup inclination angle had a maximum severity of edge loading (164 ± 72 Ns) under a 50 N swing phase load and decreased to 0 Ns at a swing phase load of 250 N. The 45° and 55° cup inclination angle also decreased in severity of edge loading as the swing phase loads increased. However, the 45° and 55° cup inclination angle had lower severity of edge loading compared to the 65° cup inclination angle for any of the swing phase load condition.

Larger magnitudes of severity of edge loading (>300 Ns) were measured under a 4 mm translational mismatch for a 65° cup inclination angle under low swing phase load conditions with a spring constant of 50 N/mm (Figure 5-3). These reached a mean (\pm CI) severity of edge loading of 550 ± 652 , 563 ± 684 , 468 ± 572 and 375 ± 898 Ns for the swing phase loads of 50, 75, 100 and 125 N respectively. The large CI for these swing phase load conditions was due to the incidence of interrupted relocation leading to high severity of edge loading which occurred in two out of three samples. At higher swing phase loads conditions, the severity of edge loading did not decrease and was found to plateau at approximately 200 Ns. The 45° and 55° cup inclination angle exhibited a small increment in severity of edge loading under a 4 mm translational mismatch under low swing phase load conditions with a spring constant of 50 N/mm. These both reached approximately 100 Ns for a 50 N swing phase load and steadily decrease to 0 Ns as the swing phase load increased to 175 N.

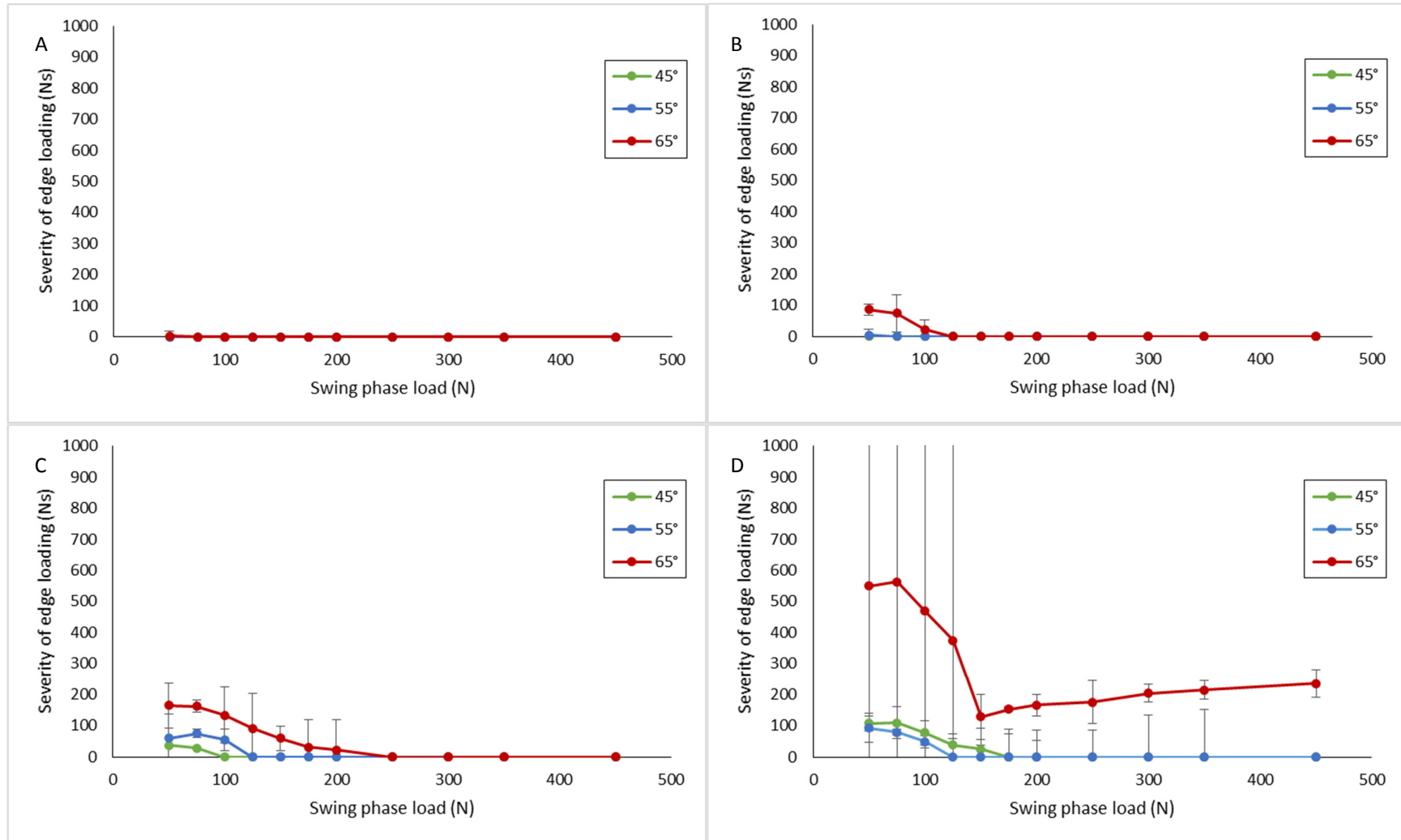


Figure 5-3. Mean ($n=3$, $\pm 95\%$ CI) severity of edge loading for 36 mm ceramic-on-ceramic (BIOLOX® delta) bearings under 1, 2, 3 and 4 mm translational mismatch conditions (A, B, C and D respectively) with a cup inclination angle of 45°, 55° and 65°, different swing phase loads and a spring stiffness of 50 N/mm.

Spring constant of 100 N/mm

The dynamic separation and severity of edge loading results from Chapter 4 are presented below. Further details of the results can be found in Chapter 4.4.3. Overall; the increased translational mismatch and cup inclination angle increased the dynamic separation (Figure 5-4). When the swing phase load was increased, the dynamic separation decreased. Increasing the translational mismatch and cup inclination angle increased the severity of edge loading (Figure 5-5). When the swing phase load was increased, the severity of edge loading decreased.

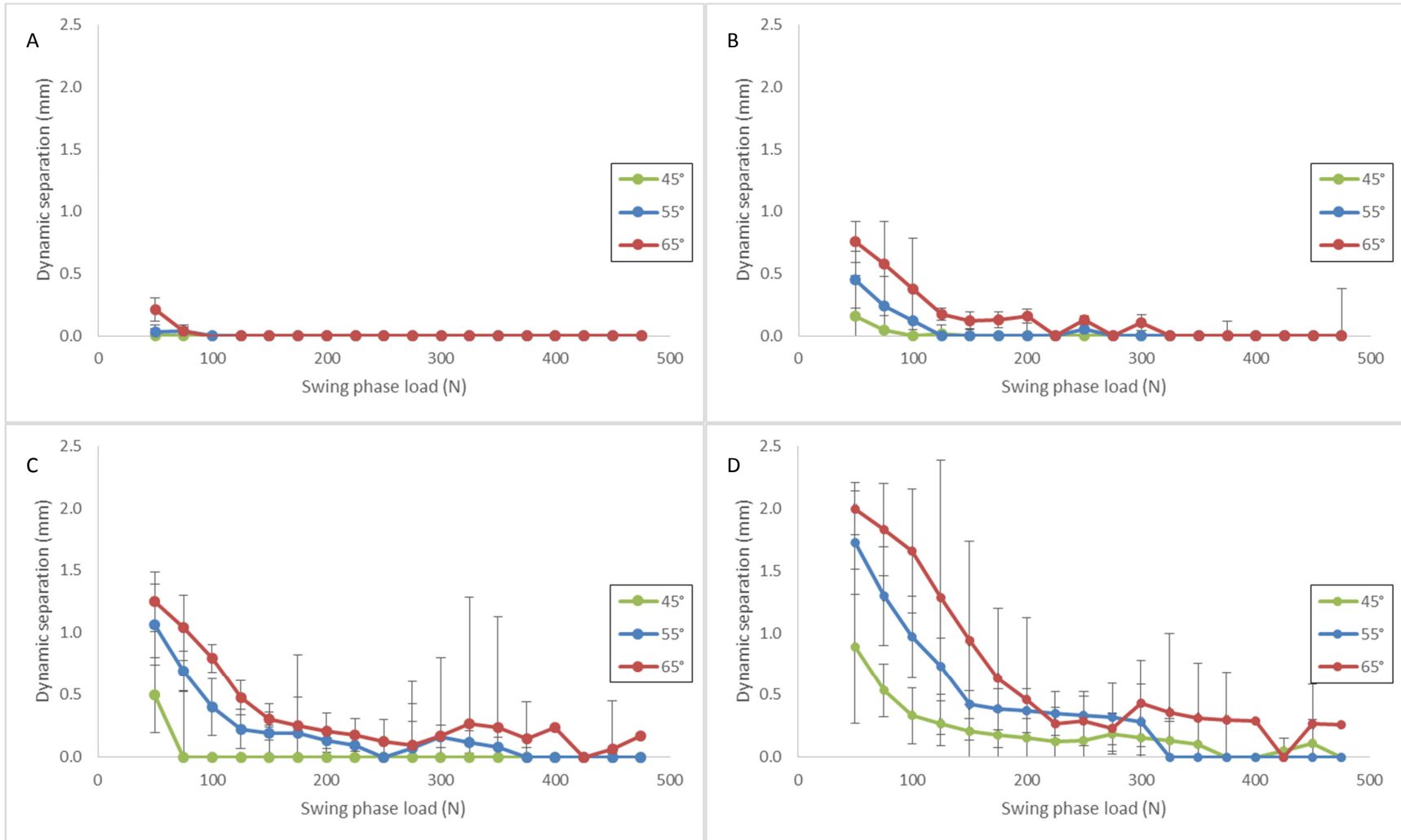


Figure 5-4. Mean ($n=3$, $\pm 95\%$ CI) dynamic separation for 36 mm ceramic-on-ceramic (BIOLOX® delta) bearings under 1, 2, 3 and 4 mm translational mismatch conditions (A, B, C and D respectively) with a cup inclination angle of 45°, 55° and 65°, different swing phase loads and a spring stiffness of 100 N/mm.

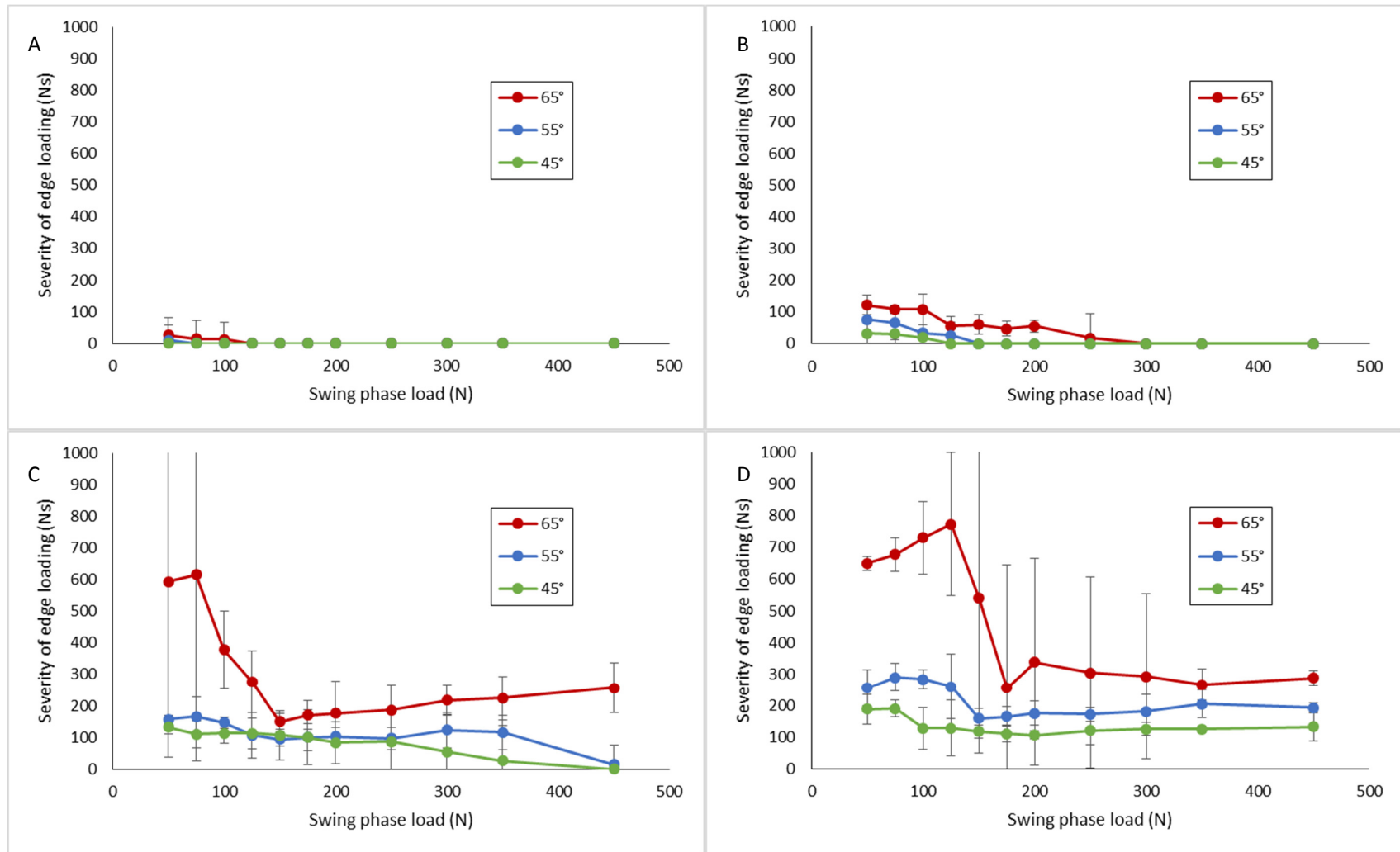


Figure 5-5. Mean ($n=3$, $\pm 95\%$ CI) severity of edge loading for 36 mm ceramic-on-ceramic (BIOLOX® delta) bearings under 1, 2, 3 and 4 mm translational mismatch conditions (A, B, C and D respectively) with a cup inclination angle of 45°, 55° and 65°, different swing phase loads and a spring stiffness of 100 N/mm.

Spring constant of 200 N/mm

Under a translational mismatch of 1 mm and a 200 N/mm spring rate, hardly any dynamic separation was observed for all the three cup inclination angles (45°, 55° and 65°), Figure 5-6. A small (less than 0.35 mm) dynamic separation was observed for the 65° cup inclination angle under a low swing phase load (50 N).

When the translational mismatch was increased to 2 mm and a 200 N/mm spring rate, different levels of dynamic separation were observed for the three cup inclination angles through the different swing phase load conditions (Figure 5-6). The largest dynamic separation was detected under the 65° cup inclination angle, followed by the 55° and finally the 45° cup inclination angle under a low swing phase load (50 N). As the swing phase load increased, the dynamic separation decreased for all the cup inclination angles, until no separation was detected.

Larger levels of dynamic separation resulted from the 3 mm translational mismatch and 200 N/m spring rate for all the cup inclination angles under low swing phase load (50 N) conditions (Figure 5-6).

Under 4 mm of translational mismatch and 200 N/mm spring rate, higher levels of dynamic separation were observed for all the cup inclination angles under low swing phase load conditions (50 N), Figure 5-6.

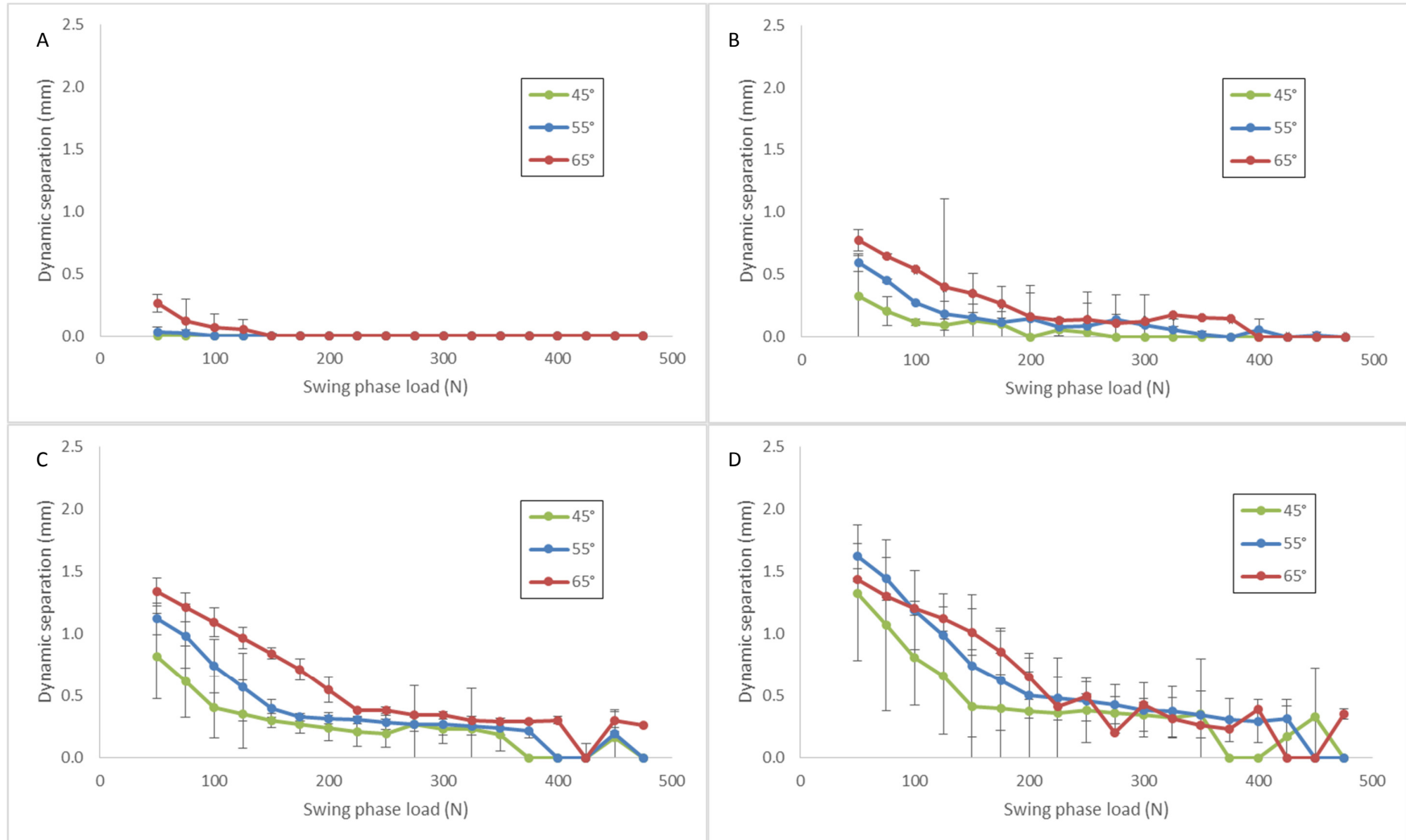


Figure 5-6. Mean ($n=3$, $\pm 95\%$ CI) dynamic separation for 36 mm ceramic-on-ceramic (BIOLOX® delta) bearings under 1, 2, 3 and 4 mm translational mismatch conditions (A, B, C and D respectively) with a cup inclination angle of 45°, 55° and 65°, different swing phase loads and a spring stiffness of 200 N/mm.

There was no dynamic separation leading to edge loading under a 200 N/mm spring constant and a 1 mm translational mismatch measured for the 45° and 55° cup inclination angles for any of the swing phase load conditions. Only the 65° cup inclination angle indicated a small (<50 Ns) severity of edge loading for the low swing phase load conditions of 50 and 75 N (Figure 5-7).

When the translational mismatch was increased to 2 mm under a 200 N/mm spring constant, the severity of edge loading increased for all the cup inclination angles under low swing phase load conditions (Figure 5-7). The mean (\pm CI) severity of edge loading under a 50 N swing phase load increased with the increased inclination angle from 97 ± 60 to 126 ± 35 to 195 ± 66 for the 45° to 55° to 65° cup inclination angle respectively. As the swing phase load increased, the trend indicated that the severity of edge loading decreased for all the cup inclination angles.

Larger magnitudes of severity of edge loading (>300 Ns) were measured under a 3 mm translational mismatch with a 200 N/mm spring constant for the 65° cup inclination angle and low swing phase load conditions (Figure 5-7). The tests indicated the incidence of interrupted relocation for these conditions to be consistent for the three samples until a swing phase load of 200 N was reached. At 200 N swing phase load, single type relocation was observed which increased the CI for that particular swing phase load condition. Overall, the 65° cup inclination angle under a 3 mm translational mismatch and 200 N/mm spring constant indicated to decrease the severity of edge loading from 150 N swing phase load onwards. The 45° and 55° cup inclination angles under a 3 mm translational mismatch and 200 N/mm spring constant had a severity of edge loading of approximately 250 Ns for the 50 and 75 N swing phase load conditions. The trend indicate a steady decrease up to 200 N swing phase load for these two cup inclination angles were the severity of edge loading didn't decrease any further for higher swing phase load conditions.

High magnitudes of severity of edge loading (>300 Ns) were observed (Figure 5-7) under a 4 mm translational mismatch and 200 N/mm spring constant for all the cup inclination angle under low swing phase load conditions (<150 N). The 45° cup inclination angle resulted in the lowest severity of edge loading while the 55° and 65° cup inclination angle resulted in much higher magnitudes under

the low swing phase load conditions for these test combinations. The 45° cup inclination angle had a gradual decrease in the severity of edge loading up until a swing phase load of 300 N where it seemed to stabilize at approximately 200 Ns. The 55° cup inclination angle under a 4 mm translational mismatch and 200 N/mm spring constant exhibited a gradual decrease in the severity of edge loading as the swing phase load increased. The large CI for the severity of edge loading in the low swing phase load conditions indicated that the interrupted relocation was not consistent with all three samples tested. In contrast, the 65° cup inclination angle indicated consistency with the type of edge loading up until a 200 N swing phase load. At a swing phase load of 200 N the severity of edge loading decreased to 400 Ns and continued to decrease to approximately 200 Ns as the swing phase load increased.

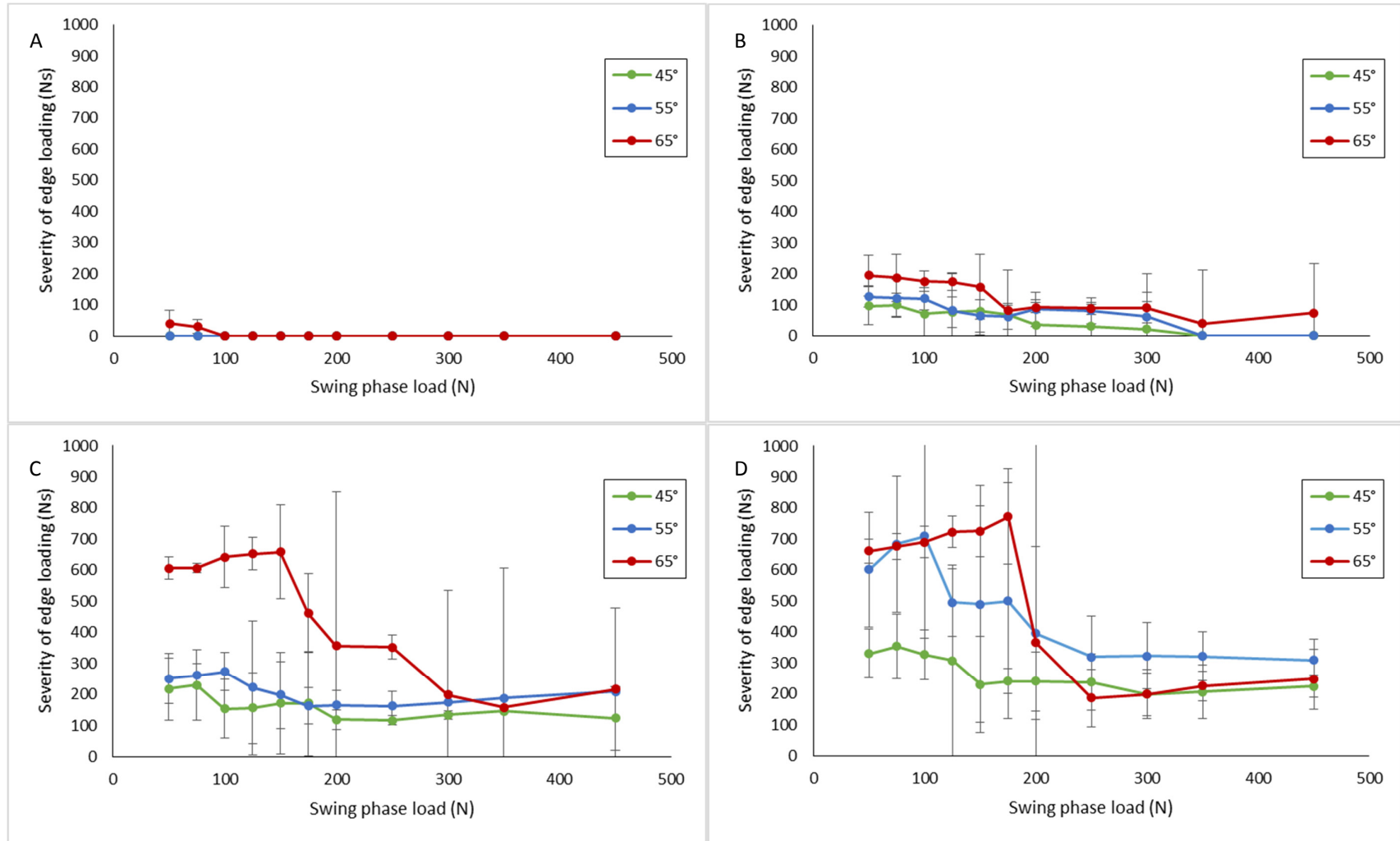


Figure 5-7. Mean ($n=3$, $\pm 95\%$ CI) severity of edge loading for 36 mm ceramic-on-ceramic (BIOLOX® delta) bearings under 1, 2, 3 and 4 mm translational mismatch conditions (A, B, C and D respectively) with a cup inclination angle of 45°, 55° and 65°, different swing phase loads and a spring stiffness of 200 N/mm.

As the separation ratio increased, the dynamic separation increased for all the cup inclination angles tested under a translational mismatch and a spring rate of 50 N/mm (Figure 5-8). A steeper linear correlation resulted from the 65° cup inclination angle, leading to higher dynamic separation for a given separation ratio in comparison to the 45° and 55°. The results from the 200 N/mm spring rate indicated that as the separation ratio increased, the dynamic separation also increased for all the cup inclination angles and translational mismatches applied (Figure 5-10). The slope of the linear correlations indicated that for the 200 N/mm spring rate, a larger separation ratio was required to achieve the same magnitude of dynamic separation as that of a spring rate of 50 N/mm.

As the separation threshold increased for all the cup inclination angles (45°, 55° and 65°) tested under a translational mismatch with a 50 N/mm spring rate, the dynamic separation decreased (Figure 5-11). The power correlation for each cup inclination angle (45°, 55° and 65°) indicated that the capacity for dynamic separation increased with a steeper cup inclination angle. The separation threshold had the same trend for the conditions tested under a spring constant of 200 N/mm (Figure 5-13). However, a lower separation threshold was required in comparison to the 50 N/mm spring constant test conditions. There was no observed dynamic separation for a separation threshold higher than 1.0 for conditions tested under a 200 N/mm spring constant.

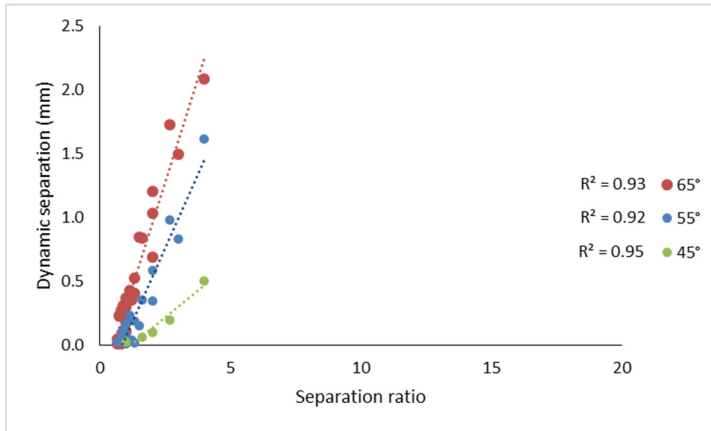


Figure 5-8

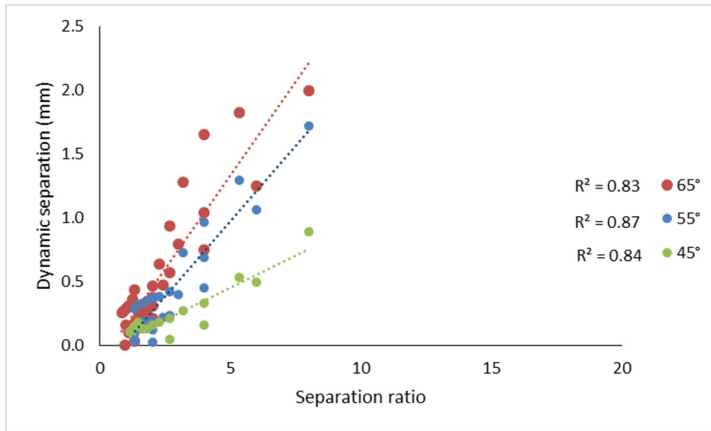


Figure 5-9

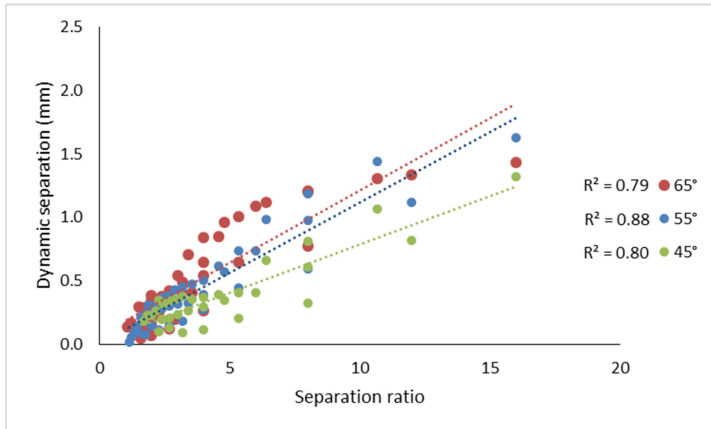


Figure 5-10

Figure 5-8. Dynamic separation against separation ratio for 1, 2, 3 and 4 mm translational mismatches grouped per inclination angle of 45° (green), 55° (blue) and 65° (red) for different swing phase loads conditions with a spring constant of 50 N/mm.

Figure 5-9. Dynamic separation against separation ratio for 1, 2, 3 and 4 mm translational mismatches grouped per inclination angle of 45° (green), 55° (blue) and 65° (red) for different swing phase loads conditions with a spring constant of 100 N/mm.

Figure 5-10. Dynamic separation against separation ratio for 1, 2, 3 and 4 mm translational mismatches grouped per inclination angle of 45° (green), 55° (blue) and 65° (red) for different swing phase loads conditions with a spring constant of 200 N/mm.

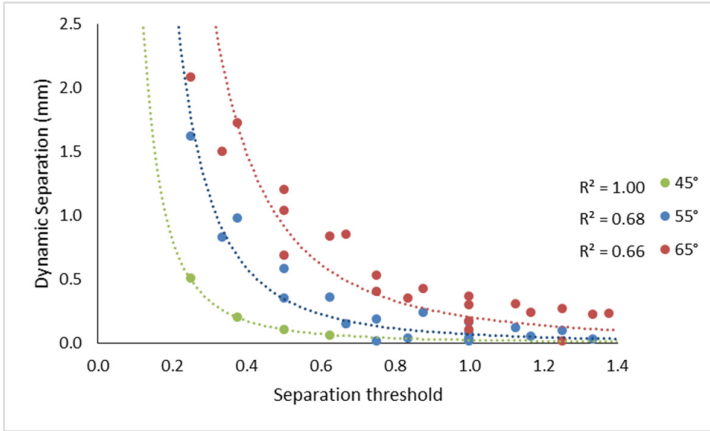


Figure 5-11

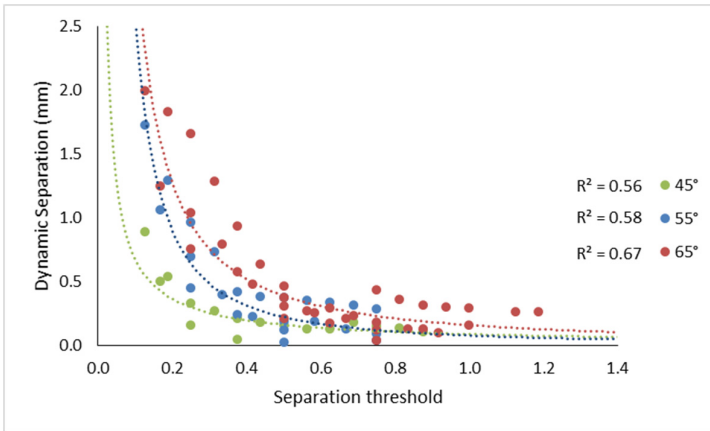


Figure 5-12

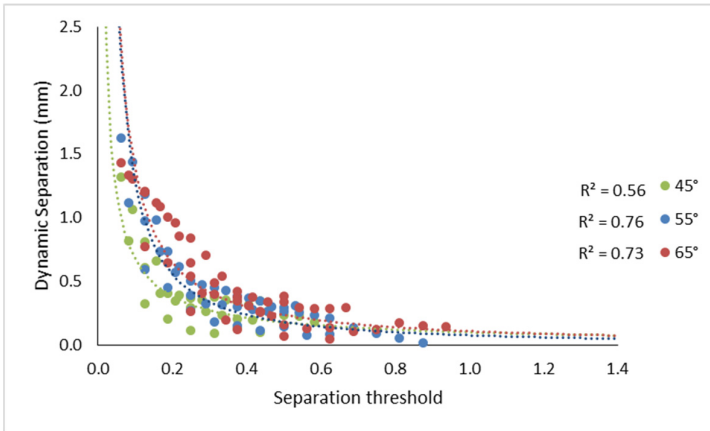


Figure 5-13

Figure 5-11. Separation threshold against dynamic separation for 1, 2, 3 and 4 mm translational mismatches grouped per inclination angle of 45° (green), 55° (blue) and 65° (red) for different swing phase loads conditions with a spring constant of 50 N/mm.

Figure 5-12. Separation threshold against dynamic separation for 1, 2, 3 and 4 mm translational mismatches grouped per inclination angle of 45° (green), 55° (blue) and 65° (red) for different swing phase loads conditions with a spring constant of 100 N/mm.

Figure 5-13. Separation threshold against dynamic separation for 1, 2, 3 and 4 mm translational mismatches grouped per inclination angle of 45° (green), 55° (blue) and 65° (red) for different swing phase loads conditions with a spring constant of 200 N/mm.

Different types of edge loading conditions were observed. Under a 45° cup inclination angle, the cup relocated in a single action as the vertical load increased. When the swing phase load increased under low levels of translational mismatches, no separation was detected for the 45° cup inclination angle. The 55° cup inclination angle indicated the same trend. However, under a 200 N/mm spring rate and a 4 mm translational mismatch with a low swing phase load (50 N), an interrupted relocation where the cup did not indicate to return to its centre assembly point was observed. There was no indication of an interrupted relocation under a 45° cup inclination angle.

An interrupted relocation was evident for the 65° cup inclination angle when a translational mismatch of 4 mm was applied for the 50 and 200 N/mm spring rate for swing phase loads lower than 250 N. However under a 3 mm translational mismatch, the 65° cup inclination angle only indicated an interrupted relocation for a 200 N/mm spring rate and low swing phase loads (less than 250 N).

Thus, overall three observations were seen; no separation, single relocation, and interrupted edge loading. These were dependent on the cup inclination angles, the levels of component translational mismatch, the swing phase load and spring constant (Figure 5-14). For a different representation of data see Appendix A.

In summary both the translational mismatch and spring constant increase the force delivered medial-laterally, hence an increase in force changes from no separation to a single type of relocation that can be measured. When increasing the force medial-laterally further, then an interrupted relocation was observed.

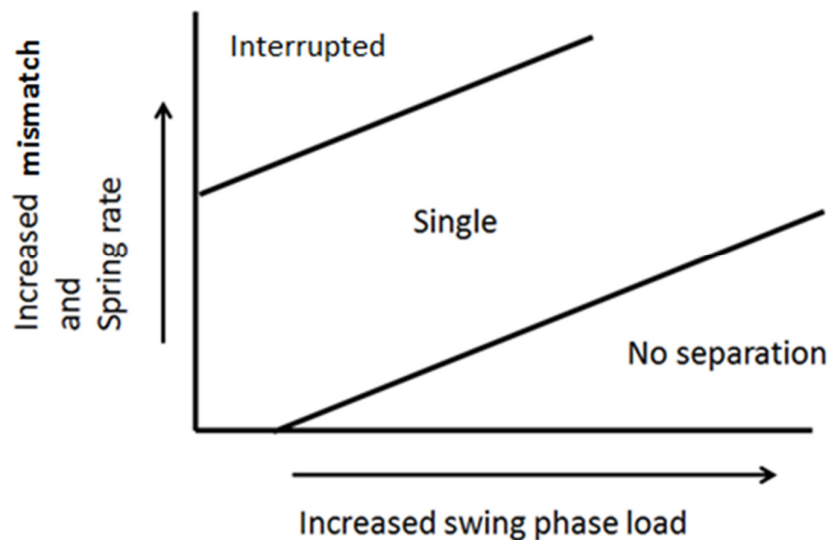


Figure 5-14. Schematic for the type of edge loading observed from the variables considered for testing.

5.5. Biomechanical study Phase 2. Evaluation of the severity of edge loading for specific spring constant test conditions under a translational mismatch

5.5.1. Aim & methodology

This study (Biomechanical study Phase 2) only investigated two spring constant conditions, were only the maximum force during edge loading and the severity of edge loading were evaluated. In this study the samples size was increased to six and all six stations were used. The two conditions applied were; 50 and 200 N/mm spring constants, were only one cup inclination angle and one translational mismatch was applied (Table 5-2). The data from Chapter 3, Phase 2 with a 100 N/mm spring constant (i.e. 4 mm translational mismatch and 65° cup inclination angle and 70 N swing phase load) was used to compare against the two spring constants evaluated in this study.

Table 5-2. Details of the biomechanical study for the evaluation of the severity of edge loading for selective spring constants under a translational mismatch.

Study	Details (Unit)	Input
Biomechanical study	Equipment	Six-station Leeds Mark II (A)
	Materials	Ceramic-on-ceramic (BIOLOX® delta)
	Design	PINNACLE
	Head size diameter (mm)	36
	Frequency (Hz)	1
	Loading profile	Paul walking cycle (twin peak load)
	Max peak force (N)	3300
	Trough load (N)	1500
	Swing phase load (N)	70
	Motion profile	Leeds walking cycle (Barbour <i>et al.</i> , 1999)
	Flexion / Extension (°) of the head	+30 / -15
	Internal / External rotation (°) of the cup	+10 / -10
	Stem antversion angle (°)	20
	Cup version angle (°)	0
	Translational mismatch (mm)	4
	Spring constant (N/mm)	50 and 200
	Number of total bearings tested	6
	Cup inclination angle (°)	65
	Cycles completed	900
	Stations used (#)	1, 2, 3, 4, 5, 6

5.5.2. Results

The maximum force under edge loading for the 50 N/mm spring constant resulted in 2299 ± 761 N (Figure 5-15). The test condition under a 200 N/mm resulted in a higher maximum force under edge loading (2983 ± 43 N), but was not found significantly different ($p=0.07$). However a larger variation was observed under the 50 N/mm test condition indicating the variability within the test group.

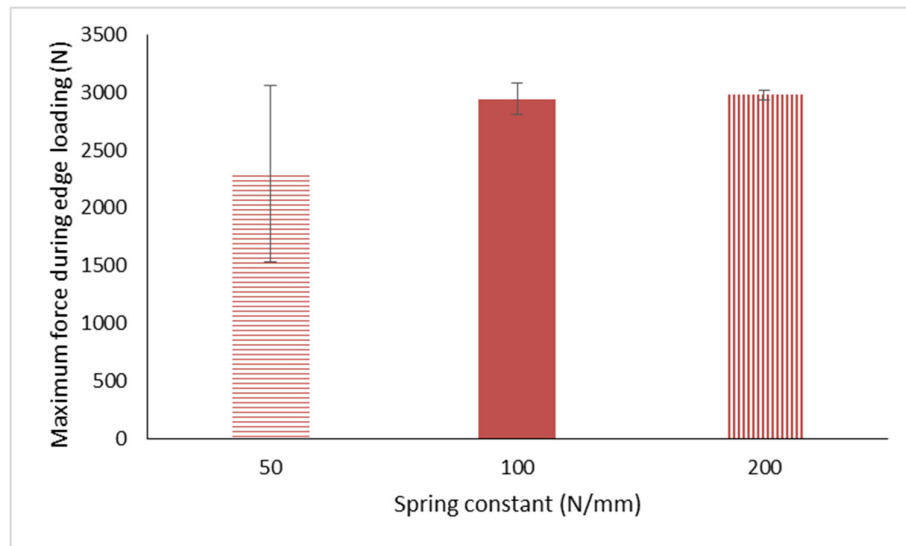


Figure 5-15. Mean ($n=6$, $\pm 95\%$ CI) maximum force under edge loading for 36 mm ceramic-on-ceramic (BIOLOX® delta) bearings under 4 mm translational mismatch conditions with a cup inclination angle of 65° for two spring constants (50, 100 and 200 N/mm).

The severity of edge loading for the 50 and 200 N/mm spring constant is plotted in Figure 5-16, in addition, the severity of edge loading from the 100 N/mm spring constant (refer to Chapter 3.5.3) with the same test combination (4 mm translational mismatch and 65° cup inclination angle and 70 N swing phase load) was added for comparison. The mean ($\pm 95\%$ CI) severity of edge loading increased from 450 ± 256 to 624 ± 161 to 762 ± 171 Ns as the spring constant increased from 50 to 100 to 200 N/mm respectively. In some cases, the 50 N/mm conditions exhibited interrupted relocation, but not found consistent. This led to higher CI under the 50 N/mm condition. There was no significant difference found between the 50 and 100 N/mm spring rate ($p=0.20$) and between the 100 and 200 N/mm ($p=0.18$) spring rate. Only a significant difference was found between the 50 and 200 N/mm spring rate ($p=0.03$).

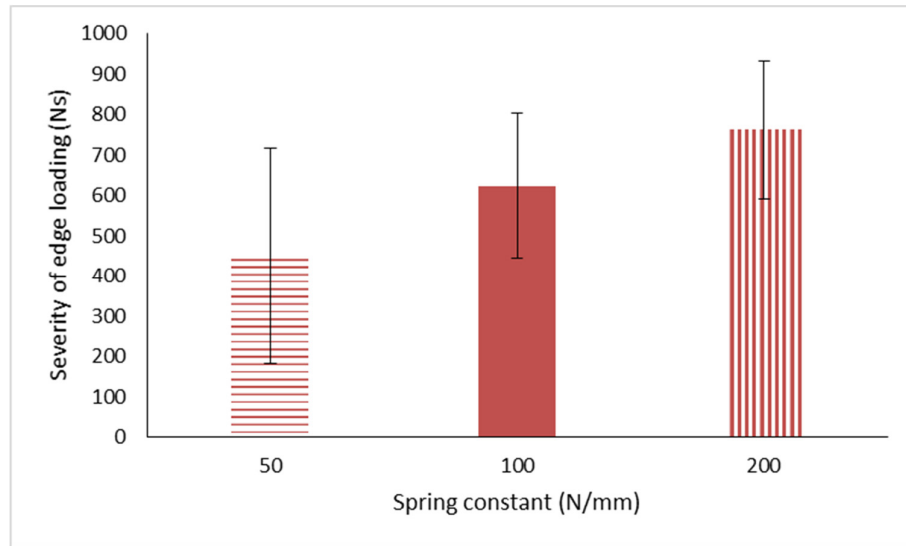


Figure 5-16. Mean ($n=6$, $\pm 95\%$ CI) severity of edge loading for 36 mm ceramic-on-ceramic (BIOLOX® delta) bearings under 4 mm translational mismatch conditions with a cup inclination angle of 65° for three spring constants (50, 100 and 200 N/mm).

5.6. The wear of 36 mm CoC (BIOLOX® delta) under edge loading due to a medial-lateral component translational mismatch of 4 mm for 50 and 200 N/mm spring constants with a cup inclination of 65°

5.6.1. Aim

The aim of this study was to determine the wear and damage of CoC under edge loading due to a medial-lateral component translational mismatch with a spring constant of 50 and 200 N/mm.

5.6.2. Methodology

The six-station Leeds Mark II Physiological Anatomical Hip Joint Wear Simulator was used, and the methodology described in Chapter 2 was followed. The bearing used was BIOLOX® delta as detailed in Chapter 2.1. A 65° cup inclination angle relative to the joint force vector was chosen for this study. A translational mismatch was applied at the start of the test to the hip simulator. This was achieved by moving the cup in the medial direction away from the femoral head centre by 4 mm Figure 5-17. This mismatch was maintained constant and regular checks were performed for consistency.

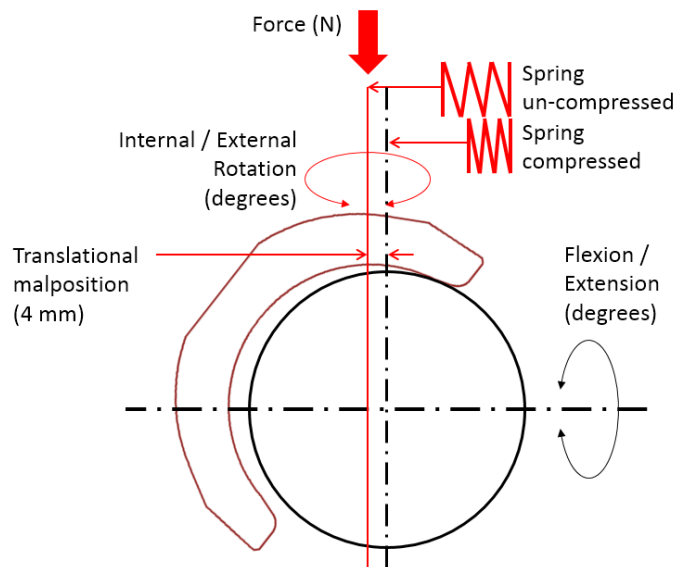


Figure 5-17. Schematic of the 4 mm translational mismatch input in the Hip Simulator.

The test was run for 3 million cycles (n=6). Details of the inputs for the test are described in Table 5-3. The first few cycles (approximately 30 minutes) were run without any medial-lateral mismatch to ensure a good performance of the equipment e.g. check the bone cement and fixtures hold without any malfunction. Afterwards, the cycle count was reset. A 4 mm medial-lateral mismatch was applied to all the stations. During the swing phase i.e. the low load phase (70 N), the spring forced the cup away. When the load was increased, the spring was compressed. As a routine check, an LVDT was employed to measure the displacement of the cup holder where the spring was placed. During intermissions i.e. either at serum change or at a measurement point (one million cycles), the fixtures and mounts were checked to ensure that no change occurred to the input mismatch. Checks on the hip simulator were done daily for good performance. Mean values and $\pm 95\%$ CI were determined and statistical analysis (one way ANOVA) completed (significance taken at $p < 0.05$).

Table 5-3. Details of the spring constant wear study under a translational mismatch.

Study	Details (Unit)	Input
Wear study	Equipment	Leeds II (A)
	Materials	Ceramic-on-ceramic (BIOLOX® delta)
	Design	PINNACLE
	Head size diameter (mm)	36
	Frequency (Hz)	1
	Loading profile	Paul walking cycle (twin peak load)
	Max twin peak force (N)	3000
	Trough peak load (N)	1500
	Swing phase load (N)	150 and 300
	Motion profile	Leeds walking cycle (Barbour <i>et al.</i> , 1999)
	Flexion / Extension (°) of the head	+30 / -15
	Internal / External rotation (°) of the cup	+10 / -10
	Stem anteverision angle (°)	20
	Cup version angle (°)	0
	Translational mismatch (mm)	4
	Spring constant (N/mm)	50 and 200
	Number of total bearings tested	12
	Cup inclination angle (°)	65
Cycles completed	3×10^6	

5.6.3. Results

The outputs from the study were the wear from the ceramic bearings, the scar depth on the femoral heads, the change in surface roughness and volumetric assessment of the heads via the CMM due to edge loading under a 4 mm translational mismatch for 65° cup inclination angle with 70 N swing phase load and a spring constant of 50 and 200 N/mm.

The total displacement of the cup holder during routine checks for the 50 N/mm spring constant measured using the LVDT indicated some variation (CV = 28%) between the stations (Figure 5-18).

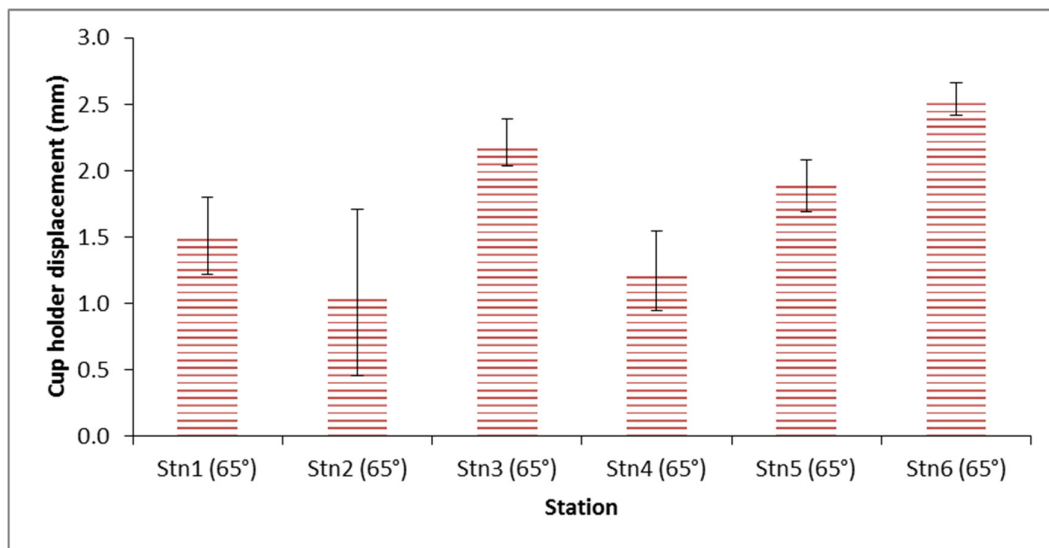


Figure 5-18. Average displacement of the cup holder (\pm CV) for 65° inclination angle under a 4 mm translational mismatch with a 70 N swing phase load and 50 N/mm spring constant.

The total displacement of the cup holder during routine checks for the 200 N/mm spring constant measured using the LVDT indicated some variation (CV = 17%) between the stations (Figure 5-19).

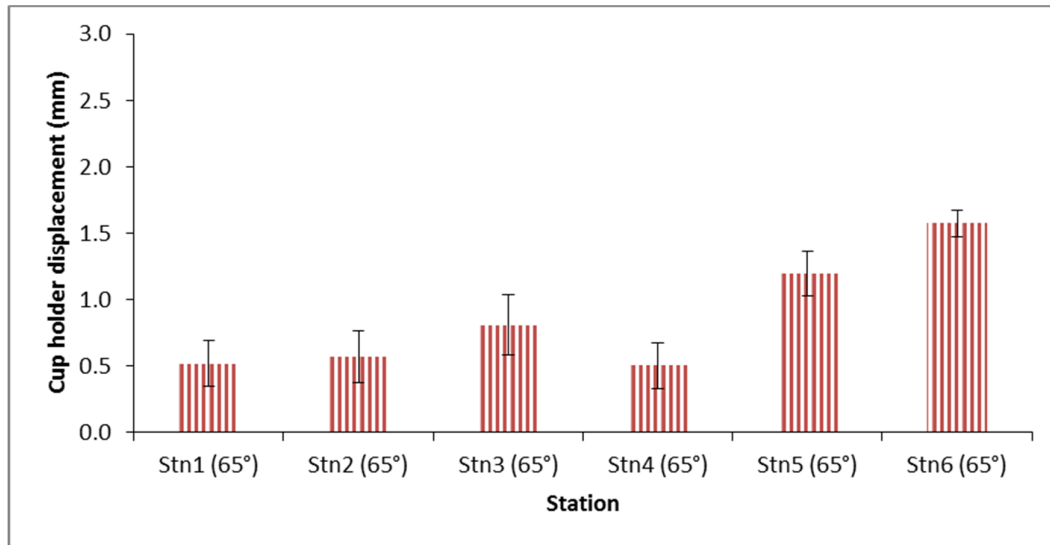


Figure 5-19. Average displacement of the cup holder (\pm CV) for 65° inclination angle under a 4 mm translational mismatch with a 70 N swing phase load and 200 N/mm spring constant.

The individual wear from all the stations tested with a 50 N/mm spring rate is shown in Figure 5-20. The wear rate on the femoral heads and the acetabular cups was relatively consistent at every interval and small decrease in wear were observed in some stations after the first million cycles. Overall, the mean wear rate decreased from 0.91 to 0.81 mm³/10⁶ cycles from first to the second measurement point.

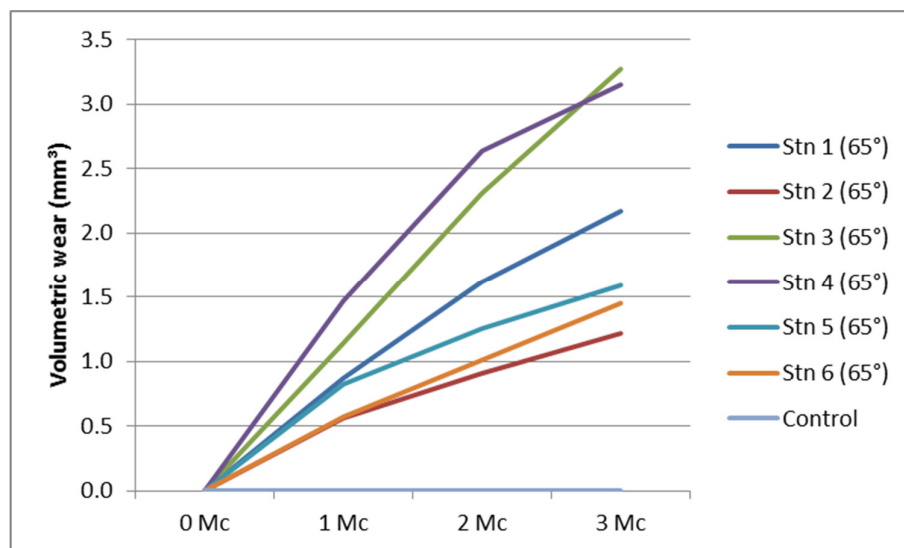


Figure 5-20. Individual volumetric wear under a 4 mm translational mismatch for 65° cup inclination angle with a 70 N swing phase load and 50 N/mm spring constant. Stn = Station.

The individual wear from all the stations tested with a 200 N/mm spring rate is shown in Figure 5-21. The wear rate on the femoral heads and the acetabular decreased after the first million cycles from 1.17 to 0.80 mm³/10⁶ cycles at two million cycles and then continued in approximately the same rate for the last measurement point.

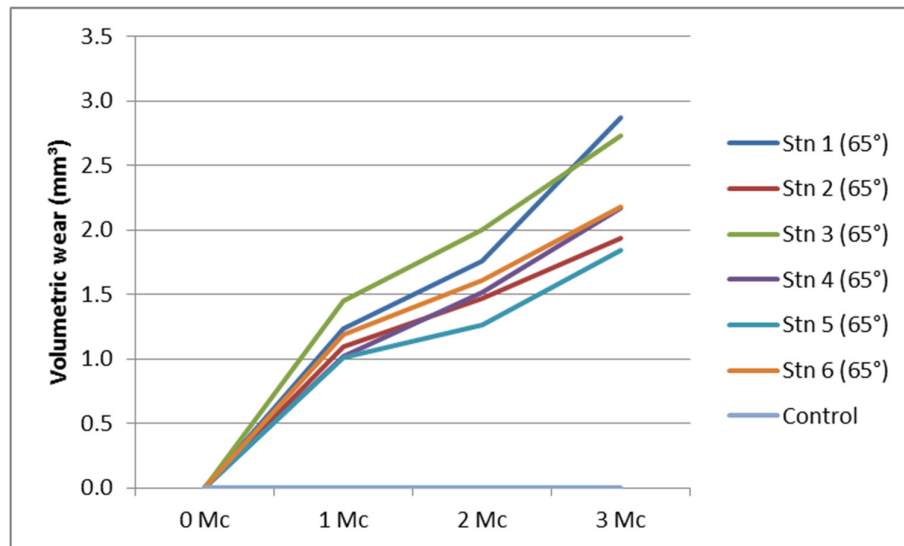


Figure 5-21. Individual volumetric wear under a 4 mm translational mismatch for 65° cup inclination angle with a 70 N swing phase load and a 200 N/mm spring constant. Stn = Station.

After three million cycles of testing, the mean wear rate was 0.71 ± 0.31 mm³/10⁶ cycles, and 0.76 ± 0.15 mm³/10⁶ cycles for the 50 and 200 N/mm spring rate respectively (Figure 5-22). No significant difference was found between the wear rates for the 50 and 200 N/mm spring rates ($p=0.72$). However the coefficient of variation was higher for the 50 N/mm compared to the 200 N/mm (0.41 and 0.18 respectively) indicating a tighter group for the 200 N/mm spring rate.

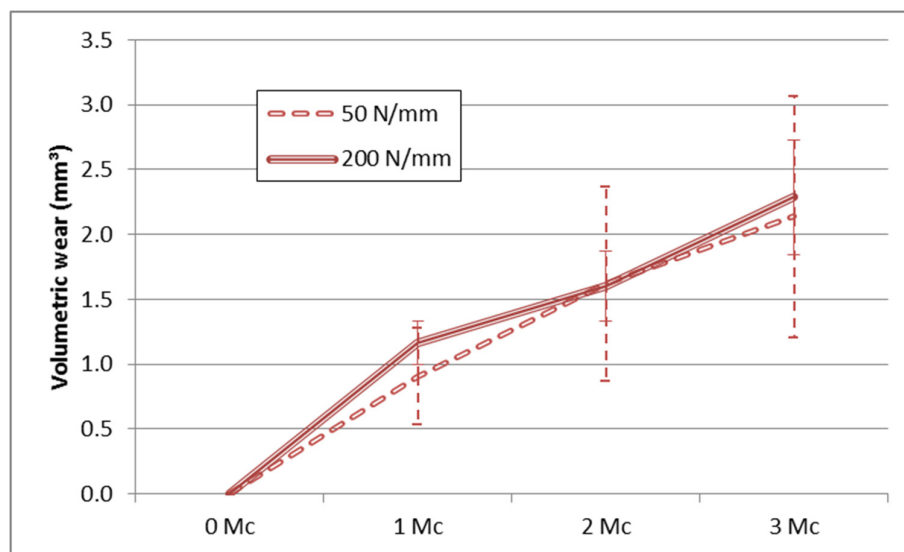


Figure 5-22 Mean ($n=6$, $\pm 95\%$ CI) wear rates for 50 and 200 N/mm spring constant under a 4 mm translational mismatch and 65° inclination angles with a 70 N swing phase load.

A representation of the damage seen on the surface of the heads after 3 million cycles for the 50 N/mm spring constant condition is shown in Figure 5-23. The point of maximum penetration in the stripe wear was varied between the stations. Sample #3 and #4 had signs of wearing towards the right hand side, whilst the rest of the samples resulted with the highest depth point of the scar on the left hand side.

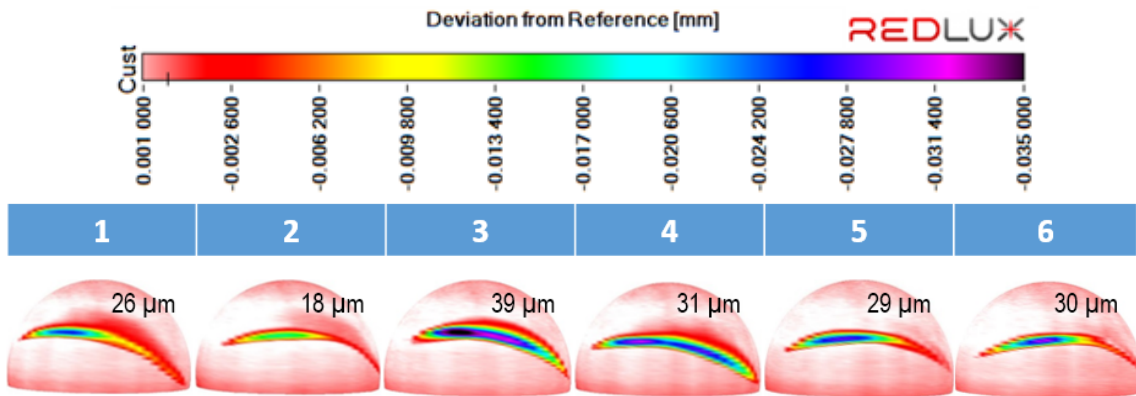


Figure 5-23. Visualisation of the heads under a 4 mm translational mismatch and 50 N/mm spring constant via RedLux software at the end of the wear test. The maximum depth of the scar is aligned to each head accordingly.

A representation of the damage seen on the surface of the heads after 3 million cycles for the 200 N/mm spring constant condition is shown in Figure 5-24. The point of maximum penetration in the stripe wear was varied between the stations. Whilst all samples indicated wear in the right hand side, only sample #6 resulted with the highest depth point of the scar on the left hand side.

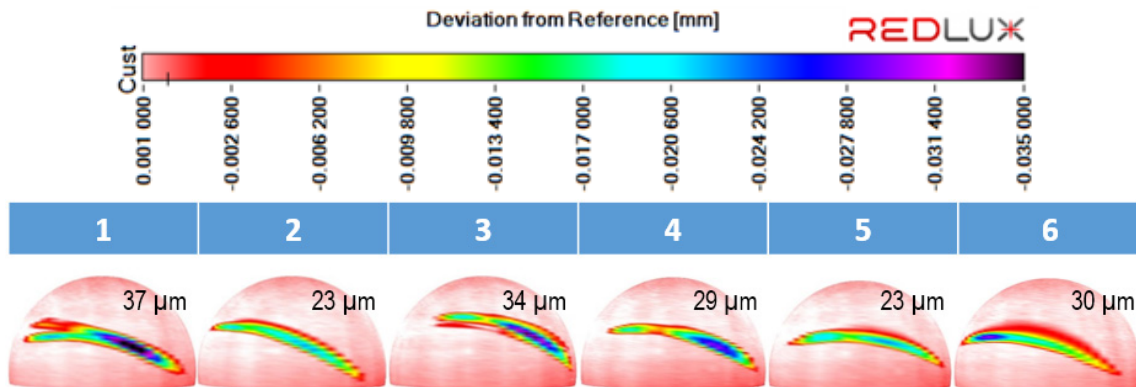


Figure 5-24. Visualisation of the heads under a 4 mm translational mismatch and 200 N/mm spring constant via RedLux software at the end of the wear test. The maximum depth of the scar is aligned to each head accordingly.

The mean scar penetration of the heads due to edge loading was $28.8 \pm 7.4 \mu\text{m}$ and $29.4 \pm 6.0 \mu\text{m}$ after 3 million cycles for the 50 and 200 N/mm spring constants respectively Figure 5-25. No significant difference was found between the 50 and 200 N/mm spring constants ($p=0.86$).

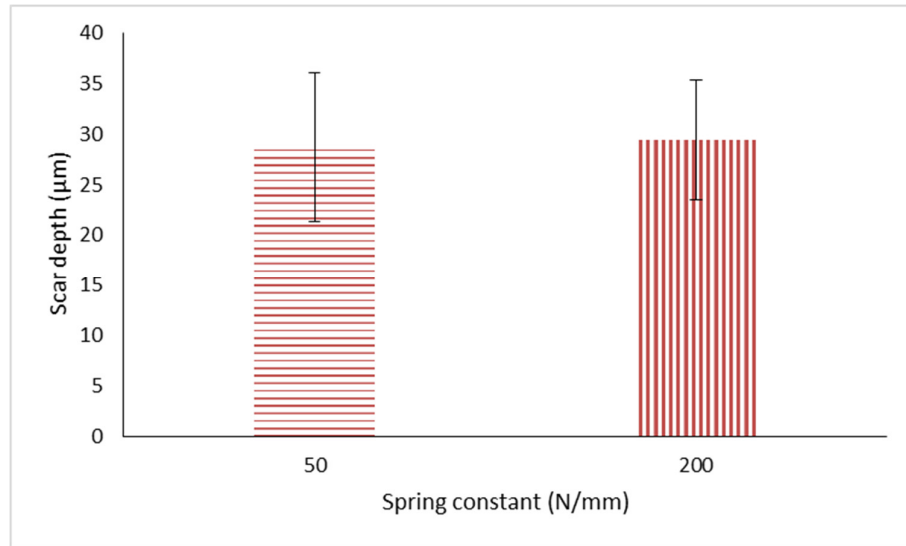


Figure 5-25. Mean ($n=6$, $\pm 95\%$ CI) maximum scar penetration after 3 million cycles under 50 and 200 N/mm spring constant and a 4 mm translational mismatch condition with a 65° cup inclination angle and a 70 N swing phase load.

Post-test, the surface roughness (Ra) was found to significantly increase ($p=0.01$ and $p<0.01$) for both spring constants (50 and 200 N/mm respectively) at the wear stripe when comparing to the pole region of the head samples 'P1 (tested)'. However, the conditions tested under a 50 N/mm spring constant were not found to increase as much as the 200 N/mm. The surface roughness for the 50 N/mm spring constant increased from 3 ± 3 to 19 ± 3 nm and the 200 N/mm increased from 6 ± 1 to 26 ± 5 nm. The difference between the surface roughness of the 50 and 200 N/mm at the wear stripe location 'P2 (tested)' were found significantly different ($p=0.01$).

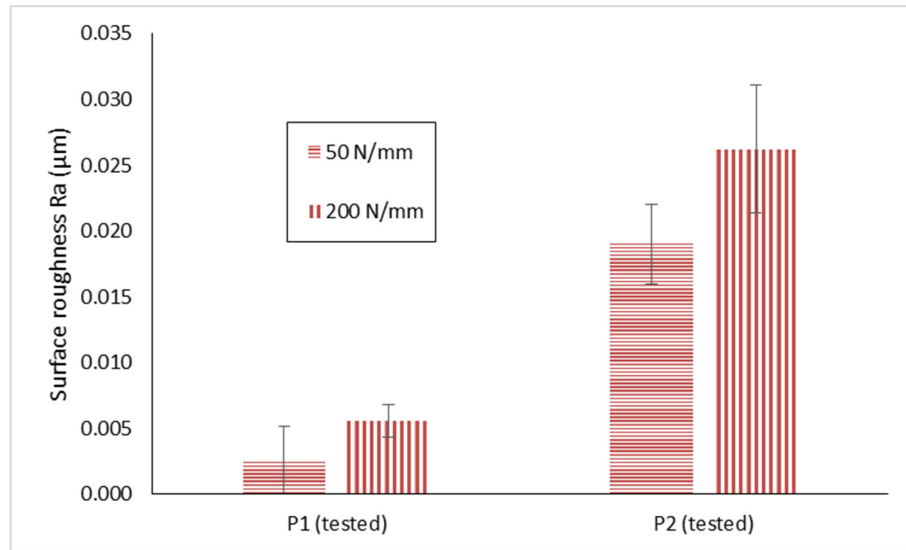


Figure 5-26. Mean ($n=6$, $\pm 95\%$ CI) surface roughness (Ra) for head samples post-test at the pole 'P1 (tested)', and the wear scar 'P2 (tested)' under 4 mm translational mismatch with a 65° cup inclination angle and a 70 N swing phase load for 50 and 200 N/mm spring constant.

Volumetric wear assessment via the CMM

The mean volumetric wear rate of the heads under a 4 mm translational mismatch with a 65° cup inclination angle and 70 N swing phase under a 50 N/mm spring constant condition calculated via the surface analysis was $0.32 \pm 0.15 \text{ mm}^3/10^6$ cycles. This was similar to the gravimetric results which was $0.35 \pm 0.17 \text{ mm}^3/10^6$ cycles.

The mean volumetric wear rate of the heads under a 4 mm translational mismatch with a 65° cup inclination angle and 70 N swing phase under a 200 N/mm spring constant condition calculated via the surface analysis was $0.36 \pm 0.07 \text{ mm}^3/10^6$ cycles. This was similar to the gravimetric results which was $0.38 \pm 0.07 \text{ mm}^3/10^6$ cycles.

5.7. Discussion

5.7.1. Dynamic separation

Previous *in vitro* testing which applied a dynamic separation, has been performed using a spring constant of 100 N/mm (Nevelos *et al.*, 2000). The effect of the spring constant was not investigated before. When replicating edge loading due to a translational mismatch, the translational mismatch has been found to affect the results due to the magnitude of the force applied medial-laterally. The medial-lateral force is exerted by the spring as the spring compresses under an axial load. Thus the magnitude of the force is dependent on the spring constant employed for the same translational mismatch.

The dynamic separation results from a 50 and 200 N/mm spring constant indicated the same pattern as those of 100 N/mm (Figure 5-28). The translational mismatch influenced the level of dynamic separation and was in alignment with the previous studies in Chapter 3, which demonstrated that a higher translational mismatch led to larger dynamic separation, and the cup inclination angle influenced the resistance to separation as shown in Figure 5-27 and Figure 5-29 for the 50 and 200 N/mm spring constant respectively for a 70 N swing phase load. Under a large translational mismatch, the effect of changing the spring from 50 to 200 N/mm can be particularly noted for the low swing phase load with a 45° and 55° cup inclination angle. These conditions resulted in small dynamic separation for the 50 N/mm, however under a 200 N/mm spring constant with the same conditions the dynamic separation increased.

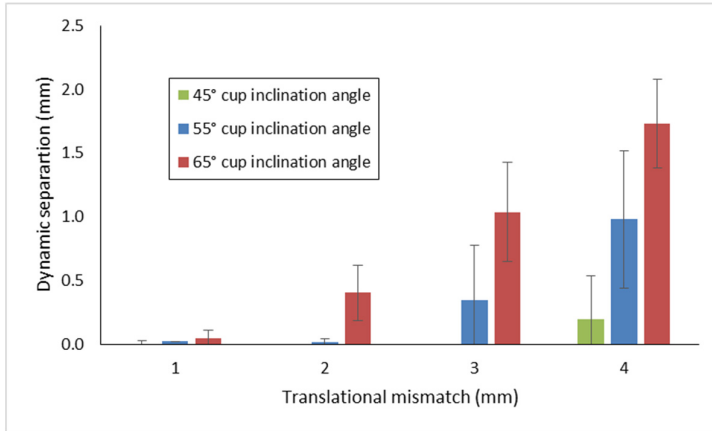


Figure 5-27

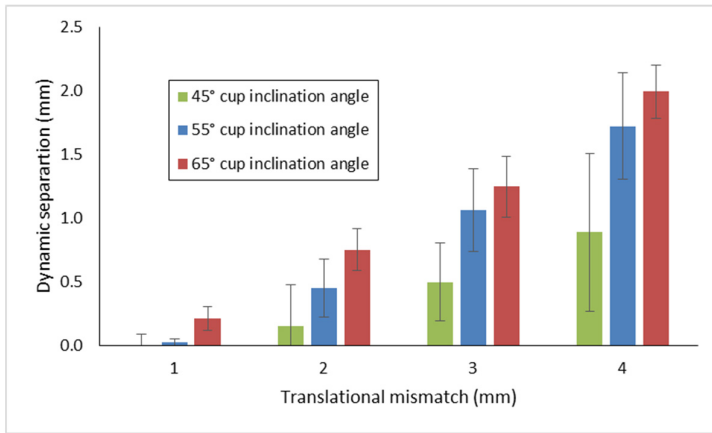


Figure 5-28

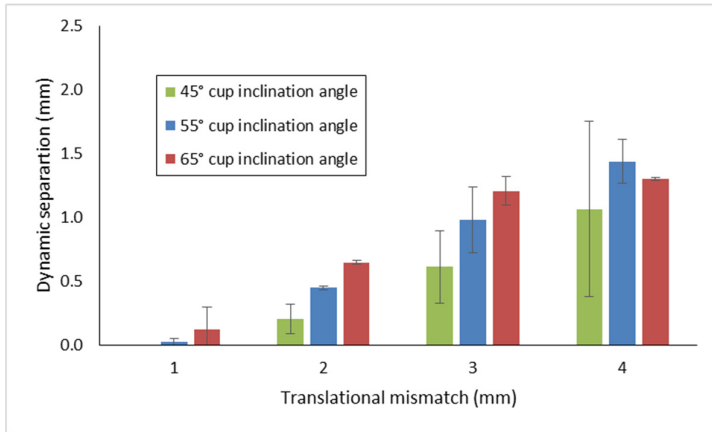


Figure 5-29

Figure 5-27. Mean (n=3, ±95% CI) dynamic separation of 36 mm ceramic-on-ceramic (BIOLOX® delta) bearings under 1, 2, 3 and 4 mm translational mismatch conditions for three cup inclination angle conditions, 45°, 55° and 65° for a 70 N swing phase load and a 50 N/mm spring constant.

Figure 5-28. Mean (n=3, ±95% CI) dynamic separation of 36 mm ceramic-on-ceramic (BIOLOX® delta) bearings under 1, 2, 3 and 4 mm translational mismatch conditions for three cup inclination angle conditions, 45°, 55° and 65° for a 70 N swing phase load and a 100 N/mm spring constant.

Figure 5-29. Mean (n=3, ±95% CI) dynamic separation of 36 mm ceramic-on-ceramic (BIOLOX® delta) bearings under 1, 2, 3 and 4 mm translational mismatch conditions for three cup inclination angle conditions, 45°, 55° and 65° for a 70 N swing phase load and a 200 N/mm spring constant.

Theoretically, a higher spring constant would apply a higher force for the same level of compressed displacement (translational mismatch) leading to a higher dynamic separation. In practice it was found that the force exerted did not match that of a 'perfect' system for all the test conditions. The dynamic separation of the 200 N/mm under a 4 mm translational mismatch and 65° cup inclination angle was found to be about the same magnitude (1.4 mm of dynamic separation) than that of a 45° cup inclination angle under a 50 N swing phase load. Furthermore, when the dynamic separation was evaluated across different spring constants and keeping the rest of the input conditions the same, (i.e. translational mismatch, cup inclination angle and swing phase load), it was found that the 200 N/mm spring constant condition could be lower than the 50 and 100 N/mm conditions (Figure 5-30). During these comparisons, it was also found that the biomechanical studies (Phase 1), the dynamic separation for the 200 N/mm spring constant indicated a very tight group from the three samples tested in comparison to the 50 and 100 N/mm spring constant.

Overall, the 50 N/mm spring constant gave a lower dynamic separation when comparing against the same translational mismatch and cup inclination angle applied with a 100 and 200 N/mm spring constant for different conditions. This was due to the higher force that was exerted by the stiffer spring, resulting in a higher dynamic separation.

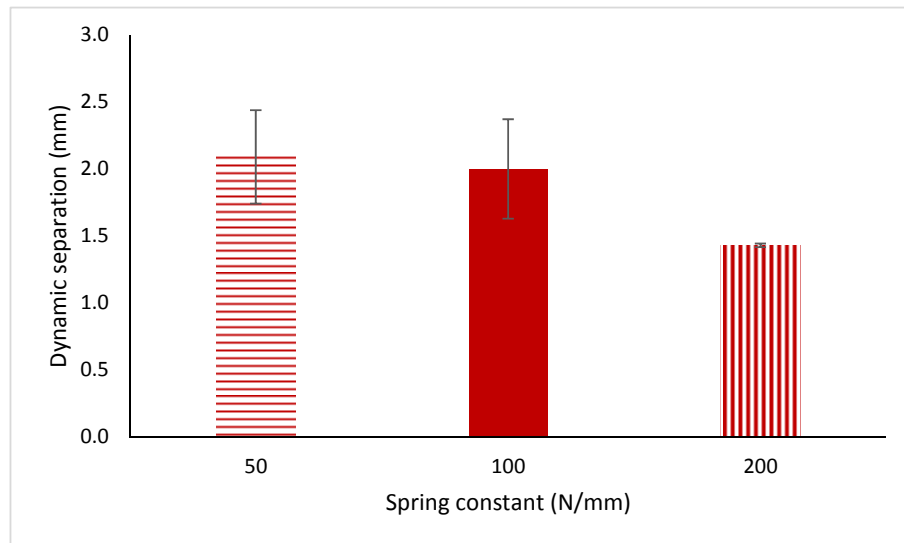


Figure 5-30. Mean (n=3, ±95% CI) dynamic separation for 36 mm ceramic-on-ceramic (BIOLOX® delta) bearings under a 4 mm translational mismatch with a cup inclination angle of 65° and a swing phase load of 70 N for three spring constants (50, 100 and 200 N/mm) conditions.

5.7.2. Wear correlations

Previously, in Chapter 3.6, the wear rate for a 100 N/mm under a translational mismatch of 4 mm and a cup inclination angle of 65° with a swing phase load of 70 N indicated to be the highest wear rate ($1.01 \pm 0.17 \text{ mm}^3/10^6 \text{ cycles}$) condition. The wear rate for the conditions tested under a 50 N/mm spring constant was not found to be significantly different to 100 N/mm ($p=0.06$), however the wear rate for the conditions tested under a 200 N/mm spring constant was found statistically different ($p=0.02$) to the 100 N/mm (Figure 5-31). While the 50 N/mm spring constant was just short of being significant to the 100 N/mm spring constant, there was a larger variation observed on the wear rate of the 50 N/mm compared to the 100 N/mm spring constant. This increased variation was due to the large wear rate of two samples (samples #3 and #4) which exhibited interrupted relocation and higher wear rates (approximately $1.00 \text{ mm}^3/10^6 \text{ cycles}$), whereas the rest of the samples had lower wear rate (approximately $0.50 \text{ mm}^3/10^6 \text{ cycles}$).

Surprisingly the wear rate for the 200 N/mm spring constant conditions was lower than the 100 N/mm. The wear rate decreased after the first million cycles. The decrease in wear rate could potentially be due to a decrease in severity as with increasing number of cycles the demand on the equipment was thought to be too high and it was not able to maintain the input peak loads. The peak loads decreased from 3000 to 2500 N. Furthermore, during the wear tests of the 200 N/mm spring constant, the cup holder displacement was found in some cases to operate with a displacement of 0.5 mm. This low displacement is not in line with the approximate range expected from the biomechanical study in Phase 1. The lower displacement may be an indication of high bending of the cup holder thus not aligning with the expected results from the biomechanical studies.

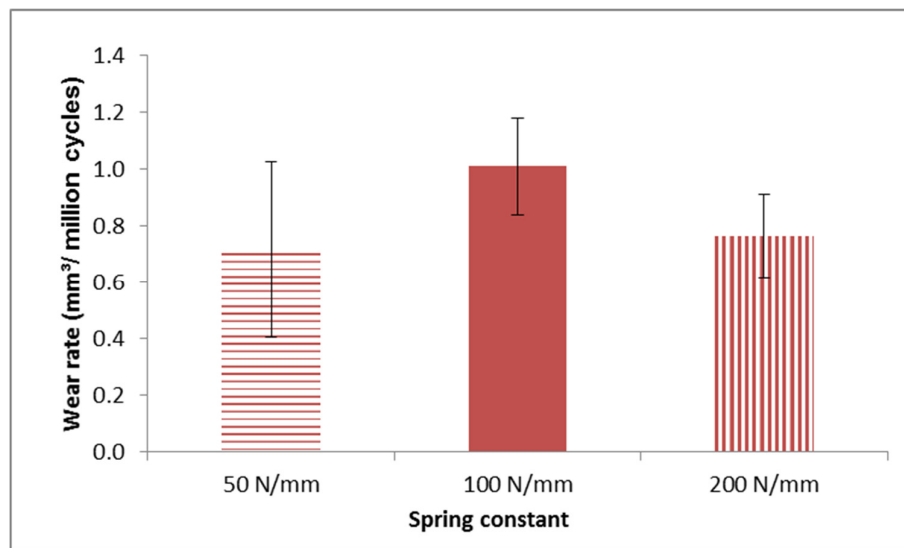


Figure 5-31. Mean ($n=6$, $\pm 95\%$ CI) wear rates 36 mm ceramic-on-ceramic (BIOLOX® delta) bearings under a 4 mm translational mismatch with a cup inclination angle of 65° for three spring constants (50, 100 and 200 N/mm) conditions.

The Phase 1 biomechanical study for different translational mismatches, cup inclination angles, swing phase loads and different spring constants gave an indication of the test conditions however not all scenarios correlated well. Based on three samples, the 200 N/mm wear test conditions (4 mm, 65°, and 70 N) gave a very small variation which was only consistent with the maximum force under edge loading (Phase 2 of the biomechanical study, n=6), but not the wear data variability. The increase in dynamic separation was found to correlate ($R^2=0.74$) with an increase in the wear rate (Figure 5-32). This holds true for all conditions tested under a translational mismatch, as the increase in separation was mainly affected by the increase in translational mismatch. Secondly, the larger the separation, the longer the head was in contact with the rim hence increased magnitude of load and severity. However, this assumption cannot hold true for all conditions, specifically when relating to clinical scenarios as demonstrated that the severity of edge loading correlation where the amount of force and duration play a role relating to the amount of wear. Furthermore, the condition termed as interrupted relocation does not particularly equate to a large dynamic separation, which skews the data correlation between dynamic separation and wear. The tests conditions under an interrupted relocation affect the wear due to the time spent under edge loading rather than the magnitude of the separation. The test conditions without interrupted relocation may indicate a linear relationship rather than an exponential curve.

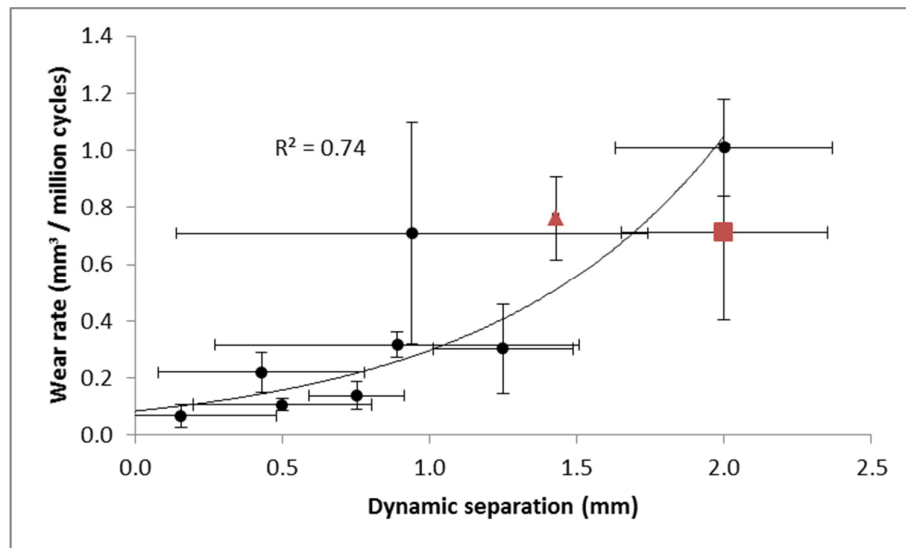


Figure 5-32. Mean ($n=3$, $\pm 95\%$ CI) dynamic separation against mean ($n=6$, $\pm 95\%$ CI) wear rate for 36 mm ceramic-on-ceramic (BIOLOX® delta) bearings under 100 N/mm spring constant with a 2, 3 and 4 mm translational mismatches with a cup inclination angle of 45° and 65° under 70 N swing phase load, and 4 mm translational mismatch with a cup inclination angle of 65° under 150 and 300 N (black circles), and 50 N/mm (red triangle) and 200 N/mm (red square) spring constants under a 4 mm translational mismatch and 65° cup inclination angle.

The severity of edge loading from the Phase 2 biomechanical study (n=6) under a 200 N/mm wear test condition (4 mm, 65°, and 70 N) gave a good representation of the variability between the stations. In some instances interrupted relocation was not observed. The same applies for the 50 N/mm spring constant test condition. A good correlation ($R^2=0.90$) was found between the severity of edge loading and the wear rate for all the conditions tested in this study (Chapter 3, 4 and 5) shown in Figure 5-33. Both 50 and 200 N/mm spring constant wear test conditions exhibited a large duration of edge loading and experienced high forces while the head was in contact with the rim which resulted in high severity of edge loading (greater than 400 Ns) and high wear.

The surface roughness within the wear stripe increased compared to the areas of the head that are not in contact with the rim. This is in alignment to the disruption of the surface and indicating the surface is wearing. The differences between the 50 and 200 N/mm spring constants surface roughness is unknown, however the point used to take the trace may have influenced the results.

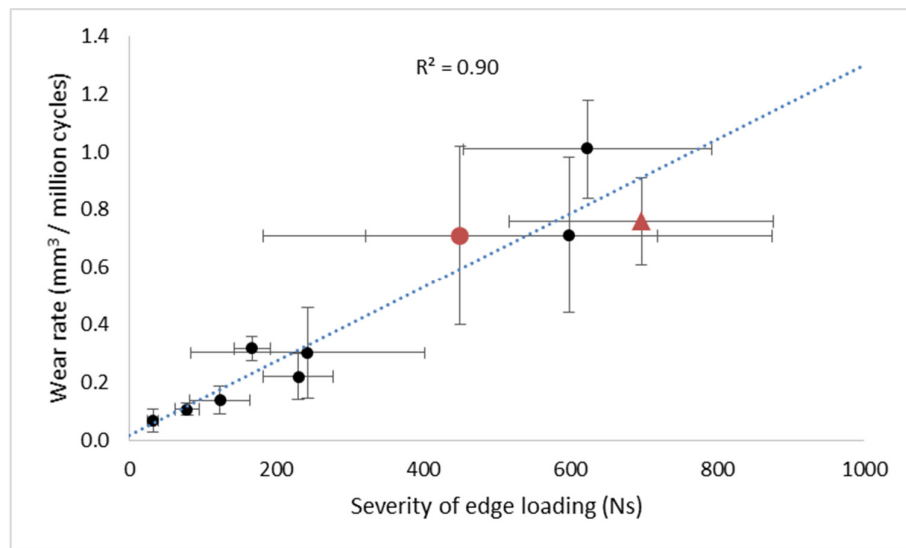


Figure 5-33. Mean (n=6, $\pm 95\%$ CI) severity of edge loading against mean (n=6, $\pm 95\%$ CI) wear rate for 36 mm ceramic-on-ceramic (BIOLOX® delta) bearings under 100 N/mm spring constant with a 2, 3 and 4 mm translational mismatch with a cup inclination angle of 45° and 65° under 70 N swing phase load, and 4 mm translational mismatch with a cup inclination angle of 65° under 150 and 300 N (black circles), and 50 N/mm (red circle) and 200 N/mm (red triangle) spring constants under a 4 mm translational mismatch and 65° cup inclination angle.

5.7.3. Separation ratio and threshold

When evaluating the 50, 100 and 200 N/mm spring constant for multiple conditions (i.e. different translational mismatches and swing phase loads, it was found that as the spring constant decreased, the slope between the separation ratio and dynamic separation increased (Figure 5-34). Meaning a larger translational mismatch would be required for a 200 N/mm spring constant to have the same dynamic separation for that of a 50 N/mm.

Theoretically, by incorporating the same inputs leading to a specific separation ratio, the outputs should be equivalent. However, that was not the case as different slopes were found with different spring constant between the separation ratio and dynamic separation. This was thought to be due to the different response the springs have in practice when employed to generate a force on the cup holder. For example, a test condition under a 4 mm translational mismatch for 200 N/mm equates to 800 N, whereas the medial-lateral load cell only recorded a maximum load of 400 N.

Increasing the spring constant for the same translational mismatch should increase the medial-lateral force as described in Hooke's Law, however in the experimental set-up the force didn't increase linearly and a considerable amount of force was 'lost' by tilting the cup holder.

A more realistic separation ratio can be obtained if the actual output medial-lateral force is used to correlate against the dynamic separation. These values can serve as a comparison between different equipment as the friction, cell stiffness and linear-bearing design manufactured can produce different results.

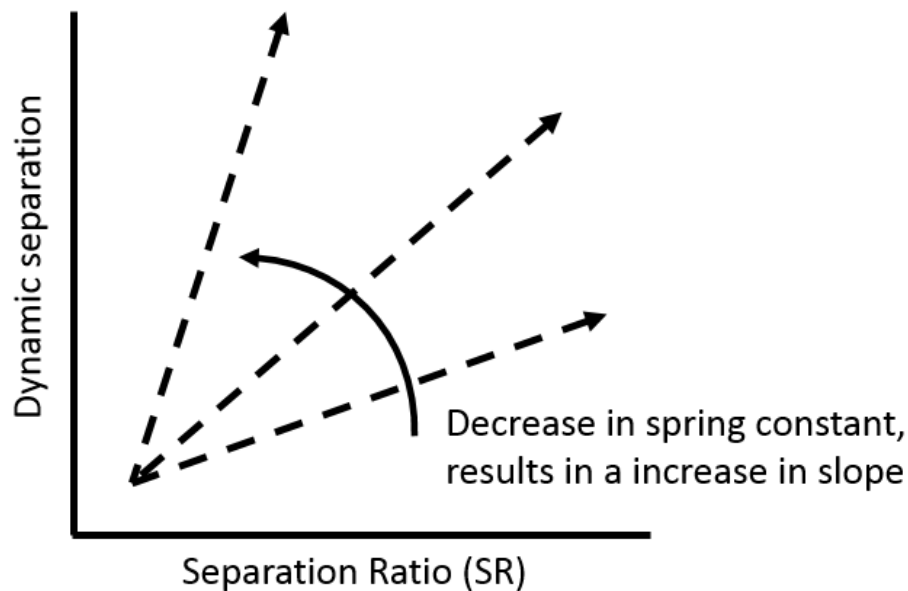


Figure 5-34. Schematic to describe the overall effect between the dynamic separation and separation ratio relationship for different spring constants and different input conditions.

The separation threshold results were not the same for different spring constants. Overall, when evaluating the separation threshold for different springs, it was found that as the spring constant increased, the separation threshold point decreased (Figure 5-35).

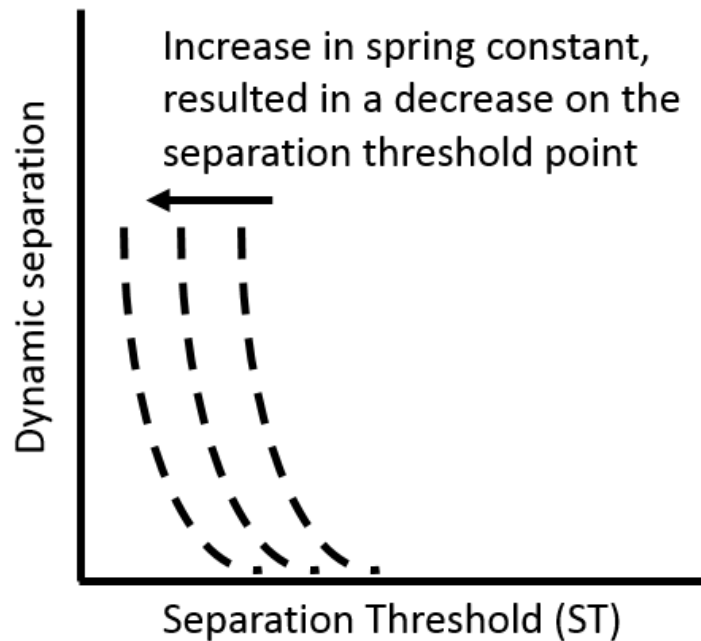


Figure 5-35. Schematic to describe the overall effect between the dynamic separation and separation threshold relationship for different spring constants and different input conditions.

5.7.4. Type of edge loading

All the three wear conditions evaluated in this chapter (50, 100 and 200 N/mm) had an incidence of interrupted relocation for at least one sample of each separate cohort. The Phase 2 biomechanical study indicated the prevalence of interrupted relocation by the level of severity of edge loading. The wear studies confirmed that interrupted relocation occurred by having a deeper scar on the right hand side of the heads. However not all samples tested in the biomechanical and wear studies demonstrated interrupted relocation or consistently through every cycle. The biomechanical study (Phase 2) results under a 50 N/mm spring constant with a translational mismatch of 4 mm, a cup inclination of 65° and a swing phase load of 70 N gave three samples which did not have interrupted relocation. This variation matched well with results from the wear study where the incidence of interrupted relocation was found in two samples based on the location of the deepest point of the scar. If the results from the biomechanical studies (Phase 2) under a 50 N/mm spring constant are split between the conditions of interrupted relocation and those that do not indicate interrupted relocation and correlated along the wear samples with interrupted relocation, a good agreement ($R^2=0.90$) is found (Figure 5-36).

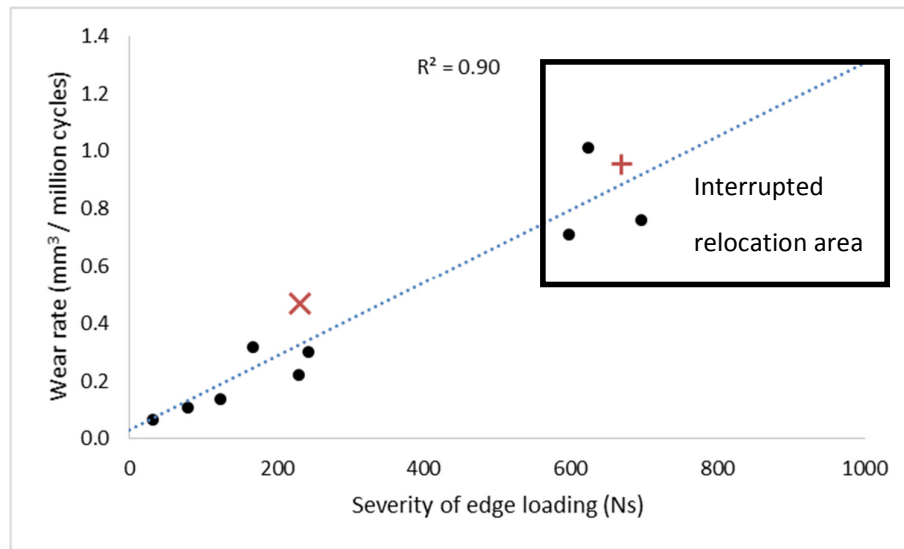


Figure 5-36. Mean ($n=6$, $\pm 95\%$ CI) severity of edge loading against mean ($n=6$, $\pm 95\%$ CI) wear rate for 36 mm ceramic-on-ceramic (BIOLOX® delta) bearings adapted from Figure 5-33 were the 50 N/mm spring constant under a 4 mm translational mismatch, a cup inclination angle of 65° with a swing phase load of 70 N is split with interrupted relocation (red '+') and with-out interrupted relocation (red 'x'). All other conditions from Figure 5-33 remain the same (black circles).

5.7.5. Limitations

The representation of *in vivo* dynamic separation generated by a spring in a hip joint simulator has some limitations. The magnitude of soft tissue tension in a patient with a hip joint replacement when there is and when there isn't a translational mismatch between the centre of the cup and the centre of the head is not known. The input hip joint kinematics affect the output of the dynamic separation as demonstrated by the different levels of swing phase loads (Chapter 4) and, effectively the dynamic separation only occurs during the swing phase load of the cycle as that is the point the spring can decompress. Furthermore, during an activity the muscles are activated which generated forces that are not accounted in this *in vitro* test model and cannot be represented by a spring.

There is uncertainty when measuring the severity of edge loading while interrupted relocation is exhibited, as under these conditions it is more difficult to conclude the point where the cup is relatively concentric with the head based on measuring with one axis. The LVDT provides an estimation, however with the interrupted relocation the high loads (from force profile while under the twin peak of 3000 N) can change the value of the severity of edge loading significantly if another point is selected as the point defined as the assembly point and the end of the separation between centres of the head and the cup.

The results are influenced by the input load profile conditions. When the inputs are changed to a swing phase load of less than 300 N, for example a 70 N swing phase load, the load response changes and the decrease in load rate is much slower. This can potentially affect the result in the sense of the

time the severity of edge loading starts which is dependent on the minimum swing phase load. Refer to Figure 4-28 in Chapter 4.7.6.

While the biomechanical studies give an indication of the results, the short tests could show dissimilarities when applying millions of cycles. A better evaluation is to input the severity of edge loading from the actual wear tests into the model to more accurately compare other tests conditions. However currently it is not possible with this equipment to accurately measure all the outputs.

The spring as a physical unit can only react to the system around it and does not represent the complexity of a hip joint replacement with a translational mismatch (offset deficiency).

5.8. Conclusion

While the spring stiffness study does not show a representation of differences of *in vivo* scenarios for different levels of translational mismatches, it has informed the practicality of using springs and how the forces applied due to a translational mismatch affect not only the samples under investigation but the system on which they are placed i.e. the cup holder, the bearings on which the test cell moves, which led to different test conditions.

The 50 and 200 N/mm spring constant did not alter the combined effect of the translational mismatch and cup inclination angle as it resulted in the same pattern as that of the 100 N/mm spring constant conditions. However, the 200 N/mm spring constant was found too stiff and much of the force was distributed away from the test samples and not in alignment with the intended purpose.

The severity of edge loading indicated high wear due to the interrupted relocation conditions and this was comparable to the 100 N/mm spring constant test condition. The wear under a 50 and 200 N/mm spring constant was of the same range as that of the 100 N/mm spring constant under the same translational mismatch, cup inclination angle and swing phase load.

There was no clear correlation between increasing the spring constant and wear.

6. Discussion and conclusion

6.1. Summary

Retrieval studies indicate that stripe wear due to edge loading is still occurring on the new generation of ceramic (BIOLOX® delta) bearings (Affatato *et al.*, 2012, Brandt *et al.*, 2013), indicating that edge loading is not specific to a type of material. Edge loading is multifactorial and among retrievals studies edge loading is thought to occur due to impingement (Dorlot *et al.*, 1989) and without impingement (Esposito *et al.*, 2012).

The testing of hip joint replacement bearings under a high cup inclination angle alone does not replicate the *in vivo* condition and does not produce the stripe wear as found on retrievals due to the approach and design of most hip joint simulators which maintain the contact area between the femoral head and acetabular cup in the bearing surface (Nevelos *et al.*, 2001). In order to replicate edge loading, the contact area between the components needs to migrate away from the bearing surface such that the head contacts the rim of the cup. This led to the development of a methodology with the current hip simulator (Leeds Mark II) to allow a medial-lateral displacement of the cup during a test profile (Nevelos *et al.*, 2000) with relevant displacements as found in clinical studies (Lombardi *et al.*, 2000) termed microseparation.

Clinical studies indicate variability in the surgical delivery (cup inclination angle) and different patient activities leading to different conditions (Callanan *et al.*, 2011 and Bergmann *et al.*, 2001). A high cup inclination angle was identified as one of the parameters leading to a higher occurrence of edge loading and higher wear. However, previous testing carried out at different cup inclination angles were not able to differentiate the influence of cup inclination angle on the wear when tested under a controlled dynamic microseparation (Nevelos *et al.*, 2001 and Al-Hajjar *et al.*, 2013). The variability in surgical implantation relating the position of the cup in the pelvis and the position of the implanted head in the femur for a total hip joint replacement is thought to be a potential factor which influences the occurrence of edge loading. Thus, a translational mismatch (offset deficiency) could influence the level of dynamic separation or occurrence of edge loading for an activity.

The methodology in this work applies a translational mismatch as an input, and the results indicate the influence of the magnitude of the *in vitro* medial-lateral translational mismatch on the output dynamic separation. With the increased translational mismatch the dynamic separation increased due to the magnitude of the medial-lateral load applied during axial loading. The boundary conditions used in this methodology differ from that of a fixed dynamic separation, and by using the translational mismatch as a fixed control input, it was possible to determine the influence of the cup

inclination angle for a specific translational mismatch. The lower cup inclination angle provided a greater resistance to dynamic separation in the medial-lateral plane (Figure 6-1). Furthermore, another factor found to influence the results was the swing phase load. Increasing the swing phase load decreased the magnitude of the dynamic separation due to the increased resistance on the cup to translate away.

All wear studies presented here resulted with a stripe wear on the head due to edge loading. Higher wear rates occurred due to edge loading when compared to standard conditions (Al-Hajjar *et al.*, 2013). However the magnitude of the wear was dependent on the input parameters.



Figure 6-1. Schematic demonstrating a higher dynamic separation under the same translational mismatch for a low (A) and high (B) cup inclination angle.

While the translational mismatch, cup inclination angle and swing phase load were found to be input parameters which influenced the results when studied in isolation *in vitro*, *in vivo*, it is unclear what specific or combination of factors influence the dynamic separation for all the cases documented in the literature.

The influence of the soft tissue tension and magnitude of loading experienced between the bearing components during edge loading are still unknown. Modifying the magnitude of the force delivered with different spring constants indicated to influence the results. The increase in spring stiffness under a high translational mismatch increased the level of bending on the system, and it does not elaborate on the *in vivo* scenarios for different patients exhibiting different conditions. The spring used to deliver a force remains as a limitation in the model as it is a physical unit not capable to comply with the complexity of an activity and patient variability. The spring for this activity can only change the contact area while under a high swing phase load, or apply a dynamic separation during a low swing phase load of the walking cycle as a response to the compression of the spring (Figure 6-2).

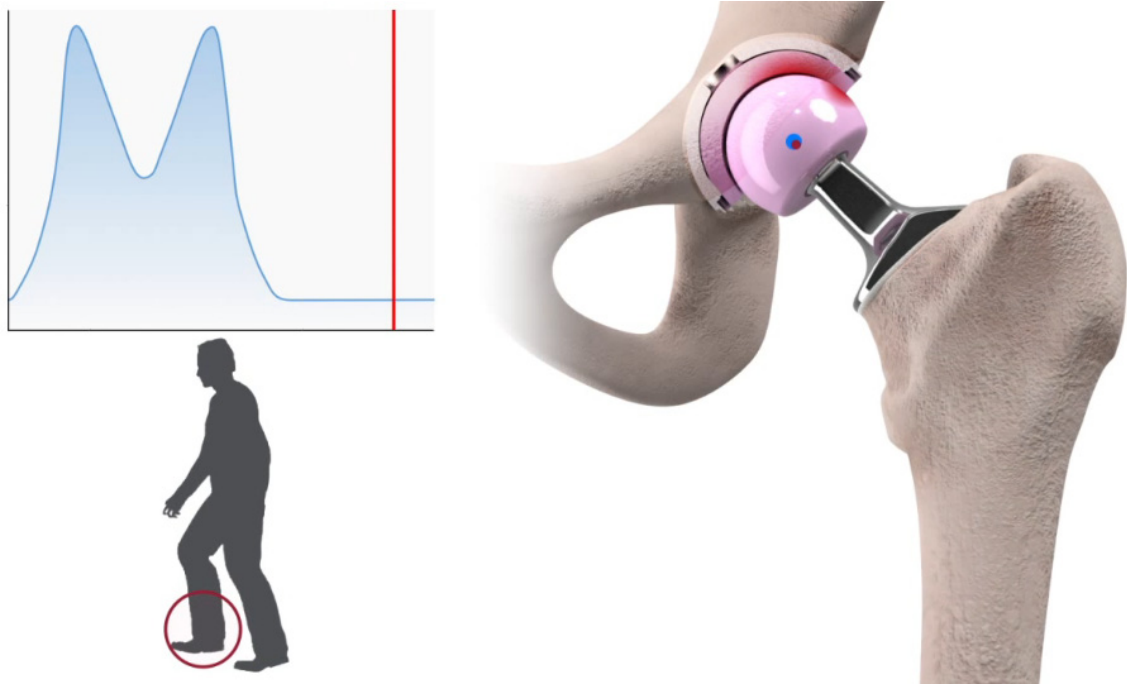


Figure 6-2. Schematic demonstrating dynamic separation occurring during the swing phase load of the walking cycle, leading to edge loading conditions in the hip joint simulator.

The wear of ceramic-on-ceramic under a translational mismatch was influenced by the magnitude of dynamic separation, and the time and force under edge loading. The larger the dynamic separation, the longer it takes the cup to return back to the head centre leading to a higher axial force acting during edge loading. The increase in magnitude of dynamic separation correlated positively with an increase in wear. However, the time and magnitude of the force under edge loading also affected the wear as described by the severity of edge loading where the combined axial and media-lateral force are evaluated for the time the head is in contact with the rim of the cup. Thus a higher severity of edge loading condition led to a higher wear rate when evaluated for different translational mismatches, cup inclination angles, swing phase load and spring constants (Figure 6-3).

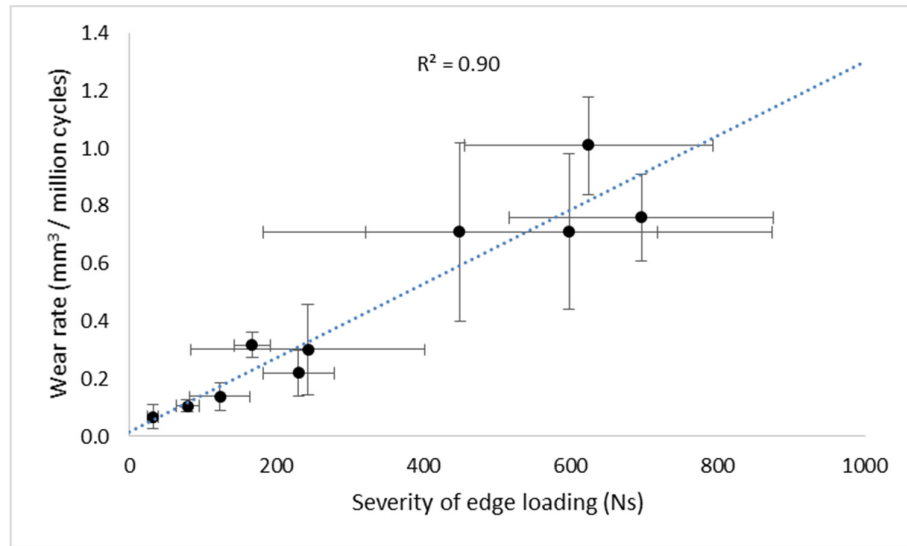


Figure 6-3. Mean ($n=6$, $\pm 95\%$ CI) severity of edge loading against mean ($n=6$, $\pm 95\%$ CI) wear rate for 36 mm ceramic-on-ceramic (BIOLOX[®] delta) bearings under different translational mismatches (2, 3 and 4 mm) for different cup inclination angles (45° and 65°) under 100 N/mm spring constant along with two different swing phase load (150 and 300 N) conditions (tested under 4 mm, 65° and 100 N/mm), and two different spring constants (50 and 200 N/mm) conditions (tested under 4 mm, 65° and 70 N).

6.2. Conclusion

A methodology was developed to evaluate the individual and combined performance of different clinical scenarios under a translational mismatch leading to edge loading conditions. These different parameters can include; cup inclination, version angle, head size, cup design, etc. The analysis and evaluation in the biomechanical studies provided useful information to determine the bearing performance and assess the worst case scenario under edge loading conditions without the need to evaluate all the possible wear test conditions leading increased time and cost. This method can be used as a pre-clinical testing technique to better predict the efficacy and reliability of hip joint replacements.

This study demonstrated how the boundary conditions associated with the test method (i.e. edge loading) alters the behaviour and results. When a translational mismatch was used as an input parameter, the conditions under a lower cup inclination angle (45°) resulted in significantly lower wear due to the greater resistance to dynamic separation and reduced severity of edge loading.

The swing phase load affected the occurrence and magnitude of the dynamic separation. Increasing the swing phase load led to a lower dynamic separation and reduced the severity of edge loading leading to significantly lower wear for a 65° cup inclination angle under a 4 mm translational mismatch and 100 N/mm spring constant.

Overall, the different spring constants affected the dynamic separation and severity of edge loading. However under a large translational mismatch with a steep cup inclination angle and a low swing phase load, the severity of edge loading was of similar magnitude, and similar test conditions were exhibited for different spring constants, all resulting in high wear rates.

All conditions tested under edge loading increased the wear rate compared to standard conditions.

The increase in dynamic separation and maximum force at the rim correlated positively with an increase in wear. However the test conditions in these studies elaborated on how the duration and force under edge loading contributed to the wear. The severity of edge loading was found to positively correlate with the increase in wear.

These studies created a foundation for analysing the occurrence and severity of edge loading in a hip joint simulator for different testing parameters that can be utilised for the development of ISO standards.

6.3. Future work

The results from these studies elaborated on the boundary conditions in the hip joint simulator for edge loading and the differences it can cause. The model used to replicate edge loading is based on a spring response and while it aids evaluating the tribological performance under edge loading, it has limitations on how much it can be used or stretched to replicate different conditions. Thus, future research could be addressed by:

Using equipment with higher capabilities to control individual stations to decrease variability and measure more accurately could help improve the model.

One future study could investigate how does the magnitude and profile of the joint reaction force influences the occurrence and severity of edge loading. These studies focused on using one loading profile that does not encompass the variability found clinically, and the different magnitude of forces under edge loading were found to influence the wear. Moreover, the loading and direction can affect the severity of edge loading thus other cases may be found as higher risk or worst case scenario.

It is also worth considering evaluating what is the effect of the pelvic rotation on the occurrence and severity of edge loading. This study used a hip simulator to mimic a walking cycle. However it does not incorporate any pelvic rotation as it does not have the capability to do so. This study indicated how the cup inclination angle affected dynamic separation and the severity of edge loading. Other activities where the pelvic tilt influences the occurrence and severity of edge loading could be explored to determine its effects and risk associated with increased wear.

Another future study could investigate what is the *in vivo* contribution of the soft tissue tension in hip joint replacements and how different activities influence the occurrence and severity of edge loading. One of the main limitations of this study is not knowing the resultant force between the head and the cup after implantation. This resultant force would be dependent on the magnitude and direction of the mismatch. These studies have demonstrated that using different spring constants is not an adequate approach which can elaborate on the soft tissue tension when considering a translational mismatch as an input condition which leads to edge loading.

The current work has elaborated on the ceramic wear, however ceramics are not the only materials used for THR. Further studies could be carried out on polymer materials and the results from those studies can increase the knowledge on the thickness and fatigue limit under edge loading conditions.

The points mentioned above can include a similar style of testing where short biomechanical studies with different input conditions can be employed in order to determine correlations between the wear.

7. Publications and abstracts

Accepted publication:

Journal of Biomedical Materials Research. Part B.

- O'Dwyer *et al.*, 2017, An *in vitro* simulation model to assess the severity of edge loading and wear, due to variations in component positioning in hip joint replacements

Abstracts:

Orthopaedics Research Society.

- O'Dwyer *et al.*, 2015, Different levels of Rotational and Translational Surgical Mal-Positioning Affects the Occurrence and Severity of Edge Loading and Wear in Total Hip Replacements
- O'Dwyer *et al.*, 2016, The Combined Effect of Head and Cup Centres Mismatch and Different Cup Inclination Angles on the Occurrence and Severity of Edge Loading and Wear in Hip Replacement
- O'Dwyer *et al.*, 2017, The Effect of the Swing Phase Load Under Head and Cup Centre Mismatch on the Severity of Edge Loading and Wear of Ceramic-on-ceramic Hip Joint Replacements

International Society of Biomechanics.

- O'Dwyer *et al.*, 2015, Surgical Translational Malposition Affects the Level of the Dynamic Microseparation, the Severity of Edge Loading and the Wear in Total Hip Replacements

European Orthopaedic Research Society.

- O'Dwyer *et al.*, 2015, Effect of Hip Implant Positioning on Edge-Loading Occurrence and Severity

Institute of Mechanical Engineers, Hip Surgery: A Joint Engineering and Surgical Challenge.

- O'Dwyer *et al.*, 2015, Surgical Medial-Lateral Translational Positioning Affects the Level of the Dynamic Microseparation, the Severity of Edge Loading and the Wear in Total Hip Replacements

International Society of Technology in Arthroplasty.

- O'Dwyer *et al.*, 2015, The Influence of Surgical Positioning on the Severity of Edge Loading, and Wear Rate in Total Hip Replacement
- O'Dwyer *et al.*, 2016, Edge Loading Wear Prediction of Hip Joint Simulators Under Head and Cup Centre Mismatch
- O'Dwyer *et al.*, 2016, The Effect of Swing Phase Load on the Occurrence and Severity of Edge Loading in Ceramic-on-ceramic Total Hip Replacement

8. References

- Affatato, S., Bersaglia, G., Foltran, I., Emiliani, D., Traina, F. and Toni, A. 2004. The influence of implant position on the wear of alumina-on-alumina studied in a hip simulator. *Wear*. **256**(3),pp.400–405.
- Affatato, S., Leardini, W., Jedenmalm, A., Ruggeri, O. and Toni, A. 2006. Larger diameter bearings reduce wear in metal-on-metal hip implants. *Clinical orthopaedics and related research*. **456**,pp.153–8.
- Affatato, S., Modena, E., Toni, A. and Taddei, P. 2012. Retrieval analysis of three generations of BioloX® femoral heads: Spectroscopic and SEM characterisation. *Journal of the Mechanical Behavior of Biomedical Materials*. **13**,pp.118–128.
- Al-Hajjar, M., Fisher, J., Tipper, J., Williams, S. and Jennings, L. 2012. Wear of Ceramic-on-ceramic Bearings in THRs: Effect of Head Size Under Steep Cup Inclination Angle and Microseparation and Edge Loading Conditions. *Journal of Bone & Joint Surgery, British Volume*. **94-B**(SUPP XL),p.1.
- Al-Hajjar, M., Fisher, J., Tipper, J.L., Williams, S. and Jennings, L.M. 2013. Wear of 36-mm BIOLOX(R) delta ceramic-on-ceramic bearing in total hip replacements under edge loading conditions. *Proceedings of the Institution of Mechanical Engineers. Part H, Journal of engineering in medicine*. **227**(5),pp.535–42.
- Al-Hajjar, M., Fisher, J., Williams, S., Tipper, J.L. and Jennings, L.M. 2012. Effect of femoral head size on the wear of metal on metal bearings in total hip replacements under adverse edge-loading conditions. *Journal of biomedical materials research. Part B, Applied biomaterials*. **101**(2),pp.213–22.
- Al-Hajjar, M., Jennings, L.M., Begand, S., Oberbach, T., Delfosse, D. and Fisher, J. 2013. Wear of novel ceramic-on-ceramic bearings under adverse and clinically relevant hip simulator conditions. *Journal of biomedical materials research. Part B, Applied biomaterials*.,pp.1–7.
- Al-Hajjar, M., Leslie, I.J., Tipper, J., Williams, S., Fisher, J. and Jennings, L.M. 2010. Effect of cup inclination angle during microseparation and rim loading on the wear of BIOLOX® delta ceramic-on-ceramic total hip replacement. *Journal of biomedical materials research. Part B, Applied biomaterials*. **95**(2),pp.263–8.
- Al-Hajjar, M., Silvia, C., Sophie, W., Louise M, J. and John, F. 2014. Effect of Acetabular Cup Version Angle on the Wear of BIOLOX® Delta Ceramic-on-ceramic Bearings under standard and Edge Loading Conditions *In: Orthopaedic Research Society*.
- Amadò, R., Werner, G. and Neukom, H. 1976. Water content of human articular cartilage and its determination by gas chromatography. *Biochemical Medicine*. **16**(2),pp.169–172.
- Angadji, A., Royle, M., Collins, S.N. and Shelton, J.C. 2009. Influence of cup orientation on the wear performance of metal-on-metal hip replacements. *Proceedings of the Institution of Mechanical Engineers. Part H, Journal of engineering in medicine*. **223**(4),pp.449–57.

- Van Arkel, R.J., Amis, A.A., Cobb, J.P. and Jeffers, J.R.T. 2015. The capsular ligaments provide more hip rotational restraint than the acetabular labrum and the ligamentum teres : an experimental study. *The bone & joint journal*. **97-B**(4),pp.484–91.
- Armfield, A. and Towers, J. 2007. Radiographic Evaluation of the Hip *In: J. Callaghan, A. Rosenberg and H. Rubash, eds. The Adult Hip*. Philadelphia: Lippincott Williams & Wilkins, pp. 349–391.
- Barbour, P.S.M., Stone, M.H. and Fisher, J. 1999. A hip joint simulator study using simplified loading and motion cycles generating physiological wear paths and rates. *Proceedings of the Institution of Mechanical Engineers, Part H: Journal of Engineering in Medicine*. **213**(6),pp.455–467.
- Barrack, R.L., Stephen, R. and Burnett, J. 2007. Preoperative Planning *In: J. Callaghan, A. Rosenberg and H. Rubash, eds. The Adult Hip*. Philadelphia: Lippincott Williams & Wilkins, pp. 884–910.
- Bennett, D., Humphreys, L., O'Brien, S., Kelly, C., Orr, J.F. and Beverland, D.E. 2008. Gait kinematics of age-stratified hip replacement patients—a large scale, long-term follow-up study. *Gait & posture*. **28**(2),pp.194–200.
- Bergmann, G., Deuretzbacher, G., Heller, M., Graichen, F., Rohlmann, A., Strauss, J. and Duda, G.. 2001. Hip contact forces and gait patterns from routine activities. *Journal of Biomechanics*. **34**(7),pp.859–871.
- Bigsby, R.J. a, Hardaker, C.S. and Fisher, J. 1997. Wear of ultra-high molecular weight polyethylene acetabular cups in a physiological hip joint simulator in the anatomical position using bovine serum as a lubricant. *Proceedings of the Institution of Mechanical Engineers, Part H: Journal of Engineering in Medicine*. **211**(3),pp.265–269.
- Black, J., Levine, B. and Jacobs, J. 2007. Biomaterials Overview *In: J. Callaghan, A. Rosenberg and H. Rubash, eds. The Adult Hip*. Philadelphia: Lippincott Williams & Wilkins, pp. 102–111.
- Boutin, P. 1971. Arthroplastie totale de la hanche par prothèse en alumine frittée. Étude expérimentale et premières applications cliniques. *Revue de chirurgie orthopédique et réparatrice de l'appareil moteur*. **58**(3),pp.229–46.
- Boutin, P., Christel, P., Dorlot, J.M., Meunier, A., de Roquancourt, A., Blanquaert, D., Herman, S., Sedel, L. and Witvoet, J. 1988. The use of dense alumina-alumina ceramic combination in total hip replacement. *Journal of biomedical materials research*. **22**(12),pp.1203–32.
- Bowsher, J.G. and Shelton, J.. 2001. A hip simulator study of the influence of patient activity level on the wear of crosslinked polyethylene under smooth and roughened femoral conditions. *Wear*. **250**(1-12),pp.167–179.
- Brandt, J.-M., Gascoyne, T.C., Guenther, L.E., Allen, A., Hedden, D.R., Turgeon, T.R. and Bohm, E.R. 2013. Clinical failure analysis of contemporary ceramic-on-ceramic total hip replacements. *Proceedings of the Institution of Mechanical Engineers. Part H, Journal of engineering in medicine*. **227**(8),pp.833–46.
- Brockett, C., Williams, S., Jin, Z., Isaac, G. and Fisher, J. 2007. Friction of Total Hip Replacements With Different Bearings and Loading Conditions. *Journal of biomedical materials research. Part B, Applied biomaterials*. (81B),pp.508–515.

- Brockett, C.L., Williams, S., Jin, Z., Isaac, G.H. and Fisher, J. 2013. Squeaking Hip Arthroplasties: A Tribological Phenomenon. *The Journal of Arthroplasty*. **28**(1),pp.90–97.
- Buechel, F.F. and Pappas, M.J. 2012. *Principles of Human Joint Replacement*. Berlin, Heidelberg: Springer Berlin Heidelberg.
- Callaghan, J., Rosenberg, A. and Rubash, H. 2007. *The Adult hip* 2nd Editio. Lippincott Williams & Wilkins.
- Callanan, M.C., Jarrett, B., Bragdon, C.R., Zurakowski, D., Rubash, H.E., Freiberg, A.A. and Malchau, H. 2011. The John Charnley Award: risk factors for cup malpositioning: quality improvement through a joint registry at a tertiary hospital. *Clinical orthopaedics and related research*. **469**(2),pp.319–29.
- Campbell, P., Beaulé, P.E., Ebramzadeh, E., Le Duff, M.J., LeDuff, M., De Smet, K., Lu, Z. and Amstutz, H.C. 2006. The John Charnley Award: a study of implant failure in metal-on-metal surface arthroplasties. *Clinical orthopaedics and related research*. **453**,pp.35–46.
- CeramTec 2014. *BIOLOX®delta – Nanocomposite for Arthroplasty - The Fourth Generation of Ceramics - Scientific Information and Performance Data*.
- Chan, F.W., Bobyn, J.D., Medley, J.B., Krygier, J.J. and Tanzer, M. 1999. The Otto Aufranc Award. Wear and lubrication of metal-on-metal hip implants. *Clinical orthopaedics and related research*. (369),pp.10–24.
- Charnley, J. 1961. ARTHROPLASTY OF THE HIP A New Operation. *The Lancet*. **277**(7187),pp.1129–1132.
- Clarke, I.C., Gustafson, A., Jung, H. and Fujisawa, A. 1996. Hip-simulator ranking of polyethylene wear: comparisons between ceramic heads of different sizes. *Acta orthopaedica Scandinavica*. **67**(2),pp.128–32.
- Clarke, I.C., Ludema, K.C., Shaffer, S.J., Green, D.D., Williams, P.A., Kubo, K., Pezzotti, G., Lombardi, A., Turnbull, A. and Donaldson, T.K. 2009. Hip-simulator wear studies of an alumina-matrix composite (AMC) ceramic compared to retrieval studies of AMC balls with 1–7 years follow-up. *Wear*. **267**(5),pp.702–709.
- Crowninshield, R.D., Johnston, R.C., Andrews, J.G. and Brand, R.A. 1978. A biomechanical investigation of the human hip. *Journal of Biomechanics*. **11**(1-2),pp.75–85.
- Currier, J.H., McHugh, D.J., Tower, D.R., Dini, D., Kennedy, F.E. and Van Citters, D.W. 2013. Gouge features on metal-on-metal hip bearings can result from high stresses during rim contact. *Tribology International*. **63**,pp.89–96.
- Delp, S.L. and Maloney, W. 1993. Effects of hip center location on the moment-generating capacity of the muscles. *Journal of Biomechanics*. **26**(4-5),pp.485–499.
- Dennis, D.A., Komistek, R.D., Northcut, E.J., Ochoa, J.A. and Ritchie, A. 2001. 'In vivo' determination of hip joint separation and the forces generated due to impact loading conditions. *Journal of Biomechanics*. **34**(5),pp.623–629.

- Derbyshire, B., Fisher, J., Dowson, D., Hardaker, C. and Brummitt, K. 1994. Comparative study of the wear of UHMWPE with zirconia ceramic and stainless steel femoral heads in artificial hip joints. *Medical Engineering & Physics*. **16**(3),pp.229–236.
- Digas, G., Johansson, P.-E. and Kärrholm, J. 2013. Inducible displacements of the cup and the femoral head during active range of motion: dynamic RSA studies of cemented total hip replacements. *Journal of orthopaedic research : official publication of the Orthopaedic Research Society*. **31**(11),pp.1686–93.
- Dorlot, J.M. 1992. Long-term effects of alumina components in total hip prostheses. *Clinical orthopaedics and related research*. (282),pp.47–52.
- Dorlot, J.-M., Christel, P. and Meunier, A. 1989. Wear analysis of retrieved alumina heads and sockets of hip prostheses. *Journal of Biomedical Materials Research*. **23**(S14),pp.299–310.
- Dowd, J.E., Sychterz, C.J., Young, A.M. and Engh, C.A. 2000. Characterization of long-term femoral-head-penetration rates. Association with and prediction of osteolysis. *The Journal of bone and joint surgery. American volume*. **82-A**(8),pp.1102–7.
- Dowson, D., Hardaker, C., Flett, M. and Isaac, G.H. 2004. A hip joint simulator study of the performance of metal-on-metal joints. *The Journal of Arthroplasty*. **19**(8),pp.124–130.
- Dowson, D., Longfield, M.D., Walker, P.S. and Wright, V. 1967. Paper 9: An Investigation of the Friction and Lubrication in Human Joints. *Proceedings of the Institution of Mechanical Engineers, Conference Proceedings*. **182**(14),pp.68–76.
- Dowson, D., McNie, C.M. and Goldsmith, A.A.J. 2000. Direct experimental evidence of lubrication in a metal-on-metal total hip replacement tested in a joint simulator. *Proceedings of the Institution of Mechanical Engineers, Part C: Journal of Mechanical Engineering Science*. **214**(1),pp.75–86.
- Elfick, A.P.D., Green, S.M., Krikler, S. and Unsworth, A. 2003. The nature and dissemination of UHMWPE wear debris retrieved from periprosthetic tissue of THR. *Journal of Biomedical Materials Research*. **65A**(1),pp.95–108.
- Esposito, C., Maclean, F., Campbell, P., Walter, W.L., Walter, W.K. and Bonar, S.F. 2013. Periprosthetic tissues from third generation alumina-on-alumina total hip arthroplasties. *The Journal of arthroplasty*. **28**(5),pp.860–6.
- Esposito, C., Walter, W.L., Roques, A., Tuke, M. a, Zicat, B. a, Walsh, W.R. and Walter, W.K. 2012. Wear in alumina-on-alumina ceramic total hip replacements: a retrieval analysis of edge loading. *The Journal of bone and joint surgery. British volume*. **94**(7),pp.901–7.
- Firkins, P.J., Tipper, J.L., Ingham, E., Stone, M.H., Farrar, R. and Fisher, J. 2001a. A novel low wearing differential hardness, ceramic-on-metal hip joint prosthesis. *Journal of biomechanics*. **34**(10),pp.1291–8.
- Firkins, P.J., Tipper, J.L., Ingham, E., Stone, M.H., Farrar, R. and Fisher, J. 2001b. Influence of simulator kinematics on the wear of metal-on-metal hip prostheses. *Proceedings of the Institution of Mechanical Engineers. Part H, Journal of engineering in medicine*. **215**(1),pp.119–21.

- Fisher, J. 2012. A stratified approach to pre-clinical tribological evaluation of joint replacements representing a wider range of clinical conditions advancing beyond the current standard. *Faraday Discussions*. **156**,p.59.
- Fisher, J. 2011. Bioengineering reasons for the failure of metal-on-metal hip prostheses: an engineer's perspective. *The Journal of bone and joint surgery. British volume*. **93**(8),pp.1001–4.
- Frankel, V.H. and Nordin, M. 1980. *Basic Biomechanics of the Skeletal System*. Philadelphia: Lea & Febiger.
- French, K., Moore, R., Gawel, H., Kurtz, S.M., Kraay, M.J., Xie, K., Goldberg, V.M. and Rimnac, C.M. 2012. Retrieval analysis of Harris-Galante I and II acetabular liners in situ for more than 10 years. *Acta orthopaedica*. **83**(4),pp.366–73.
- Gilbert, J. 2007. Metals *In*: J. Callaghan, A. Rosenberg and H. Rubash, eds. *The Adult Hip*. Philadelphia: Lippincott Williams & Wilkins, pp. 128–143.
- Glaser, D., Dennis, D.A., Komistek, R.D. and Miner, T.M. 2008. In vivo comparison of hip mechanics for minimally invasive versus traditional total hip arthroplasty. *Clinical Biomechanics*. **23**(2),pp.127–134.
- Glaser, D., Komistek, R.D., Cates, H.E. and Mahfouz, M.R. 2010. A non-invasive acoustic and vibration analysis technique for evaluation of hip joint conditions. *Journal of Biomechanics*. **43**(3),pp.426–432.
- Glaser, D., Komistek, R.D., Cates, H.E. and Mahfouz, M.R. 2008. Clicking and Squeaking: In Vivo Correlation of Sound and Separation for Different Bearing Surfaces. *The Journal of bone and joint surgery. American volume*. **90**,pp.112–20.
- Green, T.R., Fisher, J., Stone, M., Wroblewski, B.M. and Ingham, E. 1998. Polyethylene particles of a 'critical size' are necessary for the induction of cytokines by macrophages in vitro. *Biomaterials*. **19**(24),pp.2297–2302.
- Griss, P. and Heimke, G. 1981. Five years experience with ceramic-metal-composite hip endoprotheses. I. clinical evaluation. *Archives of orthopaedic and trauma surgery*. **98**(3),pp.157–164.
- De Haan, R., Campbell, P.A., Su, E.P. and De Smet, K.A. 2008. Revision of metal-on-metal resurfacing arthroplasty of the hip: THE INFLUENCE OF MALPOSITIONING OF THE COMPONENTS. *Journal of Bone and Joint Surgery - British Volume*. **90-B**(9),pp.1158–1163.
- Hadley, M., Hardaker, C., Isaac, G. and Fisher, J. 2014. In-vitro Wear Simulation of Diferent Materials for Total Hip Replacement under Stop-Dwel-Start Conditions *In: Orthopaedic Reasearch Sorciety*.
- Halma, J.J., Señaris, J., Delfosse, D., Lerf, R., Oberbach, T., van Gaalen, S.M. and de Gast, A. 2014. Edge loading does not increase wear rates of ceramic-on-ceramic and metal-on-polyethylene articulations. *Journal of biomedical materials research. Part B, Applied biomaterials*.

- Harris, W.H. 1978. Advances in surgical technique for total hip replacement: without and with osteotomy of the greater trochanter. *Clinical orthopaedics and related research*. (146),pp.188–204.
- Hatton, A., Nevelos, J.E., Matthews, J.B., Fisher, J. and Ingham, E. 2003. Effects of clinically relevant alumina ceramic wear particles on TNF- α production by human peripheral blood mononuclear phagocytes. *Biomaterials*. **24**(7),pp.1193–1204.
- Hatton, A., Nevelos, J.E., Nevelos, A.A., Banks, R.E., Fisher, J. and Ingham, E. 2002. Alumina–alumina artificial hip joints. Part I: a histological analysis and characterisation of wear debris by laser capture microdissection of tissues retrieved at revision. *Biomaterials*. **23**(16),pp.3429–3440.
- Hersey, M.D. 1935. A short account of the theory of lubrication. I. Introduction; viscosity and friction. *Journal of the Franklin Institute*. **219**(6),pp.677–702.
- Hua, X., Li, J., Jin, Z. and Fisher, J. 2016. The contact mechanics and occurrence of edge loading in modular metal-on-polyethylene total hip replacement during daily activities. *Medical engineering & physics*.
- Hua, X., Li, J., Wang, L., Jin, Z., Wilcox, R. and Fisher, J. 2014. Contact mechanics of modular metal-on-polyethylene total hip replacement under adverse edge loading conditions. *Journal of biomechanics*. **47**(13),pp.3303–9.
- Ingham, E. and Fisher, J. 2000. Biological reactions to wear debris in total joint replacement. *Proceedings of the Institution of Mechanical Engineers, Part H: Journal of Engineering in Medicine*. **214**(1),pp.21–37.
- Ingham, E. and Fisher, J. 2005. The role of macrophages in osteolysis of total joint replacement. *Biomaterials*. **26**(11),pp.1271–86.
- ISO14242-1 2014. Implants for surgery — Wear of total hip-joint prostheses.
- Jacobson, B. 2003. The Stribeck memorial lecture. *Tribology International*. **36**,pp.781–789.
- Jin, Z.M., Dowson, D. and Fisher, J. 1997. Analysis of fluid film lubrication in artificial hip joint replacements with surfaces of high elastic modulus. *Proceedings of the Institution of Mechanical Engineers. Part H, Journal of engineering in medicine*. **211**(3),pp.247–56.
- Jin, Z.M., Stone, M., Ingham, E. and Fisher, J. 2006. (v) Biotribology. *Current Orthopaedics*. **20**(1),pp.32–40.
- John, K. St. 2010. The Effect of Serum Protein Concentration on Wear Rates in a Hip Simulator. *Journal of Biomaterials Applications*. **25**(2),pp.145–159.
- Johnson, K.L., Greenwood, J.A. and Poon, S.Y. 1972. A simple theory of asperity contact in elastohydro-dynamic lubrication. *Wear*. **19**(1),pp.91–108.
- Kärrholm, J. 2012. Radiostereometric analysis of early implant migration - a valuable tool to ensure proper introduction of new implants. *Acta orthopaedica*. **83**(6),pp.551–2.

- Kärrholm, J., Borssén, B., Löwenhielm, G. and Snorrason, F. 1994. Does early micromotion of femoral stem prostheses matter? 4-7-year stereoradiographic follow-up of 84 cemented prostheses. *The Journal of bone and joint surgery. British volume*. **76**(6),pp.912–7.
- Kiernan, S., Hermann, K.L., Wagner, P., Ryd, L. and Flivik, G. 2013. The importance of adequate stem anteversion for rotational stability in cemented total hip replacement: a radiostereometric study with ten-year follow-up. *The bone & joint journal*. **95-B**(1),pp.23–30.
- Komistek, R.D., Dennis, D.A., Ochoa, J.A., Haas, B.D. and Hammill, C. 2002. In vivo comparison of hip separation after metal-on-metal or metal-on-polyethylene total hip arthroplasty. *The Journal of bone and joint surgery. American volume*. (84),pp.1836–41.
- Korim, M., Scholes, S., Unsworth, A. and Power, R. 2014. Retrieval analysis of alumina ceramic-on-ceramic bearing couples. *Acta orthopaedica*. **85**(2),pp.133–40.
- Kretzer, J.P., Kleinhans, J.A., Jakubowitz, E., Thomsen, M. and Heisel, C. 2009. A meta-analysis of design- and manufacturing-related parameters influencing the wear behavior of metal-on-metal hip joint replacements. *Journal of Orthopaedic Research*. **27**(11),pp.1473–1480.
- Kwon, Y.-M., Glyn-Jones, S., Simpson, D.J., Kamali, A., McLardy-Smith, P., Gill, H.S. and Murray, D.W. 2010. Analysis of wear of retrieved metal-on-metal hip resurfacing implants revised due to pseudotumours. *The Journal of bone and joint surgery. British volume*. **92**(3),pp.356–361.
- Kwon, Y.-M., Mellon, S.J., Monk, P., Murray, D.W. and Gill, H.S. 2012. In vivo evaluation of edge-loading in metal-on-metal hip resurfacing patients with pseudotumours. *Bone & joint research*. **1**(4),pp.42–9.
- Lerouge, S., Huk, O., Yahia, L., Witvoet, J. and Sedel, L. 1997. Ceramic-ceramic and metal-polyethylene total hip replacements: comparison of pseudomembranes after loosening. *The Journal of bone and joint surgery. British volume*. **79**(1),pp.135–9.
- Leslie, I., Williams, S., Brown, C., Isaac, G., Jin, Z., Ingham, E. and Fisher, J. 2008. Effect of bearing size on the long-term wear, wear debris, and ion levels of large diameter metal-on-metal hip replacements-An in vitro study. *Journal of biomedical materials research. Part B, Applied biomaterials*. **87**(1),pp.163–72.
- Leslie, I.J., Williams, S., Isaac, G., Ingham, E. and Fisher, J. 2009. High cup angle and microseparation increase the wear of hip surface replacements. *Clinical orthopaedics and related research*. **467**(9),pp.2259–65.
- Liao, Y.-S., Benya, P.D. and McKellop, H.A. 1999. Effect of protein lubrication on the wear properties of materials for prosthetic joints. *Journal of Biomedical Materials Research*. **48**(4),pp.465–473.
- Liu, F., Fisher, J. and Jin, Z. 2012. Computational modelling of polyethylene wear and creep in total hip joint replacements: Effect of the bearing clearance and diameter. *Proceedings of the Institution of Mechanical Engineers, Part J: Journal of Engineering Tribology*. **226**(6),pp.552–563.
- Liu, F., Williams, S., Jin, Z. and Fisher, J. 2013. Effect of head contact on the rim of the cup on the offset loading and torque in hip joint replacement. *Proceedings of the Institution of Mechanical Engineers. Part H, Journal of engineering in medicine*.

- Lombardi, A. V, Mallory, T.H., Dennis, D. a, Komistek, R.D., Fada, R. a and Northcut, E.J. 2000. An in vivo determination of total hip arthroplasty pistoning during activity. *The Journal of Arthroplasty*. **15**(6),pp.702–9.
- Lombardi, A. V., Berend, K.R., Seng, B.E., Clarke, I.C. and Adams, J.B. 2010. Delta Ceramic-on-Alumina Ceramic Articulation in Primary THA: Prospective, Randomized FDA-IDE Study and Retrieval Analysis. *Clinical Orthopaedics and Related Research*®. **468**(2),pp.367–374.
- Lusty, P.J., Watson, A., Tuke, M.A., Walter, W.L., Walter, W.K. and Zicat, B. 2007. Wear and acetabular component orientation in third generation alumina-on-alumina ceramic bearings: an analysis of 33 retrievals [corrected]. *The Journal of bone and joint surgery. British volume*. **89**(9),pp.1158–64.
- Mak, M.M., Besong, A.A., Jin, Z.M. and Fisher, J. 2002. Effect of microseparation on contact mechanics in ceramic-on-ceramic hip joint replacements. *Proceedings of the Institution of Mechanical Engineers, Part H: Journal of Engineering in Medicine*. **216**(6),pp.403–408.
- Manaka, M., Clarke, I.C., Yamamoto, K., Shishido, T., Gustafson, A. and Imakiire, A. 2004. Stripe wear rates in alumina THR--comparison of microseparation simulator study with retrieved implants. *Journal of biomedical materials research. Part B, Applied biomaterials*. **69**(2),pp.149–57.
- Massin, P., Lopes, R., Masson, B. and Mainard, D. 2014. Does Biolox Delta ceramic reduce the rate of component fractures in total hip replacement? *Orthopaedics & traumatology, surgery & research : OTSR*. **100**(6 Suppl),pp.S317–21.
- Matthies, A., Underwood, R., Cann, P., Ilo, K., Nawaz, Z., Skinner, J. and Hart, A.J. 2011. Retrieval analysis of 240 metal-on-metal hip components, comparing modular total hip replacement with hip resurfacing. *The Journal of bone and joint surgery. British volume*. **93**(3),pp.307–314.
- McGann, W. 2007. Surgical Approaches In: J. Callaghan, A. Rosenberg and H. Rubash, eds. *The Adult Hip*. Philadelphia: Lippincott Williams & Wilkins, pp. 683–733.
- McGrory, B.J., Morrey, B.F., Cahalan, T.D., An, K.N. and Cabanela, M.E. 1995. Effect of femoral offset on range of motion and abductor muscle strength after total hip arthroplasty. *The Journal of bone and joint surgery. British volume*. **77**(6),pp.865–9.
- McKellop, H., Clarke, I., Markolf, K. and Amstutz, H. 1981. Friction and wear properties of polymer, metal, and ceramic prosthetic joint materials evaluated on a multichannel screening device. *Journal of Biomedical Materials Research*. **15**(5),pp.619–653.
- Miki, H., Kyo, T., Kuroda, Y., Nakahara, I. and Sugano, N. 2014. Risk of edge-loading and prosthesis impingement due to posterior pelvic tilting after total hip arthroplasty. *Clinical Biomechanics*. **29**(6),pp.607–613.
- Murray, D.W. 1993. The definition and measurement of acetabular orientation. *The Journal of bone and joint surgery. British volume*. **75**(2),pp.228–32.
- Nam, K.W., Yoo, J.J., Lae Kim, Y., Kim, Y.-M., Lee, M.-H. and Kim, H.J. 2007. Alumina-debris-induced osteolysis in contemporary alumina-on-alumina total hip arthroplasty. A case report. *The Journal of bone and joint surgery. American volume*. **89**(11),pp.2499–503.

- Nevelös, A.B., Evans, P.A., Harrison, P. and Rainforth, M. 1993. Examination of alumina ceramic components from total hip arthroplasties. *Proceedings of the Institution of Mechanical Engineers. Part H, Journal of engineering in medicine*. **207**(3),pp.155–62.
- Nevelos, J., Ingham, E., Doyle, C., Streicher, R., Nevelos, A., Walter, W. and Fisher, J. 2000. Microseparation of the centers of alumina-alumina artificial hip joints during simulator testing produces clinically relevant wear rates and patterns. *The Journal of Arthroplasty*. **15**(6),pp.793–5.
- Nevelos, J.E., Ingham, E., Doyle, C., Fisher, J. and Nevelos, a B. 1999. Analysis of retrieved alumina ceramic components from Mittelmeier total hip prostheses. *Biomaterials*. **20**(19),pp.1833–40.
- Nevelos, J.E., Ingham, E., Doyle, C., Nevelos, a B. and Fisher, J. 2001. The influence of acetabular cup angle on the wear of ‘BIOLOX Forte’ alumina ceramic bearing couples in a hip joint simulator. *Journal of Materials Science. Materials in Medicine*. **12**(2),pp.141–4.
- Nevelos, J.E., Ingham, E., Doyle, C., Nevelos, A.B. and Fisher, J. 2001. Wear of HIPed and non-HIPed alumina–alumina hip joints under standard and severe simulator testing conditions. *Biomaterials*. **22**(16),pp.2191–2197.
- Nevelos, J.E., Prudhommeaux, F., Hamadouche, M., Doyle, C., Ingham, E., Meunier, a, Nevelos, a B., Sedel, L. and Fisher, J. 2001. Comparative analysis of two different types of alumina-alumina hip prosthesis retrieved for aseptic loosening. *The Journal of bone and joint surgery. British volume*. **83**(4),pp.598–603.
- NICE 2013. *Overview – Arthritis of the hip (end stage)- hip replacement (total) and resurfacing arthroplasty (Rev TA2, TA44)*.
- Nieuwenhuijse, M.J., Valstar, E.R., Kaptein, B.L. and Nelissen, R.G.H.H. 2012. Good diagnostic performance of early migration as a predictor of late aseptic loosening of acetabular cups: results from ten years of follow-up with Roentgen stereophotogrammetric analysis (RSA). *The Journal of bone and joint surgery. American volume*. **94**(10),pp.874–80.
- O’Kelly, J., Unsworth, A., Dowson, D., Hall, D.A. and Wright, V. 1978. A Study of the Role of Synovial Fluid and its Constituents in the Friction and Lubrication of Human Hip Joints. *Engineering in Medicine*. **7**(2),pp.73–83.
- Oliveira, A.L.L., Lima, R.G., Cueva, E.G. and Queiroz, R.D. 2011. *Comparative analysis of surface wear from total hip prostheses tested on a mechanical simulator according to standards ISO 14242-1 and ISO 14242-3*.
- Partridge, S., Tipper, J.L., Al-Hajjar, M., Isaac, G.H., Fisher, J. and Williams, S. 2017. Evaluation of a new methodology to simulate damage and wear of polyethylene hip replacements subjected to edge loading in hip simulator testing. *Journal of Biomedical Materials Research Part B: Applied Biomaterials*.
- Parvizi, J., Sharkey, P.F., Bissett, G.A., Rothman, R.H. and Hozack, W.J. 2003. Surgical treatment of limb-length discrepancy following total hip arthroplasty. *The Journal of bone and joint surgery. American volume*. **85-A**(12),pp.2310–7.

- De Pasquale, D., Stea, S., Beraudi, A., Montesi, M., Squarzone, S. and Toni, A. 2013. Ceramic debris in hip prosthesis: correlation between synovial fluid and joint capsule. *The Journal of arthroplasty*. **28**(5),pp.838–41.
- Pasquier, G., Ducharme, G., Sari Ali, E., Giraud, F., Mouttet, A. and Durante, E. 2010. Total hip arthroplasty offset measurement: Is C T scan the most accurate option? *Orthopaedics & Traumatology: Surgery & Research*. **96**(4),pp.367–375.
- Paul, J. 1967. Forces at the human hip joint.
- Pijls, B.G., Nieuwenhuijse, M.J., Fiocco, M., Plevier, J.W., Middeldorp, S., Nelissen, R.G. and Valstar, E.R. 2012. Early proximal migration of cups is associated with late revision in THA: a systematic review and meta-analysis of 26 RSA studies and 49 survivalstudies. *Acta orthopaedica*. **83**(6),pp.583–91.
- Rieger, W. 2001. *Ceramics in Orthopedics - 30 Years of Evolution and Experience*. Verlag Hans Huber.
- Sahin, O., Tuncdemir, A.R., Cetinkara, H.A., Guder, H.S. and Sahin, E. 2011. Production and Mechanical Behaviour of Biomedical CoCrMo Alloy. *Chinese Physics Letters*. **28**(12),p.126201.
- Saikko, V. 2003. Effect of Lubricant Protein Concentration on the Wear of Ultra-High Molecular Weight Polyethylene Sliding Against a CoCr Counterface. *Journal of Tribology*. **125**(3),p.638.
- Sariali, E., Klouche, S., Mouttet, A. and Pascal-Moussellard, H. 2014. The effect of femoral offset modification on gait after total hip arthroplasty. *Acta orthopaedica*. **85**(2),pp.123–7.
- Saxler, G., Marx, A., Vandeveld, D., Langlotz, U., Tannast, M., Wiese, M., Michaelis, U., Kemper, G., Grützner, P.A., Steffen, R., von Knoch, M., Holland-Letz, T. and Bernsmann, K. 2004. The accuracy of free-hand cup positioning--a CT based measurement of cup placement in 105 total hip arthroplasties. *International orthopaedics*. **28**(4),pp.198–201.
- Scholes, S.C., Green, S.M. and Unsworth, A. 2001. The wear of metal-on-metal total hip prostheses measured in a hip simulator. *Proceedings of the Institution of Mechanical Engineers. Part H, Journal of engineering in medicine*. **215**(6),pp.523–30.
- Scholes, S.C. and Unsworth, A. 2000. Comparison of friction and lubrication of different hip prostheses. *Proceedings of the Institution of Mechanical Engineers, Part H: Journal of Engineering in Medicine*. **214**(1),pp.49–57.
- Scholes, S.C. and Unsworth, A. 2006. The Effects of Proteins on the Friction and Lubrication of Artificial Joints. *Proceedings of the Institution of Mechanical Engineers, Part H: Journal of Engineering in Medicine*. **220**(6),pp.687–693.
- Schroeder, D., Durham, S. and Elliott, M. 2014. SMALL-DIAMETER CERAMIC-ON-CERAMIC HIP WEAR TESTING WITH ADVERSE MICROSEPARATION CONDITIONS. *Bone & Joint Journal Orthopaedic Proceedings Supplement*. **96-B**(SUPP 11),p.143.
- Sexton, S.A., Yeung, E., Jackson, M.P., Rajaratnam, S., Martell, J.M., Walter, W.L., Zicat, B.A. and Walter, W.K. 2011. The role of patient factors and implant position in squeaking of ceramic-on-ceramic total hip replacements. *The Journal of bone and joint surgery. British volume*. **93**(4),pp.439–42.

- Shishido, T., Yamamoto, K., Tanaka, S., Masaoka, T., Clarke, I.C. and Williams, P. 2006. A Study for a retrieved implant of ceramic-on-ceramic total hip arthroplasty. *The Journal of arthroplasty*. **21**(2),pp.294–8.
- Silva, M., Heisel, C. and Schmalzried, T.P. 2005. Metal-on-metal total hip replacement. *Clinical orthopaedics and related research*. (430),pp.53–61.
- Smith, S.L., Dowson, D. and Goldsmith, A.A. 2001. The effect of femoral head diameter upon lubrication and wear of metal-on-metal total hip replacements. *Proceedings of the Institution of Mechanical Engineers. Part H, Journal of engineering in medicine*. **215**(2),pp.161–70.
- Smith, S.L. and Unsworth, A. 2001. An *in vitro* wear study of alumina—alumina total hip prostheses. *Proceedings of the Institution of Mechanical Engineers, Part H: Journal of Engineering in Medicine*. **215**(5),pp.443–446.
- Soong, M., Rubash, H.E. and Macaulay, W. 2004. Dislocation after total hip arthroplasty. *The Journal of the American Academy of Orthopaedic Surgeons*. **12**(5),pp.314–21.
- Stewart, T., Tipper, J., Streicher, R., Ingham, E. and Fisher, J. 2001. Long-term wear of HIPed alumina on alumina bearings for THR under microseparation conditions. *Journal of Materials Science. Materials in Medicine*. **12**(10-12),pp.1053–6.
- Stewart, T., Tipper, J.L., Insley, G., Streicher, R.M., Ingham, E. and Fisher, J. 2003. Long-term wear of ceramic matrix composite materials for hip prostheses under severe swing phase microseparation. *Journal of biomedical materials research. Part B, Applied biomaterials*. **66**(2),pp.567–73.
- Tateiwa, T., Clarke, I.C., Pezzotti, G., Sedel, L., Kumakura, T., Shishido, T. and Yamamoto, K. 2007. Surface micro-analyses of long-term worn retrieved ‘Osteal’ alumina ceramic total hip replacement. *Journal of biomedical materials research. Part B, Applied biomaterials*. **83**(2),pp.562–70.
- Tateiwa, T., Clarke, I.C., Shirasu, H., Masaoka, T., Shishido, T. and Yamamoto, K. 2006. Effect of low protein concentration lubricants in hip simulators. *Journal of Orthopaedic Science*. **11**(2),pp.204–211.
- Tipper, J.L., Hatton, A., Nevelos, J.E., Ingham, E., Doyle, C., Streicher, R., Nevelos, a B. and Fisher, J. 2002. Alumina-alumina artificial hip joints. Part II: characterisation of the wear debris from in vitro hip joint simulations. *Biomaterials*. **23**(16),pp.3441–8.
- Tsai, T.-Y., Li, J.-S., Wang, S., Lin, H., Malchau, H., Li, G., Rubash, H. and Kwon, Y.-M. 2013. A novel dual fluoroscopic imaging method for determination of THA kinematics: In-vitro and in-vivo study. *Journal of Biomechanics*. **46**(7),pp.1300–1304.
- Tsai, T.-Y., Li, J.-S., Wang, S., Scarborough, D. and Kwon, Y.-M. 2014. In-vivo 6 degrees-of-freedom kinematics of metal-on-polyethylene total hip arthroplasty during gait. *Journal of biomechanics*. **47**(7),pp.1572–6.
- Unsworth, A., Dowson, D. and Wright, V. 1975. Some new evidence on human joint lubrication. *Annals of the rheumatic diseases*. **34**(4),pp.277–85.

- Uribe, J., Geringer, J., Gremillard, L. and Reynard, B. 2013. Degradation of alumina and zirconia toughened alumina (ZTA) hip prostheses tested under microseparation conditions in a shock device. *Tribology International*. **63**,pp.151–157.
- Vassiliou, K., D Elfick, A.P., Scholes, S.C. and Unsworth, A. 2006. The effect of ‘running-in’ on the tribology and surface morphology of metal-on-metal Birmingham hip resurfacing device in simulator studies. *Proceedings of the Institution of Mechanical Engineers, Part H: Journal of Engineering in Medicine*. **220**(2),pp.269–277.
- Walter, W.L., Insley, G.M., Walter, W.K. and Tuke, M.A. 2004. Edge loading in third generation alumina ceramic-on-ceramic bearings. *The Journal of Arthroplasty*. **19**(4),pp.402–413.
- Wang, A., Polineni, V.K., Stark, C. and Dumbleton, J.H. 1998. Effect of femoral head surface roughness on the wear of ultrahigh molecular weight polyethylene acetabular cups. *The Journal of Arthroplasty*. **13**(6),pp.615–620.
- Wasielewski, R. 2007. The Hip *In*: J. Callaghan, A. Rosenberg and H. Rubash, eds. *The Adult Hip*. Philadelphia: Lippincott Williams & Wilkins, pp. 51–67.
- Widmer, K.-H. and Zurfluh, B. 2004. Compliant positioning of total hip components for optimal range of motion. *Journal of orthopaedic research : official publication of the Orthopaedic Research Society*. **22**(4),pp.815–21.
- Wierer, T., Forst, R., Mueller, L. a and Sesselmann, S. 2013. Radiostereometric migration analysis of the Lubinus SP II hip stem: 59 hips followed for 2 years. *Biomedizinische Technik. Biomedical engineering*. **58**(4),pp.333–41.
- Williams, S., Butterfield, M., Stewart, T., Ingham, E., Stone, M. and Fisher, J. 2003. Wear and deformation of ceramic-on-polyethylene total hip replacements with joint laxity and swing phase microseparation. *Proceedings of the Institution of Mechanical Engineers. Part H, Journal of engineering in medicine*. **217**(2),pp.147–53.
- Williams, S., Jalali-Vahid, D., Brockett, C., Jin, Z., Stone, M.H., Ingham, E. and Fisher, J. 2006. Effect of swing phase load on metal-on-metal hip lubrication, friction and wear. *Journal of biomechanics*. **39**(12),pp.2274–81.
- Williams, S., Leslie, I., Isaac, G., Jin, Z., Ingham, E. and Fisher, J. 2008. Tribology and wear of metal-on-metal hip prostheses: influence of cup angle and head position. *The Journal of bone and joint surgery. American volume*. **90 Suppl 3**,pp.111–7.
- Williams, S., Schepers, A., Isaac, G., Hardaker, C., Ingham, E., van der Jagt, D., Breckon, A. and Fisher, J. 2007. The 2007 Otto Aufranc Award. Ceramic-on-metal hip arthroplasties: a comparative in vitro and in vivo study. *Clinical orthopaedics and related research*. **465**(465),pp.23–32.
- Williams, S.R., Wu, J.J., Unsworth, A. and Khan, I. 2011. Wear and surface analysis of 38 mm ceramic-on-metal total hip replacements under standard and severe wear testing conditions. *Proceedings of the Institution of Mechanical Engineers, Part H: Journal of Engineering in Medicine*. **225**(8),pp.783–796.
- Wirganowicz, P.Z. and Thomas, B.J. 1997. Massive osteolysis after ceramic on ceramic total hip arthroplasty. A case report. *Clinical orthopaedics and related research*. (338),pp.100–4.

- Yamamoto, T., Saito, M., Ueno, M., Hananouchi, T., Tokugawa, Y. and Yonenobu, K. 2005. Wear analysis of retrieved ceramic-on-ceramic articulations in total hip arthroplasty: Femoral head makes contact with the rim of the socket outside of the bearing surface. *Journal of biomedical materials research. Part B, Applied biomaterials*. **73**(2),pp.301–7.
- Yoder, S.A., Brand, R.A., Pedersen, D.R. and O’Gorman, T.W. 1988. Total hip acetabular component position affects component loosening rates. *Clinical orthopaedics and related research*. (228),pp.79–87.
- Yoon, T.R., Rowe, S.M., Jung, S.T., Seon, K.J. and Maloney, W.J. 1998. Osteolysis in association with a total hip arthroplasty with ceramic bearing surfaces. *The Journal of bone and joint surgery. American volume*. **80**(10),pp.1459–68.

9. Appendices

Appendix A. Type of edge loading for different conditions based on the analysis of data and interpretation of the observer

Type of edge loading for the 50 N/mm spring constant

Swing phase load (N)		50	75	100	125	150	175	200	225	250	275	300	325	350	375	400	425	450	475	500	
Mismatch (mm)	Cup inclination angle (deg)																				
1	45°																				
2																					
3																					
4																					
1	55°																				
2																					
3																					
4																					
1	65°																				
2																					
3																					
4																					?

Notes:

- Gray cells indicated no separation observed
- Green cells indicated separation observed
- Red cells indicated interrupted relocation observed
- ? Can't confirm based on observation and data actual result

Type of edge loading for the 100 N/mm spring constant

Swing phase load (N)		50	75	100	125	150	175	200	225	250	275	300	325	350	375	400	425	450	475	500	
Mismatch (mm)	Cup inclination angle (deg)																				
1	45°																				
2																					
3																					
4																					
1	55°																				
2																					
3																					
4																					
1	65°																				
2																					
3																					?
4																					

Notes:

- Gray cells indicated no separation observed
- Green cells indicated separation observed
- Red cells indicated interrupted relocation observed
- ? Can't confirm based on observation and data actual result

Type of edge loading for the 200 N/mm spring constant

Swing phase load (N)		50	75	100	125	150	175	200	225	250	275	300	325	350	375	400	425	450	475	500	
Mismatch (mm)	Cup inclination angle (deg)																				
1	45°																				
2																					
3																					
4																					
1	55°																				
2																					
3																					
4																					
1	65°																				
2																					
3																					
4																					

Notes:

- Gray cells indicated no separation observed
- Green cells indicated separation observed
- Red cells indicated interrupted relocation observed
- ? Can't confirm based on observation and data actual result

Appendix B. Variability of the springs close end finish and the effect on its performance under axial compression

Aim: To determine what is the effect of the close end finish of the springs used for the edge loading testing methodology and variability associated with each station in the hip simulator due to the spring

Objective: To test the springs under an axial compression

Method:

Vertical electromechanical (universal) testing machine (Instron 3365, Bucks, UK) with a 500 N load cell

Compression test with a rate of 1 mm/min, to a max compression of approximately 300 N.

n=6, spring rate of 50, 100 and 200 N/mm

Measure the distance required to grip under a compression load before the spring is fully supported by the active coils and operating between the specified spring rate.

Results:

An example of load and displacement curve from the Instron demonstrating the distance required to grip under compression before the spring was fully supported by the active coils is shown in Figure 9-1.

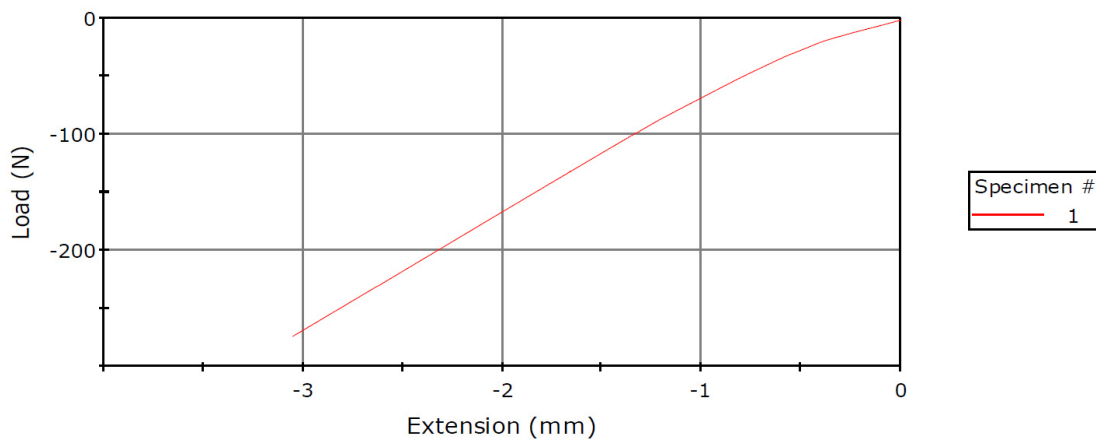


Figure 9-1. Load vs displacement curve for a 100 N/mm spring tested under a 1 mm/min compressive load.

Spring constant of 50 N/mm

The distance required to grip each of the 6 springs tested varied from approximately 0.00 to 0.20 mm (Figure 9-2). The mean (\pm standard deviation) distance required to grip the springs was 0.06 ± 0.09 mm.

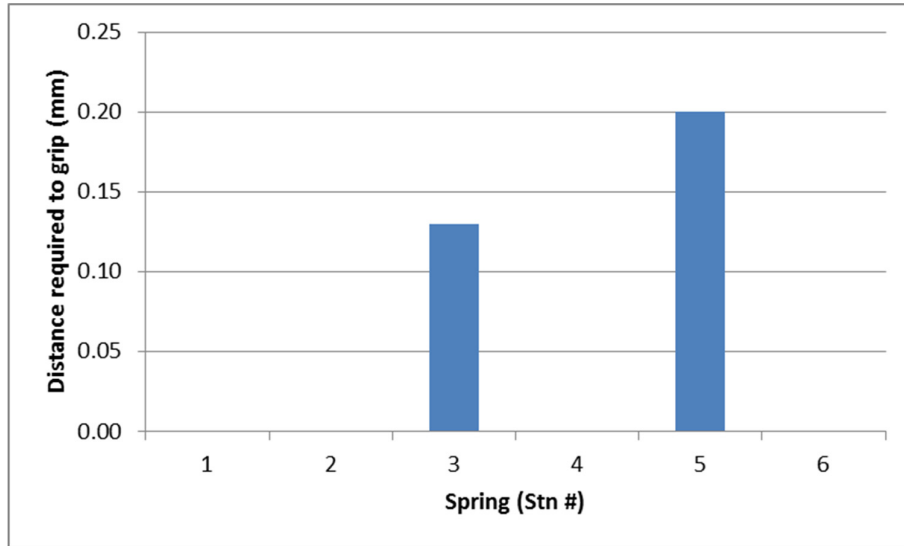


Figure 9-2. Distance required to grip the 50 N/mm spring constant before the active coils respond to the appropriate spring stiffness for the 6 stations of the Leeds II Hip Joint Simulator.

Spring constant of 100 N/mm

The distance required to grip each of the 6 springs tested varied from approximately 0.05 to 0.60 mm (Figure 9-3). The mean (\pm standard deviation) distance required to grip the springs was 0.31 ± 0.20 mm.

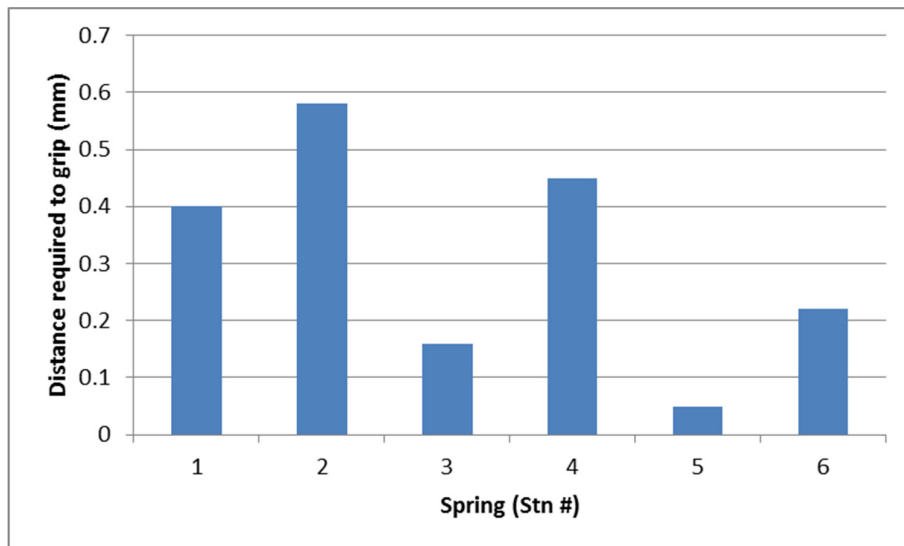


Figure 9-3. Distance required to grip the 100 N/mm spring constant before the active coils respond to the appropriate spring stiffness for the 6 stations of the Leeds II Hip Joint Simulator.

Spring constant of 200 N/mm

The distance required to grip each of the 6 springs tested varied from approximately 0.30 to 0.70 mm (Figure 9-4). The mean (\pm standard deviation) distance required to grip the springs was 0.46 ± 0.14 mm.

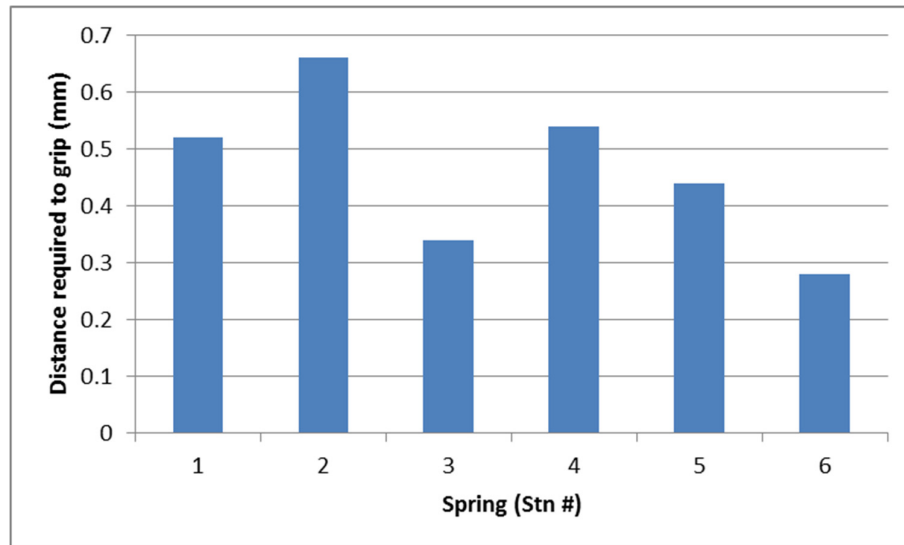


Figure 9-4. Distance required to grip the 200 N/mm spring constant before the active coils respond to the appropriate spring stiffness for the 6 stations of the Leeds II Hip Joint Simulator.

Discussion and conclusion:

A compression force was generated by an input displacement (translational mismatch) with a spring in the studies from this thesis. The springs were manufactured with closed ends and ground. Small variations were observed between the spring's ends. This was dependant on how much material was machined off, and the geometry of the ends of the springs. This variation can create a slight effect on the compressive force required to grip properly before the springs are fully supported by the active coils. A 1 mm/min compression test was performed on a single axis compression machine on all the springs used in these studies to measure the amount of distance required to compress before the springs were fully supported by the active coils. The results from these tests demonstrated the variation between the springs. This distance could influence the medial-lateral load applied during dynamic loading.

Appendix C. Effect of the input translational mismatch on the displacement and tilt of the cup holder

Aim: To determine the effect of the input translational mismatch on the cup holder under cyclic loading.

Objective: To measure the displacement of the cup holder and define the assembly point where the head and the cup are relatively concentric under cyclic conditions.

Method:

Using two LVDTs positioned in two different locations along the cup holder (Figure 9-5), the assembly point during cyclic loading while under a translational mismatch was evaluated. The assembly point was defined as the position of the cup holder when a high swing phase load was applied such that the components are relatively concentric while a translational mismatch (active spring) was present. Different conditions were applied as described in Table 9-1. Three samples were used per condition. One station was used and the methodology as described in Chapter 2 was followed.

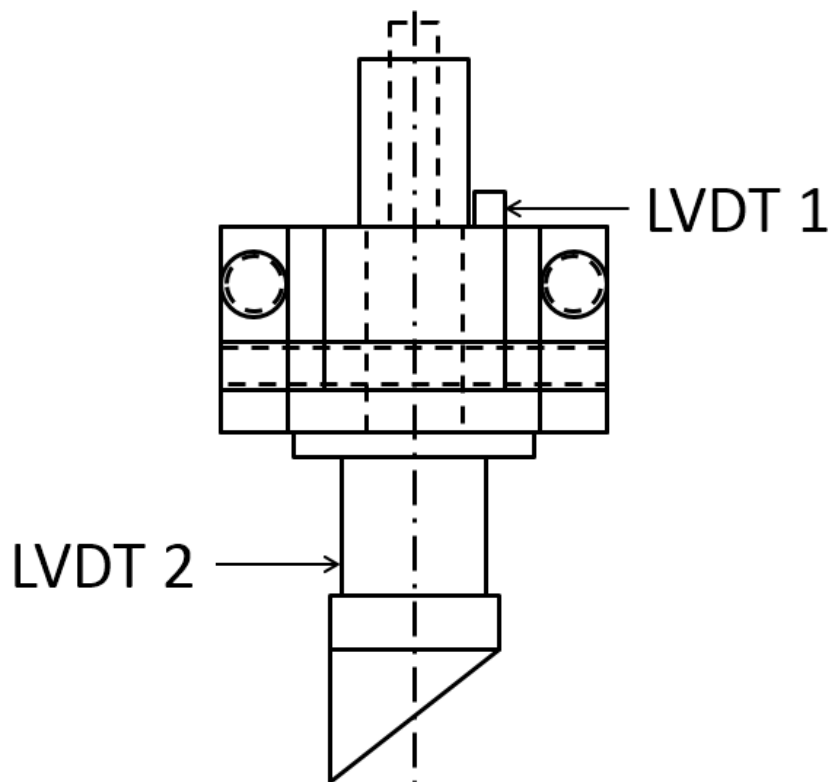


Figure 9-5. Schematic of the cup holder and the positions where the LVDTs were placed in the Leeds Mark II Hip Joint Simulator to measure the displacement of the cup centre relative to the head centre.

Table 9-1. Details of the study to define the centre assembly point of the head and the cup under a translational mismatch condition to replicate edge loading.

Study	Details (Unit)	Input
Biomechanical study	Equipment	Six-station Leeds Mark II (A)
	Materials	Ceramic-on-ceramic (BIOLOX® delta)
	Design	PINNACLE®
	Head size diameter (mm)	36
	Frequency (Hz)	1
	Loading profile	Paul walking cycle (twin peak load)
	Max peak force (N)	3000
	Trough load (N)	1500
	Swing phase load (N)	50, 75, 100, 125, 150, 175, 200, 250, 300, 350, and 450
	Motion profile	Leeds walking cycle (Barbour <i>et al.</i> , 1999)
	Flexion / Extension (°) of the head	+30 / -15
	Internal / External rotation (°) of the cup	+10 / -10
	Stem anteverision angle (°)	20
	Cup version angle (°)	0
	Medial-lateral mismatch (mm)	1, 2, 3 and 4
	Spring constant (N/mm)	50, 100 and 200
	Number of total bearings tested	3
	Cup inclination angle (°)	45, 55 and 65
	Cycles completed	3000
	Station used (#)	3

Results:

The results indicate that when the level of translational mismatch was increased, the tilt level on the cup holder also increased due to the force generated by the translational mismatch (Figure 9-6). The cup inclination angle did not seem to affect the magnitude of the cup holder tilt for the 100 N/mm spring constant conditions. The spring constant affected the centre assembly point (Figure 9-7).

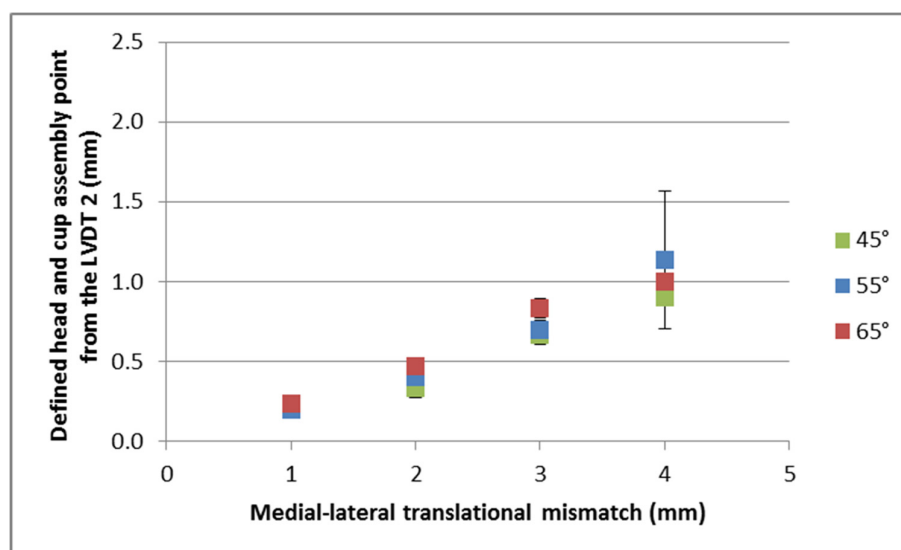


Figure 9-6. Mean ($n=3$, \pm SD) defined centre assembly point for different translational mismatches (1, 2, 3 and 4 mm) and different cup inclination angles (45°, 55° and 65°) for the 100 N/mm spring constant.

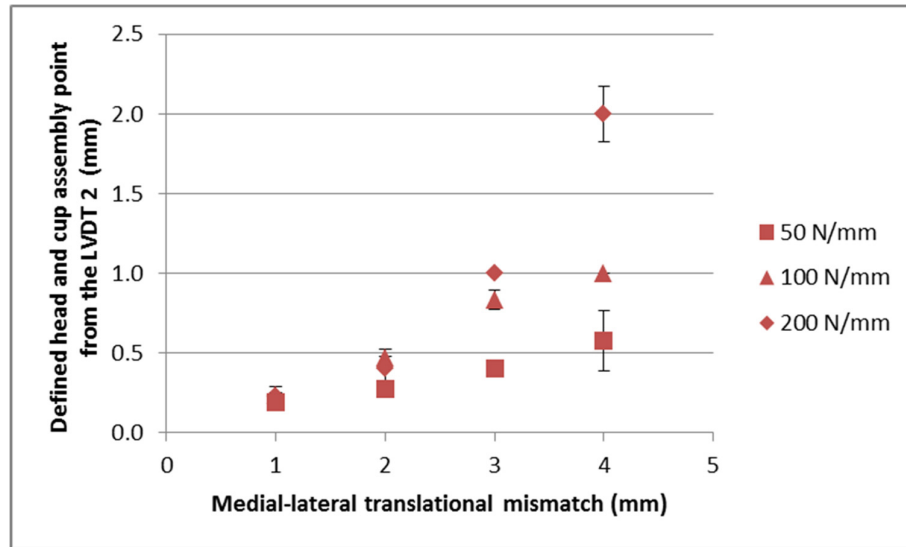


Figure 9-7. Mean ($n=3$, \pm SD) defined centre assembly point for different translational mismatches (1, 2, 3 and 4 mm) for the 65° cup inclination angle for the 50, 100 and 200 N/mm spring constant.